Università degli Studi di Ferrara

UCA Universidad de Cádiz

INTERNATIONAL DOCTORAL COURSE IN
"EARTH AND MARINE SCIENCES (EMAS)"

CYCLE XXXIV

COORDINATOR Prof. MASSIMO COLTORTI

MIOCENE LARGER FORAMINIFERAL BIOSTRATIGRAPHY IN THE MEDITERRANEAN AND THE INDO-PACIFIC AREAS

Scientific/Disciplinary Sector (SDS) GEO/01 (PALEONTOLOGY AND PALEOECOLOGY)

Candidate
Mónica Bolívar Feriche

Supervisors
Prof. Davide Bassi

Prof. Juan Carlos Braga

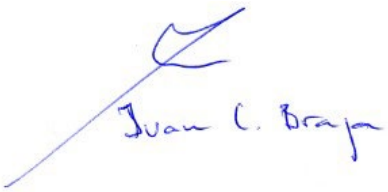

Prof. Massimo Coltorti

Years 2018/2021

To my family

ABSTRACT

Larger benthic foraminifera (LBF) constitute an outstanding tool for biostratigraphic, palaeoecological and palaeobiogeographic studies because of their widespread geographical distribution, fast evolutionary changes, high susceptibility to environmental changes, and high abundance in the sedimentary successions. The PhD project dealt with Miocene LBF (alveolinoids, austrotrillinids, lepidocyclinids and nummulitids) newly recorded in the Mediterranean (southeastern Spain) and Indo-Pacific areas (Indonesia, northern Philippine sea, the Maldives and Ryukyu Islands).

The new LBF record from the Sierra de Marmolance (Granada province, southeasrtern Spain) belongs to a 270-m thick continuous and *in situ* limestone succession of middle Miocene age (dated by the occurrence of Langhian–Serravallian planktonic foraminifera at the bottom of the succession). The LBF assemblage is represented by *Austrotrillina brunni*, *Austrotrillina striata, Borelis inflata, Eulepidina formosoides*, *Eulepidina* ex.interc *dilatata et formosoides*, *Heterostegina assilinoides*, *Neorotalia viennoti, Nephrolepidina* ex.interc. *morgani et praemarginata*, *Nephrolepidina tournoueri, Nummulites fichteli*, *Nummulites kecskemetii, Nummulites vascus*, *Operculina complanata*, *Risananeiza crassaparies* and *Spiroclypeus* sp. These species, up to now considered indicative of Rupelian–Chattian and Aquitanian–Burdigalian, extend their time ranges from the Rupelian to the early Serravallian. Since they are considered as Neogene biochronostratigraphic markers, this study highlights the need of a substantial revision of the Oligocene–Miocene SBZs.

The new records of *Austrotrillina* from Ibi and Sierra de Marmolance (southeastern Spain), Indonesia (Mankalihat and Wailawi) and western Pacific (Kitadaito-jima and Kikai Seamount) allowed to assess their taxonomy according to the shell structure (tectum and a parakeriotheca with subsutural alcoves), biostratigraphy and palaeobiogeography. *Austrotrillina eocaenica* first appears in the middle–late Eocene of Iran. Two Rupelian descendants, *A. brunni* and *A. striata*, migrated from the western Tethys into the Indo-Pacific. *Austrotrillina striata* reached Indonesia and western Australia in the Chattian, then disappeared in the Langhian of Kita-daito-jima. *Austrotrillina brunni* first occurred in the Burdigalian of Indonesia and western Australia and disappeared in the early Serravallian of western and South Australia. *Austrotrillina brunni* and *A. striata* disappeared in the Serravallian westernmost Mediterranean (southeastern Spain). From the Burdigalian the exclusive occurrence of *A. howchini* in the Indo-Pacific areas is a possible result of the closing Tethyan Seaway, which differentiated the Mediterranean and Indo-Pacific bioprovinces. This species disappears in the latemost Langhian–early Serravallian of South Australia and in the Kikai Seamount. The palaeobiogeographical distribution of these species suggests an early Miocene active connection of Eastern Africa with the Central Indo–West Pacific.

The new records (fossil and Recent) from the Maldives, Indonesia and Ryukyu Islands (Okinawa) were analysed to assess the taxonomic status of *Flosculinella* and *Alveolinella* species and to understand the alveolinoid phylogeny in the Indo-Pacific area. The latest Oligocene–middle Miocene *Flosculinella globulosa*, the early–middle Miocene *F. reicheli*, *F. bontangensis*, *F. cucumoides*, *Alveolinella borneensis* and the late Miocene–Recent *A. quoyi* are herein circumscribed in terms of shell length, diameter of the proloculus, whorl number of the first attic occurrence, and number of supplementary chamberlets in the attic floor per chamberlet in the main floor. The occurrence of the preseptal passage only and Y-shaped septula in *Borelis schlumbergeri, Flosculinella* and *Alveolinella* are characters of phylogenetic significance. Oligocene–early Miocene *Borelis philippinensis* is inferred as the common ancestor of these taxa. The diversification of *Flosculinella* and *Alveolinella* occurred in the Coral Triangle of southeast Asia during the early–middle Miocene. The northernmost occurrence of the Tortonian–Recent *A. quoyi*, widespread from Central to the Eastern Indo-Pacific areas, is in the Ryukyu Islands.

TABLE OF CONTENTS

INTRODUCTION

Larger Benthic Foraminifera (LBF) are a group of unicellular marine benthic organisms characterized by complex internal shell structures and usually large size. Living representatives of LBF occur in tropical and warm-temperate, shallow-water seas, confined to the euphotic zone (Hottinger, 1997). LBF are abundant in coral reef-related environments, where extreme densities have been recorded on reef flats in the West Pacific and East Indian Ocean (Langer and Hottinger, 2000). The higher diversities have been reported as well from the Indo-Pacific region (Hallock, 1999). Aproximately the 5% of the total carbonate production in the world's reef shelf areas is produced by LBF (Langer, 2008).

Because of their widespread geographical distribution, fast evolutionary changes, high susceptibility to environmental changes (due to their specific depth and temperature requirements) and high abundance in the sedimentary successions, LBF constitute an outstanding tool for biostratigraphic, palaeoecological and palaeobiogeographic studies (e.g. Hottinger, 1997; Boudagher-Fadel, 2018).

Cenozoic shallow-marine Tethyan deposits contain several age-diagnostic groups of hyaline and porcelaneous larger foraminifera, including alveolinoids, miogypsinids, lepidocyclinids and nummulitids, which can be used for biostratigraphic zonation and regional correlations (Papazzoni et al., 2017; Simmons, 2020). These groups have been reported across a huge area stretching from Europe to the central Pacific and central America (e.g. Adams et al., 1983).

In the last twenty years one of the most important achievements of LBF biostratigraphy has been the Tethyan Shallow Benthic Zonation (SBZ), which was defined for the Paleocene and Eocene by Serra-Kiel et al. (1998; SBZ1 to SBZ20) and for the Oligocene and Miocene by Cahuzac and Poignant (1997; SBZ21 to SBZ26). Several works dealt with the Oligocene–Miocene biostratigraphy of shallow-water sedimentary successions especially for the Indo-Pacific and Central America areas (e.g. Boudagher-Fadel and Banner, 1999; Renema, 2007; Özcan and Less, 2009; Less et al., 2018) and the eastern Mediterranean (e.g. Özcan et al., 2009a, b; Özcan and Less, 2009; Gedik et al., 2014). However, no significant SBZ revision has been performed in the last two decades for the western Mediterranean region.

The PhD project deals with Miocene LBF (i.e. alveolinoids, austrotrillinids, lepidocyclinids, nummulitids) newly recorded in the Mediterranean (southeastern Spain) and Indo-Pacific areas (Indonesia, northern Philippine sea, the Maldives and Ryukyu Islands) aiming to assess their taxonomy and biostratigraphical settings, as well as their palaeobiogeographical distributions.

Thesis outlines

In this thesis the assessment of the Miocene larger benthic foraminiferal biostratigraphy in the Mediterranean and Indo-Pacific areas is organized in three chapters.

Chapter 1 presents the studied middle Miocene sedimentary succession cropping out in Sierra de Marmolance (SE Spain) with the microfacies analysis and the systematic paleontology of the identified larger benthic foraminifera.

Chapter 2 provides the new records of *Austrotrillina* species from southern Spain (Ibi and Sierra de Marmolance), Indonesia (Mankalihat and Wailawi) and western Pacific (Kitadaito-jima and Kikai Seamount). These records allowed the species circumscriptions according to the shell structure. The biostratigraphic records and the paleobiogeographic distributions of the *Austrotrillina* species in the Mediterranean and Indo-Pacific areas are discussed.

Chapter 3 introduces the new records of *Alveolinella* and *Flosculinella* species from the Maldives, Indonesia and Ryukyu Islands (Okinawa). According to these records the species circumscriptions based on shell structures, the biostratigraphic settings and the paleobiogeographic distributions are described and discussed.

Chapter 1. Middle Miocene larger foraminifera in SE Spain: biostratigraphical assessment

1. Introduction

Larger benthic foraminiferal (LBF) biozonations are of great importance for dating Cenozoic shallow-water carbonate deposits (Papazzoni et al., 2017; Simmons, 2020). In the last twenty years one of the most important achievements of LBF biostratigraphy has been the Tethyan Shallow Benthic Zonation (SBZ), which was defined for the Paleocene and Eocene by Serra-Kiel et al., (1998; SBZ1 to SBZ20) and for the Oligocene and Miocene by Cahuzac and Poignant (1997; SBZ21 to SBZ26).

The SBZ emerged after the taxonomic and stratigraphic revisions of the most diverse groups of Paleogene–Neogene LBF (i.e. alveolinoids, nummulitids, orthophragminids, miogypsinids, lepidocyclinids) in the 1970s–1980s. The SBZs follow the Oppelian criteria of superposed key localities forming an ideal succession, key assemblages and vicariant taxa, and thus represent a discrete biozonation (e.g. Pignatti and Papazzoni, 2017). The SBZs are correlated to pelagic zones (calcareous plankton and nannofossils), as well as to magnetostratigraphic chrons for the Paleocene–Eocene western Tethys (modern Mediterranean), adding a significant information useful for worldwide correlation and achieving the status of a 'standard' zonation (Pignatti and Papazzoni, 2017). Although the western Tethyan Oligocene–Miocene SBZs have been tentatively correlated to the planktonic zones, the SBZs are independent from the classic standard biozonations (Cahuzac and Poignant, 1997, p. 157) and further chronostratigraphic ties are required for accurate correlations (Papazzoni et al., 2017).

Since the establishment of the SBZ, new information about systematics, biostratigraphy and palaeobiogeography of Paleogene LBF became available (e.g. Less, 1999; Özcan et al., 2006; Less et al., 2006; Bassi et al., 2007; Less et al., 2008; Less and Özcan, 2008; Özcan et al., 2010; Benedetti, 2010; Less and Özcan, 2012; Boudagher-Fadel and Price, 2013; Özcan et al., 2014; Less et al., 2015; Ferràndez-Cañadell and Bover-Arnal, 2017; Hadi et al., 2019; Özcan et al., 2019; Akbar-Baskalayeh et al., 2020; Gedik and Karadenizli, 2021). Several works applied the Oligocene–Miocene SBZ especially for the Indo-Pacific and Central America areas (e.g. Boudagher-Fadel and Banner, 1999; Renema, 2007; Özcan and Less, 2009; Less et al., 2018) and the eastern Mediterranean (e.g. Özcan et al., 2009a; Özcan and Less, 2009; Gedik et al., 2014). However, no significant SBZ revision for the Neogene has been performed since the Cahuzac and Poignant's (1997) proposal for the Mediterranean region.

In the Neogene Mediterranean basins dating the widespread Miocene shallow-water deposits remains very inaccurate except when lateral changes of facies to pelagic materials in which planktonic foraminifera abundantly occur (Braga et al., 2006, 2010). In most cases, however, planktonic index fossils are either scarce or absent and no lateral transitions to pelagic fine-grained sediments can be traced (Papazzoni et al., 2017). In addition, in shallow-water deposits magnetostratigraphy often cannot be applied (Papazzoni et al., 2017). Isotopic stratigraphy ($^{86}Sr/^{87}Sr$ dating) attempted to solve this problem (e.g. Sælen et al., 2016; Ando et al., 2011) but it resulted in controversial outcomes owing to the disturbance of original geochemical signals as a result of rock alteration and the local character of the basin water masses.

The sampled Miocene deposits from the Sierra de Marmolance (southeastern Spain) were analysed to assess a LBF biozonation. The presence of planktonic marls at the base and laterally interfingering with limestones containing autochthonous LBF in the studied section (Sierra de Marmolance, southeastern Spain) represents an exceptional opportunity to correlate the planktonic foraminiferal zones and the LBF occurrences, making possible a re-assessement of the age range of Miocene SBZs for the western Mediterranean area. This will allow dating Miocene shallow-water carbonates from the western Mediterranean region, for the first time, using the standard chronostratigraphic scale based on planktonic foraminifera.

2. Geological and stratigraphical setting

The LBF specimens were collected in Miocene bioclastic limestones from the Sierra de Marmolance near Huéscar in the Granada province (southeastern Spain). This limestone succession belongs to the Subbetic Domain of the External Zones of the Betic Cordillera. The Subbetic was the distal domain of the Southern Iberian Margin, which in middle Miocene times was already deformed and partially emergent.

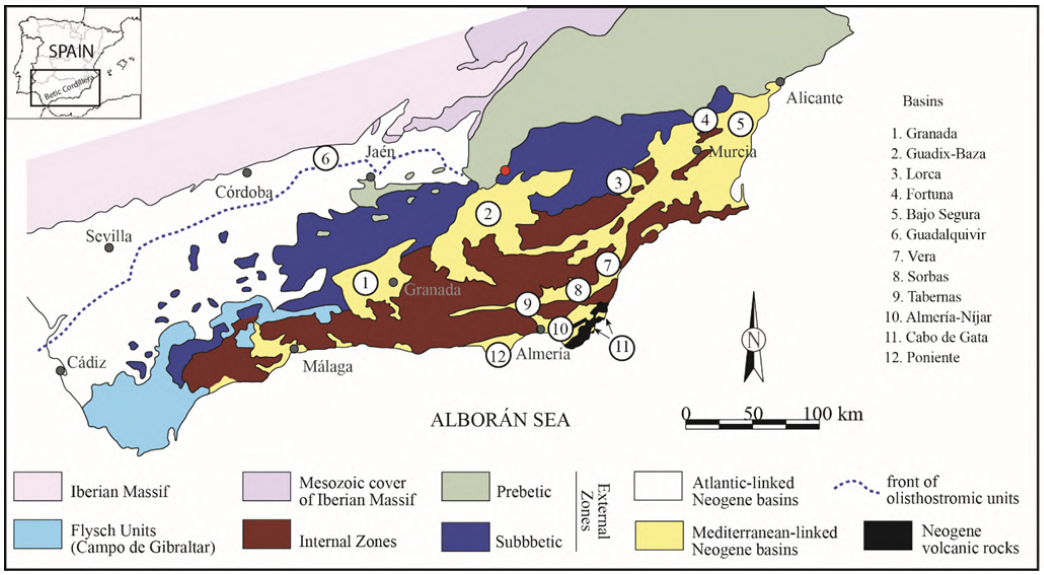

Figure 1. Location of the study area (red point) in the southeastern Spain (Granada province).

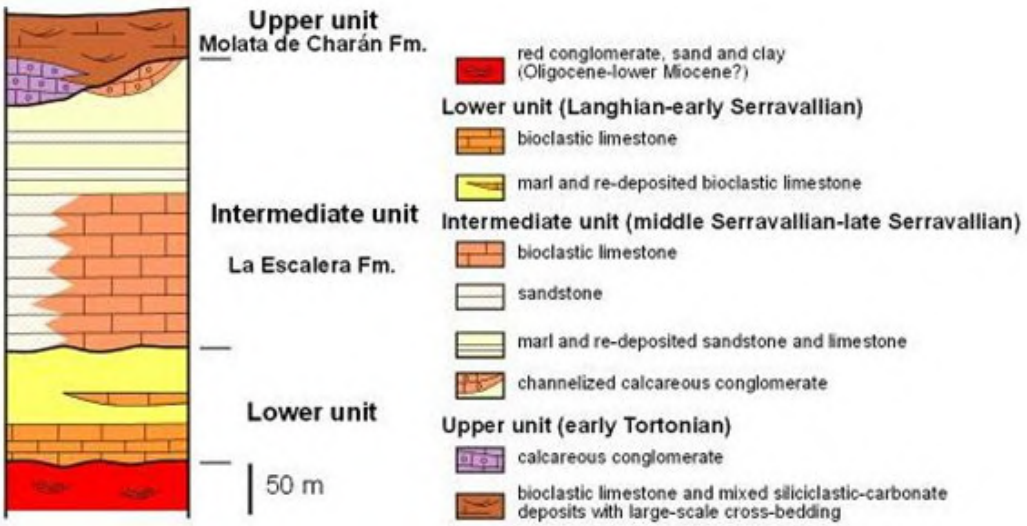

Figure 2. Stratigraphic column showing the stratigraphy of Prebetic domain. Taken from Braga et al., 2010.

The Betic cordillera, together with the Rif in North Africa, forms the westernmost segment of the Alpine chains surrounding the western Mediterranean. Two main geological domains can be differentiated in the Betic Cordillera according to their lithological, stratigraphic and structural features, as well as their paleogeographic meaning: the Internal Zones (or Alboran Block) to the south, and the External Zones (or South-Iberian Palaeomargin) to the north. The Internal Zones constitute an alloctonous lithospheric fragment dominated by metamorphic rocks Palaeozoic to Miocene in age and comprises the Nevado-Filábride, Alpujárride and Maláguide complexes. The External Zones (Prebetic and Subbetic) consist of sedimentary rocks Mesozoic to Miocene in age and formed most of the southern and part of the eastern margin of the Iberian Massif (Sanz de Galdeano, 1990).

Both domains underwent convergence and collisional processes that ended in the early Miocene and gave rise to substantial crustal thickening. This was followed by an extensional phase dominated by detachment processes (García Dueñas et al., 1992; Jabaloy et al., 1992) and strike-slip movements (Sanz de Galdeano, 1997). Since the late Miocene, the convergence of Eurasian and African plates produced regional uplift and the development of large late regional E–W to NE–SW folds, which determine the main reliefs. The Betic Neogene basins evolved and were deformed under this compressional context.

In the Subbetic domain, the collision of the Internal Zones produced considerable dragging and stretching during Burdigalian, whereas throughout the Langhian–Serravallian the tectonic regime diminished in intensity (Sanz de Galdeano, 1990). An important marine basin appeared in the Subbetic and in the southern part of the Prebetic, which evolved during the Middle Miocene (Sanz de Galdeano y Vera, 1992). From the Tortonian onwards the geodynamic situation changed drastically: the westward drift of the Internal Zones practically ceased and the generally compressive context between Africa and Iberia (NNW–SSE approximately) was reestablished in the whole Betic Cordilllera (Sanz de Galdeano y Vera, 1992).

Shallow-water carbonate sedimentation prevailed in the Prebetic domain during the late early and middle Miocene (Braga et al., 2010; fig. 2), whereas deeper water sediments extended over most of the Subbetic domain. In the latter domain, however, shallow-water carbonates formed around already emergent reliefs in the middle Miocene. This is the case of the study area, in which the antecendent reliefs of the Sagra and Montilla mountains were emergent. The study deposits formed on the shallow-water area west of those two uplands.

2.1. Sierra de Marmolance section

The Sierra de Marmolance (37° 50' 8" N, 2° 36' 42" W) is located in the Huéscar region, Granada province (southern Spain). It is an elongated mountain (up to 9 km and 1.519 m altitude) with orientation N45°E emerging from a plateau, la Hoya de Baza. It belongs to a system of isolated reliefs aligned NE–SW, between Cazorla and Huéscar, that constitute the southernmost part of Sierra de Segura (Foucault, 1971; fig. 3).

Well-exposed bioclastic limestones (reaching up to 300 m in thickness) are the dominant sedimentary deposits in Sierra de Marmolance. Marls occur at the base and interfinger with limestones.

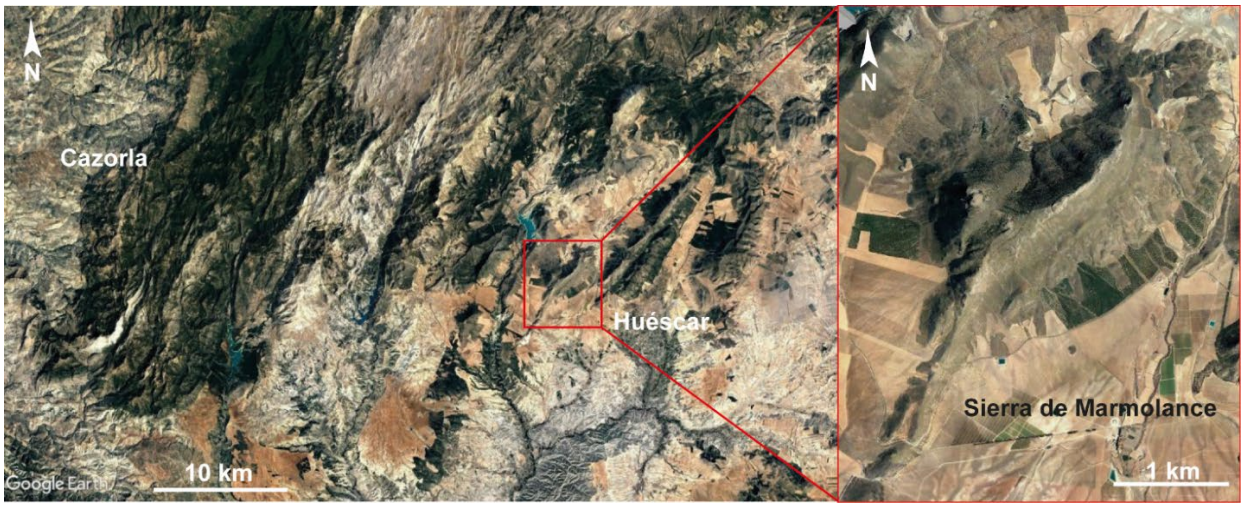

Figure 3. Sierra de Marmolance (SE Spain). Google earth panoramic view.

Studies on the geology of Sierra de Marmolance are rare and relatively old (Fallot, 1945, p.107; Foucault, 1960, 1971). For more than 50 years, the only published work on the area is the geological map (MAGNA 0929, 0950: Lupiani-Moreno et al., 1994). Regarding the stratigraphy of the rocks forming the sierra, Fallot (1945) attributed to the bioclastic limestones a Paleogene

age due to the presence of *Nummulites*. Foucault (1971) only dated as Paleogene the lowest limestones in the mountain and, in turn, gave a maximum age of lower Miocene to the upper limestone deposits because of the presence of *Nephrolepidina*. Foucault (1971) pointed out the hindrances on studying this area, namely the presence of Quaternary deposits and debris covering the lowermost part of the outcrop making difficult to follow the lateral continuity of stratigraphic succession.

3. Materials and methods

3.1. Field work

The palaeontological survey and sampling was carried out in a c. 300 m-thick succession of lower to middle Miocene bioclastic limestones. The succession was logged and 229 rock samples were collected from composite sections. Composite sections comprise one section in the San Clemente channel part (A), one section in the western (B) part and three sections in the eastern part (C, D, E) (fig. 4). The central part of the Sierra was not sampled because of the presence of landslides. This implies that older materials coming from the upper part are found together with younger materials from lower levels, precluding the section logging. Besides, in the lowermost part of the mountain Quaternary materials and debris cover the succession, making difficult to follow the lateral continuity of strata.

Marls at the base and interfingering with limestones, were sampled for analysing their planktonic foraminiferal content to constrain the age of the succession (fig. 4 and 5). The study has been based on seven samples (M1, M0, MARMO 1, MARMO 2, MARMO 3, MARMO 4 MARMO 5) located in the occidental part (M1, M0) and oriental part (MARMO 1–5) in Sierra de Marmolance. Stratigraphically, the lowest samples correspond to MARMO 1–5 and the uppermost to M1.

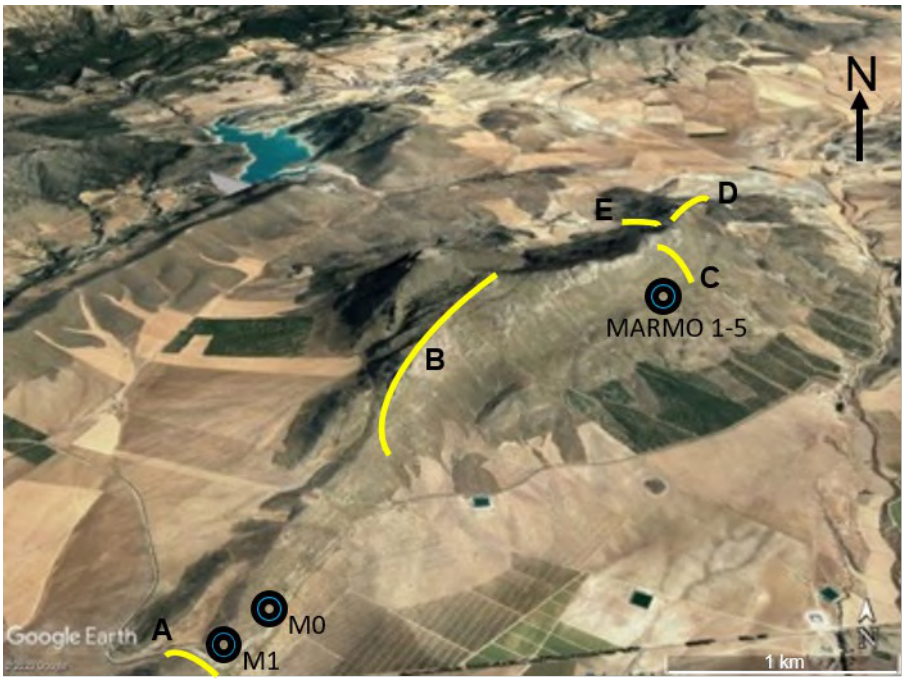

Figure 4. Location of the stratigraphic sections (bioclastic limestones, lines in yellow: A–E) and sampling points (marls, circles in blue: M1, M0, MARMO 1–5) in Sierra de Marmolance (SE Spain). A: San Clemente channel section. B: western section. C–E: eastern sections.

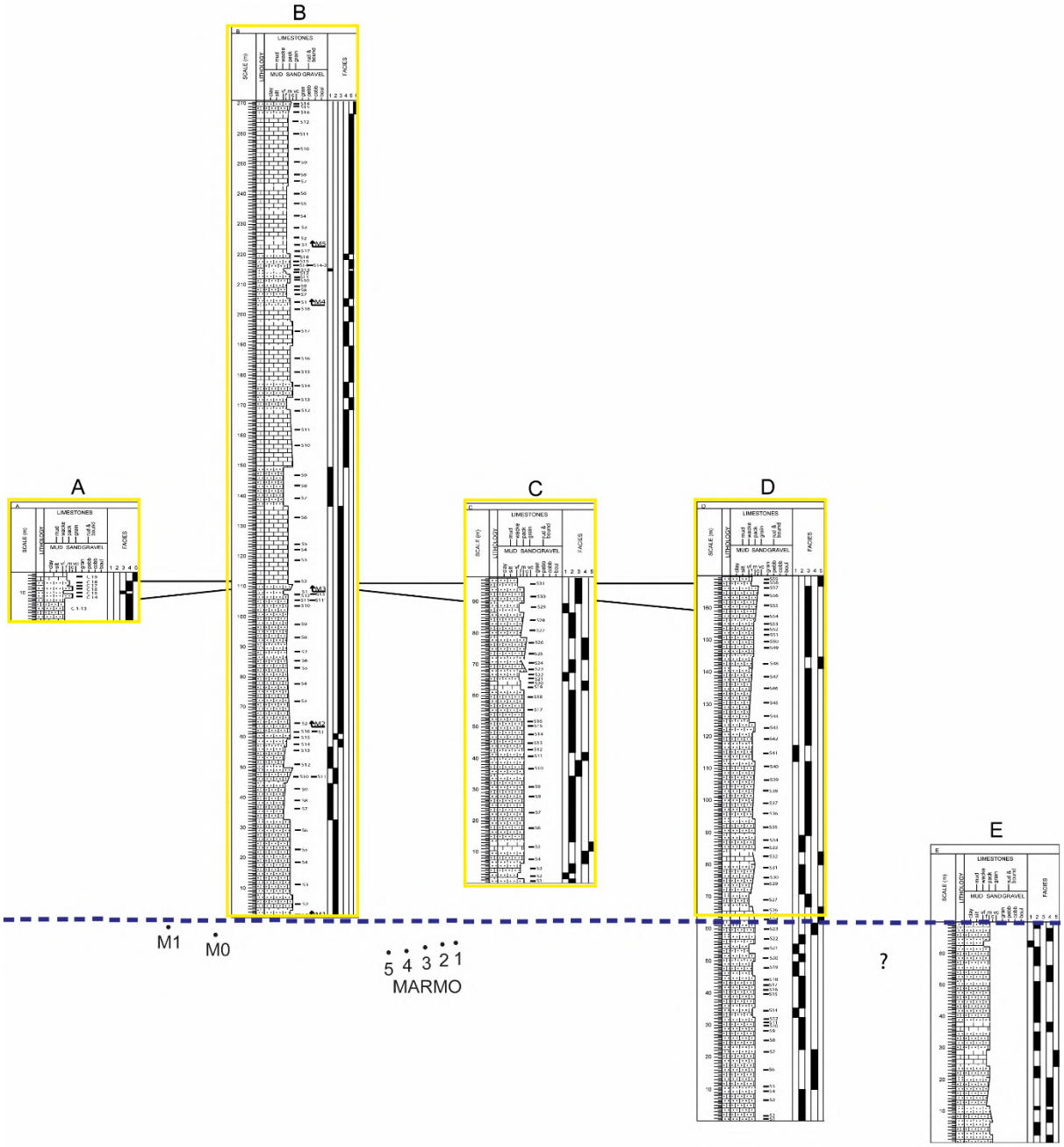

Figure 5. Stratigraphic setting of the logged sections showing the studied bioclastic limestones (A–E, up to 270 m in thickness; yellow) and the underlying planktonic marls (black spots; samples M1, M0, MARMO 1-5; see Fig. 8). The boundary between the marls and the limestones is marked by the blue dashed line. Relative stratigraphic locations of the planktonic samples and sections are not to scale. For the legend, see Fig. 6.

3.2. Laboratory work

In order to study the taxonomy and taphonomy of larger benthic and planktonic foraminifera assemblages, two methods were performed. Planktonic foraminifera were analyzed by optical microscopy and by Scanning Electron Microscopy (SEM) and larger benthic foraminifera by optical microscopy (Lab. of Dpto. Estrat. Paleontol., Univ. Granada; Lab. Dip. Fis. Sci. Terra, Unife).

From the marl deposits, planktonic foraminifera were picked out from the sediment matrix since rock samples were unconsolided.

For SEM analysis (Centro de Instrumentación Científica, CIC, Univ. Granada), isolated foraminifera specimens were picked up and selected according to their preservation state before

being analyzed. SEM images allowed the characterization of the outer shell of planktonic foraminifera specimens (Fig. 8).

The samples from bioclastic limestones were all hard-cemented, so it was no possible to isolate LBF specimens. However, numerous thin sections (339) were made in order to look for appropriate shell sections showing diagnostic characters for LBF species identification. Rocks were cut perpendicular and parallel to the bedding plane. The microfacies analysis was performed on thin sections (Fig. 10).

Anatomical and morphological terms are those used by Hottinger et al. (1993) and Hottinger (1977, 2001, 2006). The suprageneric classification adopted follows Loeblich and Tappan (1987). Shell shape is defined according to Racey (1995). The LBF-shell breakage patterns proposed by Beavington-Penney (2004) as a guide to the autochthonous/allochthonous nature of fossil LBF in thin section (index ranging from 0 to 3, being 0 the best preservation level; Beavington-Penney, 2004, fig. 7) were assessed on the studied thin sections.

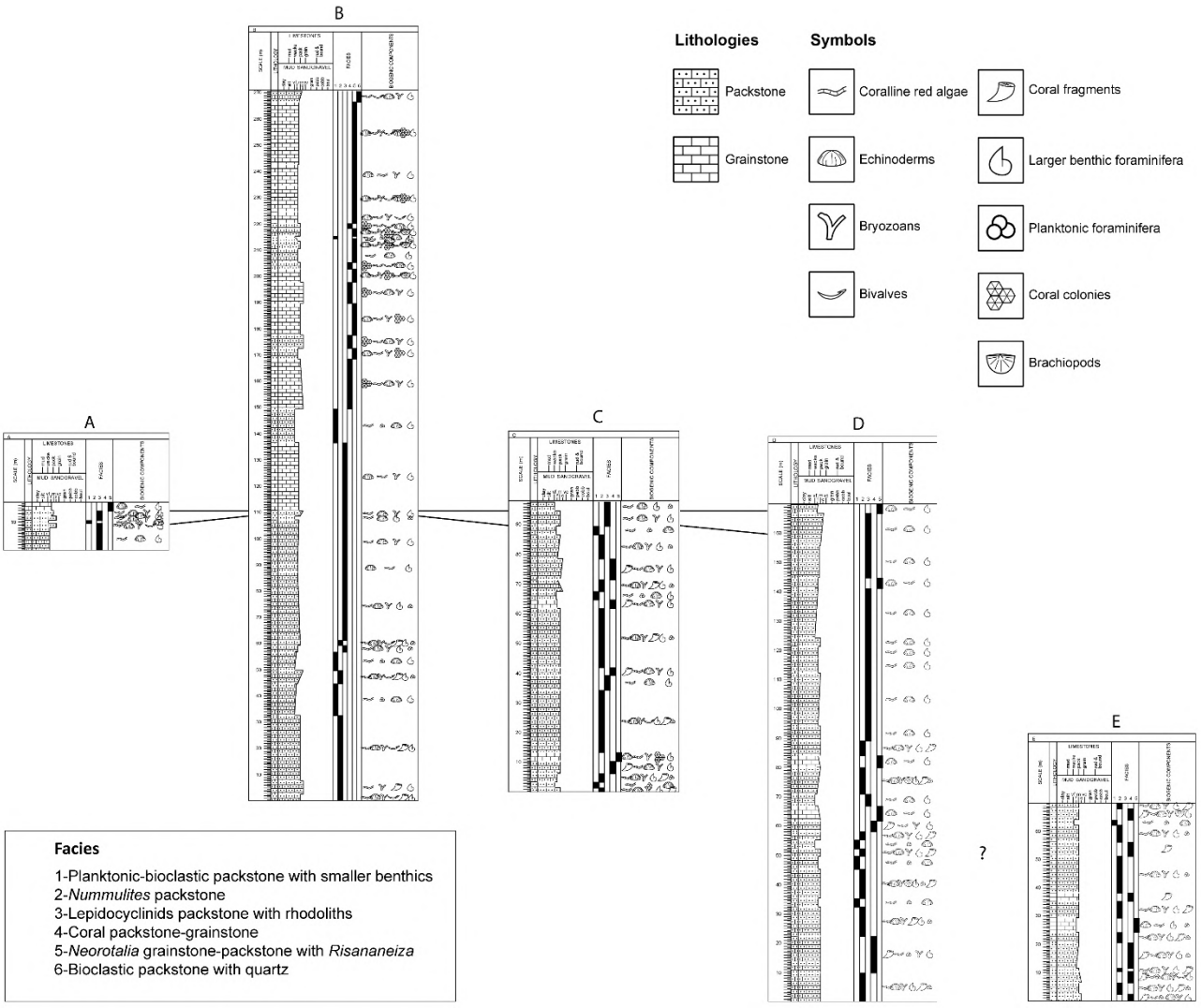

Figure 6. Stratigraphic sections (A–E) from Sierra de Marmolance and their correlation with the main section (B). See fig. 4 for their locations. Below, the studied sections (A, B, C and upper part of D) showing the location of samples.

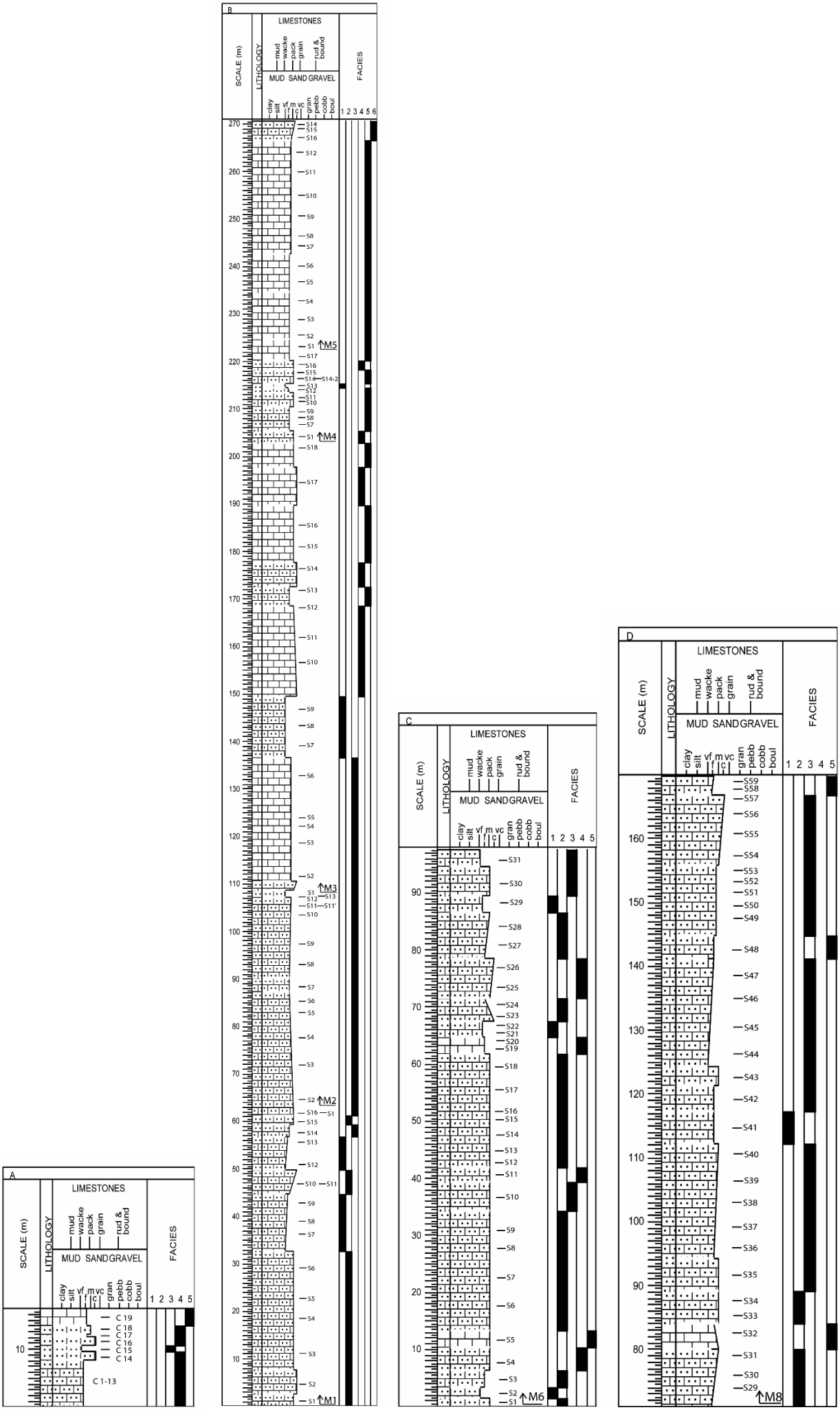
A
B
C
D
SCALE (m)
LITHOLOGY
LIMESTONES
mud
wacke
pack
grain
rud &
bound
MUD SAND GRAVEL
clay
silt
vf
f
m
c
vc
gran
pebb
cobb
boul
FACIES
1 2 3 4 5
C 19
C 18
C 17
C 16
C 15
C 14
C 1-13
M1
M2
M3
M4
M5
M6
M8

4. Results

4.1. General features of the study limestones

The predominant materials in Sierra de Marmolance are bioclastic limestones that can be found as massive-poorly bedded limestones (metric scale; generally coarse-grained; greyish-whitish) alternating with well-stratified micritic limestones (centimetric scale; generally finer-grained; greyish-brownish). Usually, limestones seem more massive and thicker to the SW and thinner to the NE of Sierra de Marmolance. Recrystallization of limestones is common. LBF are generally found in massive medium to coarse-grained limestones. There are beds of high concentration of LBF and algae (e.g. samples C14, M1S4, M2S13, M6S10, M6S30, M8S35, M8S43, M8S54–57). In some beds, LBFs can be seen at hand sample and by a magnifying glass (e.g. samples M1S3, M2S10, M3S3, M5S4, M6S7, M6S9, M6S13, M6S16, M6S28, M8S9, M8S16, M8S35, M8S57).

Strata show, in general, a slight inclination to the NW. In the western part, at the base, strata are dipping slightly to the NW (5–10 degrees), whereas to the top and in the central-eastern part beds are almost horizontal or showing changes in the dipping direction pointing to a gentle folding of materials. In general, the studied stratigraphic succession is continuous.

Occasionally, cross-bedding stratification occurs at small (e.g. M1S9, M5S5, M6S21, M6S27, M8S3, M8S8, M8S10, M8S12, M8S22, M8S25, M8S30, M8S33-35, M8S57) and big scale (e.g. M6S17), as well as lenticular bedding (e.g. M1S4, M1S16). Bioturbation has only been identified at a few points (samples M1S14, M2S12A, M3S1, M3S7, M3S9, M4S5-8, M6S8-9, M6S31, M8S17). Coarse to fine terrigenous (siliciclastic grains) are common in the upper part of the succession.

The logged columns are illustrated in fig. 6.

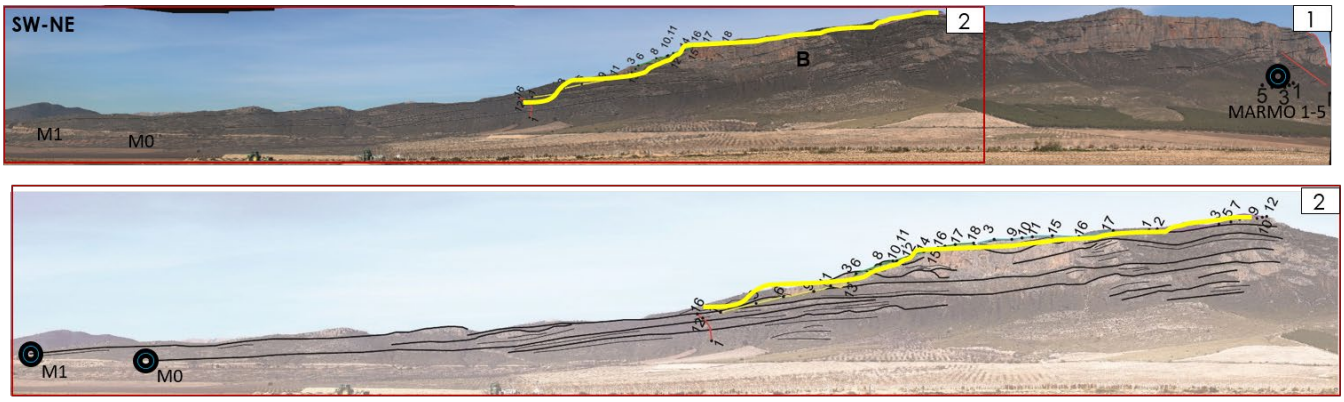

Figure 7. Sierra de Marmolance panoramic view (bedding and sample locations). Stratigraphic distinctions made by Jesús Reolid (Univ. Granada). 1. Panoramic view of the whole Sierra. 2. Zoomed image. In yellow, the stratigraphic section B (main succession of the bioclastic limestones). Marl samples are represented by M1, M0, MARMO 1–5.

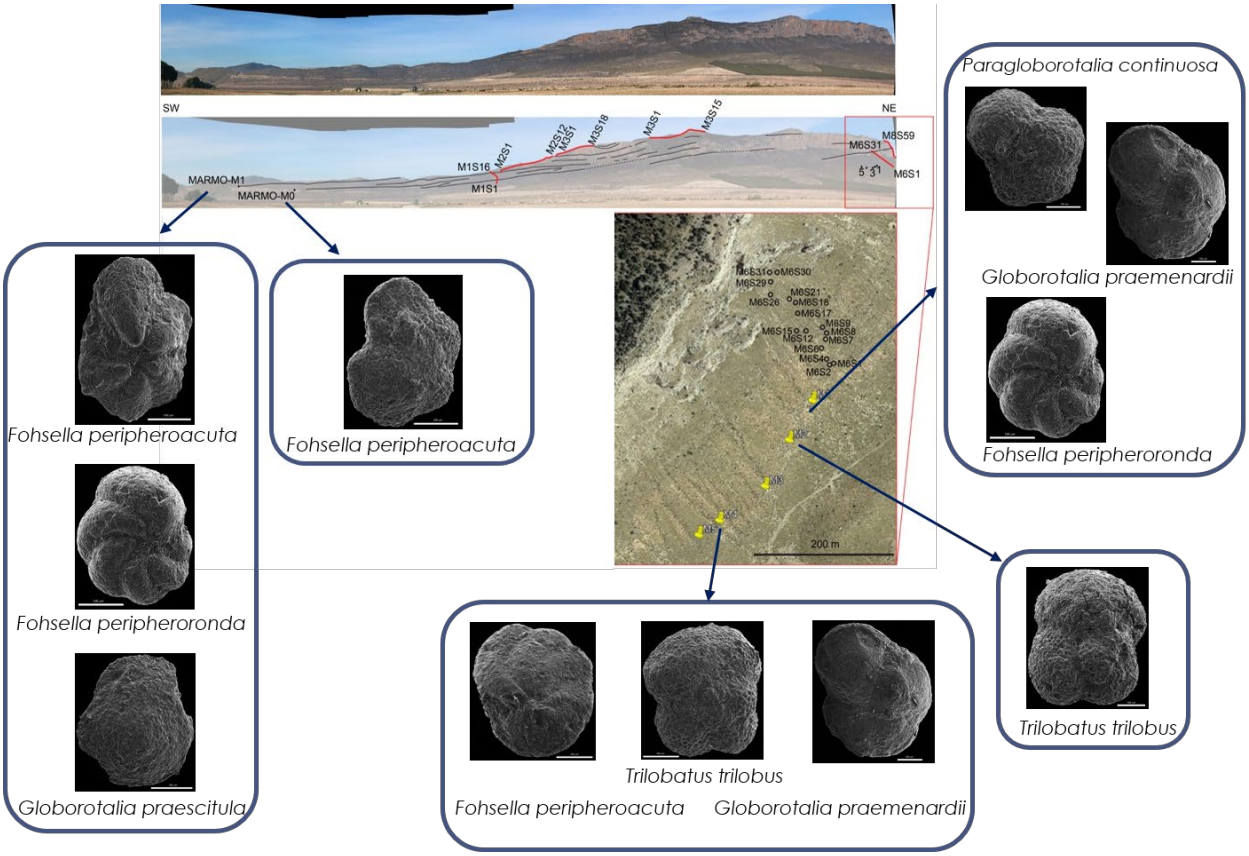

Figure 8. Stratigraphical setting of the analyzed planktonic foraminiferal marly samples in Sierra de Marmolance (M1, M0, MARMO 1–5) and illustrations of the planktonic foraminiferal biostratigraphic markers (SEM photos). Taxonomic identification made by Julio Aguirre (University of Granada).

4.2. Biogenic components

The biogenic components are dominated by coralline red algae, corals and foraminifera (larger and small benthic and encrusting forms), as well as echinoderms and bryozoans. Bivalves and serpulids (*Ditrupa*) are subordinate. Balanids and brachiopods are local ly present.

Planktonic foraminifera occur in the deeper facies at the base of and interfingering with the bioclastic limestones.

Biogenic components are usually well preserved, even if many of them show slight abrasion, fragmentation and/or microbioerosion.

Terrigenous grains, such as quartz, from euhedral (hexagonal shape) to rounded forms with varying amounts of inclusions, occur in the middle-upper part of the succession, being more abundant and of bigger sizes towards the top.

4.2.1. Planktonic foraminifera

Four genera and six species of planktonic foraminifera were identified from Sierra de Marmolance (Fig. 8): *Fohsella peripheroacuta, Fohsella peripheroronda, Globorotalia praescitula, Globorotalia praemenardii, Paragloborotalia continuosa* and *Trilobatus trilobus.* The identification has been performed by Julio Aguirre and Juan Carlos Braga (UGR). They occur at the bottom of the succession and intercalating with the bioclastic limestones (e.g. *Nummulites* facies). See Figs. 4, 5, 7 and 8 for the location of the samples.

The planktonic foraminiferal assemblage identified in Marmolance (Fig. 8) allows to ascribe the marly samples to the biozone M7, between the Langhian-Serravallian boundary and the lowermost Serravallian (Wade et al., 2011).

4.2.2. Larger benthic foraminifera (LBF)

Nineteen larger benthic foraminifera genera and fourteen species were distinguished in the composite sections (Table 1; further details in the Chapter 4.4. on systematic paleontology). The LBF are represented by hyaline perforated, porcelaneous and agglutinated forms, including nummulitids (*Heterostegina, Nummulites, Operculina, Spiroclypeus*), calcarinids (*Neorotalia*), cuvillierinins (*Risananeiza*), amphisteginids (*Amphistegina*), lepidocyclinids (*Eulepidina, Nephrolepidina*), miliolaceans (*Austrotrillina*), alveolinoids (*Borelis*), soritoids (*Archaias, Peneroplis, Sorites*), acervulinids (*Acervulina, Sphaerogypsina*), *Planorbulina*, *Carpenteria*/*Victoriella*. Small benthic foraminifera such as textulariids, miliolids along with agglutinated encrusting foraminifera (*Haddonia*) are also present.

In general, the LBF preservation is good along the succession, showing slight to no abrasion and fragmentation, suggesting that these materials are not reworked.

The lower part of the sedimentary succession (first c. 60 m) is characterized by the presence of *Nummulites* (represented by *Nummulites vascus* and *Nummulites kecskemetii*) with subordinate *Amphistegina sp.* and *Neorotalia viennoti.* In the middle part (next c. 100 m), the dominant components are lepidocyclinids (represented by *Eulepidina* sp. and *Nephrolepidina* sp.) with subordinate *Operculina complanata*, *Neorotalia viennoti* and *Nummulites fichteli*. In the upper part (last c. 120 m), the dominant components are calcarinids and cuvillierinins (represented by *Neorotalia viennoti* and *Risananeiza crassaparies*) with subordinate *Heterostegina assilinoides*, *Spiroclypeus sp*., *Austrotrillina striata*, *A. brunni* and *Borelis inflata*.

The study of the LBF assemblages was focused on the species with biostratigraphic relevance (in fig. 9 is shown the stratigraphic distribution of the relevant species in the Sierra de Marmolance sections).

Table 1. LBF genera and species identified in Sierra de Marmolance.

Superfamily	Family	Genus	Species
Nummulitoidea	*Nummulitidae*	*Nummulites*	*N. fichteli* Michelotti, 1841 *N.* cf. *kecskemetii* Less, 1991 *N.* cf. *vascus* Joly and Leymerie, 1848
		Operculina	*O. complanata* Defrance, 1822
		Heterostegina	*H.* cf. *assilinoides* Blanckenhorn, 1890 emend. Henson, 1937
		Spiroclypeus	*S.* sp.
Asterigerinoidea	*Lepidocyclinidae*	*Eulepidina*	*E. formosoides* Douvillé, 1925 *Eulepidina* ex. interc. *dilatata* (Michelotti, 1861) et *formosoides* Douvillé, 1925
		Nephrolepidina	*Nephrolepidina* ex. interc. *morgani* Lemoine and R. Douvillé, 1904 et *praemarginata* R. Douvillé, 1908 *N. tournoueri* Lemoine et Douvillé, 1904
	Amphisteginidae	*Amphistegina*	*A.* sp.
Rotalioidea	*Rotaliidae*	*Neorotalia*	*N. viennoti* Greig, 1935
Rotaliacea	*Ornatorotaliidae*	*Risananeiza*	*R. crassaparies* Benedetti and Briguglio, 2012
Milioloidea	*Austrotrillinidae*	*Austrotrillina*	*A. brunni* Marie, 1955 *A. striata* Todd and Post, 1954
Alveolinoidea	*Alveolinidae*	*Borelis*	*B. inflata* Adams, 1965
Soritoidea	*Peneroplidae*	*Peneroplis*	*P.* sp.
	Soritidae	*Sorites*	*S.* sp.
		Archaias	*A.* sp.
Acervulinoidea	*Acervulinidae*	*Acervulina*	*A.* sp.
		Sphaerogypsina	*S.* sp.
Planorbulinoidea	*Planorbulinidae*	*Planorbulina*	*P.* sp.
	Victoriellidae	*Carpenteria/Victoriella*	sp.
Coscinophragmatoidea	*Haddoniidae*	*Haddonia*	*H.* sp.

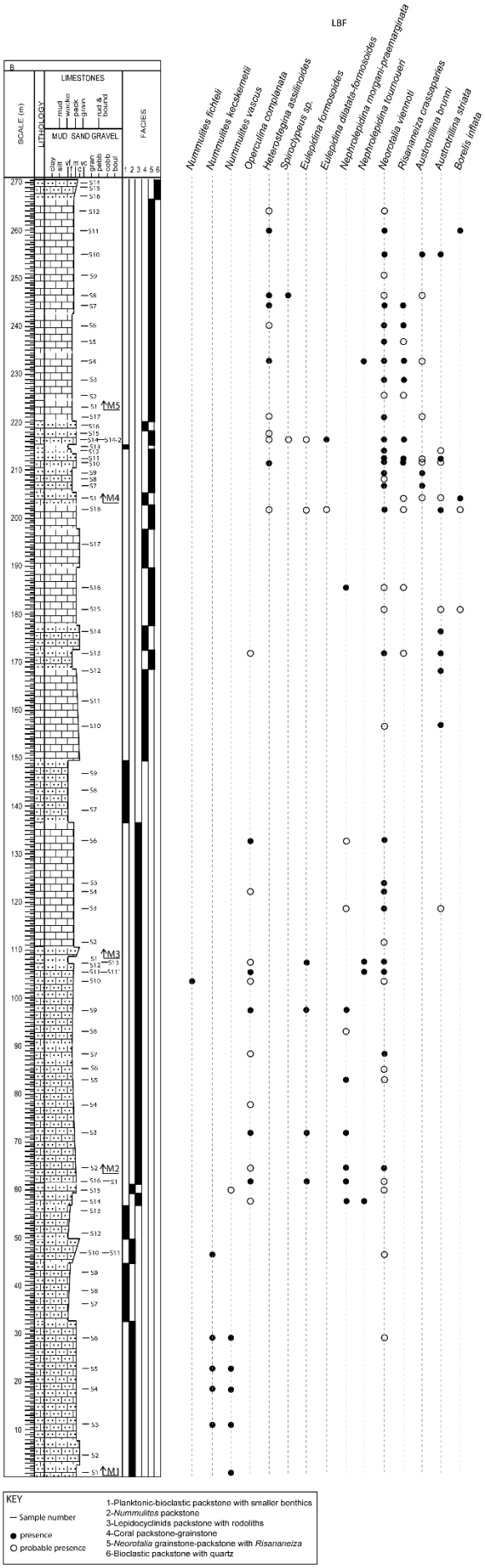

Figure 9. Distribution of the identified larger foraminiferal species along the main stratigraphic succession (B). Below, the complementary correlated sections (A, C, D).

A
SCALE (m)
LITHOLOGY
LIMESTONES
mud
wacke
pack
grain
rud. & bound
MUD SANDGRAVEL
clay
silt
vf
f
m
c
vc
gran
pebb
cobb
boul
FACIES
1 2 3 4 5
C 19
C 18
C 17
C 16
C 15
C 14
C 1-13
10
LBF
Nummulites fichtelli
Nummulites kecskemetii
Nummulites vascus
Operculina complanata
Heterostegina assilinoides
Spiroclypeus sp.
Eulepidina formosoides
Eulepidina dilatata-formosoides
Nephrolepidina morgani-praemarginata
Nephrolepidina tournoueri
Neorotalia viennoti
Risananeiza crassaparies
Austrotrillina brunni
Austrotrillina striata
Borelis inflata

C
SCALE (m)
LITHOLOGY
LIMESTONES
mud
wacke
pack
grain
rud. & bound
MUD SANDGRAVEL
clay
silt
vf
f
m
c
vc
gran
pebb
cobb
boul
FACIES
1 2 3 4 5
S31
S30
S29
S28
S27
S26
S25
S24
S23
S22
S21
S20
S19
S18
S17
S16
S15
S14
S13
S12
S11
S10
S9
S8
S7
S6
S5
S4
S3
S2
S1
90
80
70
60
50
40
30
20
10
LBF
Nummulites fichtelli
Nummulites kecskemetii
Nummulites vascus
Operculina complanata
Heterostegina assilinoides
Spiroclypeus sp.
Eulepidina formosoides
Eulepidina dilatata-formosoides
Nephrolepidina morgani-praemarginata
Nephrolepidina tournoueri
Neorotalia viennoti
Risananeiza crassaparies
Austrotrillina brunni
Austrotrillina striata
Borelis inflata

D
SCALE (m)
LITHOLOGY
LIMESTONES
mud
wacke
pack
grain
rud. & bound
MUD SANDGRAVEL
clay
silt
vf
f
m
c
vc
gran
pebb
cobb
boul
FACIES
1 2 3 4 5
S58
S57
S56
S55
S54
S53
S52
S51
S50
S49
S48
S47
S46
S45
S44
S43
S42
S41
S40
S39
S38
S37
S36
S35
S34
S33
S32
S31
S30
S29
160
150
140
130
120
110
100
90
80
LBF
Nummulites fichtelli
Nummulites kecskemetii
Nummulites vascus
Operculina complanata
Heterostegina assilinoides
Spiroclypeus sp.
Eulepidina formosoides
Eulepidina dilatata-formosoides
Nephrolepidina morgani-praemarginata
Nephrolepidina tournoueri
Neorotalia viennoti
Risananeiza crassaparies
Austrotrillina brunni
Austrotrillina striata
Borelis inflata

4.2.3. Coralline red algae

Coralline red algae, represented by geniculate and non-geniculate forms. Non-geniculate red algae occur as algal fragments (algal debris), branches, rhodoliths and very thin crusts encrusting corals. Rodoliths show encrusting, warty to lumpy growth forms and are sub-spheroidal to ellipsoidal in shape, reaching up to 8 mm in diameter. Encrusting acervulinid foraminifera contribute in the rhodolith formation. Eight genera of red algae have been identified from Sierra de Marmolance, mostly coralline red algae (Table 2).

Table 2. Red algae identified in Sierra de Marmolance. Note: all are coralline red algae except the genus *Polystrata alba.*

Order	Family	Subfamily	Genus
Corallinales	Corallinaceae	Neogoniolithoideae	*Neogoniolithon* Setchell and Mason *Spongites* Kützing
	Mastophoraceae	Mastophoroideae	*Lithoporella* (Foslie) Foslie
-	-	-	*Subterraniphyllum thomasii* Elliot
-	Lithophyllaceae		*Karpathia* Maslov
Hapalidiales	-	-	*Lithothamnion* Heydrich
Sporolithales	-	-	*Sporolithon* Heydrich
Peyssonneliales	Peyssonneliaceae	-	*Polystrata alba* (Pfender) Denizot

4.3. Microfacies

Six microfacies were distinguished based on textural and biogenic features (dominating biotic components). Mixed carbonate-siliciclastic and carbonate textures are present and they include mostly packstones and subordinate grainstones, with abundant LBF, coralline algae and corals (figs. 10–11, Table 3).

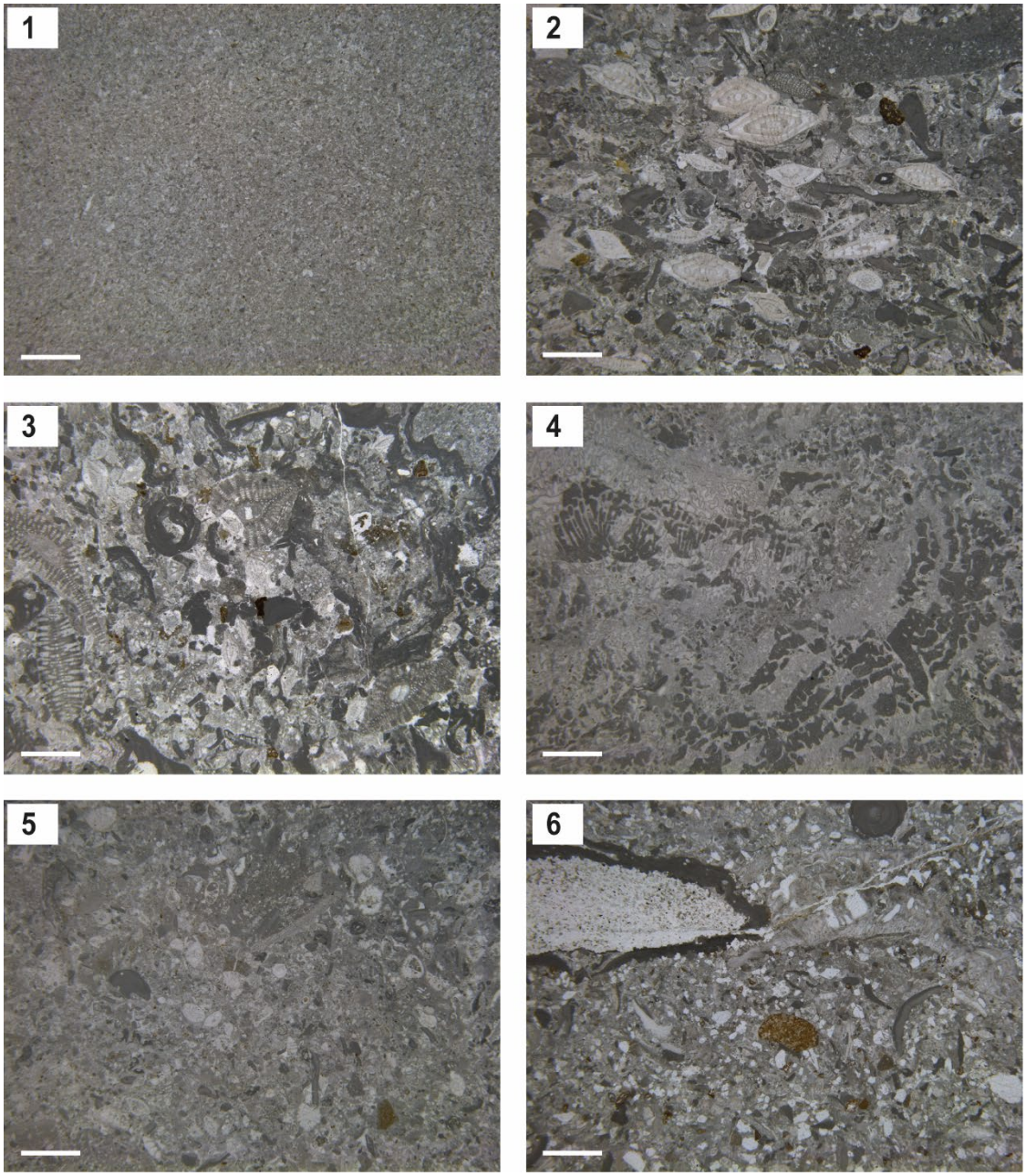

Figure 10. 1–6. Microfacies distinguished in Sierra de Marmolance. 1. Planktonic-bioclastic packstone with smaller benthics. Sample M3S9; 2. *Nummulites* packstone. Sample M1S3; 3. Lepidocyclinid packstone with rhodoliths. Sample M2S13; 4. Coral packstone-grainstone. Sample M3S11; 5. *Neorotalia* packstone-grainstone with *Risananeiza*. Sample M4S11; 6. Bioclastic packstone with quartz. Sample M5S14. Scale bar represents 2 mm.

Table 3. Microfacies distinguished in Sierra de Marmolance showing the dominant components, subordinant components, their distinctive characters and the interpreted depositional environment for each one. Facies are listed from distal to proximal environment.

Microfacies name	**Dominant components**	**Subordinant components**	**Distinctive characters**	**Depositional environment**
1. Planktonic-bioclastic packstone with smaller benthics	Planktonic foraminifera, smaller benthic foramninifera, glauconite	Coralline red algae, echinoderms and LBF debris (*Neorotalia, Amphistegina, Nummulites, Carpenteria/Victoriella, Acervulina, Sphaerogypsina*)	Common to abundant glauconite Highly abraded and fragmented coralline algae, echinoderms and LBF	Distal middle ramp Low energy
2. Nummulites packstone	*N. vascus, N. kecskemetii,* coralline red algae debris	Corals, echinoderms, branching bryozoans, *Amphistegina*, *Carpenteria/Victoriella, Neorotalia viennoti,* smaller benthic foraminifera, planktonic foraminifera, glauconite. Very rare *Acervulina*, *Peneroplis, Archaias*, *Planobulina, Ditrupa,* bivalve fragments.	*Subterranyphyllum* Locally common planktonics and glauconite *Archaias*	Distal-proximal middle ramp Low energy
3. Lepidocyclinids packstone with rodoliths	*Eulepidina* (*E. formosoides*), *Nephrolepidina* (*N. morgani-praemarginata, N. tournoueri*), rhodoliths, *Operculina complanata, Amphistegina*	*Neorotalia viennoti*, *Nummulites fichteli*, echinoderms, bryozoans, smaller benthic foraminifera, quartz grains. Very rare *Carpenteria/Victoriella*, *Ditrupa,* bivalves, glauconite, planktonic foraminifera, miliolids, *Planorbulina, Sphaerogypsina*	Common rhodoliths Microbioerosion in algae *N. fichtelli*	Proximal middle ramp Low energy
4. Corals packstone-grainstone	Colonial corals, thin encrusting coralline algae	Porcelaneous foraminifera (miliolids), encrusting foraminifera (mostly *Carpenteria), Amphistegina, Austrotrillina striata, Neorotalia viennoti*, echinoderms, bryozoans. Very rare *Nephrolepidina, Risananeiza, Sorites, Peneroplis, Planorbulina, Sphaerogypsina,* smaller benthic foraminifera, *Ditrupa,* planktonics.	Common porcelaneous foraminifera Thin coralline algae encrusting corals Micritic matrix with sparite in corals	Proximal middle ramp- distal inner ramp Reef Low energy
5. Neorotalia packstone-grainstone with *Risananeiza*	*Neorotalia viennoti*, echinoids, coralline red algae debris, *Risananeiza crassaparies*	Corals, bryozoans, miliolids (*Austrotrillina brunni, Austrotrillina striata*), *Heterostegina assilinoides*, *Eulepidina dilatata-formosoides, Nephrolepidina tournoueri*, *Amphistegina*, bivalves, siliciclastics. Very rare *Spiroclypeus, Carpenteria/Victoriella*, smaller benthic foraminifera, *Borelis inflata*, *Peneroplis, Sorites*, *Sphaerogypsina, Planorbulina, Operculina complanata, Ditrupa*, green algae (*Halimeda*), brachiopods, planktonic foraminifera.	Small quartz grains *Austrotrillina striata* *Borelis inflata* *Heterostegina assilinoides* *Spiroclypeus* terebratellacean brachiopods *Halimeda*	Distal inner ramp Reef area Low-moderate energy
6. Bioclastic packstone with quartz	Coralline red algae debris, *Acervulina*, ostreids, balanids, *Ditrupa*, quartz grains	Echinoderms, bryozoans, *Amphistegina*, *Haddonia*, smaller benthic foraminifera and planktonic foraminifera. Very rare miliolids	Balanids ostreids Big and abundant quartz grains *Haddonia* Traces	Distal inner ramp Submarine bars Moderate-high energy

4.3.1. Planktonic-bioclastic packstone with smaller benthics

This subfacies is a packstone with planktonic foraminifera (globorotalids, globigerinids, orbulinids) and smaller benthic foraminifera (rotaliids, textulariids) associated with coralline algae, echinoderms and LBF debris. Most of the bioclasts could not be determined/cuantified because of their high fragmentation. Among the LBF were identified *Neorotalia*, *Amphistegina, Nummulites*, *Acervulina, Carpenteria/Victoriella,* and *Sphaerogypsina*. Coralline algae (non-geniculate and geniculate) and echinoderms occur as very little fragments. Glauconite grains are present.

Grain size is fine to very fine. Beavington-Penney's index ranges from 2 to 3. Abrasion (algae, echinoderms) is high.

This facies occurs mostly in the lower part of the stratigraphic succession, intercalated with *Nummulites* facies, and also in the middle part, between the lepidocyclinid and coral facies. Facies thickness ranges from 5 to 15 m.

This facies is interpreted as the deepest facies in a carbonate ramp (distal middle-ramp) because of the presence of planktonics and smaller benthic foraminifera together with abundant glauconite grains (Fig. 11). The high fragmentation and abrasion of LBF, coralline algae and echinoderms present in this facies suggests that they are not authoctonous, but reworked from the shallower settings.

4.3.2. *Nummulites* packstone

This packstone facies is characterized by *Nummulites* (*N. vascus* and *N. Kecskemetii*), which are associated with abundant to common coralline algae (mostly *Subterraniphyllum*). Subordinate components are corals, echinoderms (fragments), branching bryozoans, *Amphistegina* sp*., Carpenteria/Victoriella, Neorotalia viennoti*, small benthics (represented by rotaliids, textulariids and miliolids). Very rare encrusting foraminifera (*Acervulina*), *Peneroplis, Archaias*, *Planobulina*, *Ditrupa* and bivalve fragments also occur. Planktonic foraminifera and glauconite grains are locally common (samples M1S10, M1S15b).

Coralline algae occur mostly as debris (little fragments of non-geniculate branches, intergenicula of geniculates). Rhodoliths, sub-spheroidal to ellipsoidal in shape (around up to 3 mm diameter), are rare. The identified taxa are *Lithoporella, Lithothamnion, Spongites, Sporolithon* and *Subterranyphyllum*.

Grain size is medium. Beavington-Penney's index ranges from 1 to 2. Abrasion occurring on algae and echinoderms is low. In coralline algae microbioerosion is very rare.

This facies occurs in the lower part of the succession (first 60 m). Intercalates with planktonic foraminiferal facies and underlies the lepidocyclinid facies. This facies mostly occurs as massive beds, but also as well-stratified limestones, in packages from 2.5 to 25 m in thickness.

The presence of planktonic foraminifera in some levels together with glauconite grains (samples M1S10 and M1S15) and branching bryozoans can suggest that this facies represents a distal-proximal middle ramp (Fig. 11).

4.3.3. Lepidocyclinid packstone with rhodoliths

This facies is a packstone with *Eulepidina* (*E. formosoides, E. dilatata*) and *Nephrolepidina* (*N. morgani, N. tournoueri*) associated with abundant-common coralline algae (mostly rodoliths), *Operculina complanata* and *Amphistegina* sp. Subordinate components are *Neorotalia viennoti,* echinoderms, bryozoans, smaller benthic foraminifera (textulariids, rotaliids) and quartz grains. Very rare *Nummulites fichteli*, *Carpenteria/Victoriella*, *Ditrupa,* bivalves, glauconite, planktonic foraminifera (locally common in M1S14, M1S16a, M2S1, M2S2'), miliolids, *Planorbulina, Sphaerogypsina* were identified.

Coralline algae occur mostly as rhodoliths, sub-spheroidal to ellipsoidal in shape (up to 8 mm in diameter); rare encrusting, branching and warty-lumpy forms along with geniculates are

present. The identified red algae taxa are *Karpathia, Lithoporella, Lithothamnion, Polystrata, Spongites* and *Sporolithon*.

Grain size is predominantly coarse. Beavington-Penney's index (LBF) ranges from 1 to 2. Abrasion (algae, echinoderms) is low. Microbioerosion in algae is common. Bioturbation occurs in massive and stratified limestones. Locally (M2S4-S12), the biogenic components are highly fragmented and abraded, and coralline algae are found mostly as small fragments of non-geniculate plants.

This facies occurs in the lower-middle part of the succession (60–135 m), overlying the *Nummulites* facies and underlying the coral facies. Facies thickness ranges between 2.5 and 15 m.

Because of the common occurrence of rhodoliths together with lepidocyclinids, this facies deposited in the proximal middle-ramp (Fig. 11).

4.3.4. Coral packstone-grainstone

This facies is a packstone-grainstone with corals colonies associated with coralline algae. Coralline algae mostly occur as thin crusts encrusting corals; rare as non-geniculate debris. *Spongites* and *Lithoporella* were identified in the algal assemblage.

Subordinate components are porcelaneous foraminifera (mostly miliolids), encrusting foraminifera (mostly *Carpenteria*), *Amphistegina, Austrotrillina striata, Neorotalia viennoti,* echinoderms and bryozoans fragments. Very rare *Nephrolepidina*, *Risananeiza, Sorites, Peneroplis, Planorbulina, Sphaerogypsina*, *Ditrupa*, planktonics and small benthic foraminifera (rotaliids, textulariids). Peloids are also present. The encrusting foraminifera occur together with coralline algae encrusting corals.

Grain size is predominantly coarse. Beavington-Penney's index ranges from 1 to 2. Abrasion (algae, echinoderms) is low. No microbioerosion was observed.

This facies occurs in the middle part of the succession (150–200 m), between the lepidocyclinid and *Neorotalia* with *Risananeiza* facies, intercalating with the latter. This facies occurs as massive and stratified beds and the facies thickness oscilates from 3 to 20 m.

Porcelaneous foraminifera like *Sorites* and *Peneroplis*, as well as miliolids, are usually found on shallow-water reef sites (Hallock, 1999). The presence of porcelaneous foraminifera associated to the corals would suggest a proximal middle- to distal inner ramp setting (Fig. 11).

4.3.5. *Neorotalia* packstone-grainstone with *Risananeiza*

This packstone-grainstone is characterized by *Neorotalia* (represented by *N. viennoti*) associated with echinoderms (echinoids), coralline algae and *Risananeiza* (represented by *R. crassaparies*). Subordinate components are corals, bryozoans fragments, miliolids (*Austrotrillina brunni, Austrotrillina striata*), *Heterostegina assilinoides*, lepidocyclinids (*Nephrolepidina* tournouer, *Eulepidina dilatata-formosoides*), *Amphistegina*, bivalves and siliciclastics. Very rare *Carpenteria/Victoriella*, smaller benthic foraminifera (textulariids, undetermined), *Borelis inflata*, *Peneroplis, Sorites*, *Sphaerogypsina, Planorbulina, Operculina complanata, Spiroclypeus, Ditrupa*, green algae (*Halimeda*), terebratellacean brachiopods and planktonic foraminifera also occur. Peloids are present.

Red algae occur mostly as debris (mostly small fragments, branches); and are rare as rhodoliths, subspheroidal-ellipsoidal in shape (up to 8 mm diameter) and encrusting other bioclasts. The identified taxa are *Lithoporella, Lithotamnion, Polystrata* and *Sporolithon*.

Siliciclastics occur as very little grains, sub-angular, around 0.25 mm in diameter.

Grain size is coarse to fine. Beavington-Penney's index ranges from 1 to 2. Abrasion (algae, echinoderms) is generally low, but locally high (M4S7-S9).

This facies occurs in the upper part of the succession (200–265 m), overlying and intercalating with the coral facies and underlying the bioclastic packstone with quartz facies. Facies thickness ranges from 4 to 25 m.

In this facies the occurrence of rotaliiforms (*Neorotalia, Risananeiza*), echinoids and nummulitids (*Heterostegina, Spiroclypeus*) together with larger porcelaneous foraminifera (*Borelis, Austrotrillinia* and other miliolids) suggests shallow-water conditions of the distal inner-ramp. The robust and ornamented shells that characterize *Neorotalia* and *Risananeiza* has been interpreted as attachment mechanisms to thrive in high energy environments (Hallock, 1999; Beavington-Penney and Racey, 2004). The occurrence of *Halimeda* together with nummulitid foraminifera and rhodoliths has been described as indicative of deposits in the upper part of the euphotic zone (Bourrouilh-Le Jan and Hottinger, 1988; Fig. 11).

4.3.6. Bioclastic packstone with quartz

This facies is a packstone with bioclasts and abundant quartz. Common bioclasts are coralline algae, encrusting foraminifera (*Acervulina*), bivalves (ostreids), balanids and *Ditrupa*. Subordinate components are echinoderms, bryozoans, *Amphistegina*, agglutinated foraminifera (textulariids, *Haddonia*), smaller benthic foraminifera and planktonic foraminifera. Very rare miliolids are also present.

Coralline algae occur mostly as debris (little fragments and branches) and as rhodoliths, spheroidal to ellipsoidal in shape (around 1–6 mm in diameter), represented by the genera *Lithothamnion* and *Neogoniolithon*. Quartz grains are bad sorted, with sub-angular shape and sizes mostly ranging from 0.25 to 1 mm in diameter, reaching up to 3–4 mm (sample M5S14 and M5S15).

Grain size is coarse. Beavington-Penney's index ranges from 1 to 2. Abrasion (algae, echinoderms) is moderate. Microbioerosion in algae is present. Locally (M5S16), the biogenic components are highly fragmented and abraded, and coralline algae occur as very little fragments of non-geniculate plants.

This facies occurs in the uppermost part of the succession (last 5 m; from 265 m upwards), overlying the *Neorotalia* with *Risananeiza* facies. Facies thickness is about 5 m.

This facies is located in a distal inner ramp and represents the shallowest facies of the studied succession. Because of the abundant siliciclastics suggesting a higher input of terrigenous material and the presence of ostreids and balanids higher energy environments are assessed (Fig. 11).

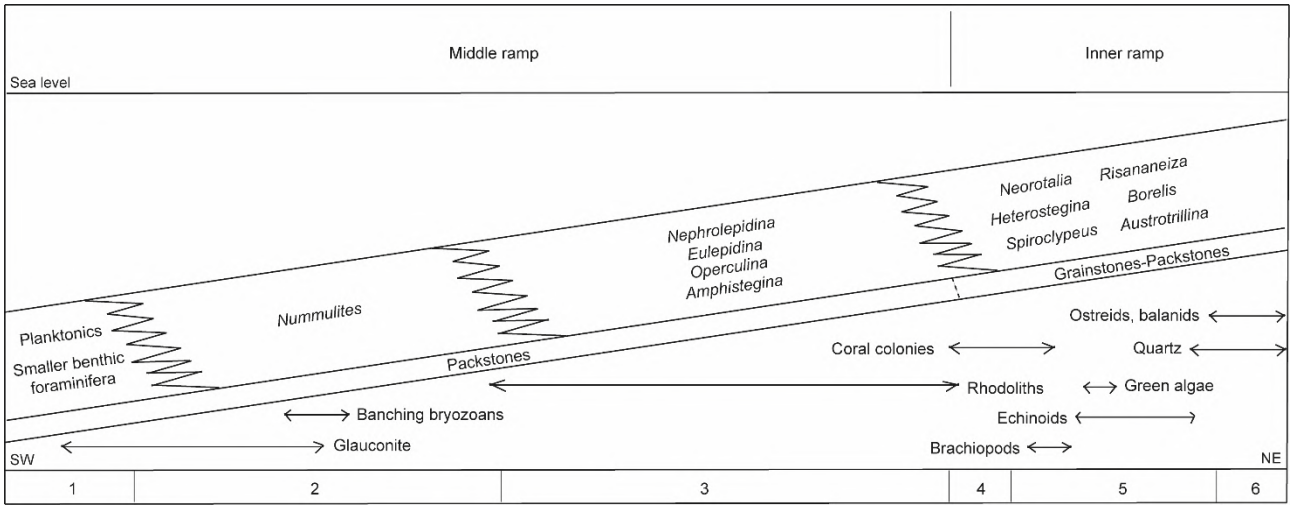

Figure 11. Facies distribution in the Marmolance carbonate ramp showing the characteristic foraminifera of each facies (1–6). The arrows point the subordinate biotic facies components. Not to scale. Abbreviations: 1, Planktonic-bioclastic packstone with smaller benthics; 2, *Nummulites* packstone; 3, Lepidocyclinid packstone with rhodoliths; 4, Coral packstone-grainstone; 5, *Neorotalia* packstone-grainstone with *Risananeiza*; 6, Bioclastic packstone with quartz.

According to the biogenic components, their stratigraphical distribution and the microfacies analysis (e.g. Hallock, 1999; Beavington-Penney and Racey, 2004; Bassi and Nebelsick, 2010; Braga and Bassi, 2011), the distinguished microfacies in the Marmolance sedimentary succession represent middle-inner carbonate ramp settings (Fig. 11, Table 3).

The deepest microfacies are represented by packstones with planktonic foraminifera and smaller benthics (1), overlain by nummulitids and lepidocyclinids packstones associated with bryozoans and rhodoliths (2 and 3, respectively). Shallower facies are represented by grainstone-packstone with mixed LBF fauna (hyaline perforated and porcelaneous forms; facies 5) associated with coral colonies (4) and green algae. The shallowest microfacies are represented by packstones with bioclastics (ostreids, balanids) and quartz grains.

4.4. Systematic palaeontology

Family NUMMULITIDAE de Blainville, 1827

Remarks. In the family Nummulitidae the presence or absence of trabeculae and the type of stolon system are important characters at the generic level (Hottinger 1977, pp. 9–10). However, in randomly sectioned specimens these characters are visible only on well-preserved specimens and on sub-equatorial and tangential sub-equatorial sections. This structural analysis is necessary in order to recognize the diagnostic traits of each genus. To assess the occurrence of trabeculae and the type of stolon system sections tangential to the lateral chamber walls and to the nearly equatorial plane respectively are necessary. A tangential section cutting the lateral chamber wall shows the grooves in the porous wall created by the trabecular canals. Nearly equatorial sections through the successive septa show the stolon system (Hottinger 1977, fig. 7).

The main characteristic trait of the identified five species belonging to this group is the completely involute test, which leads to thick lenticular tests in small individuals (i.e. *Nummulites*). In large specimens, the chambers of the last whorl become flat and thin (i.e. *Spiroclypeus*, *Operculina*, *Heterostegina*). Although one species belonging to this group (*Heterostegina*) can be differentiated by the division of chambers into chamberlets, morphological distinction between the others (*Nummulites*, *Spiroclypeus* and *Operculina*) needs detailed assessements of the preserved characters shown in thin section and has led to taxonomic uncertainties. See Table 4, after Blondeau (1972) and Hottinger (1977), for the distinction between the nummulitid genera based on their internal structures.

Table 4. Classification of the Nummulitidae (Blondeau 1972; Hottinger 1977).

GENERA	SPIRE	SEPTA	CHAMBERS	LATERAL CHAMBERS	TEST
Nummulites	slowly opening	short, arcuate	simple	absent	involute
Assilina	slow and regularly opening	straight or slightly inclined	simple	absent	evolute
Operculina	rapidly opening	long, thin, arcuate	simple	absent	evolute
Operculinella	rapidiy opening	long, thin, tangential to spire at base	simple	absent	involute
Ranikothalia	slow and regularly opening	short, arcuate	simple	absent	semi-involute
Heterostegina	rapidly opening	secondary septa present	divided into chamberlets	absent	evolute
Grzybowskia	rapidly opening	secondary septa present, appear as ridges on test surface	divided into chamberlets	absent	involute
Spiroclypeus	rapidly opening	secondary septa present	divided into chamberlets	present	evolute
Cycloclypeus	rapidly opening becoming annular	secondary septa present	divided into chamberlets	absent	evolute

Remarks. The specimens showing trabeculae in sub-equatorial sections were assigned to *Nummulites* (see fig. 13; pl. 3, D). The identification of *Nummulites* species is usually based on the surface characteristics and the internal morphology of the equatorial section (e.g. Drooger et al., 1971, Less 1999; Özcan et al., 2009a; Less et al., 2018; Akbar-Baskalayeh et al., 2020). According to Bassi et al. (2007) and Ferràndez-Cañadell and Bover-Arnal (2017), in the absence of isolated material and equatorial sections, the species ascriptions were assessed by means of the size (test diameter, D; mean proloculus diameter, P; chamber length in the third whorl, L; see fig. 14) and shell outline in axial section of the studied specimens (all megalospheric forms). According to the shell shape, three groups were distinguished: *N. vascus* (inflated lenticular), *N. fichteli* (flat) and *N. kecskemetii* (flattened lenticular). The synonymy lists are limited to those works including comparable axial sections.

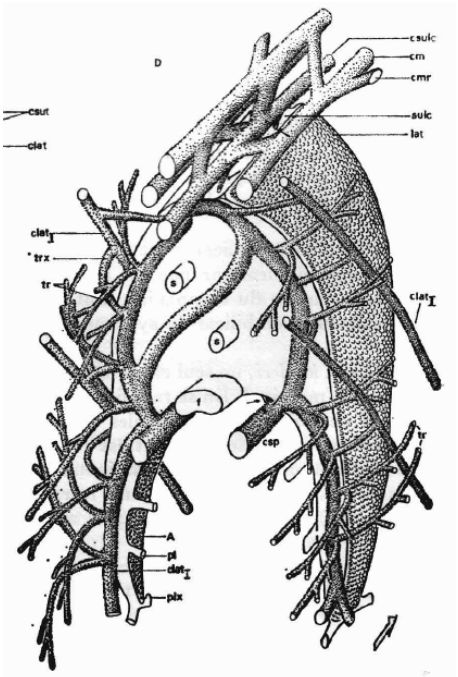

Figure 13. Canal system in operculiniform foraminifera *Nummulites planulatus* (lower Eocene). Scheme (not to scale) showing the internal geometry of the protoplasmic chamber lumen corresponding to a single whorl. Black arrows: communications between the cavities of the chamber and the canal system. White arrows: growth direction. The plane containing the arrow is parallel to the equatorial plane of the test. Alphabetic legend: A, lumen of alar prolongations; clat, lateral canal; cm, marginal canals; cmr, radial or oblique marginal canals grouped at the periphery of the shell or inside the spiral canals of the successive whorl; csp, spiral canal; c sulc, sulcus canal; f, foramen; pl, lateral passages from lumen of alar prolongations to canal system of the previous whorl in *Nummulites*; plx, passages created by partial resorption of the septum at the end of the lumen of alar prolongations; s, stolon; sulc, sulcus; NOTE the tr, sutural canals at the origin of the transversal trabeculae in *Nummulites*; trx, trabecular canals transformed into passage within the canal system of a whorl with that of the successive whorl. Taken from Hottinger, 1977.

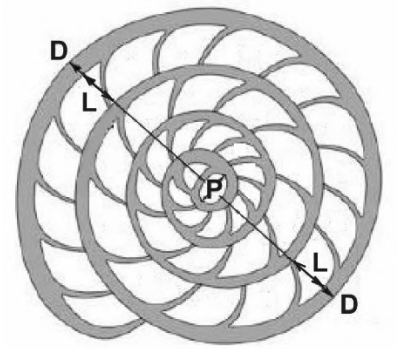

Figure 14. Schematic drawing of *Nummulites* showing the shell parameters used for measure the specimens from Sierra de Marmolance. Abbreviations: D, test diameter; P, proloculus diameter; L, chamber length in the third whorl. Measurement system modified from Özcan et al., 2009a (fig. 10, p.746).

Nummulites fichteli Michelotti, 1841

Plate 1. Figures A–H

1995 *Nummulites fichteli* Michelotti; Racey, pl. 4, figs. 1–7.
2010 *Nummulites fichteli* Michelotti; Benedetti 2010 Pl. 3, fig. 6; Text-fig. 8, figs. 15–16.
2010 *Nummulites fichteli* Michelotti; Özcan et al., pl. 4, figs. 2–16.
2013 *Nummulites fichteli* Michelotti; Amirshahkarami, pl. 1, figs. 1–3.
2016 *Nummulites fichteli* Michelotti; Serra-Kiel et al., fig. 50, 10–19.
2018 *Nummulites fichteli* Michelotti; Habibi, pl. 1, figs. 1, 3; pl. 2, figs. 2, 5.
2020 *Nummulites fichteli* Michelotti; Sirel et al., fig. 13, A–C.

Description. Specimens are flat, biconvex in shape. From fourteen axial sections of megalospheric specimens were measured the test diameter (D=2.2–4.8 mm; mean 3.4 mm), the proloculus size (P= 112–418 μm; mean 234 μm) and chamber length in the third whorl (L= 103–191 μm; mean 143 μm).

Remarks. *N. fichteli* and *N. bormidiensis* belong to the same lineage (*N. fabianii*). Although similar in shape they can be differentiated by the ornamentation and the size of the protoconch, being bigger that of *N. bormidiensis* (see Less et al., 2006: *N. fichteli* 200–320 microns, *N. bormidiensis* 320–450 microns; Özcan et al., 2009a, tab. 4). Because the studied specimens only occur in thin sections, we could only assess the proloculus diameter for the species identification.

Comparing with the literature (i.e. Schaub 1981; Kleiber 1991; Racey 1995; Less et al., 2006; Benedetti 2010; Özcan et al., 2010; Amirshahkarami, 2013; Serra-Kiel et al., 2016; Habibi, 2018; Less et al., 2018; Sirel et al., 2020; see Table 5) the studied specimens were identified as *N fichteli* (P mean between 200–300μm).

Stratigraphical distribution. In Sierra de Marmolance, this species occurs in the lower-middle part of the succession (section A, samples C14, 16, 18; section B, sample M2S10; section D, samples M8S40, 50, 52), in the Lepidocyclinid facies, associated with *Operculina complanata, Neorotalia viennoti, Eulepidina formosoides, Nephrolepidina* ex.interc. *morgani* et *praemarginata and Nephrolepidina tournoueri* (see fig. 7; table 3.3).

In the literature, its biostratigraphic range is from Rupelian to early Chattian (SBZ 21–22) (e.g. Schaub 1981; Racey 1994, 1995; Cahuzac and Poignant 1997). See Table 5 for the stratigraphical and palaeogeographical distributions with their references.

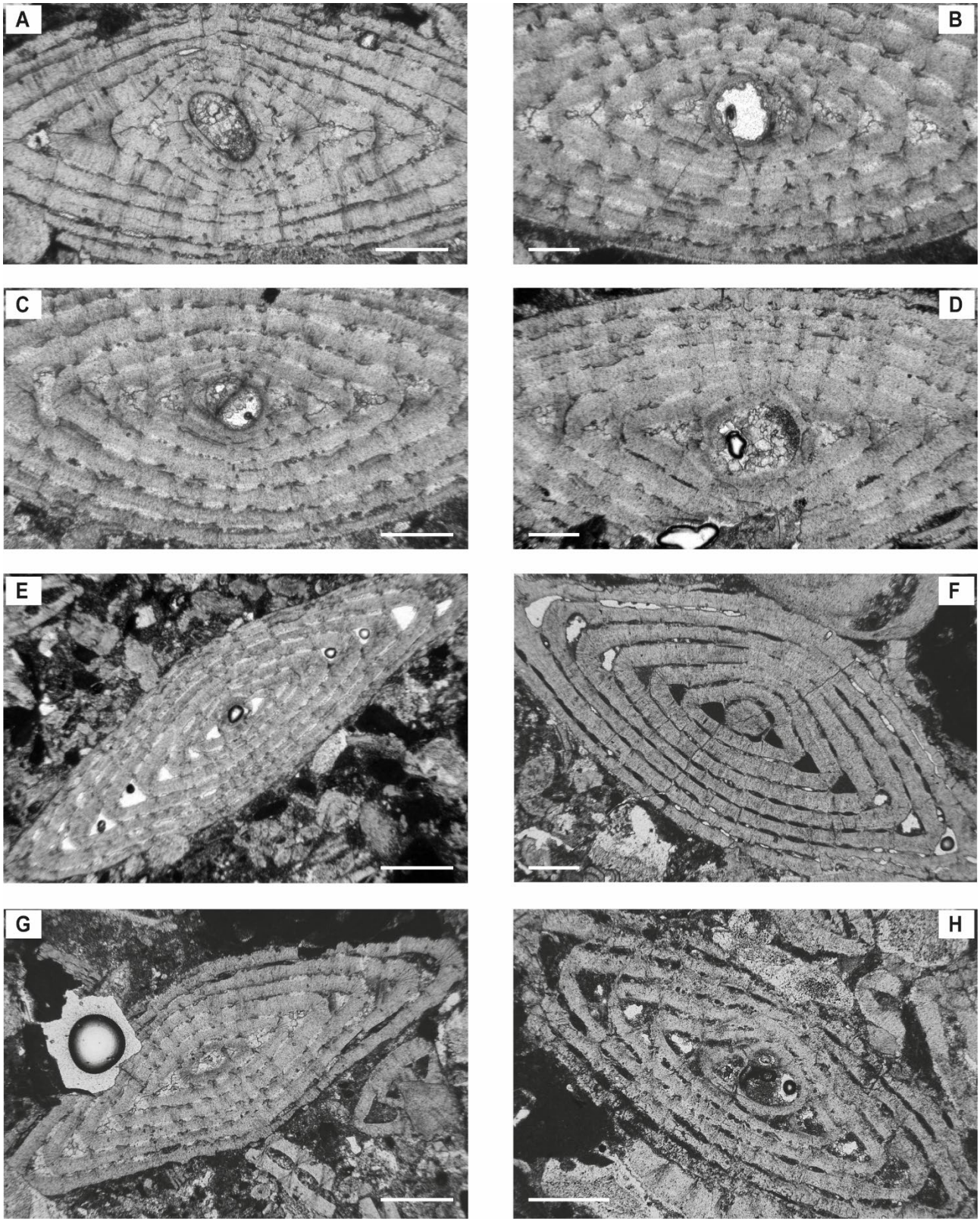

Plate 1. A–H. *Nummulites fichteli* from Sierra de Marmolance, Spain. A: Sample M8S52; B–D; F, G: Sample C14; E: Sample M2S10; H: Sample C18. Scale bar represents 400 µm.

Table 5. Biometric parameters and stratigraphical distribution of *Nummulites fichteli* from Marmolance (this study) with other localities for comparison (megalospheric forms). Abbreviations: Prol., proloculus diameter (mean); L, chamber length in the third whorl (mean); D, test diameter (mean); SBZ, Shallow Benthic Zonations. Serrav., Serravallian; Illustr., illustrations; Ax/Eq, axial/equatorial sections measured from illustrations.

Referred to as	References	Prol. (□m)	L (□m)	D (mm)	Age	Locality	Illustr.
N. fichteli	Schaub 1981	250–300	-	3.4–4.8	Rupelian (SBZ21–22)	-	pl. 50, figs. 5–18
N. fichteli	Kleiber 1991	250–300	-	3.4–4.8	-	-	-
N. fichteli	Racey 1995	250–350	-	3.83–4.25 (4.04)	early Oligocene (SBZ21–22)	Wadi Rusayl, Oman	pl. 4, figs. 1–7
N. fichteli (= N. intermedius)	Cahuzac and Poignant 1997	-	-	-	Rupelian–early Chattian (SBZ21–22B)	Aquitaine basin, SW France	pl. 1, figs. 3, 4
N. fichteli	Less *et al.* 2006	200–320	-	-	late Priabonian–early Rupelian (SBZ 20–21)	W Tethys (SW France–Armenia)	-
N. fichteli	Özcan *et al.* 2010	190–410 (261)	192–329 (249)	-	late Rupelian (SBZ22A)	Kelereşdere, E Turkey	pl. 4, figs. 2–16
N. fichteli	Benedetti 2010	Ax:357	Ax:178	Ax:4.3	early Rupelian (SBZ21)	N Sicily	pl. 3, fig. 6; Text-fig. 8, figs. 15–16
N. fichteli	Amirshahkarami 2013	Ax: 409	Ax: 250	Ax: 4.3–5.2	Rupelian	Zagros basin (Iran)	pl. 1, figs. 1–3
N. fichteli	Serra-Kiel *et al.* 2016	320–330; Ax:330	Ax:125	4–4.6; Ax:3.6	Rupelian (SBZ 21–22)	Dhofar and Socotra island	fig. 50, 10–19
N. ex. interc. *fichteli–bormidiensis*	Less *et al.* 2018	190–440 (292)	235–362 (279)	-	-	Waior, W India	-
N. fichteli	Habibi 2018	250–450	-	3–4.75	Rupelian	SW Iran	pl. 1, figs. 1, 3; Pl. 2, figs. 2, 5
N. fichteli	Sirel *et al.* 2020	Ax: 143; Eq: 214	Ax: 143; Eq: 178	3.1–3.6	early Oligocene	NW Turkey	fig. 13, A–C
N. fichteli	**This study**	112–418 (234)	103–191 (143)	2.2–4.8 (3.4)	Serrav.	SE Spain	Pl. 1

Nummulites cf. *kecskemetii* Less, 1991

Plate 2. Figures A–H

2007 *Nummulites* cf. *bouillei* de la Harpe; Bassi et al., pl. 4, fig. 13.
2017 *Nummulites* aff. *kecskemetii* Less; Ferràndez-Cañadell and Bover-Arnal, fig. 10, J–R.

Description. Specimens with a flattened test with a mean diameter of 2.6 mm. Small protoconch (71–97 microns in diameter; mean 90 μm) and chamber length in the third whorl ranging from 198 to 376 microns (mean 272 μm).

Remarks. Nummulites kecskemetii is a small radiate form determined by its very small proloculus, curved septa and open spire (Özcan et al., 2009a, 2010). *N. kecskemetii* was previously included into *N. bouillei* de la Harpe 1879, which spans from the Priabonian to the late Oligocene (Cahuzac and Poignant, 1997) in Europe and the Middle East (e.g. Grimsdale, 1952). Less (1991) defined this late Oligocene new species because of its characteristic small proloculus. In equatorial section *N. kecskemetii* can be confused with *Operculina* sp. because both have an operculiniform growth, with a higher last whorl than the preceding whorls (see Less et al., 2018 for more detailed distinction). Since no equatorial section or isolated specimens have been found in Marmolance, the species identification was based on the proloculus size and shell outline from axial sections. Even if the lack of figured axial sections in literature to compare with makes difficult the identification of this species in thin section, few specimens could be differentiated from *N. vascus* (thicker tests and bigger proloculus diameters) and were attributed to *N. kecskemetii.*

Comparing with literature, comparable values of the protoconch diameter assigned to *N. kecskemetii* have been reported from northeastern Hungary, 40–100 μm (Less et al., 1991); northern Spain, 70–115 μm (Ferràndez-Cañadell et al., 1999); southwestern Turkey, 50–95 μm (Özcan et al., 2009a); eastern Turkey, 55–135 μm (Özcan et al., 2010) and wetern India, 40–90 μm (Less et al., 2018). However, lower values (58–68 μm) have been reported from northeastern Hungary by Less (1999). Even if slightly higher values have been reported from southeastern Spain, 94–141 μm (Ferràndez-Cañadell and Bover-Arnal, 2017) and northeastern Italy, c. 133 μm (Bassi et al., 2007), illustrated specimens show similar axial outlines to those from Sierra de Marmolance. See Table 6.

Stratigraphical distribution. In Sierra de Marmolance, this species occurs in the lower part of the succession (section B, samples M1S3, M1S4, M1S5, M1S6, M1S11; section C, samples M6S14, M6S16, M6S24), in the *Nummulites* facies, associated with *Nummulites vascus* (see fig. 7; table 3.2).

In the Tethys realm, *N. kecskemetii* has been set to the whole duration of the Chattian (SBZ 22B–23), based on data from Spain (Ferràndez-Cañadell et al. 1999), Hungary (Less 1991; Less et al., 2008; Báldi et al. 1999) and southwestern Turkey (Özcan et al., 2009a, 2010). During this time-span no considerable evolution within this species have been observed (Less et al., 2018). See Table 6 for the stratigraphical and palaeogeographical distributions with their references.

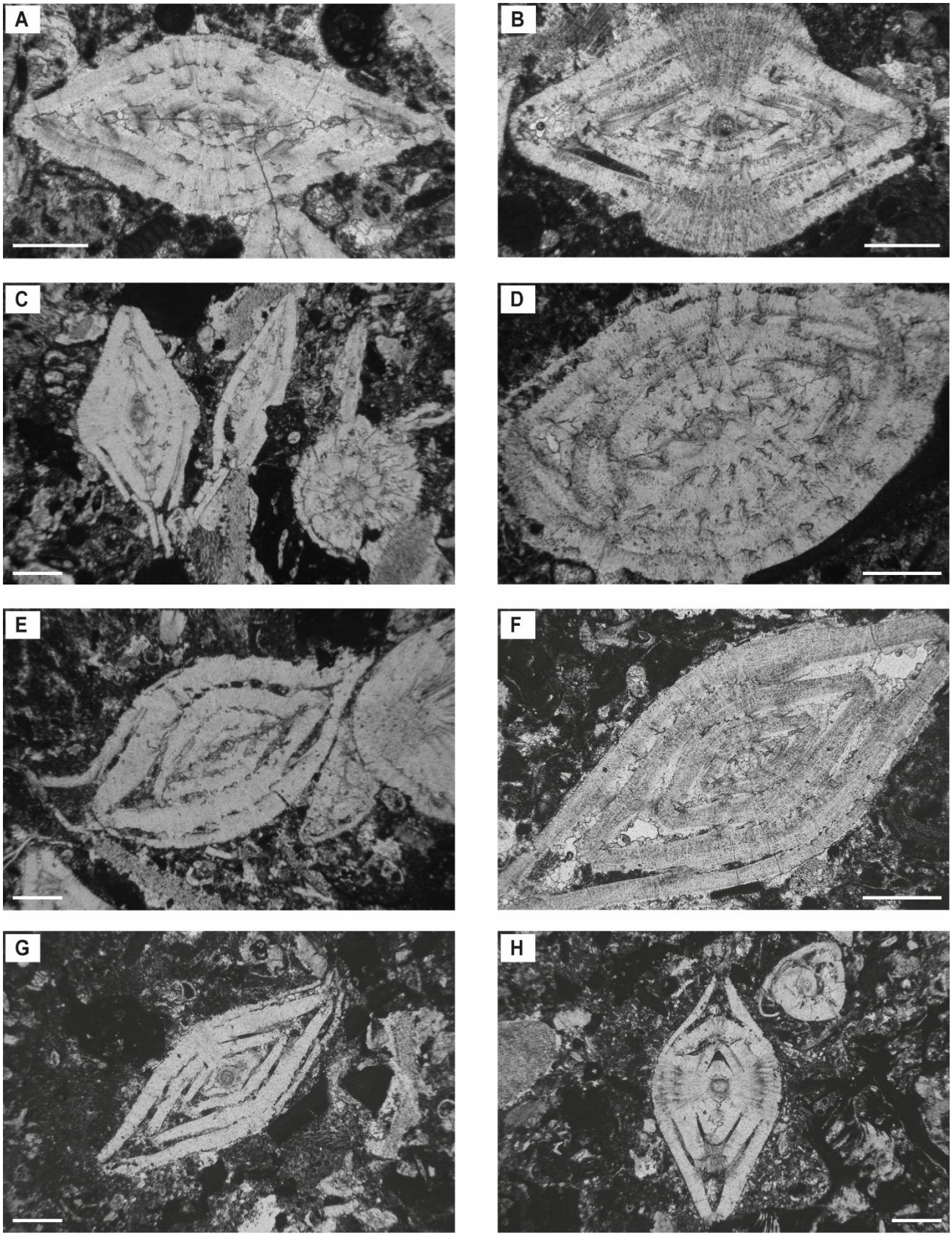

Plate 2. A–H. *Nummulites* cf. *kecskemetii* from Sierra de Marmolance, Spain. A: Sample M6S16; B: Sample M6S14; C: Sample M1S3; D: Sample M1S5; E, G, H: Sample M1S6; F: Sample M1S11. Scale bar represents 400 μm.

Table 6. Biometric parameters and stratigraphical distribution of *Nummulites kecskemetii* present in Marmolance (this study) with other localities for comparison (megalospheric forms). Abbreviations: Prol., proloculus diameter (mean); L, chamber length in the third whorl (mean); D, test diameter (mean); SBZ, Shallow Benthic Zonation. Serrav., Serravallian; Illustr., illustrations; Ax/Eq, axial/equatorial sections measured from illustrations.

Referred to as	References	Prol. (□m)	L (□m)	D (mm)	Age	Locality	Illustr.
N. kecskemetii	Less *et al.* 1991	40–100	-	-	late Chattian (SBZ23)	NE Hungary	-
N. bouillei	Cahuzac and Poignant 1997	-	-	-	Priabonian–late Oligocene	Aquitaine basin, SW France	pl. 1, figs. 5, 6
N. kecskemetii	Less 1999	(58–68)	(156–164)	-	late Chattian (SBZ23)	NE Hungary	pl. 2, figs. 14–16
N. kecskemetii	Ferràndez-Cañadell *et al.* 1999	70–115	Eq: 360	Eq: 1.9	Chattian (SBZ22B–23)	N Spain	pl. 1, h; fig. 3, n–o
N. cf. *bouillei*	Bassi *et al.* 2007	Ax: 133	-	-	Priabonian–late Oligocene	NE Italy	pl. 4, fig. 13
N. kecskemetii	Özcan *et al.* 2009a	50–95	145–260	Eq: 2.6	late Chattian (SBZ23)	SW Turkey	fig. 17. 6–10
N. kecskemetii	Özcan *et al.* 2010	55–135	155–221	Eq: 1.3–3	Chattian (SBZ22B–23)	E Turkey	pl. 4, figs. 23, 24
N. kecskemetii	Less *et al.* 2018	40–90	Eq: 286	Eq: 2.25	Chattian (SBZ22B–23)	W India	fig. 10, 1–5
N. aff. *kecskemetii*	Ferràndez-Cañadell and Bover-Arnal, 2017	94–141	Ax:257	Ax: 2–2.5	late Chattian (SBZ23)	SE Spain	fig. 10, J–R
N. cf. *kecskemetii*	**This study**	71–97 (90)	198–376 (272)	2.1–3.7 (2.6)	Serrav.	SE Spain	Pl. 2

Nummulites cf. *vascus* Joly and Leymerie, 1848

Plate 3. Figures A–H

1995 *Nummulites vascus* Joly and Leymerie; Racey, pl. 2, figs. 24–26.
1997 *Nummulites vascus* Joly and Leymerie; Cahuzac and Poignant, pl. 1, figs. 1, 2.
2007 Nummulites cf. vascus Joly and Leymerie 1848; Bassi et al., pl. 4, figs. 7, 11, 12.
2010 *Nummulites vascus* Joly and Leymerie; Benedetti, pl. 3, fig. 7; Text-fig. 8, figs. 9–10.
2011 *Nummulites vascus* Joly and Leymerie; Less et al., fig. 39, s–u, w.
2013 *Nummulites vascus* Joly and Leymerie; Amirshahkarami, pl. 1, figs. 4–5, 7.
2014 *Nummulites* cf. *vascus* Joly and Leymerie; Gedik, pl. 13, figs. 16–19.
2017 *Nummulites* cf. *vascus* Joly and Leymerie; Ferràndez-Cañadell and Bover-Arnal, fig.10I.
2020 *Nummulites vascus* Joly and Leymerie; Sirel et al., fig. 13, D–J.

Description. Specimens with thick lenticular test and more or less defined central boss. Test diameter (D) ranges between 1.9 and 4.8 mm, with a mean diameter of 2.7 mm. Proloculus (P) is c. 160 microns in diameter (ranging from 108 to 235 μm) and the chamber length in the third whorl ranges from 139 to 338 microns (mean 204 μm).

Remarks. In the absence of equatorial sections (only oblique and paraequatorial sections were found in randomly oriented thin sections), specimens from Marmolance were measured from

nineteen axial sections of megalospheric forms. *Nummulites* showing comparable size and axial outline to those ascribed so far to *N. vascus* in the literature were assigned to this species, following Bassi et al., 2007. The synonymy list is limited to those works including comparable axial sections.

Comparing with literature, similar proloculus and test diameter have been reported from Oman (Racey, 1995: P=80–270 μm, D=2.18–4.37 mm), northwestern Turkey (Sirel et al., 2020: P=200–250 μm, D=2.1–3.2 mm), northeast Italy (Bassi et al., 2007: P c. 150 μm; D c. 2.2 mm), eastern Turkey (Gedik 2014: D=1.5–2.2 mm) and Sicily (Benedetti 2010: P c. 155 μm, D c. 2.7 mm). Smaller test dimensions have been reported from southern Spain (Ferràndez-Cañadell and Bover-Arnal, 2017: P=67–133 μm; D= 1.7–2.2 μm). See Table 7.

Stratigraphical distribution. In Sierra de Marmolance, this species occurs in the lower part of the succession (section B, samples M1S1, M1S3, M1S4, M1S5, M1S6; section C, samples M6S9, M6S12, M6S16, M6S19, M6S20, M6S24), in the *Nummulites* facies together with *N. kecskemetii* (see fig. 7; table 3.2).

In the literature, there is no consensus about the stratigraphic range of *N. vascus,* possibly due to systematic discrepancies, as suggested by Ferràndez-Cañadell and Bover-Arnal (2017). According to several authors, the stratigraphic range of *N. vascus* is limited to the Rupelian (Laursen et al., 2009; Amirshahkarami 2013; Moghadam et al., 2014) or Rupelian–early Chattian, SBZ 21–22B (e.g. Cahuzac and Poignant 1997, 1998; Bádi et al., 1999; Gedik 2014, 2015; Braga and Bassi 2011). Even its possible persistence into the late Oligocene (SBZ 23) was also proposed (e.g. Schaub 1981; Drooger and Laagland 1986; Bassi et al., 2007; Ferràndez-Cañadell and Bover-Arnal 2017). See Table 7 for the stratigraphical and palaeogeographical distributions with their references.

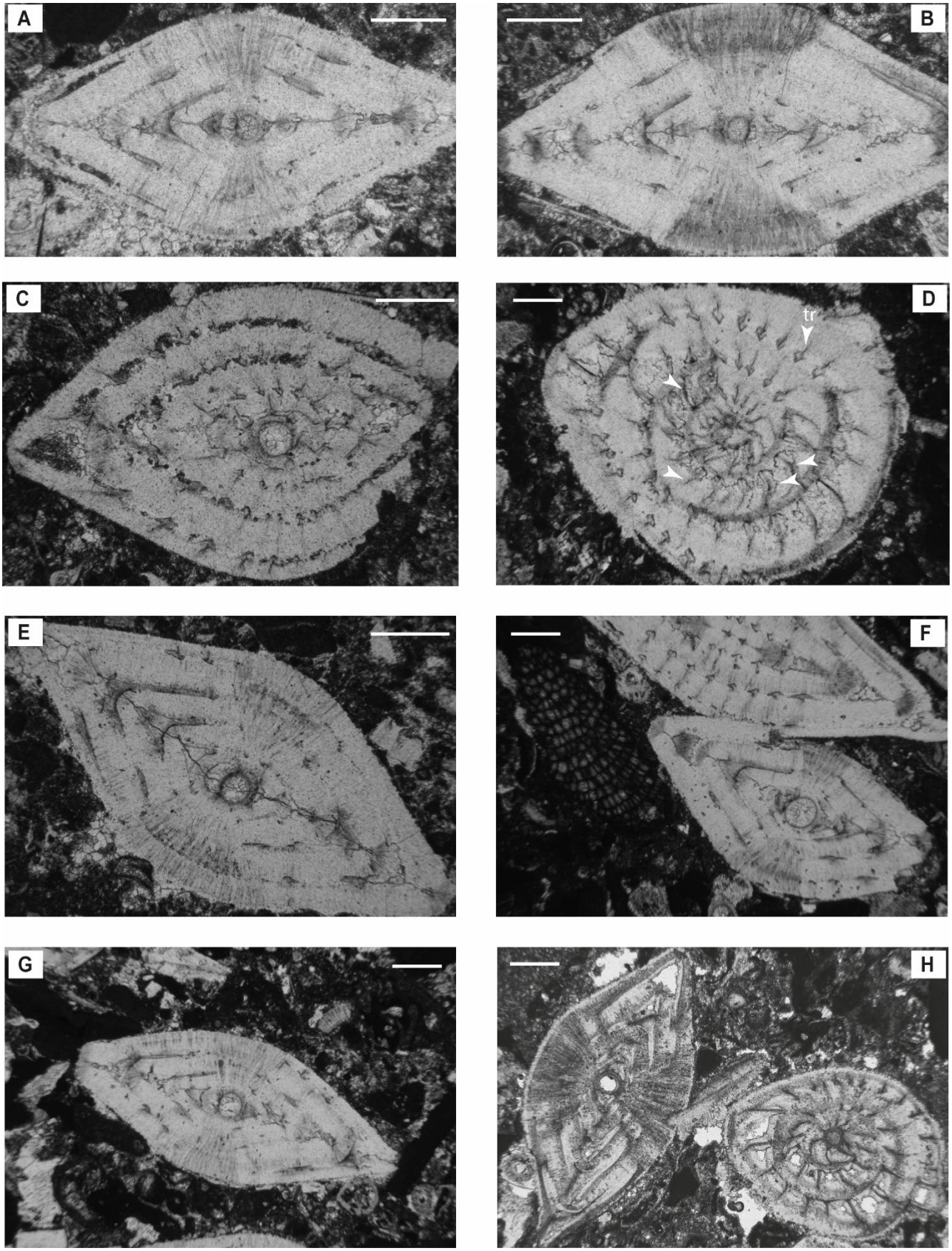

Plate 3. A–H. *Nummulites* cf. *vascus* from Sierra de Marmolance, Spain. All axial sections except two Sub-equatorial sections (fig. D and right specimen in fig. H). Notice the presence of trabecule (tr) in fig. D. A–D: Sample M1S6; E: Sample M1S5; F–G: Sample M1S3; H: Sample M1S1. Scale bar represents 400 μm.

Table 7. Biometric parameters and stratigraphical distribution of *Nummulites vascus* present in Marmolance (this study) with other localities for comparison (megalospheric forms). Abbreviations: Prol., proloculus diameter (mean); L, chamber length in the third whorl (mean); D, test diameter (mean); SBZ, Shallow Benthic Zonations. Serrav., Serravallian; Illustr., illustrations; Ax/Eq, axial/equatorial sections measured from illustrations.

Referred to as	References	Prol. (□m)	L (□m)	D (mm)	Age	Locality	Illustr.
N. vascus	Schaub 1981	-	-	-	Rupelian–Chattian	-	pl. 53, figs. 1–6
N. vascus	Racey 1995	80–270	-	2.18–4.37 (3.85)	Priabonian–early Oligocene	Quriyat (Oman)	pl. 2, figs. 24–26
N. vascus	Cahuzac and Poignant 1997	-	-	-	Rupelian–early Chattian (SBZ21–22B)	Aquitaine basin (SW France)	pl. 1, figs. 1, 2
N. cf. *vascus*	Bassi *et al.* 2007	Ax: 150	Ax: 185	Ax: 2.2	Rupelian–early Chattian (SBZ21–22B)	NE Italy	pl. 4, figs. 7, 11–12
N. vascus	Laursen *et al.* 2009	-	-	-	Rupelian	Turkey	-
N. vascus	Benedetti 2010	180–270; Ax: 155	Ax: 190	1.9–3.2; Ax: 2.7	Rupelian (SBZ21–22A)	N Sicily	pl. 3, fig. 7; text-fig. 8, figs. 9–10
N. vascus	Braga and Bassi 2011	-	-	-	Rupelian–early Chattian (SBZ21–22B)	SE Spain	fig. 5, D
N. vascus	Less *et al.* 2011	145–360 (236)	167–287 (222)	Eq: 2.5	early Rupelian (SBZ21)	NW Turkey	fig. 39s–u, w
N. vascus	Amirshahkarami 2013	-	-	-	Rupelian	SW Iran	pl. 1, Figs. 4–5, 7
N. cf. *vascus*	Gedik 2014	-	Ax:192	1.5–2.2	Rupelian–early Chattian (SBZ21–22B)	E Turkey	pl. 13, figs. 16–19
N. cf. *vascus*	Gedik 2015	-	Ax:192	Ax: 2.2	Rupelian–early Chattian (SBZ21–22B)	E Turkey	pl. 6, figs. 14–16
N. cf. *vascus*	Ferràndez-Cañadell and Bover-Arnal, 2017	67–133	Ax: 171	1.7–2.2	Chattian (SBZ23)	SE Spain	fig. 10, A–I
N. vascus	Sirel *et al.* 2020	200–250	Ax: 120–240 Eq: 280	2.1–3.2	early Oligocene	NW Turkey	fig. 13, D–J
N. cf. *vascus*	**This study**	108–235 (160)	139–338 (204)	1.9–4.8 (2.7)	Serrav.	SE Spain	pl. 3

Genus *OPERCULINA* d'Orbigny, 1826

Operculina complanata (Defrance, 1822)

Plate 4. Figures A–D

2009 *Operculina Complanata* Defrance; Özcan and Less, pl. 2, fig. 22.
2009a *Operculina Complanata* Defrance; Özcan et al., fig. 20. 1, 2.
2010 *Operculina Complanata* Defrance; Benedetti, pl. 3, fig. 2; text-fig. 8, figs. 11–14.
2010 *Operculina Complanata* Defrance; Özcan et al., pl. 4, fig. 25–31.
2011 *Operculina Complanata* Defrance; Less et al., fig. 40, s.
2017 *Operculina Complanata* Defrance; Ferràndez-Cañadell and Bover-Arnal, fig. 7. F, G.

Description. Specimens with rapidly opening spire, few whorls and folded septa (Pl. 4, fig. A; for comparison, see fig. 15). From five equatorial sections was only measured the proloculus diameter (P), ranging between 94 and 133 microns (mean 111 μm).

Remarks. Operculina is represented in the Eocene by the involute *O. ex. gr. gomezi* Colom and Bauzá 1950 with very dense and high chambers and in the Oligocene by the evolute *O. complanata* Defrance 1822 (see Less et al., 2011). *O. complanata* shows a great range of intraspecific variability (Less, 1991), hampering the species identification and, therefore, the literature did not put special attention on this taxon (except Hottinger, 1977 and Less, 1991).

Comparing with literature, similar shell morphometrical characters ascribed to *O. complanata* have been reported from Burdigalian (SBZ 25) specimens of eastern Turkey (Özcan and Less, 2009: P=85–140 μm, mean 110 μm; Özcan et al., 2010: P c. 108 microns) and early Chattian (SBZ 22B) specimens from southwestern Turkey (Özcan et al., 2009a: P c. 105 μm). Greater values have been observed for late Chattian (SBZ 23) specimens from Spain (*i.e.* Ferràndez-Cañadell and Bover-Arnal, 2017: P=220–245 μm) and eastern Turkey (Özcan et al., 2010: P c. 188 μm). Lower values have been reported from Sicily (Benedetti, 2010: P=54–132 μm, mean 82 μm).

Özcan et al. (2010) described a fluctuation in the proloculus size with an increase of the diameter mean in Chattian from about 108 μm in SBZ 22B to about 188 μm in SBZ 23, followed by a subsequent reduction in lower Burdigalian specimens to values similar to those in SBZ 22B. So, specimens from Sierra de Marmolance could represent a minimum in that trend.

Stratigraphic distribution. In Sierra de Marmolance, this species occurs in the lower-middle part of the succession (section A, samples C-14, 16, 18; section B, samples M1S16, M2S3, M2S9, M2S11, M3S6), in the Lepidocyclinid facies, associated with *Neorotalia viennoti, Eulepidina formosoides, Nephrolepidina* ex.interc. *morgani* et *praemarginata and Nephrolepidina tournoueri* and *Nummulites fichteli* (see fig. 7; table 3.3).

O. complanata has a rather long stratigraphic range, from the base of the Oligocene to the Tortonian (SBZ 21–26; Cahuzac and Poignant, 1997) without showing significant evolutionary change during this interval (Özcan et al., 2009a, 2009b, 2010).

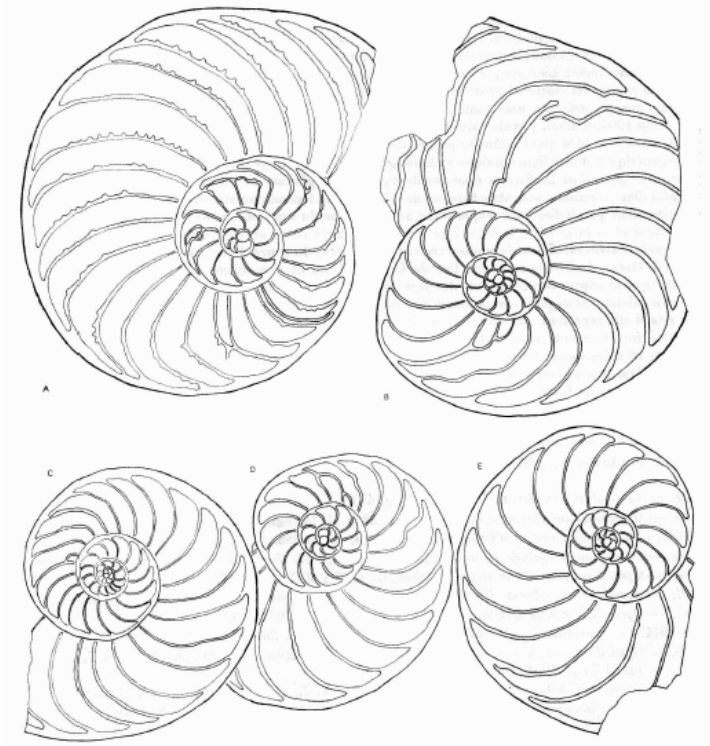

Figure 15. *Planoperculina complanata* (Defrance). Megalospheric specimens, equatorial sections. Oligocene. A: Specimen from Handilloh, bordelaise region, Aquitaine occidentale, France. B–E: Little specimens. From southeast Borneo. Lower Oligocene. From Hottinger (1977, p. 102, fig. 39).

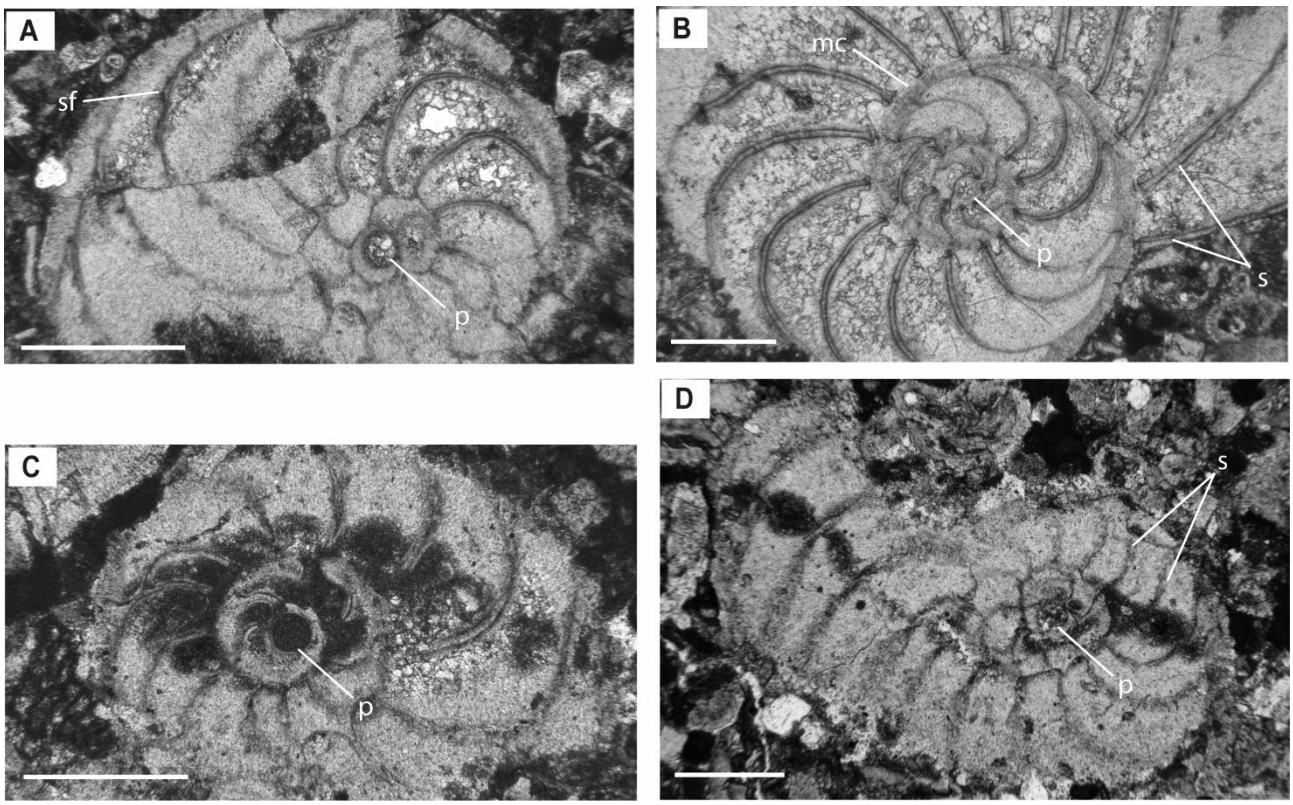

Plate 4. A–D. *Operculina complanata* from Sierra de Marmolance, Spain. A: Sample M2S3; B: M1S16; C: Sample C-16; D: Sample M2S9. Abbreviations: sf, septal flap; mc, marginal cord; s, septum; p, proloculus. Scale bar represents 400 µm.

Genus HETEROSTEGINA d'Orbigny, 1826

Heterostegina cf. *assilinoides* Blackenhorn 1890 emend. Henson 1937

Plate 5. Figures A–D

1995 *Heterostegina assilinoides* Blanckenhorn emend. Henson; Racey, pl. 11, figs. 1, 2.
2008 *Heterostegina (Vlerkina) assilinoides* Blanckenhorn emend. Henson; Boukhary et al., pl. 3, figs. 8–21.
2008 *Heterostegina assilinoides* Blanckenhorn emend. Henson; Less et al., fig. 18. A, B.
2009a *Heterostegina assilinoides* Blanckenhorn emend. Henson; Özcan et al., fig. 20. 5–9.
2010 *Heterostegina assilinoides* Blanckenhorn emend. Henson; Özcan et al., pl. 5, figs. 1–4, 7.
2014 *Heterostegina assilinoides* Blanckenhorn emend. Henson; Gedik, pl. 13, figs. 8–10, 12–15.
2017 *Heterostegina assilinoides* Blanckenhorn emend. Henson; Ferràndez-Cañadell and Bover-Arnal, figs. 3G, H; 8A–F, L, M.
2018 *Heterostegina assilinoides* Blanckenhorn emend. Henson; Less et al., fig. 10, 6–13.

Description. The specimens show a protoconch (P) c. 116 microns in diameter, measured from axial and oblique sections. In the sections axially oriented, thick pillars can be observed throughout the inflated umbonal region (see pl. 5, fig. C). From two oblique sections equatorially oriented can be perceived internal stellate chambers surrounding the protoconch and the deuteroconch (pl. 5, fig. A; see for comparison Less et al., 2008: fig. 18; Boukhary et al., 2008: pl. 3, fig. 11; Özcan et al., 2009a: fig. 20. 4, 10; Ferràndez-Cañadell and Bover-Arnal, 2017: fig. 8, D; Less et al., 2018: fig. 10).

Remarks. No equatorial sections were found useful to measure the specimens using the parameters introduced by Less et al. (2008) after Drooger and Roelofsen (1982). These parameters characterize the equatorial section of A-forms of the western Tethyan late Bartonian and Priabonian *Heterostegina* (applied also for the Oligo–Miocene forms by Özcan et al., 2009a, 2010 and Less et al., 2018). The parameters are the number of undivided chambers, the pattern of the spiral and the density of chambers. However, comparing with illustrated axial sections in the literature (i.e. Tosquella et al., 2001; Özcan et al., 2010; Ferràndez-Cañadell and Bover-Arnal, 2017; Boukhary et al., 2008; Gedik, 2014), Marmolance specimens show similar outline to the Chattian *H. assilinoides* specimens from other localities in the Mediterranean region like southeastern Spain (see fig. 8L in Ferràndez-Cañadell and Bover-Arnal, 2017), northern Sinai (see pl. 3, figs. 17–21 in Boukhary et al., 2008) or eastern Turkey (see pl. 5, fig. 7 in Özcan et al., 2010; figs. 8–9, 14–15 in Gedik, 2014). In contrast, very different axial outlines (see figs. 8, 2, 4–6 in Tosquella et al., 2001) have been reported from southwestern Spain for specimens ascribed to *H. gomez-angulensis*, even if they have closer protonconch diameters (P = 100–250 µm).

Regarding the protoconch size, Henson (1937) and Hottinger (1966) noted that it is highly variable in *H. assilinoides*. Specimens from Marmolance fall within the range of the proloculus diameter observed in *H. assilinoides*, from 110–330 µm (Henson, 1937), with smaller dimensions comparing to other publications (e.g. Ferràndez-Cañadell and Bover-Arnal, 2017: P = 210–338 µm; mean 268 µm; Özcan et al., 2010: P = 140–350 µm; mean 214 µm; Boukhary et al., 2008: P = 200–300 µm; Racey, 1995: P = 230–290 µm). Proloculus measures reported from western India (Less et al., 2018: P = 110–295 µm; mean 182 µm) would be the most similar.

Stratigraphic distribution. In Sierra de Marmolance, these specimens have been found in the upper part of the succession (section B, samples M4S10, M5S4, M5S7, M5S8, M5S11), in the *Neorotalia* with *Risananeiza* facies, associated with *Neorotalia viennoti, Risananeiza crassaparies, Austrotrillina brunni, Austrotrillina striata, Spiroclypeus sp., Eulepidina* ex.interc. *dilatata* et *formosoides, Nephrolepidina tournoueri* and *Borelis inflata* (see fig. 7; talbe 3.5).

In the literature, *H. assilinoides* is known to occur from the Rupelian (SBZ 21–22) (southern Spain, Hottinger 1977; northern Oman, Racey 1995; eastern Turkey, Gedik 2014) to the

late Chattian (SBZ 23) (southwestern France, Cahuzac and Poignant 1997; southeastern Spain, Ferràndez-Cañadell and Bover-Arnal 2017).

Genus *SPIROCLYPEUS* Douvillé, 1905

Spiroclypeus sp.

Plate 5. Figures E, F

2010 *Spiroclypeus blanckenhorni* Henson; Özcan et al., 2010, pl. 5, figs. 11, 14, 15, 17, 18.
2017 *Spiroclypeus blanckenhorni* Henson; Ferràndez-Cañadell and Bover-Arnal, figs. 3I, 8A–8F, 8L, 8M.

Remarks. Hottinger (1977) circumscribed *Spiroclypeus* Douvillé, 1905 by the occurrence of Y-shaped stolons on the single equatorial plane, alar prolongations, spiral chambers subdivided in secondary chamberlets and lateral chambers formed by the backward folding of the entire proximal primary lateral wall (Loeblich and Tappan, 1987). In the studied materials a few of paraxial sections (see pl. 5, figs. E, F) show lateral chambers (diagnostic character of *Spiroclypeus*), but no others characters could be measured since no centered sections (containing the proloculus) were found. Therefore, the Marmolance specimens cannot be identified to species level, even if they show similarities to the *Spiroclypeus* specimens reported from Spain (fig. 8, K, M–O in Ferràndez-Cañadell and Bover-Arnal, 2017) or Turkey (pl. 5, fig. 17 in Özcan et al., 2010) identified as *S. blanckenhorni*.

Stratigraphic distribution. In Sierra de Marmolance, *Spiroclypeus* sp. only occurs in the upper part of the succession (section B, sample M5S8), in the *Neorotalia* with *Risananeiza* facies, together with *Neorotalia viennoti, Risananeiza crassaparies, Heterostegina assilinoides, Austrotrillina brunni, Austrotrillina striata, Eulepidina* ex.interc. *dilatata* et *formosoides, Nephrolepidina tournoueri* and *Borelis inflata* (see fig. 7; table 3.5).

Along the circum-Mediterranean region, this genus has been commonly reported (e.g. Hottinger, 1977; Racey, 1995; Bassi et al., 2007; Less and Özcan, 2008; Özcan et al., 2010; Ferràndez-Cañadell and Bover-Arnal, 2017). Age ranges from late Eocene (Priabonian) to early Miocene (Aquitanian; Hottinger, 1977).

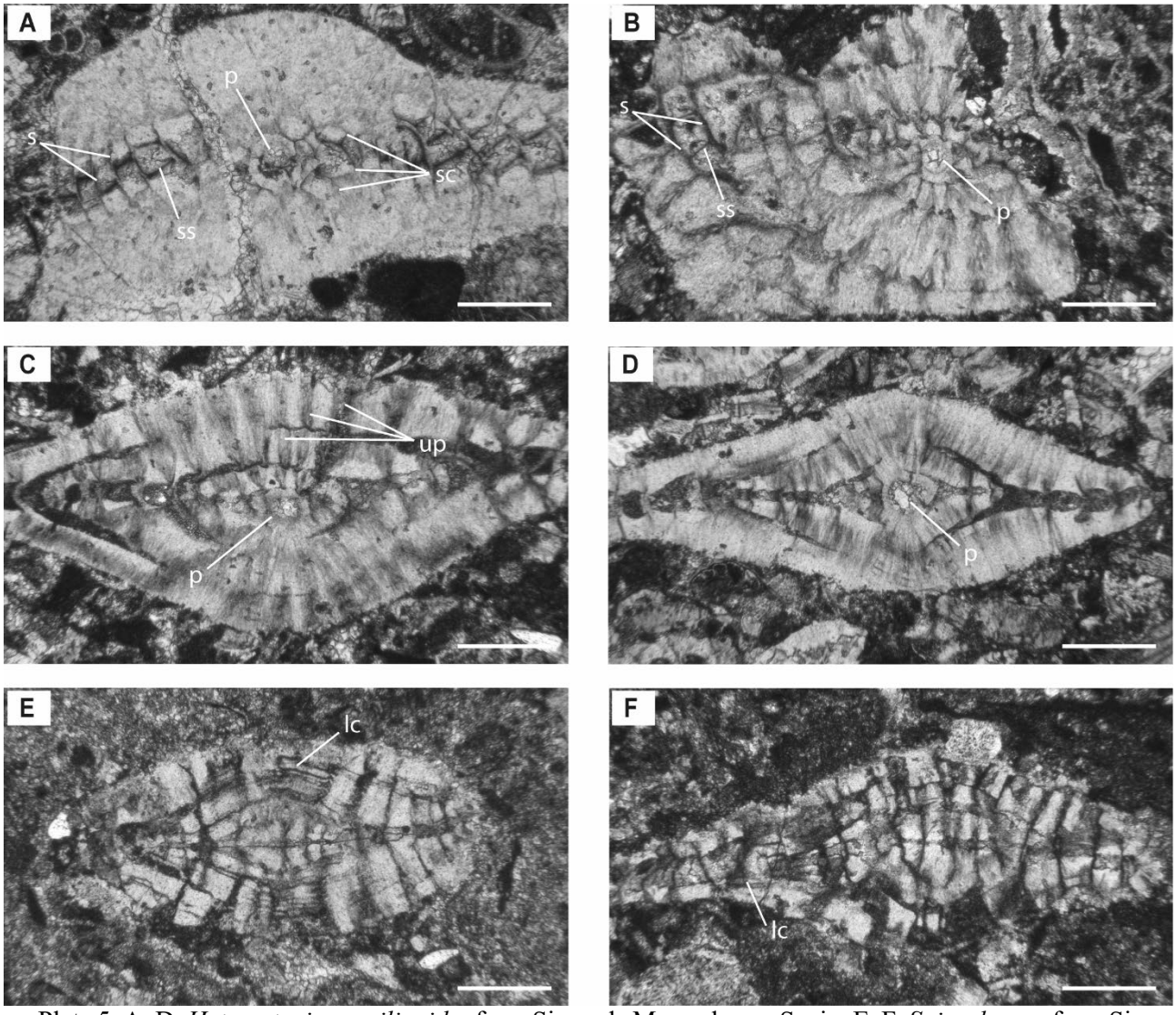

Plate 5. A–D. *Heterostegina assilinoides* from Sierra de Marmolance, Spain. E, F. *Spiroclypeus* from Sierra de Marmolance, Spain. A: Sample M4S10; B, C: Sample M5S7; D: Sample M5S4; E, F: Sample M5S8. Abbreviations: s, septa; ss, secondary septa; p, proloculus; sc, stellate chamberlets; up, umbonal pillars; lc, lateral chambers. Scale bar represents 400 µm.

Family LEPIDOCYCLINIDAE Scheffen, 1932

Lepidocyclinids have been described extensively in the literature (e.g. Atlantic: Sachs, 1964; Seiglie and Frost, 1979; Brun et al., 1982; Indo-Pacific: Cole, 1960; Van der Vlerk and Gloor 1968; Adams, 1979; Chapronière, 1980; Matsumaru, 1981; Saraswati, 1995; Muthukrishnan and Saraswati, 2001; Boudagher-Fadel, 2002; Renema 2007; Boudagher-Fadel and Price 2010; Tethyan area: Drooger and Socin, 1959; Drooger and Freudenthal 1964; Pieroni, 1965; Lange, 1968; Schiavinotto, 1979; van Heck and Drooger, 1984; Özcan et al., 2009a, 2010) with occurrences ranging from the middle Eocene in America to the late Miocene (or possibly early Pliocene) in the Indo-Pacific Tethyan sub-province (Boudagher-Fadel and Price, 2010). It is thought that during the Eocene, Lepidocyclinids were restricted to Central America and towards the early Oligocene they migrated to the Mediterranean and Indo-West Pacific provinces (Renema, 2007).

A large number of studies classified Lepidocyclinids according to the morphological features (e.g. H. Douvillé, 1899; Lemoine and R. Douville, 1904; H. Douvillé, 1911; Van der Vlerk, 1929; Cole, 1962, 1968; Eames et al., 1962). Tan Sin Hok (1936) was the first to highlight the importance of the embryonic chambers for the classification of Lepidocyclinid assemblages.

These showed a time-related increase of the degree of embracement of the protoconch by the deuteroconch and the number of chambers attached to the deuteroconch (ad-auxiliary chambers).

In the western Tethys this family is represented by two genera: *Eulepidina* H. Douvillé, 1911 and *Nephrolepidina* H. Douvillé, 1911. These two genera are distinguished by different morphological features (for more detailed description see Less et al., 2018 and references therein): (1) externally, the overall size (*Eulepidina* is significantly larger and thinner than *Nephrolepidina*); (2) the megalospheric embryon (in *Eulepidina* the size of the embryonic chambers is much larger); (3) the degree of embracement of the protoconch by the deuteroconch or parameter A (larger in *Eulepidina* than in *Nephrolepidina*); (4) the equatorial chamberlets (those of *Eulepidina* are much larger) and (5) the degree of curvature of the common wall between the protoconch and deuteroconch. By means of R-mode factor analysis Saraswati (1995) suggested that the use of biometric parameters based on characters of the embryonic apparatus (size of embryonic chambers, grade of enclosure and curvature of the common wall together) explain the maximum variance in lepidocyclinids. See figs. 13 and 14.

Twenty-four *Nephrolepidina* specimens and twenty-three *Eulepidina* specimens were measured from sub-equatorial and axial sections. The terminology and parameters used are those proposed by van der Vlerk (1959), Drooger and Socin (1959) and Özcan et al. (2009a). Measurements assigned to *Eulepidina* show deuteroconch sizes ranging from 598 to 1470 µm (mean 994 µm), while *Nephrolepidina* values are much smaller (199–574 µm; mean 338 µm). Protoconch size ranges from 428 to 960 µm (mean 645 µm) in *Eulepidina* and from 155 to 466 µm (mean 250 µm) in *Nephrolepidina* specimens. A parameter is larger as well in *Eulepidina* specimens (A= 50–67) than in *Nephrolepidina* (A= 37–46).

Genus *EULEPIDINA* H. Douvillé, 1911

Remarks. Eulepidina has a world-wide distribution and constitute a significant biostratigraphic marker (e.g. Vlerk 1959, 1963; Matsumaru, 1971; Chapronière, 1980; Less, 1991; Robinson, 2003; Roozpeykar and Moghaddam, 2016). In the western Tethyian (Mediterranean) province, several authors studied the biometry of *Eulepidina* representatives (e.g. Lange 1968; de Mulder, 1975; Matteucci and Schiavinotto, 1977; van Heck and Drooger, 1984; Drooger and Laagland, 1986; Schiavinotto and Verrubbi, 1996; Cahuzac and Poignant, 1997; Myftary et al., 2001; Özcan et al., 2009a, 2009b, 2010; Özcan and Less, 2009; Ferràndez-Cañadell and Bover-Arnal, 2017; Akbar-Baskalayeh et al., 2020).

Four species of *Eulepidina* have been described in the Mediterranean domain: *E. formosoides, E. dilatata, E. elephantina* and *E. anatolica* (for more detailed information see van Heck and Drooger, 1984; Less, 1991, 2018; Özcan et al., 2009a, 2010; Less et al., 2018). After the study of their morphometric parameters (test size and megalospheric embryo; see fig. 16), the Marmolance specimens of *Eulepidina* correspond to the main *formosoides-dilatata* Mediterranean lineage (pl. 6 and 7). The parameters used here to distinguish the species *E. formosoides* and *E. dilatata* are D (the average size of the deuteroconch) and A (the average degree of embracement of the protoconch by the deuteroconch), following the morphometric limits proposed by Özcan et al. (2009a, 2010) as to D_{mean} = 1250 µm and A_{mean} = 83.

Stratigraphical distribution. In the Mediterranean region, *Eulepidina* occurrences are restricted to the Oligocene (Europe: Cahuzac and Poignant, 1997; Turkey: Özcan et al., 2009a, b; Özcan and Less, 2009). While in the Indo-Pacific area this genus reaches the lower Miocene (e.g. van der Vlerk, 1928; Coleman, 1963; Adams, 1965, 1984; Hashimoto et al., 1977; Chapronière, 1984; Butterlin, 1987; Boudagher-Fadel and Lokier, 2005), reports from the Mediterranean early Miocene are still highly disputed due to the absence of adequate paleontological data (see Özcan et al., 2009b; Özcan and Less, 2009).

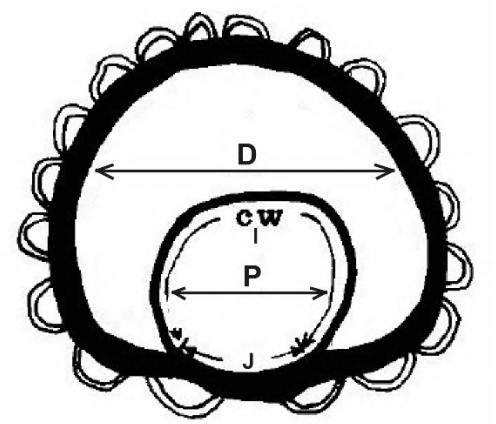

Figure 16. Schematic drawing of the embryonic apparatus of *Eulepidina* showing the chamber types and positions of measurements. P is the protoconch; D is the deuteroconch; cw is the common wall between P and D (parameter I); J is the point of contact between P and D. Modified from Chapronière, 1980, fig. 11, p. 165.

Eulepidina formosoides Douvillé, 1925

Plate 6. Figures A–H

1984 *Lepidocyclina (Eulepidina) formosoides* Douvillé; van Heck and Drooger, pl. 1, figs. 13–17; pl. 2, figs. 1–9; pl. 3, figs. 1–5.
2010 *Eulepidina formosoides* Douvillé; Özcan et al., pl. 3, figs. 1–8; text-figure 10.
2020 *Eulepidina formosoides* Douvillé; Akbar-Baskalayeh et al., figs. 19, 20.1–11; 13, 14.

Description. Four equatorial sections show the deuteroconch (D_{mean} = 996 μm) and the protoconch (P_{mean} = 697 μm). The A parameter results to be A_{mean} = 58. Measures taken in sub-oblique axial sections, the protoconch is 428–978 μm (P_{mean} = 614 μm) in diameter and the deuteroconch is 598–1326 μm (D_{mean} = 914 μm) width.

Remarks. The *Eulepidina* populations from Marmolance (see Table 8) with values of D_{mean} <1250 μm and A_{mean} < 83 were assigned to *E. formosoides* taxa. Even if A parameter of Marmolance specimens is smaller than those reported in literature for *E. formosoides* (A_{mean} around 70–80; see Özcan et al., 2010; van Heck and Drooger, 1984; unpublished data in Parente and Less 2019; Akbar-Baskalayeh et al., 2020), similar values of D and P in *Eulepidina* specimens ascribed to *E. formosoides* have been reported from eastern Turkey (Özcan et al., 2010: D = 505–1740 μm; P = 310–980 μm), northern Spain (van Heck and Drooger, 1984: D = 363–1283 μm; P = 247–700 μm), France (unpublished data in Parente and Less, 2019: D = 505–1215 μm; P = 310–645 μm) and central Iran (Akbar-Baskalayeh et al., 2020: D = 390–1170 μm; P = 230–660 μm).

Stratigraphical distribution. In Sierra de Marmolance, this species is common in the lower-middle part of the succession (section A, samples C14 and C16; section B, samples M1S16, M2S3, M2S9, M2S12, M2S13; section D, samples M8S35, M8S55, M8S56), in the Lepidocyclinid facies, associated with *Operculina complanata, Neorotalia viennoti, Nephrolepidina* ex.interc. *morgani* et *praemarginata, Nephrolepidina tournoueri* and *Nummulites fichteli* (see fig. 7; table 3.3).

E. formosoides occurs in the sedimentary record from the late Rupelian (base of SBZ 22A) to the early Chattian (middle of SBZ 22B) (Cahuzac and Poignant, 1997).

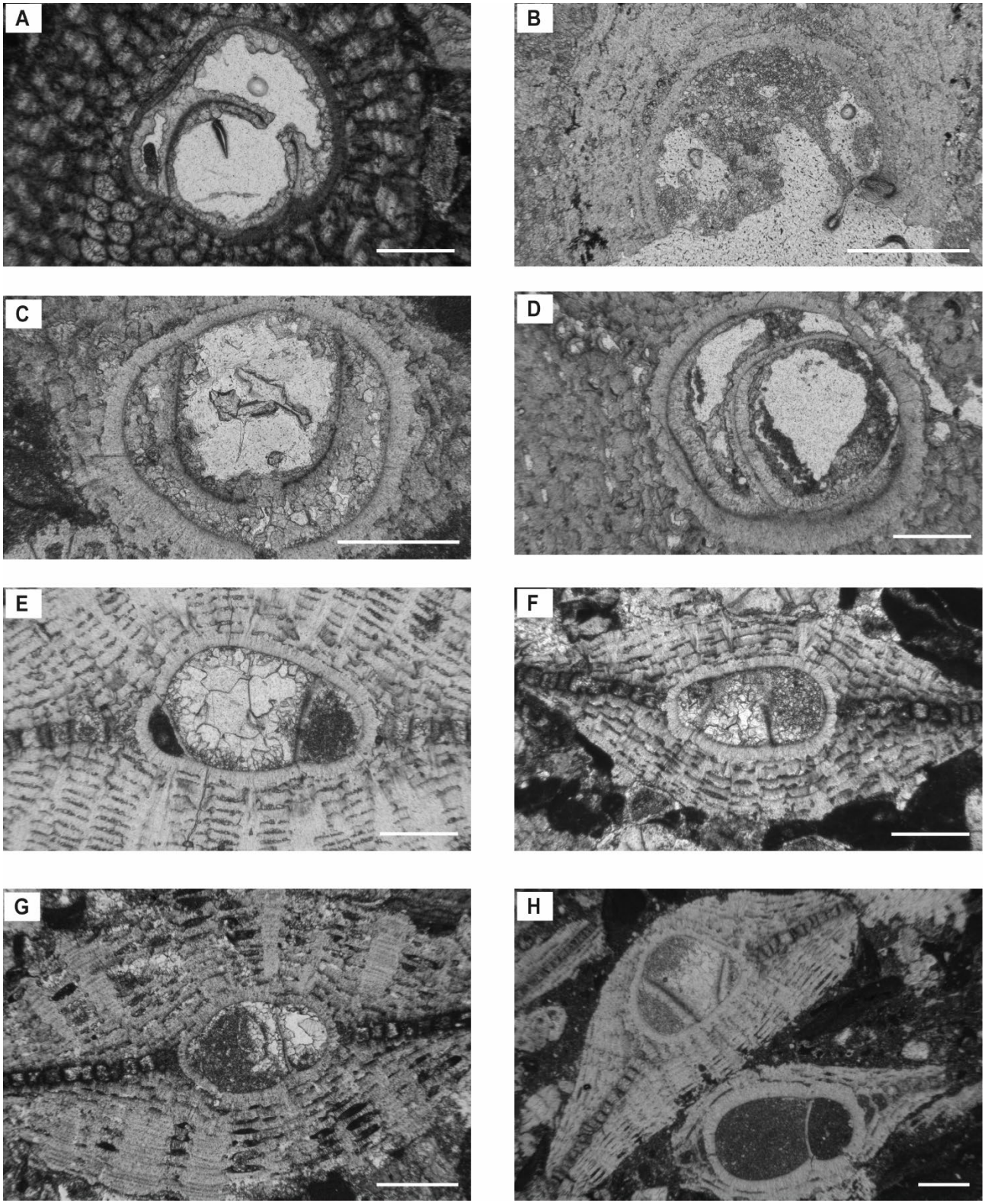

Plate 6. A–H. *Eulepidina formosoides* from Sierra de Marmolance, Spain. A: Sample M1S16; B: Sample M2S3; C, H: Sample M2S13; D: Sample M8S35; E: Sample M8S55; F: Sample M8S56; G: Sample M2S12. Scale bar represents 400 μm.

Eulepidina ex. interc. *dilatata* (Michelotti, 1861) et *formosoides* Douvillé, 1925

Plate 7. Figures A–D

2009a *Eulepidina* ex. interc. *dilatata* (Michelotti) et *formosoides* Douvillé; Özcan et al., fig. 15. 17–18.
2018 *Eulepidina* ex. interc. *formosoides* Douvillé et *dilatata* (Michelotti); Less et al., fig. 14, 1–6.
2019 *Eulepidina dilatata* (Michelotti); Parente and Less, fig. 15J–O.
2020 *Eulepidina* ex. interc. *formosoides* Douvillé et *dilatata* (Michelotti); Akbar-Baskalayeh et al., fig. 20. 15–17.

Description. Only one equatorial section was found (pl. 7, fig. B), from which the diameter of the protoconch (P = 960 μm) and deuteroconch (D = 1260 μm), as well as A parameter (A = 58), were measured. Measures taken in sub-oblique axial sections, the protoconch is 550–960 μm (P_{mean} = 785) in diameter and the deuteroconch is 1260–1470 μm (D_{mean} = 1374) width.

R*emarks.* Because of their embryo characteristics and D_{mean}, some Marmolance specimens are closer to the *E. dilatata* but with an unusually small A_{mean} value. The *Eulepidina* population (see table 8) showing values of D_{mean} typical from *E. dilatata* (D_{mean} > 1250 μm) but A_{mean} typical from *E. formosoides* (A_{mean} < 83) were assigned to this group. Comparing with other records, the Marmolance specimens have smaller sizes (smaller D and P values) than those reported for *E. dilatata* from southwestern Turkey (Özcan et al., 2009a: D_{mean} = 1743 μm; P_{mean} = 934 μm), eastern Turkey (Özcan et al., 2010: D_{mean} = 1477 μm; P_{mean} = 895 μm), Hungary (Less et al., 1991: D_{mean} = 1590 μm; P_{mean} = 911 μm), southeastern Spain (Ferràndez-Cañadell and Bover-Arnal, 2017: D = 1200–2178 μm; P = 675–1240 μm), France (unpublished data in Parente and Less, 2019: D_{mean} = 1427 μm; P_{mean} = 781 μm). Comparable sizes have been reported by other authors, which assigned the *Eulepidina* specimens to the *E. dilatata-formosoides* group (e.g. Özcan et al., 2009a from southwestern Turkey: D_{mean} = 1328 μm; P_{mean} = 699 μm; Özcan et al., 2010 from eastern Turkey: D_{mean} = 1229 μm; P_{mean} = 738 μm; Less et al., 2018 from western India: D_{mean} = 1343 μm; P_{mean} = 826 μm and Akbar-Baskalayeh et al., 2020 from central Iran: D_{mean} = 1198 μm; P_{mean} = 735 μm) or *E. dilatata* (e.g. Parente and Less, 2019 from south Italy: D_{mean} = 1380 μm; P_{mean} = 773 μm).

E. dilatata and *E. formosoides* are two successive and phylogenetically linked species belonging to the same lineage (Cahuzac and Poignant, 1997). Linages are used for biostratigraphic purposes and are stablished after the artificial separation of species by arbitrary biometric limits based on numerical evolutionary parameters which are characteristic from each chronospecies. Sometimes the mean parameter of a population can be very close (closer than 1 s.e. of the mean) to the limit between two neighbouring species. In this case, we adopt Drooger's (1993) proposal by using an intermediate notation (the notation *exemplum intercentrale*, abbreviated as *ex. interc*.), followed by the names of the two subspecies on either side of the limit, naming first the assemblage that is closer. So specimens from Marmolance were ascribed to *Eulepidina ex. interc. dilatata et formosoides* since they show intermediate characteristics between *E. dilatata* and *E. formosoides* lineages, being closer to the former.

Stratigraphical distribution. In Sierra de Marmolance, those forms occur mostly in the upper part of the succession (section B, sample M4S14; also section A, sample C16), in the *Neorotalia* with *Risananeiza* facies, together with *Neorotalia viennoti, Risananeiza crassaparies, Heterostegina assilinoides, Austrotrillina brunni, Austrotrillina striata, Nephrolepidina tournoueri, Spiroclypeus* sp. and *Borelis inflata* (see fig. 7; table 3.5).

While *E. formosoides* has been reported mainly from the Rupelian, *E. dilatata* has been reported mainly from the Chattian (Özcan et al., 2009a). *E. dilatata* occurs in the sedimentary record from the late Rupelian (middle of SBZ 22A) to the late Chattian (SBZ 23) (Cahuzac and Poignant, 1997).

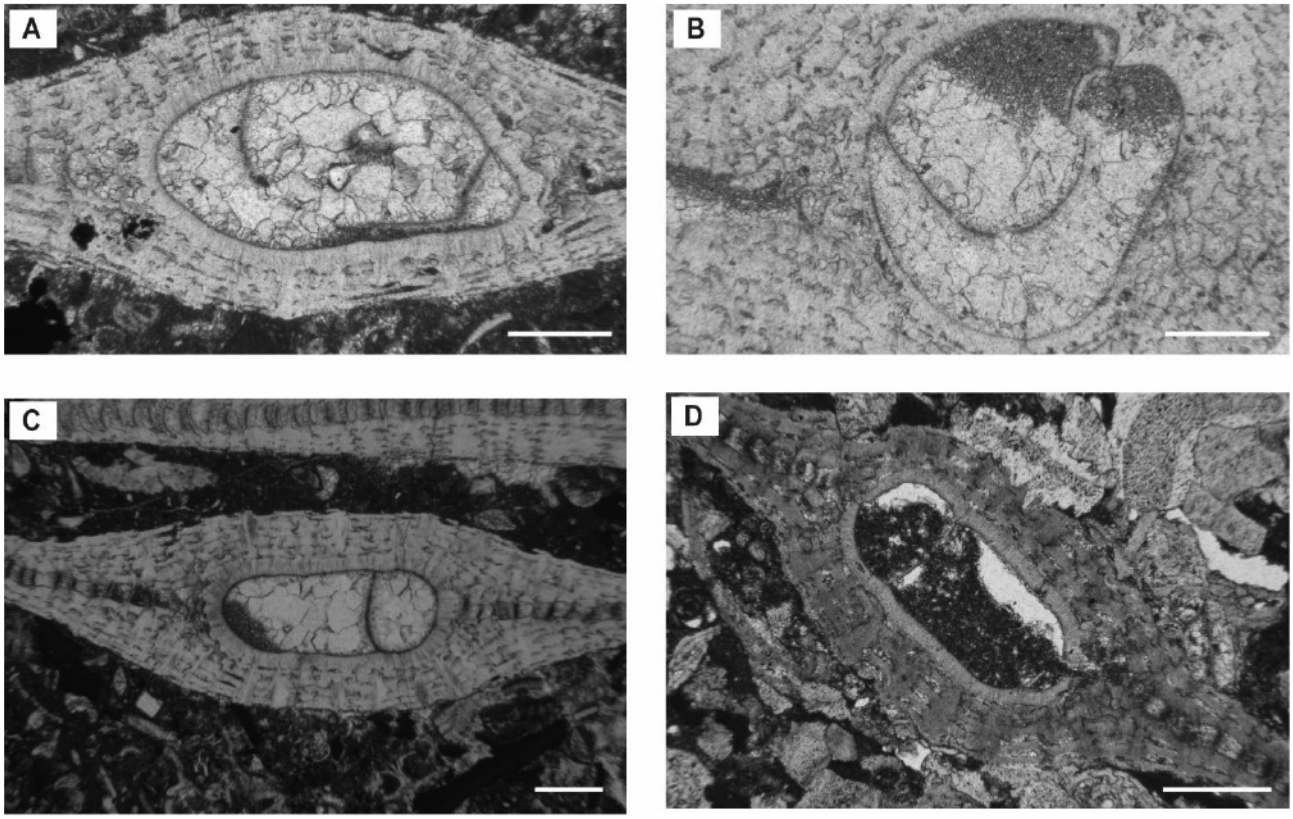

Plate 7. A–D. *Eulepidina* ex. interc. *dilatata* et *formosoides* from Sierra de Marmolance, Spain. A–C: Sample M4S14; D: Sample C16. Scale bar represents 400 µm.

Table 8. Biometric parameters and stratigraphical distribution of *Eulepidina* species present in Sierra de Marmolance (this study). Abbreviations: P, proloculus diameter (mean); A, average degree of embracement of the protoconch by the deuteroconch (mean); D, deuteroconch diameter (mean); Illustr., Illustrations.

Eulepidina species	P (□m)	A (□)	D (□m)	Age	Locality	Illustr.
E. formosoides	428–978 (614)	50–67 (58)	598–1326 (914)	Serravallian	SE Spain	Pl. 6, figs. A–H
*E.*ex.interc. *dilatata* et *formosoides*	550–960 (785)	58	1260–1470 (1374)	Serravallian	SE Spain	Pl. 7, figs. A–D

Remarks. In the western Tethyan area, *Nephrolepidina* is represented by a main evolutive lineage formed by the species *N. praemarginata, N. morgani* and *N. tournoueri* (Cahuzac and Poignant, 1997). *N. praemarginata* has been reported from the upper Rupelian (SBZ 22A) to the lower Chattian (SBZ22B) (e.g. Cahuzac and Poignant, 1997). *N. morgani* has a long stratigraphic range, from the late Chattian to the early Burdigalian (SBZ 23 to the lower part of SBZ 25), partially overlapping with *N. tournoueri*, which spans from the latest Aquitanian to the whole Burdigalian (upper SBZ 24 and SBZ 25) (Cahuzac and Poignant, 1997).

Even if the typological characterization of species is still applied (e.g. Amirshahkarami, 2013), since de Mulder (1975) most authors use a biometric method for the species designation (e.g. Benedetti and Pignatti, 2013; Schiavinotto, 2010; Özcan et al., 2009a, 2010). This method is based on the combination of two biometric parameters: the degree of embracement of the protoconch by the deuteroconch (parameter A), and the number of accessory auxiliary ("adauxiliary") chamberlets (AAC) with direct stolon connection with the deuteroconch (parameter C) (e.g. Özcan et al., 2010). Following those parameters (see fig. 17), *Nephrolepidina* specimens with C_{mean} ranging from 1 to 3 and A_{mean} between 35 and 40 are assigned to *N. praemarginata*; with C_{mean} = 3–5.25; A_{mean} = 40–45 to *N. morgani;* with C_{mean} > 5.25; A_{mean} > 45 to *N. tournoueri*. Intermediate forms are also recognized, using the terminology "ex. interc." (*exemplum intercentrale*).

In randomly sectioned specimens the parameters A and C are difficult to be assessed since centered equatorial sections are required for the measurements. And, even in centered sections, the AAC are hardly visible. Furthermore, the parameter C, since it is directly linked to the embryo size, is likely to be related to environmental factors (such as water temperature and depth) rather than to evolution (e.g. Chapronière, 1980; Schiavinotto and Verrubbi, 1994; Schiavinotto, 1995, 2010; Benedetti and Pignatti, 2013) and therefore this parameter wouldn't be adequate for discriminating the western Tethyan (Mediterranean) chronospecies of *Nephrolepidina* (Benedetti and Pignatti 2013; Ferràndez-Cañadell and Bover-Arnal 2017).

The Marmolance specimens are represented by twenty-four sub-equatorial sections (pl. 8 and 9). The parameter A and the embryo size (by means of D and P diameters) were assessed. Parameter C was not used because no good sections were found to measure it. Along the stratigraphic section, a variation in the embryos size is noted, from smaller to larger, coinciding with an increase in the A parameter that might correspond to the *N. praemarginata-tournoueri* series.

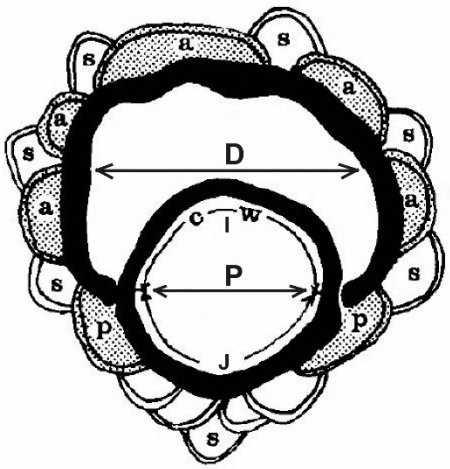

Figure 17. Schematic drawing of the embryonic apparatus of *Nephrolepidina* showing the chamber types and positions of measurements. P is the protoconch; D is the deuteroconch; cw is the common wall between P and D (parameter I); J is the circumference of the lower part of P; p are the primary auxiliary chambers; a are the adauxiliary chambers (AAC); s are the symmetrical chambers. For this specimen parameter C = 5. Modified from Chapronière, 1980, fig. 12, p 166.

Nephrolepidina ex. interc. *morgani* Lemoine and R. Douvillé 1904 et *praemarginata* R. Douvillé 1908

Plate 8. Figures A–H

1975 *L.* ex. interc. *praemarginata-morgani*; De Mulder, pl. 3, fig. 7.
1978 *L.* ex. interc. *praemarginata-morgani*; Van Vessem, no illustrations.
2010 *Nephrolepidina* ex. interc. *morgani* Lemoine and R. Douvillé - *praemarginata* R. Douvillé; Özcan et al., pl. 2, figs. 20–26; text-figure 8.
2015 *Nephrolepidina* ex. interc. *praemarginata-morgani*; Ghafor, fig. 11.7–10.
2019 *Nephrolepidina* ex. interc. *morgani* Lemoine and R. Douvillé et *praemarginata* R. Douvill**é**; Parente and Less, fig. 20F–H.
2018 *Nephrolepidina* ex. interc. *morgani* Lemoine and Douvillé et *praemarginata* R. Douvillé; Less et al., fig. 14. 7–12.

Description. From eighteen sub-equatorial sections were measured the parameter A (A= 37–44; mean 40), as well as the diameter of the protoconch (P = 155–306 µm; mean 228 µm) and deuteroconch (D = 199–398 µm; mean 300 µm). See pl. 8 (for comparison, see De Mulder, 1975: pl. 3, fig. 7; Özcan et al., 2010, pl. 2, figs. 20–26; Ghafor, 2015, figs. 11. 7–10; Less et al., 2018, fig. 14. 7–12; Parente and Less, 2019, fig. 20A–E).

Remarks. Nephrolepidina specimens showing values of parameter A very close to the biometric limit between the two successive species *N. morgani* (A_{mean} = 40–45) and *N. praemarginata* (A_{mean} = 35–40) were assigned to this group (Table 9). It could represent, as proposed by Özcan et al., 2010, a primitive developmental stage of *N. morgani.*

Comparing with the literature, similar values have been reported from Iraq (Ghafor, 2015: P_{mean} = 274 µm; D_{mean} = 322 µm; A_{mean} = 40.2 µm), eastern Turkey (Özcan et al., 2010: P_{mean} = 212.6 µm; D_{mean} = 309.4 µm; A_{mean} = 42.4 µm), northwestern India (Van Vessem, 1978: P_{mean} = 255 µm; D_{mean} = 346 µm; A_{mean} = 41.5 µm; Less et al., 2018: P_{mean} = 233 µm; D_{mean} = 315 µm; A_{mean} = 41.04 µm), southern Italy (Parente and Less, 2019: P_{mean}=212.9 µm; D_{mean} = 297.9 µm; A_{mean} = 40.1 µm), western Greece (de Mulder, 1975: P_{mean} = 231 µm; D_{mean} = 308 µm; A_{mean} = 35 µm). All of them ascribed to the *Nephrolepidina* ex. interc. *morgani–praemarginata* group.

Stratigraphical distribution: In Sierra de Marmolance, those forms occur mostly in the lower-middle part of the succession (section A, samples C-14, C-16, C-18; section B, samples M1S14, M1S16, M2S1, M2S3, M2S5, M2S9, M3S16), in the Lepidocyclinid facies, associated with *Operculina complanata, Neorotalia viennoti, Eulepidina formosoides, Nephrolepidina tournoueri* and *Nummulites fichteli* (see fig. 7; table 3.3).

In the literature, *N. morgani–praemarginata* has been reported from the late Oligocene (Chattian) to the early Miocene (Burdigalian) (Cahuzac and Poignant, 1997).

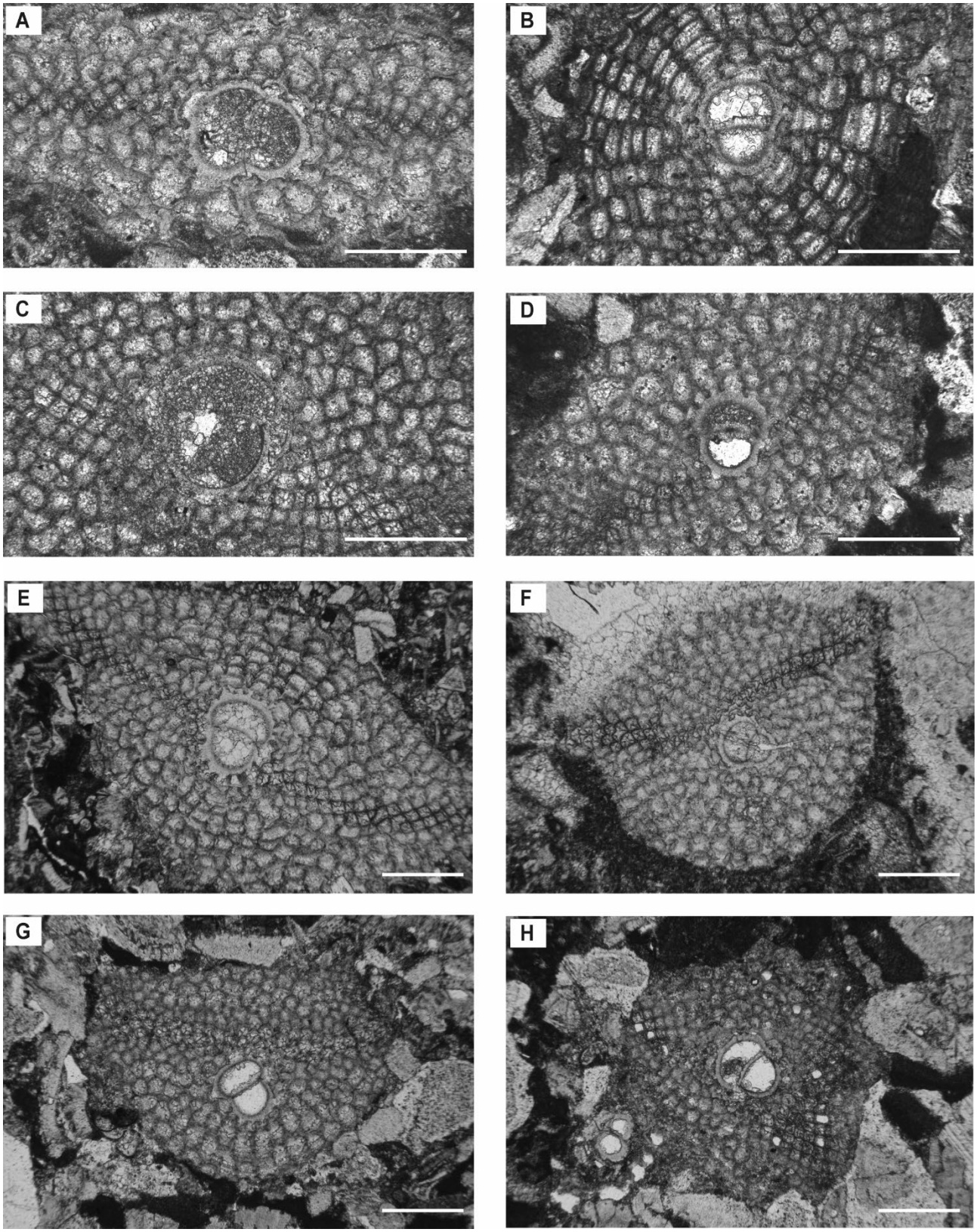

Plate 8. A–H. *Nephrolepidina* ex. interc. *morgana* et *praemarginata* from Sierra de Marmolance, Spain. A: Sample C-14; B, C: Sample M2S1; D: Sample C-16; E: Sample M1S14; F: Sample M2S16; G: Sample M2S9; H: Sample C18. Scale bar represents 400 µm.

Nephrolepidina tournoueri Lemoine and Douvillé 1904

Plate 9. Figures A–D

1975 *Lepidocyclina (Nephrolepidina) tournoueri* Lemoine and R. Douvillé; De Mulder, pl. 3, fig. 10; pl. 4, figs. 1–3.
1990 *Nephrolepidina tournoueri* Lemoine and R. Douvillé; Giovagnoli and Schiavinotto, pl. 1, figs. 1–4; pl. 2, figs. 1–6.
2009a *Nephrolepidina* ex. interc. *tournoueri-morgani* Lemoine and Douvillé; Özcan et al., fig. 15. 14; fig. 16.

Description. From six sub-equatorial sections were measured the A parameter (A = 45–46; mean 46), as well as the diameter of the protoconch (P = 224–466 μm; mean 317 μm) and deuteroconch (D = 379–574 μm; mean 453 μm).

Remarks. Populations of *Nephrolepidina* showing values of parameter A equal or higher than 45 were assigned to *N. tournoueri* (Table 9).

Comparing with the literature, similar values of *Nephrolepidina* identified as *N. tournoueri* have been reported from Greece (de Mulder, 1975: P_{mean} = 296 μm; D_{mean} = 460 μm; A_{mean} = 44.8 μm) and Italy (Giovagnoli and Schiavinotto, 1990: P_{mean} = 377 μm; D_{mean} = 485 μm; A_{mean} = 47.51 μm). Also, comparable values of *Nephrolepidina* specimens ascribed to *N. tournoueri–morgani* have been reported from southwestern Turkey (Özcan et al., 2009a: P_{mean} = 280.9 μm; D_{mean} = 440.5 μm; A_{mean} = 46.07 μm).

Stratigraphical distribution. In Sierra de Marmolance, those forms occur in the lower-middle part of the succession (section B, samples M1S14, M2S11, M2S13; section A, sample C-16), in the Lepidocyclinid facies, associated with *Operculina complanata, Neorotalia viennoti, Eulepidina formosoides, Nephrolepidina* ex.interc. *morgani* et *praemarginata* and *Nummulites fichteli* (see fig. 7; table 3.3) and in the upper part of the succession (section B, sample M5S4), in the *Neorotalia* with *Risananeiza* facies, together with *Neorotalia viennoti, Risananeiza crassaparies, Heterostegina assilinoides, Austrotrillina brunni, Austrotrillina striata, Eulepidina* ex.interc. *dilatata* et *formosoides, Spiroclypeus* sp. and *Borelis inflata* (see fig. 7; table 3.5).

In the literature, *N. tournoueri* has been reported from the latest Aquitanian to the whole Burdigalian (upper SBZ 24 and SBZ 25; Cahuzac and Poignant, 1997).

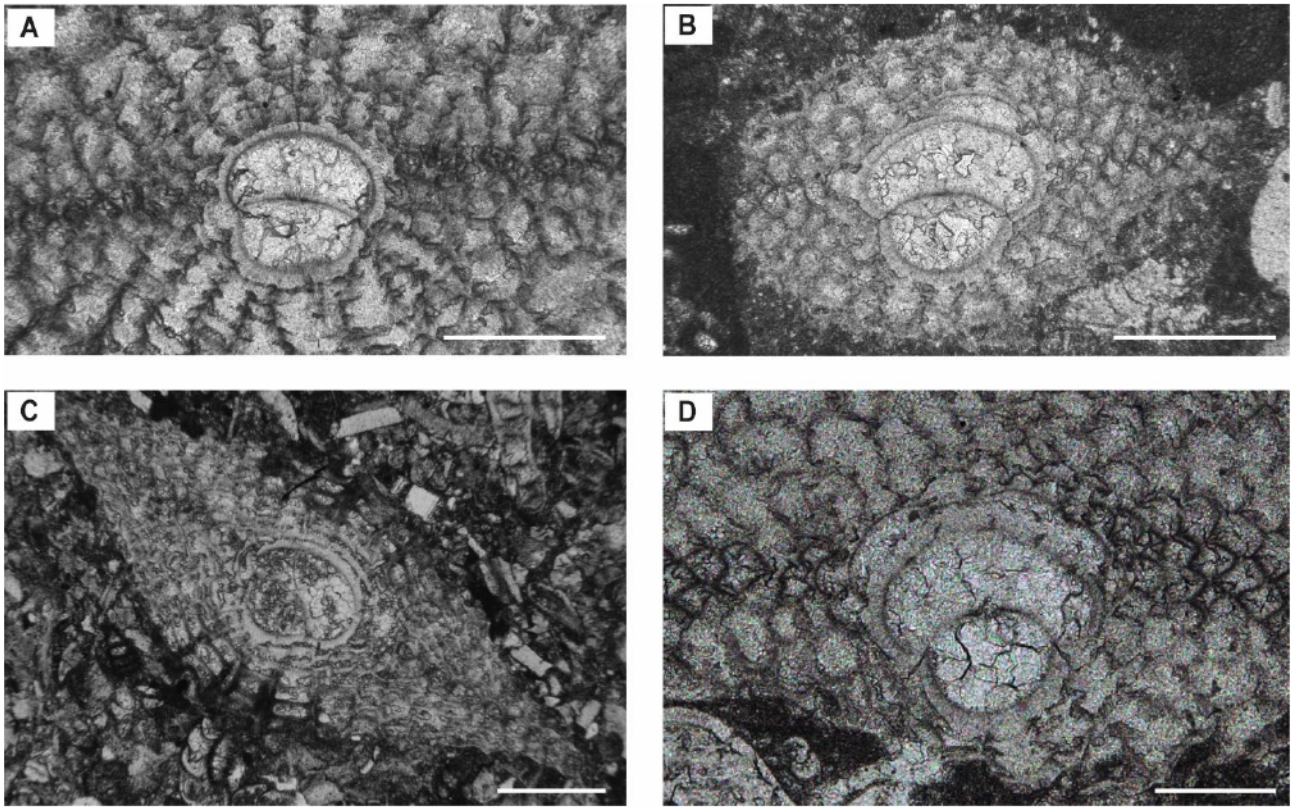

Plate 9. A–D. *Nephrolepidina tournoueri* from Sierra de Marmolance, Spain. Scale bar represents 400 µm. A, D: Sample M5S4; B: Sample M2S13; C: Sample M1S14. Scale bar represents 400 µm.

Table 9. Biometric parameters of *Nephrolepidina* species found in Sierra de Marmolance. Abbreviations: P, proloculus diameter (mean); A, average degree of embracement of the protoconch by the deuteroconch (mean); D, deuteroconch diameter (mean); Illustr., Illustrations.

Nephrolepidina species	Prol. (□m)	A (□)	D (□m)	Age	Locality	Illustr.
N. ex. interc. *morgani* et *praemarginata*	155–306 (228)	37–44 (40)	199–398 (300)	Serravallian	SE Spain	Pl. 8, figs. A–H
N. tournoueri	224–466 (317)	45–46 (46)	379–574 (453)	Serravallian	SE Spain	Pl. 9, figs. A–D

Family ROTALIIDAE Ehrenberg, 1839

Genus *NEOROTALIA* Bermúdez, 1952

Neorotalia viennoti (Greig, 1935)

Plate 10. Figures A–H

1935 *Rotalia viennoti* n. sp., Greig, pl. 58, figs. 1–14.
2007 *Neorotalia viennoti* Greig; Bassi et al., pl. 3, figs. 1–7.
2013 *N. tethyana* n. sp.; Boudagher-Fadel and Price, pl. 1, figs. 2–4.
2014 *Neorotalia viennoti* Greig; Hottinger, fig. 8.1 A–D, p. 157.
2017 *Neorotalia viennoti* Greig; Ferràndez-Cañadell and Bover-Arnal, fig. 3F; 13A–L.

Description. The studied specimens are almost in sub-axial and oblique sections showing a trochospiral test with a thick ventral pile that lead to an asymmetrical outline in axial section. The proloculus is c. 111 µm in diameter.

Remarks. *Neorotalia* Bermúdez is characterized by a spiral umbilical canal closed by a cover (enveoloping canal system due to secondary lamination). This cover extends from the ventral adaxial chamber wall to the heavy-ornamented umbilicus. The presence of a compound axial plug and an apertural lip (representing the serrated end of the toothplate) is also characteristic of all neorotaliids (Loeblich and Tappan, 1987; Bassi et al., 2007; Hottinger 1991, 2014; Ferràndez-Cañadell and Bover-Arnal, 2017; fig. 18).

The two species distinguished in the Oligocene are *N. lithothamnica* (Uhlig, 1886) and *N. viennoti* (Greig, 1935). *N. lithothamnica* differs from *N. viennoti* in having a lower trochospiral test, a less protruding ventral area with pustules and a nearly symmetrical shape in axial section. The chamber outline in axial section is less triangular and with the distal end more rounded than in *N. viennoti.* Ferràndez-Cañadell and Bover-Arnal (2017) consider *N. tethyana* Boudagher-Fadel and Price, 2013 a possible younger synonym of *N. viennoti*, whereas Cahuzac and Poignant (2005) refer *N. burdigalensis* (d'Orbigny, 1852) as a synonym of *N. lithothamnica*. Hottinger et al. (1991) pointed out that the architecture of *N. viennoti* is identical to that of *N. calcar* and *N. mexicana* (fig. 18). Cahuzac and Poignant (1997) stated that *Neorotalia* species are still present in the middle Miocene, such as *N. aculeata* (d'Orbigny) in the Serravallian. A revision of *Neorotalia* species would confer them a more precise biostratigraphic usefulness for the Oligocene (Hottinger, 2014). In addition, it could clarify the phylogenetic relationships with miogypsinids (Ferràndez-Cañadell and Bover-Arnal, 2017).

The Marmolance specimens are comparable to those reported in the literature for *N. viennoti* (e.g. Greig 1935, from Palestine; Bassi et al., 2007, from Italy; Boudagher-Fadel and Price, 2013, from the Indo-Pacific, as *N. tethyana*; Hottinger 2014, from Middel East; Ferràndez-Cañadell and Bover-Arnal 2017, from Spain). They show similar proloculus size than other western Mediterranean specimens (*e.g.* Ferràndez-Cañadell and Bover-Arnal, 2017: c. 115 µm, southeastern Spain; Bassi et al., 2007: 120–160 µm, northeastern Italy) and smaller than those reported from eastern Meditarranean (e.g. Greig, 1935: 200 µm, Ramleh, Palestine).

Stratigraphic distribution. In Sierra de Marmolance, *N. viennoti* specimens occur mainly in the upper part of the succession (section B, samples M4S7, M4S9, M4S10, M4S11, M4S12, M4S14, M4S17, M5S3, M5S4, M5S5, M5S6, M5S7, M5S10, M5S11), in the *Neorotalia* with *Risananeiza* facies, associated with *Risananeiza crassaparies, Heterostegina assilinoides, Austrotrillina brunni, Austrotrillina striata, Nephrolepidina tournoueri, Spiroclypeus* sp. and *Borelis inflata* (see fig. 7; table 3.5). but also is present in the middle part of the succession (section A, samples C-14, C-16; section B, samples M2S11, M2S12, M3S3, M3S4, M3S5, M3S6, M3S13, M3S18; section C, samples M6S28, M6S30; section D, samples M8S32, M8S35, M8S36, M8S48,

M8S59), in the Lepidocyclinid facies, associated with *Operculina complanata, Eulepidina formosoides, Nephrolepidina* ex.interc. *morgani* et *praemarginata, Nephrolepidina tournoueri* and *Nummulites fichteli* (see fig. 7; table 3.3).

In the Mediterranean realm, *N. viennoti* has been recorded from the Maestrichtian up to the Oligocene (e.g. Greig, 1935, in Palestine; Ferràndez-Cañadell and Bover-Arnal, 2017, in southern Spain).

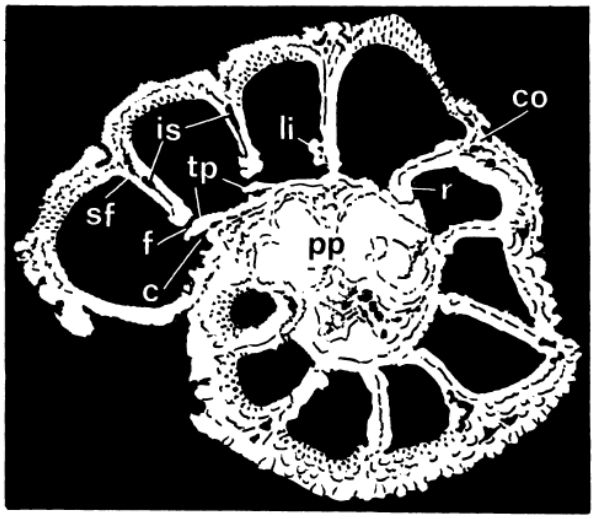

Figure 18. *Neorotalia mexicana* (Nuttall), early Miocene, Victoria, Australia. Reinterpreted drawings of a SEM photo of a horizontal section (from Hansen and Reiss, 1971). Abbreviations: c, canal (formed by toothplate); co, cover of interlocular space (enveloping system); f, intercameral foramen; is, intraseptal interlocular space; li, apertural lip; pp, compound plug; r, retral bend; sf, septal flap; tp, toothplate. From Hottinger et al. (1991, fig. 3).

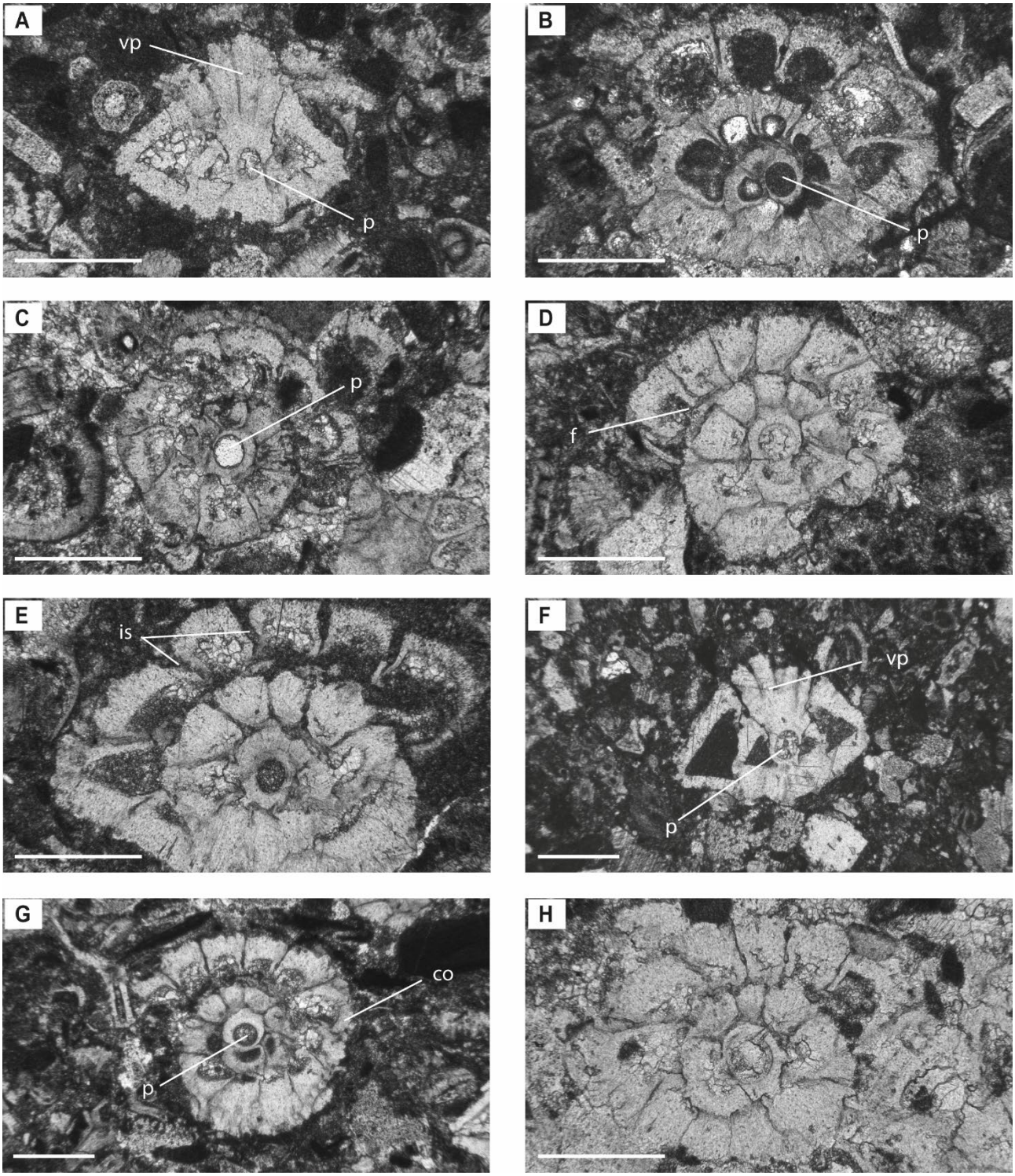

Plate 10. A–H. *Neorotalia viennoti* from Sierra de Marmolance. Axial (A, F), oblique (B, E) and equatorial sections (C, D, G, H). Notice the thick ventral pile (vp) and asymmetrical outline in axial sections. A. Sample M8S59; B. Sample C-16; C. Sample M2S11; D. Sample M3S13; E. Sample M4S14; F. Sample M5S3; G. Sample M5S4; H. Sample M5S6. Abbreviations: p, proloculus; vp, ventral pile; f, intercameral foramen; is, intraseptal interlocular space; co, cover of interlocular space. Scale bar represents 400 μm.

Family ORNATOROTALIIDAE Benedetti 2015

Subfamily Cuvillierininae Loeblich and Tappan 1964
Genus *Risananeiza* Boukhary, Kuss and Abdelraouf 2008
Type species. *Risananeiza pustulosa* Boukhary, Kuss and Abdelraouf, 2008

Remarks. According to the two *Risananeiza* species known in literature (*R. pustulosa, R. crassapiles*), the test size, the chamber size in equatorial plane and the numbers of chambers in the last whorl are reliable characters at species level.

Risananeiza crassaparies Benedetti and Briguglio 2012

Plate 11. Figures A–H

2012 *Risananeiza crassaparies* n. sp., Benedetti and Briguglio, figs. 3a–g, 4a–e; pl. 1, figs. 1–13; pl. 2, figs 1–15.

Description. Specimens show a shell diameter ranging from 0.99 to 1.78 mm. Test thickness from 0.67 to 0.95 mm. Ratio h/w (chamber height/chamber width) is c. 1.6. The subspherical proloculus ranges in sieze from 0.074–0.182 mm (mean 0.12 mm), similar than the deuteroconch. No or very very rare B-form were found.

Remarks. The occurrence in both shell sides of thick continuous piles with dorsal and ventral vertical funnels between the piles, incised sutures and intraseptal canals provide clear evidence that the studied specimens belong to *Risananeiza* (fig. 19).

Kuss and Boukhary (2008, p. 69) introduced the new genus *Risananeiza* with the name *R. nodosa* from the upper Oligocene Wadi Arish Formation at Gebel Risan Aneiza (Sinai). The authors did not describe and illustrate the taxon. This name does not meet the requirements of Articles 11 and 13.1 of the ICZN and, therefore, it is a *nomen nudum*. Successively, Boukhary et al. (2008) mentioned *R. nodosa* (p. 186) in the taxonomic remarks regarding the new species *R. pustulosa*, which is the available name and type species of this genus.

Risananeiza differs from *Neorotalia mexicana* Bermúdez, 1952 (type species) in having coarse pustules on both sides of the test and in lacking the ventral wide plug and the chambers surrounding the boss. In addition, the narrow aperture of *Neorotalia mexicana* extends from the umbilicus to the periphery, while the basal aperture in *Risananeiza* is in the peripheral view (Boukhary et al., 2008).

R. pustulosa differs from *R. crassaparies* in having larger test and chamber sizes (Boukhary et al., 2008; Benedetti and Briguglio, 2012). Proloculus size is not a distinctive character because in *R. pustulosa* is 0.90–0.140 mm and in *R. crassaparies* is 0.90–0.225 mm (Ferràndez-Cañadell and Bover-Arnal, 2017). In general, the megalospheric form of *R. pustulosa* is larger than that of *R. crassaparies* (Table 10).

Specimens from Marmolance show comparable test size to *R. crassaparies* and the same number of chambers in the last whorl. The proloculus diameter is smaller and comparable in size to the deuteroconch. In *R. pustulosa* and *R. crassaparies* the proloculus is larger than the deuteroconch (Table 10).

Stratigraphic and geographic distribution. *R. pustulosa* and *R. crassaparies* have been so far reported from Chattian deposits of western Tethys (Spain, southern Italy, Egypt). Ferràndez-Cañadell and Bover-Arnal (2017) pointed out that possible Chattian records of *Neorotalia*, *Rotalia* and *Bozorgniella* Rahaghi, 1973 have likely to be assigned to *Risananeiza*. Nonetheless, the lower Miocene *Bozorgniella* record from the Qom Formation (Iran; Daneshian and Dana, 2007, fig. 6/3 as *Elphidium* sp.) needs confirmation (Table 11).

In Sierra de Marmolance, *R. crassaparies* occurs in the middle-upper part of the succession (section B, samples M4S10, M4SS11, M4S14, M5S3, M5S4, M5S6, M5S7), in the *Neorotalia* with *Risananeiza* microfacies, together with *Neorotalia viennoti, Heterostegina assilinoides, Austrotrillina brunni, Austrotrillina striata, Borelis inflata, Nephrolepidina tournoueri* and *Eulepidina* ex.interc. *dilatata* et *formosoides* (see fig. 7; table 3.5). A similar association has been described from southern Italy (Benedetti and Briguglio 2012, p. 167) and Spain (Ferràndez-Cañadell and Bover-Arnal, 2017). In Italy, *R. crassaparies* has been found associated with *Eulepidina dilatata*, *Nephrolepidina morgani*, *Miogypsinoides* ex. interc. *complanatus–formosensis*, *Neorotalia viennoti*, *Operculina complanata, Heterostegina assilinoides, Amphistegina* sp. and *Austrotrillina* sp.

R. crassaparies seems to occur only in the western Tethys, limited to the SBZ23 (Benedetti and Briguglio, 2012), having its last occurrence in the westernmost Mediterranean (southeastern Spain) in the Serravallian.

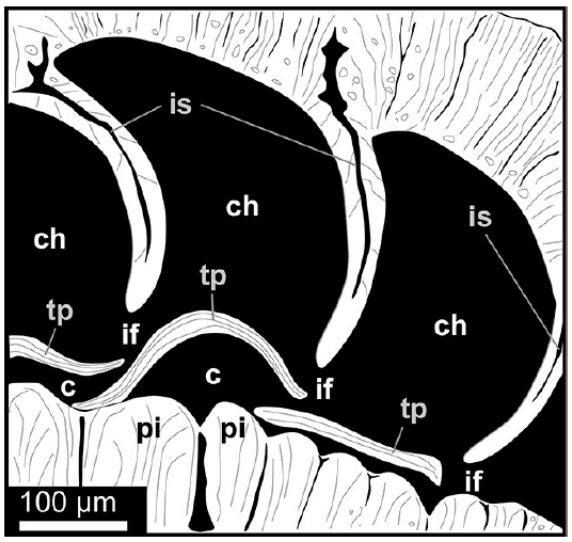

Figure 19. *Risananeiza crassaparies* from Porto Badisco. Interpreted drawing of an equatorial microspheric specimen. Abbreviations: c, canal formed by toothplate; ch, chamber lumen; if, intercameral foramen; is, intraseptal canal system; pi, pile; tp, toothplate. Scale bar represents 100 µm. From Benedetti and Briguglio (2012, fig. 5).

Table 10. Shell parameters measured in *Risananeiza* specimens from Marmolance (this study). Comparison with *R. pustulosa* (Boukhary et al., 2008) and *R. crassaparies* (Benedetti and Brigulio, 2012). Abbreviations: D, shell diameter; deut, deuteroconch; h, chamber height; m, mean; no., number; prol., proloculus; T, shell thickness; w, chamber width; B-, B-forms. All measures in mm.

Shell parameters	*R. pustulosa*	*R. crassaparies*	**This study**
D	0.925–2.9 (B-, 5.375)	1.10–1.81 (B-, 1.59–3.82)	0.99–1.78
T	0.55–1.625 (B-, 1.25)	0.6–0.9 (B-, 0.86–1.37)	0.67–0.95
Proloculus	0.15–0.25 (prol>deut)	0.09–0.225 (prol>deut), mean 0.159	0.074–0.182 (prol~deut), mean 0.120
h/w	-	1.7	1.5 (1.6)
no. chambers in the last whorl	15–16	13–15	13–15

Table 11. Stratigraphic and palaeogeographic distribution of *Risananeiza* species.

Referred to as	**References**	**Age**	**Locality**	**Illustrations**
R. pustulosa	Didon *et al.* 1961	Oligocene	SE Spain	pl. 1R
Pararotalia cf. *lithothamnica*	Bassi *et al*. 2007	Chattian	NE Italy	pl. 3, fig 8
R. pustulosa	Boukhary *et al*. 2008	Chattian	N Sinai	pl. 1, figs 1–18
R. pustulosa	Işik 2010	Oligocene	S Turkey	pl. 7, figs 1–16; pl. 8, figs 1–20
R. pustulosa	Sirel and Işik 2011	late Chattian	S Turkey	pl. 3, figs 1–13; pl. 4, figs 1–19
R. crassaparies	Benedetti and Brigulio 2012	late Chattian	S Italy	figs 3a–g; pl. 1, figs 1–13; pl. 2, figs 1–15
R. sp.	Benedetti and Brigulio 2012	late Chattian	S Italy	fig. 1
R. pustulosa	Ferràndez-Cañadell and Bover-Arnal 2017	late Chattian	SE Spain	figs 3J, 14A–N
R. crassaparies	**This study**	Serravallian	SE Spain	Pl. 11, figs A–H

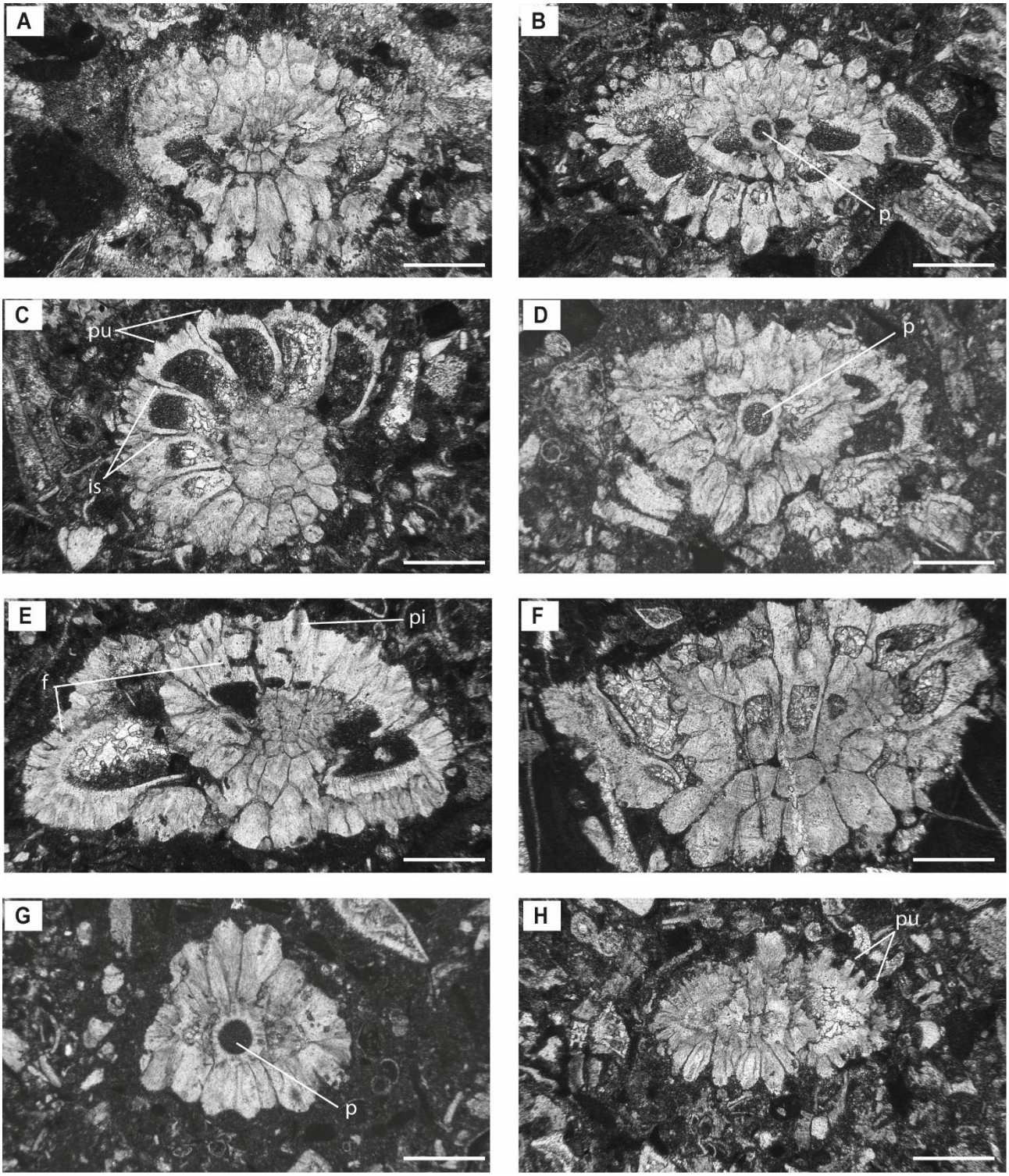

Plate 11. A–H. *Risananeiza crassaparies* from Sierra de Marmolance. A, B, D, E, F: Oblique sections; C: Sub-equatorial section; G, H: Sub-axial sections. Notice the ornamented test with coarse pustules (pu) and thick continuous piles (pi); chamber lumen higher than wide (C). A: Sample M4S10; B. Sample M4S14; C–E. Sample M4S14; F. Sample M5S2; G, H. Sample M5S4. Abbreviations: p, proloculus; pi, piles; pu, pustules; is, intraseptal canals; f, funnels. Scale bar represents 400 µm.

Superfamily MILIOLACEA Ehrenberg, 1839

Family AUSTROTRILLINIDAE Loeblich and Tappan, 1986
Genus AUSTROTRILLINA Parr, 1942

Remarks. The studied specimens were subdivided in two groups: with fine parapores and coarse parapores in the parakeriotheca covered by a thin tectum (Bassi et al., 2021a). The characters of the first group are diagnostic of *Austrotrillina brunni* Marie (in Brunn et al., 1955), whereas those of the second group of *Austrotrillina striata* Todd and Post, 1954. See Chapter 2 (Bassi et al., 2021a) for more details about *Austrotrillina*.

Austrotrillina brunni Marie, 1955

Plate 12. Figures B, C

1968 *Austrotrillina asmariensis* sp. nov. Adams, pp. 82–83, pl. 1, figs 1–12.
1968 *Austrotrillina brunni* Marie; Adams, pl. 6, figs 6, 8.
2013 *Austrotrillina brunni* Marie; Sirel et al., p. 106, pl. 11, figs 2–17.
2014 *Austrotrillina brunni* Marie; Gedik, pl. 3, figs 12–16, 18–22.
2014 *Austrotrillina asmariensis* Adams; Gedik, pl. 3, fig. 25; pl. 4, figs 1–13.
2016 *Austrotrillina brunni* Marie; Serra-Kiel et al., fig. 14, 17–19; fig. 16, 1–11.
2017 *Austrotrillina asmariensis* Adams; Ferràndez-Cañadell and Bover-Arnal, p. 88, fig. 3A; fig. 4A–G.
2018 *Austrotrillina asmariensis* Adams; Boudagher-Fadel, pl. 6.3, figs. 7–9; pl. 7.1, figs. 8–9.
2021a *Austrotrillina brunni* Marie; Bassi et al., fig. 3.

Description. Specimens with fine parapores, nepionic apparatus (prolоculi c. 250 μm in diameter) with narrow flexostyle and no parakeriotheca.

Remarks. *A. asmariensis* is considered as a junior synonym of *Austrotrillina brunni*, since the types of *A. asmariensis* (Adams, 1968, pl. 1, figs. 1–12) cannot be morphologically separated from the ones of *A. brunni* (Bassi et al., 2021a).

Comparing with literature, similar shell characters ascribed to *A. brunni/A. asmariensis* have been reported from the Philippine sea (e.g. Adams, 1968), Turkey (e.g. Sirel et al., 2013; Gedik, 2014), Spain (Ferràndez-Cañadell and Bover-Arnal, 2017; Bassi et al., 2021a), Japan (Bassi et al., 2021a), Iran (Boudagher-Fadel, 2018), Iraq (Boudagher-Fadel, 2018), Oman and Yemen (e.g. Serra-Kiel et al., 2016).

Stratigraphic distribution. In Sierra de Marmolance, those forms occur in the upper part of the succession (section B; samples M4S7 and M4S9), in the *Neorotalia* with *Risananeiza* facies, associated with *Risananeiza crassaparies, Neorotalia viennoti, Heterostegina assilinoides, Austrotrillina striata, Nephrolepidina tournoueri, Spiroclypeus* sp. and *Borelis inflata* (see fig. 7; table 3.5).

A. brunni ranges from the Rupelian to the Serravallian in the western Tethys, disappearing after the eastern closure of the Mediterranean Sea (Bassi et al., 2007, text-fig. 9; fig. 10). Nonetheless, Boudagher-Fadel and Lokier (2005, fig. 3) considered *A. striata* and *A. brunni* restricted to the early Miocene. *Austrotrillina brunni* shows a wide geographical distribution from the western Tethys (e.g. Gallardo et al., 2001; Bassi et al., 2007; Ferràndez-Cañadell and Bover-Arnal, 2017; Bassi et al., 2021a) to western Australia (Riera et al., 2019; table 2). In the Mediterranean area, the Serravallian records are represented by the studied specimens from the Sierra de Marmolance (Bassi et al., 2021a), while no Serravallian specimens have been found in the Middle East.

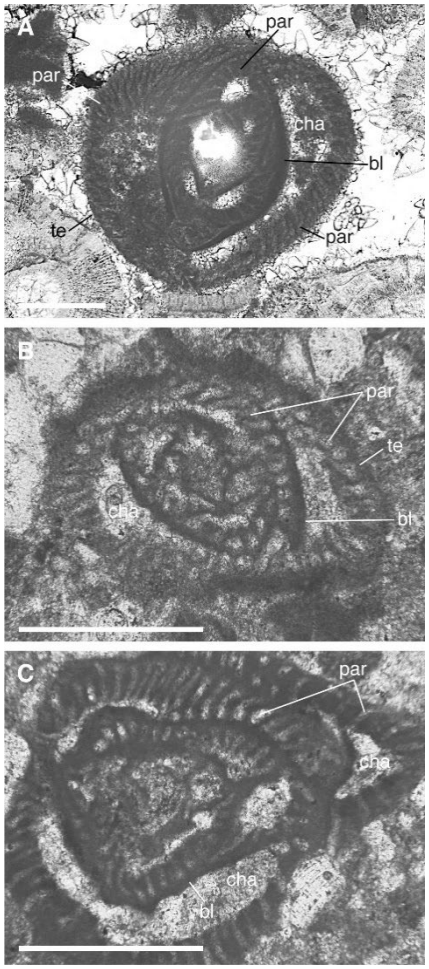

Plate 12. *Austrotrillina brunni* Marie in Brunn et al., 1955. A. Tangential sub-transversal section showing the fine parakeriotheca and the basal layer; Burdigalian–Langhian boundary, Kita-daito-jima, Hanzawa's (1940) collection, sample 835 (202.66 m); Institute of Geology and Paleontology, Graduate School of Science, Tohoku University (IGPS), Sendai, Japan. B–C. Tangential sections of deformed specimens showing the fine parakeriotheca coated by the tectum; Serravallian, Sierra de Marmolance. Abbreviations: bl, basal layer; cha, chamber; par, parapores; te, tectum. Scale bars represent 250 µm. After Bassi et al. (2021a, fig. 3).

Austrotrillina striata Todd and Post, 1954

Plate 13. Figures A–F

1968 *Austrotrillina striata* Todd and Post; Adams, pp. 92–93, pl. 4, figs 1–13; pl. 6, fig. 9.
1973 *Austrotrillina striata* Todd & Post; Adams, pl. 1, fig. 4.
2016 *Austrotrillina* sp.; Roozpeykar and Moghaddam, fig. 9A.
2016 *Austrotrillina striata* Todd and Post; Serra-Kiel et al., figs 14, 15–16; fig. 16, 12–21.
2018 *A. striata* Todd and Post; Boudagher-Fadel, pl. 7.1, figs 4–7.
2021a *Austrotrillina striata* Todd and Post; Bassi et al., figs. 4–6.

Description. Specimens with coarse parapores, nepionic apparatus (proloculus c. 130 µm in diameter) with flexostyle and no parakeriotheca in the first three chambers.

Remarks. Comparing with literature, similar shell characters ascribed to *Austrotrillina striata* have been reported from the Philippine sea (e.g. Adams 1968, 1973; Boudagher-Fadel, 2018), Iran (e.g. Roozpeykar and Moghaddam, 2016), Spain, Japan (e.g. Bassi et al., 2021a), Oman and Yemen (e.g. Serra-Kiel et al., 2016).

Stratigraphic distribution: In Sierra de Marmolance, these forms occur in the middle-upper part of the succession (section B; samples M3S10, M3S12, M3S13, M3S14, M3S18, M4S11, M5S10), in the *Neorotalia* with *Risananeiza* facies, associated with *Risananeiza crassaparies, Neorotalia viennoti, Heterostegina assilinoides, Austrotrillina brunni, Nephrolepidina tournoueri, Spiroclypeus* sp. and *Borelis inflata* (see fig. 7; table 3.5).

Austrotrillina striata appears from the Rupelian in the western Tethys (Middle East) and from the Chattian in the Indo-Pacific area (Indonesia; table 3 in Bassi et al., 2021a). In the Middle East, this species disappears in the early Burdigalian (e.g. Roozpeykar and Moghaddam, 2016; Daneshian and Dana, 2019). In the western Tethys, the two records from the Rupelian and Chattian of southeastern Spain (Hottinger, 1963; see also Adams, 1968; Ibi, Bassi et al., 2021a) are followed by a Serravallian occurrence in the southeastern Spain (Bassi et al., 2021a).

In the Pacific area, *Austrotrillina striata* ranges from the Rupelian (Eniwetok, Todd and Low, 1960; Midway Atoll, Cole, 1969; Todd and Post, 1970) to the middle Miocene (western Australia; Adams, 1984; Chapronière, 1984; Lunt and Allan, 2004; Langhian in Kita-daito-jima, Bassi et al., 2021a). This latter occurrence represents the northernmost record in the western Pacific marking the limit of shallow-water carbonate depositional systems. In Indonesia, it has been recorded from Tf1, roughly equivalent to the Burdigalian (Novak, 2014). The Serravallian record from southeastern Spain represents the last occurrence of this species in the Mediterranean area (table 3 in Bassi et al., 2021a).

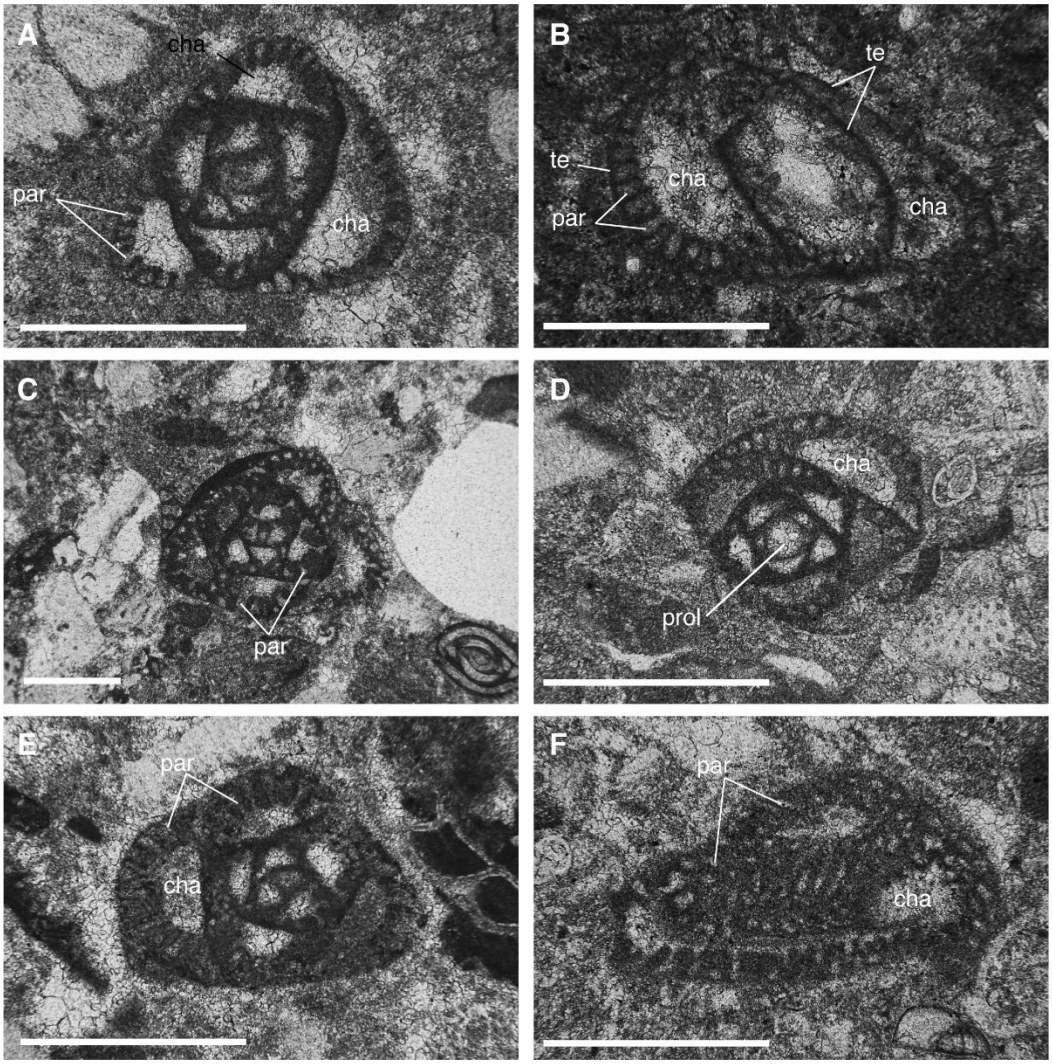

Plate 13. *Austrotrillina striata* Todd and Post, 1954; Serravallian, Sierra de Marmolance (southeastern Spain). A, C–E. Sub-transversal sections showing the miliolid trilocular growth and the coarse parakeriotheca underlying the tectum. B, F. Tangential sections of deformed specimens. Abbreviations: cha, chamber; par, parapores; prol, proloculus; te, tectum. Scale bars represent 250 µm. After Bassi et al. (2021a, fig. 6).

Superfamily ALVEOLINOIDEA Ehrenberg, 1839
Family BORELIDAE Schmarda, 1871
Subfamily BORELINAE Schmarda, 1871
Genus *BORELIS* de Montfort, 1808

The porcelaneous larger foraminifera are represented by sub-ellipsoidal tests with septula aligned from chamber to chamber and only preseptal passages present, and by tests with an exoskeletal parakeriotheca. The sub-ellipsoidal tests were ascribed to *Borelis* de Montfort, 1808 (*B. inflata*), whereas the parakeriotheca tests to *Austrotrillina* Parr 1942 (*A. brunni, A. striata*).

Borelis inflata (Adams, 1965)

Plate 14. Figs. A, B

1965 *Neoalveolina inflata* s. nov; Adams, p. 325, pl. 25, figs d–j.
2010 *Borelis inflata* Adams; Benedetti, p. 201, pl. 1, fig. 6.
2011 *Borelis inflata* Adams; Braga and Bassi, fig. 5B.
2021b *Borelis inflata* Adams; Bassi et al., fig. 3, p. 383.

Description. The specimens ascribed to *Borelis inflata* (Adams 1965) show tightly coiled shells, ellipsoidal in shape, with diameters c. 0.6 mm and length around 1.2 mm. Since no totally centered sections were found, the proloculus could not be measured (is estimated in c. 35 □m in diameter). No Y-shaped septula were recognized.

Remarks. Borelis inflata is characterized by a shell size of 0.5–1.5 mm in diameter and 0.4–1.2 mm length, with a proloculus diameter ranging from 30 to 70 □m and absence of Y-shaped septula (fig. 20; figs. 3, 8 and table 1 in Bassi et al., 2021b).

The Marmolance specimens are comparable to those reported for *B. inflata* in the literature (e.g. Adams 1965, from Sarawak; Benedetti 2010, from southern Italy; Braga and Bassi 2011, from southern Spain; Bassi et al., 2021b, from northern Italy).

Stratigraphic distribution. In Sierra de Marmolance, *B. inflata* occurs in the upper part of the succession (section B; sample M4S1 and M5S11), in the *Neorotalia* with *Risananeiza* facies, associated with *Risananeiza crassaparies, Neorotalia viennoti, Heterostegina assilinoides, Austrotrillina brunni, Austrotrillina striata, Nephrolepidina tournoueri* and *Spiroclypeus* sp. (see fig. 7; table 3.5).

In the western Mediterranean region, *B. inflata* has been recorded from the SBZ21 or Rupelian (Aquitaine basin; Cahuzac and Poignant, 1997) to the SBZ26 or Tortonian (Stazzano; Bassi et al., 2021b).

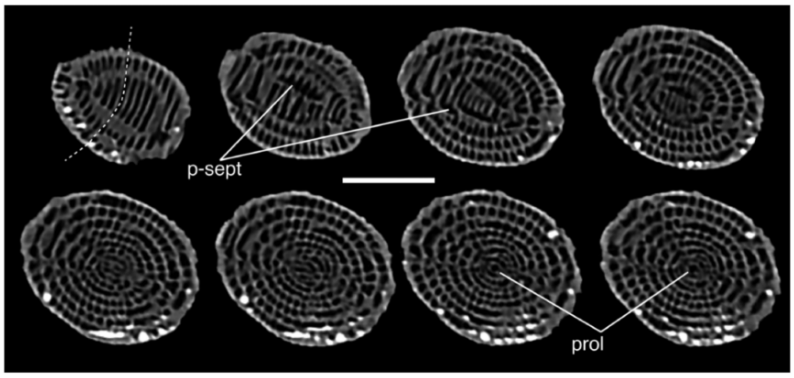

Figure 20. *Borelis inflata* (Adams, 1965). Tortonian, Sant'Agata Fossili Marl Formation cropping out in the Stazzano area (northwestern Italy). Micro-computed tomographic analysis of a megalospheric specimen illustrating the preseptal passages (p-sept) and the proloculus (prol). Note the absence of Y-shaped septula. Scale bar is 0.50 mm. After Bassi et al., 2021b, fig. 3.

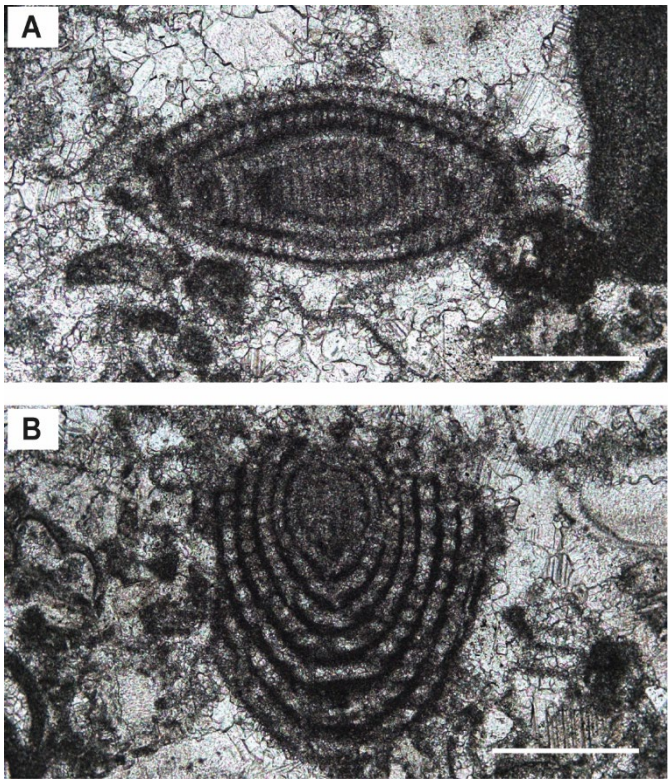

Plate 14. A, B. *Borelis inflata* from Sierra de Marmolance (southeastern Spain). Scale bar represents 400 μm. A, B. Sub-axial sections. Sample M5S11.

4.5. Biostratigraphy

The LBF assemblage from Sierra de Marmolance is represented by *Austrotrillina brunni*, *Austrotrillina striata, Borelis inflata, Eulepidina formosoides*, *Eulepidina* ex.interc *dilatata et formosoides*, *Heterostegina assilinoides*, *Neorotalia viennoti, Nephrolepidina* ex.interc. *morgani et praemarginata*, *Nephrolepidina tournoueri, Nummulites fichteli*, *Nummulites kecskemetii, Nummulites vascus*, *Operculina complanata*, *Risananeiza crassaparies* and *Spiroclypeus* sp.

Species that were though to be extinct in the Oligocene–Miocene boundary are present in the middle Miocene Marmolance section.

In the literature, the last occurrences (LAD) of *Nummulites fichteli*, *Nummulites vascus, Eulepidina formosoides*, *Nephrolepidina praemarginata, Nummulites kecskemetii*, *Eulepidina dilatata, Heterostegina assilinoides and Neorotalia viennoti* had been reported so far from the Chattian. However, their presence in the Marmolance succession would extends their stratigraphic ranges until Serravallian (see fig. 22).

Other species with LAD in the early Miocene (*Risananeiza crassaparies, Nephrolepidina morgani, Nephrolepidina tournoueri*) are present in Sierra de Marmolance, so their stratigraphic ranges would extend up to the middle Miocene (Serravallian age; see fig. 22). Furthermore, the new record of *R. crassaparies* would represents the most recent record of the subfamily Cuvillierininae and family Ornatorotaliidae found in the westernmost Mediterranean (southeastern Spain).

The age estimated for the LBF species from Sierra de Marmolance section is middle Miocene because of the planktonic foraminifera assemblage identified (fig. 21; see fig. 6 for the locations of the planktonic marl samples). This planktonic foraminifera assemblage indicate an age of 14.23–13.77 million years (Langhian–Serravallian transition, belonging to the biozone M7), given by the presence of *Foshella peripheroacuta*.

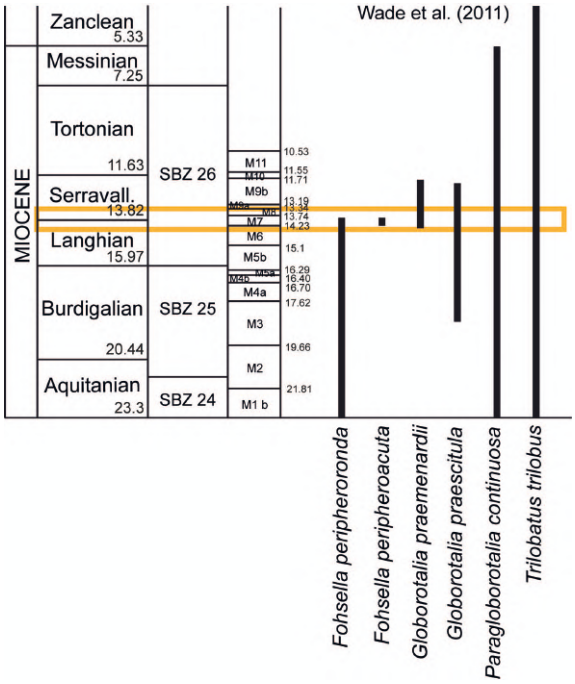

Figure 21. Biostratigraphic chart showing the stratigraphic ranges of the planktonic foraminiferal species identified in Sierra de Marmolance (taxonomic identification by Julio Aguirre). In yellow, the age interval defined by the planktonic foraminiferal assemblage (M7, Langhian–Serravallian boundary and early Serravallian). M (Miocene) zones and stratigraphic ranges after Wade et al. (2011). SBZ, Shallow benthic zonation (Cahuzac and Poignant, 1997).

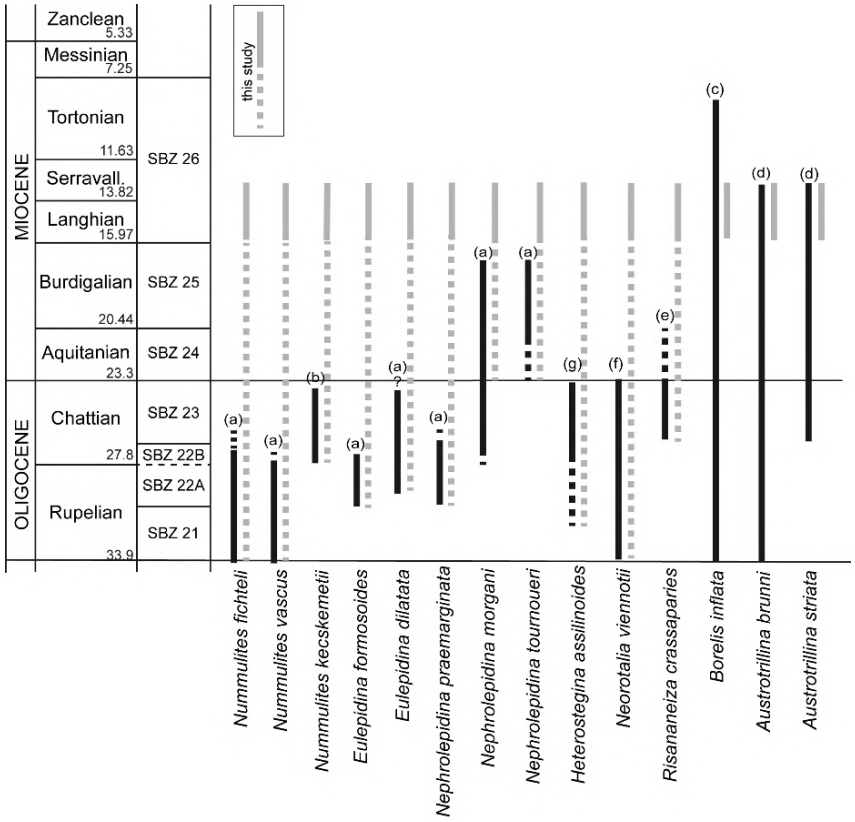

Figure 22. Stratigraphic ranges of the LBF species with relevant biostratigraphic significance identified in Sierra de Marmolance (southeastern Spain). Dashed lines represent the absence of record in the stratigraphic interval. a, Cahuzac and Poignant (1997); b, Less et al. (2011), Ferràndez-Cañadell and Bover-Arnal (2017); c, Cahuzac and Poignant (1997), Bassi et al. (2021b); d, Bassi et al (2021a); e, Benedetti and Briguglio (2012), Ferràndez-Cañadell and Bover-Arnal (2017); f, Greig (1935), Ferràndez-Cañadell and Bover-Arnal (2017); g, Hottinger (1977), Racey (1995), Ferràndez-Cañadell and Bover-Arnal (2017). Abbreviations: SBZ, shallow benthic zonation (Cahuzac and Poignant, 1997); Serravall., Serravallian.

5. Concluding remarks

The presence of planktonic marls at the base and laterally interfingering with limestones containing autochthonous LBF in the studied area (Sierra de Marmolance, southern Spain) allowed the correlation of the planktonic foraminiferal zones and the LBF occurrences, making possible a re-assessement of the age range of Miocene SBZs for the western Mediterranean area. The microfacies analysis shows the *in situ* deposition of the limestones.

The integrated analysis of planktonic and LBF stratigraphic occurrences revealed new last occurrences (LAD) of many LBF species. The LADs of these species have been so far reported from the SBZ22B, 23 and SBZ25 (Chattian–Burdigalian; Cahuzac and Poignant 1997). In Sierra de Marmolance the identified LBF assemblages should be indicative of Rupelian–Chattian and Aquitanian–Burdigalian SBZs.

However, according to the planktonic foraminifera identified in Sierra de Marmolance, the age of marls located at the bottom of the succession is middle Miocene (Langhian–Serravallian), so the overlying LBF limestones should be at least early Serravallian in age or even younger.

The LBF record in the Sierra de Marmolance extends from the Rupelian–Chattian to the early Serravallian the time ranges of the following species: *Eulepidina formosoides, Eulepidina* ex.interc *dilatata et formosoides, Heterostegina assilinoides, Neorotalia viennoti, Nephrolepidina* ex.interc. *morgani et praemarginata, Nephrolepidina tournoueri, Nummulites fichteli, Nummulites kecskemetii, Nummulites vascus* and *Risananeiza crassaparies*. Most of these species have been so far considered as biochronostratigraphic markers for the Oligocene and some of them for the early Miocene. These results highlight the need of a substantial revision of the Oligocene–Miocene SBZs.

6. References

Adams, C.G. (1965). The Foraminifera and stratigraphy of the Melinau Limestone, Sarawak, and its importance in Tertiary correlation. *Quarterly Journal of the Geological Society London, 121*, 283–338.

Adams, C.G. (1968). A revision of the foraminiferal genus *Austrotrillina* Parr. *Bull. Brit. Mus. (Nat. Hist.) 6* (2), 73–97.

Adams, C.G. (1973). Some Tertiary Foraminifera. *In* Hallam, A. (Ed.), Atlas of Palaeobiogeography. *Elsevier*, Amsterdam, 453–468.

Adams, C.G. (1984). Neogene larger foraminifera, evolutionary and geological events in the context of datum planes. *In* Ikebe, N., and Tsuchi, R. (eds.), Pacific Neogene Datum Planes. *University of Tokyo Press*, Tokyo, 47–67.

Adams, C.G., Gentry, A.W. and Whybrow, P.J. (1983). Dating the terminal Tethyan event. *Utrecht Micropaleontological Bulletins*, 30, 273–298.

Adams, C.G., Rodda, P. and Kiteley, R.J. (1979). The extinction of the foraminiferal genus *Lepidocyclina* and the Miocene/Pliocene boundary problem in Fiji. *Marine Micropaleontology, 4*, 319–339.

Akbar-Baskalayeh, N., Less, G., Ghasemi-Nejad, E., Yazdi-Moghadam, M., and Pignatti, J. (2020). Biometric study of late Oligocene larger benthic Foraminifera (Lepidocyclinidae and Nummulitidae) from the Qom Formation, Central Iran (Tajar-Kuh section*). Journal of Paleontology*, *94*(4), 593–615.

Amirshahkarami, M. (2013). Revision in the paleontology and distribution of the larger benthic foraminifera in the Oligocene–Miocene deposits of the Zagros Basin, southwest Iran. *Historical Biology*, *25*(3), 339–361.

Ando, A., Khim, B.K., Nakano, T. and Takata, H. (2011). Chemostratigraphic documentation of a complete Miocene intermediate-depth section in the Southern Ocean: Ocean Drilling Program Site 1120, Campbell Plateau off New Zealand. *Marine Geology, 279*(1-4), 52–62.

Báldi, T., Less, G. and Mandic, O. (1999). Some new aspects of the lower boundary of the Egerian stage (Oligocene, chronostratigraphic scale of the Paratethys area). *Abhandlungen- Geologischen Bundesanstalt, 56*(2), 653–668.

Bassi, D. and Nebelsick, J. H. (2010). Components, facies and ramps: redefining Upper Oligocene shallow water carbonates using coralline red algae and larger foraminifera (Venetian area, northeast Italy). *Palaeogeography, Palaeoclimatology, Palaeoecology, 295*(1-2), 258–280.

Bassi, D., Aftabuzzaman, M., Bolivar-Feriche, M., Braga, J.C., Aguirre, J., Renema, W., Takayanagi, H. and Iryu, Y. (2021a). Biostratigraphical and palaeobiogeographical patterns of the larger porcelaneous foraminifer *Austrotrillina* Parr, 1942. *Marine Micropaleontology, 169*, 102058. Elsevier. https://doi.org/10.1016/j.marmicro.2021.102058.

Bassi, D., Braga, J.C., Di Domenico, G., Pignatti, J., Abramovich, S., Hallock, P., Könen, J., Kovács, Z., Langer, M.R., Pavia, G. and Iryu, Y. (2021b). Palaeobiogeography and evolutionary patterns of the larger foraminifer *Borelis* de Montfort (Borelidae). *Papers in Palaeontology, 7*(1), 377–403.

Bassi, D., Hottinger, L. and Nebelsick, J. H. (2007). Larger foraminifera from the Upper Oligocene of the Venetian area, north-east Italy. *Palaeontology*, *50*(4), 845–868.

Beavington-Penney, S.J. (2004). Analysis of the effects of abrasion on the test of Palaeonummulites venosus: implications for the origin of nummulithoclastic sediments. *Palaios*, *19*(2), 143–155.

Beavington-Penney, S.J. and Racey, A. (2004). Ecology of extant nummulitids and other larger benthic foraminifera: applications in palaeoenvironmental analysis. Earth-Science Reviews, 67(3-4), 219–265.

Benedetti, A. (2010). Biostratigraphic remarks on the Caltavuturo Formation (Eocene-Oligocene) cropping out at Portella Colla (Madonie Mts., Sicily). *Revue de Paléobiologie*, *29*(1), 197–216.

Benedetti, A. (2015). The new family Ornatorotaliidae (Rotaliacea, Foraminiferida). *Micropaleontology, 61*(3), 231–236.

Benedetti, A. and Briguglio, A. (2012). *Risananeiza crassaparies* n. sp. from the upper Chattian of Porto Badisco (southern Apulia, Italy). *Boll Soc Paleont Ital, 51,* 167–176.

Benedetti, A. and Pignatti, J. (2013). Conflicting evolutionary and biostratigraphical trends in *Nephrolepidina praemarginata* (Douvillé, 1908) (Foraminiferida). *Historical Biology, 25*, 363–383, doi: 10.1080/08912963.2012.713949.

Bermúdez, P.J. (1952). Estudio sistemático de los foraminíferos rotaliformes. Venezuela. *Boletin de Geologia, , 2*(4), 230pp.

Blanckenhorn, M. (1890). Das Eocän in Syrien, mit besonderer Berücksichtigung Nord-Syriens, ein Beitrag zur Geologie Syriens. *Zeitschrift der Deutschen Geologischen Gesellschaft, 42*, pp. 318–359.

Blondeau, A. (1972). Les *Nummulites*. *Lib. Vuibert*, Paris.

Boudagher-Fadel, M.K. (2002). The stratigraphical relationship between planktonic and larger benthic

foraminifera in Middle Miocene to Lower Pliocene carbonate facies of Sulawesi, Indonesia. *Micropaleontology, 48*(2), 153–176.
Boudagher-Fadel, M.K. (2018). Evolution and geological significance of larger benthic foraminifera. *University College London Press*, London, UK, 2nd ed., 693 pp. doi: 10.14324/111.9781911576938.
Boudagher-Fadel, M.K. and Banner, F. T. (1999). Revision of the stratigraphic significance of the Oligocene-Miocene "Letter-Stages". *Revue de micropaléontologie, 42*(2), 93–97.
Boudagher-Fadel, M.K. and Lokier, S.W. (2005). Significant Miocene larger foraminifera from South Central Java. *Revue de Paléobiologie, 24*, 291–309.
Boudagher-Fadel, M.K. and Price, G.D. (2010). Evolution and paleogeographic distribution of the lepidocyclinids. *The Journal of Foraminiferal Research, 40*(1), 79–108.
Boudagher-Fadel, M.K. and Price, G.D. (2013). The phylogenetic and palaeogeographic evolution of the miogypsinid larger benthic foraminifera. *Journal of the Geological Society, 170*(1), 185–208.
Boukhary, M., Kuss, J. and Abdelraouf, M. (2008). Chattian larger foraminifera from Risan Aneiza, northern Sinai, Egypt, and implications for Tethyan paleogeography. *Stratigraphy, 5*(2), 179–192.
Bourrouilh-Le Jan, F.G. and Hottinger, L.C. (1988). Occurrence of rhodolites in the tropical Pacific-a consequence of Mid-Miocene paleo-oceanographic change. *Sedimentary Geology*, *60*(1-4), 355–367.
Braga, J.C. and Bassi, D. (2011). Facies and coralline algae from Oligocene limestones in the Malaguide Complex (SE Spain). Annalen des Naturhistorischen Museums in Wien. *Serie A für Mineralogie und Petrographie, Geologie und Paläontologie, Anthropologie und Prähistorie*, 291–308.
Braga, J.C., Martín, J.M., Aguirre, J., Baird, C.D., Grunnaleite, I., Jensen, N.B., Puga-Bernabéu, A., Sælen, G. and Talbot, M.R. (2010). Middle-Miocene (Serravallian) temperate carbonates in a seaway connecting the Atlantic Ocean and the Mediterranean Sea (North Betic Strait, S Spain). *Sedimentary Geology*, *225*(1-2), 19–33.
Braga, J.C., Martín, J.M., Betzler, C., and Aguirre, J. (2006). Models of temperate carbonate deposition in Neogene basins in SE Spain: a synthesis. *Geological Society*, London, *Special Publications, 255*(1), 121–135.
Brun, L., Butterlin, J. And Montell, L. (1982). Decouverte de Lépidocyclines (Foraminifères) d'âge Eocène dans le Golfe de Guinée. Implications Paléobiogéographiques. *Cahiers de Micropaléontologie, 2*, 91–109.
Brunn, J.H., Chevalier, J.-P., Marie, P. (1955). Quelques formes nouvelles de Polypiers et de Foraminifères de l'Oligocene et du Miocene du NW de la Grèce. II. Foraminifères. *Bull. Soc. géol. Fr. 5,* 193–205. https://doi.org/10.2113/gssgfbull.S6-V.1-3.193.
Butterlin, J. (1987). Origine et évolution des Lepidocyclines de la région des Caraibes. Comparisons et relations
Cahuzac, B. and Poignant, A. (1997). Essai de biozonation de l'Oligo-Miocène dans les bassins Européens à l'aide des grands foraminières néritiques. *Bulletin de la Société Géologique de France*, 168, 155–169.
Cahuzac, B. and Poignant, A. (2005). Sur les foraminifères benthiques de la base du Burdigalien dans les «Sables à Mactres» de Martillac (Gironde, SO France). *In* Annales de Paléontologie, 91, No. 1, 5–31. *Elsevier Masson.*
Cahuzac, B., Poignant, A., de Graciansky, P.C., Hardenbol, J. and Vail, P.R. (1998). Larger benthic foraminifera (Neogene). *Mesozoic–Cenozoic sequence stratigraphy of European basins: SEPM Special Publication, 60*, 766–767.
Chapronière, G.C.H. (1980). Biometrical studies of early Neogene larger Foraminiferida from Australia and New Zealand. *Alchiringa, 4,* 153–181.
Chapronière, G.C.H. (1984). Oligocene and Miocene larger Foraminiferida from Australia and New Zealand. *Bur. Min. Resour, Geology and Geophysics, Bull. 188*, 98 pp.
Cole, W.S. (1960). Variability in embryonic chambers of Lepidocyclina. *Micropalaeontology, 6*, pp 133–144.
Cole, W.S. (1962). Embryonic chambers and the subgenera of *Lepidocyclina* in India. *Bulletin of American Palaeontology, 44* (200), 28–60.
Cole, W.S. (1968). More on variation in the genus *Lepidocyclina* (Larger Foraminifera). *Bulletin of American Paleontology, 54*(243), 295–327.
Cole, W.S. (1969). Larger foraminifera from deep drill holes on Midway Atoll. *U.S. Geol. Surv. Prof. Pap*. 680-C, C1–C5. doi: 10.3133/pp680C.
Coleman, P.J. (1963). Tertiary larger foraminifera of the British Solomon Islands, southwest Pacific. *Micropaleontology, 9*, no. 1, 1–38.
Colom, G. and Bauzá, J. (1950). *Operculina canalifera gomezi* n. subesp. de Bartoniense de Cataluña. *Boletin de la Real Sociedad Espanola de Historia Natural, 47,* 219–221.
Daneshian, J. and Dana, L.R. (2007). Early Miocene benthic foraminifera and biostratigraphy of the Qom Formation, Deh Namak, central Iran. *Journal of Asian Earth Sciences, 29*(5-6), 844–858.
Daneshian, J. and Dana, L.R. (2019). Benthic foraminiferal events of the Qom Formation in the north Central

Iran Zone. *Paleontol. Res. 23*, 10–22. https://doi.org/10.2517/2018PR008.
De Mulder, E.F.J. (1975). Microfauna and sedimentary tectonic history of Oligo-Miocene of the Ionian Islands and Western Epirus (Greece). *Utrecht Micropalaentol. Bull., 13*, 139 pp.
Defrance, M.J.L. (1822). Lenticulites. *In* M.F. Cuvier (ed.), *Dictionnaire des Sciences naturelles,* Levrault F.G., Strasbourg et Le Normant, Paris, v. 25, 452–453.
Denizot, M. (1968). Les algues Floridées encroutantes (à l'exclusion des Corallinacées). *Lab. De Cryptogamie,* Mus. Nat. Hist. Paris, 310 pp.
Didon, J., Durand Delga, M., Fontboté, J. M., Magné, J. and Peyre, Y. (1961). El Oligoceno superior del Bético de Málaga (Andalucía). *Inst. Geol. y Min. España, 61*, 115–130.
Douvillé, H. (1899). Sur les couches à Orbitoides (Lepidocyclina) du Bassin de l'Adour. Bull. Soc. Géol. France, 27 (3), 497–498.
Douvillé, H. (1905). Les foraminifères dans le Tertiaire de Bornéo. *Bulletin de la Société Géologique de France, 5,* 435–464.
Douvillé, H. (1925). Revision des Lépidocyclines. *Mémoires de la Société Géologique de France, nouvelle série, 1*, no.2, 1–118.
Douvillé, R. (1908). Observations sur les faunes à foraminifères du Sommet du Nummulitique Italien. *Bulletin de la Société géologique de France, 4*, 88–95.
Douvillé., H. (1911). Les Foraminiferes dans le tertiare des Phillipines. *Phillipine Journal of Science, 6*, 53–80.
Drooger, C.W. (1993). Radial foraminifera, morphometrics and evolution. *Verhandelingen der Koninklijke Nederlandse Akademie van Wetenschappen, Afdeling Natuurkunde*. North Holland, Amsterdam, 41, 242 pp.
Drooger, C.W. and Freudenthal, T. (1964). Associations of *Miogypsina* and *Lepidocyclina* at some European localities. *Ecl. Geol. Helv, 57*(2), 509–528.
Drooger, C.W. and Laagland, H. (1986). Larger foraminiferal zonation of the European-Mediterranean Oligocene. Proceedings of the Koninklijke nederlandse akademie van wetenschappen. Series B. *Palaeontology, geology, physics, chemistry, anthropology*, *89*(2), 135–148.
Drooger, C.W. and Roelofsen, J.W. (1982). Cycloclypeus from Ghar Hassan, Malta. *In* Proceedings of the Koninkijke Nederlandse Akademie van *Wetenschappen (B), 85*, 203–218.
Drooger, C.W. and Socin, C. (1959). Miocene foraminifera from Rosignano, northern Italy. *Micropaleontology,* 415–426.
Drooger, C.W., Marks, P., Papp, A. and Bik, T.A. (1971). Smaller radiate Nummulites of northwestern Europe. *Utrecht Micropaleontological Bulletins, 5,* 137 pp.
Eames, F.E., Banner, F.T., Blow, W.H., Clarke, W.J. and Smout, A.H. (1962). Morphology, taxonomy and stratigraphic occurrence of Lepidocyclininae. *Micropalaeontology, 8,* 289–322.
Ehrenberg, C.G. (1839). Über die Bildung der Kreidefelsen und des Kreidemegels durch unsichtbare Organismen. *Phys Abh k preuss Akad Wiss, 1838*, 59–148, 1 tab, pls. 14, Berlin.
Elliot, G.F. (1957). Subterraniphyllum, a new Tertiary calcareous alga. *Palaeontology, 1*, 73–75.
Fallot, P. (1945). Estudios geológicos en la Zona Subbética entre Alicante y el río Guadiana Menor (Vol. 5). Consejo Superior de Investigaciones Científicas, *Instituto de Investigaciones Geológicas Lucas Mallada*.
Ferràndez-Canadell, C. and Bover-Arnal, T. (2017). Late Chattian larger foraminifera from the Prebetic domain (SE Spain): new data on shallow benthic zone 23. *Palaios*, 32(1), 83–109.
Ferràndez-Canadell, C., Tosquella, J. and Serra-Kiel, J. (1999). Reworked *Discocyclina* occurring together with *Lepidocyclina* in the Oligocene of San Vicente de la Barquera (Northern Spain). *Revista Española de Micropaleontología, 31,* 232–330.
Foslie, M. (1909). Algologiske notiser VI. Kongelige Norske Videnskabers Selskab Skrifter, 1909, 1–63.
Foucault, A. (1960). Sur la tectonique de la zone subbetique de la region de Huescar (prov. de Grenade, Espagne) et sur son Nummulitique. *Bulletin de la Société Géologique de France*, 7(3), 318–321.
Foucault, A. (1971). Etude géologique des environs des sources du Guadalquivir, provinces de Jaén et de Grenade, Espagne méridionale. Doctoral dissertation, *Université Pierre et Marie Curie-Paris VI*.
Gallardo, A., Serra-Kiel, J., Ferràndez-Cañadell, C., Razin, Ph., Roger, J., Boix, C., Caus, E. (2001). Macroforaminíferos porcelanados del Eoceno Superior–Oligoceno Inferior del Dhofar (Sultanato de Omán). *In* Meléndez, G., Herrera, Z., Delvene, G., Azanza, B. (Eds.), Los fósiles y la paleogeografía. Actas de las 17◦ Jornadas de la Sociedad Española de Paleontología, Albarracín (Teruel), 5 (1). *Pub. Sem. Paleontol.* Zaragoza (SEPAZ), 83–89.
García Dueñas, V., Balanyá, J.C. and Martínez-Martínez, J. M. (1992). Miocene extensional detachments in the outcropping basement of the northern Alboran basin (Betics) and their tectonic implications. *Geo-Marine Letters*, 12(2), 88–95.
Gedik, F. (2014). Benthic Foraminiferal Fauna of Malatya Oligo-Miocene Basin,(Eastern Taurids, Eastern

Turkey). *Bulletin of the Mineral Research and Exploration*, 149(149), 93–136.
Gedik, F. (2015). Benthic foraminiferal biostratigraphy of Malatya Oligo-Miocene succession (Eastern Taurids, Eastern Turkey). *Bulletin of the Mineral Research and Exploration*, 150(150), 19–50.
Gedik, F. and Karadenizli, L. (2021). Oligocene larger benthic foraminifera and sedimentation of the Burdur Basin, SW Anatolia, Turkey. *Geodiversitas*, 43(13), 377–389.
Ghafor, I.M. (2015). Evolutionary aspects of *Lepidocyclina* (*Nephrolepidina*) from Baba Formation (late Oligocene) in Bai-Hassan well-25, Kirkuk area, Northeast Iraq. *Arabian Journal of Geosciences, 8*(11), 9423–9431. Doi: 10.1007/s12517-015-1865-9.
Giovagnoli, M.C. and Schiavinotto, F. (1990). *Nephrolepidina tournoueri* (Lemoine & R. Douvillé) from the lower Miocene of Ales (Sardinia). *Bollettino della Società Paleontologica Italiana*, *29*(2), 233–244.
Greig, D.A. (1935). *Rotalia viennoti*, an important foraminiferal species from Asia Minor and Western Asia. *Journal of Paleontology, 9*, 523–526.
Grimsdale, T.F. (1952). Cretaceous and Tertiary Foraminifera from the Middle East: *Bulletin of the British Museum, Natural History (Geology), 1*, no. 8, 223–247.
Habibi, T. (2018). Biostratigraphy and Systematic Paleontology of the Oligocene Larger Benthic Foraminifera from Fars Province, Zaros Basin, SW Iran. *Iranian Journal of Science and Technology, Transactions A: Science, 42*(3), 1285–1308.
Hadi, M., Less, G. and Vahidinia, M. (2019). Eocene larger benthic foraminifera (alveolinids, nummulitids, and orthophragmines) from the eastern Alborz region (NE Iran): Taxonomy and biostratigraphy implications. *Revue de micropaléontologie*, 63, 65–84.
Hallock, P. (1999). Symbiont-bearing foraminifera. In *Modern foraminifera*, pp. 123-139. Springer, Dordrecht.
Hansen, H. J. and Reiss, Z. (1971). Electron microscopy of Rotaliacean wall structures. *Bulletin of the Geological Society of Denmark, 20*(4), 329–346.
Harpe, PH. de la (1879). Description des *Nummulites* appartenant à la zone supérieure des Falaises de Biarritz. *Bulletin de la Société Borda, 4,* 137–156.
Hashimoto, W., Matsumaru, K., Kurihara, K., David, P.P. and Balce, G.R. (1977). Larger foraminiferal assemblages useful for the correlation of the Cenozoic marine sediments in the mobile belt of the Philippines. *Geology and Palaeontology of Southeast Asia, 18*, 103–123.
Heck, van S.E. and Drooger, C.W. (1984). Primitive *Lepidocyclina* from San Vicente de la Barquera (N Spain). *Proceedings of the Koninklijke Nederlandse Akademie van Wetenschappen, ser. B, 87*, 301–318.
Henson, F.R.S. (1937). Larger foraminifera from Aintab, Turkish Syria. *Eclogae Geologicae Helvetiae, 30*, 45–57.
Heydrich, F. (1897). Corallinaceae, insbesondere Melobesieae. *Ber. Deutsch. Bot. Gesellschaft,15,* 34–71.
Hottinger L., Halicz E., Reiss Z. (1991). The foraminiferal geenra *Pararotalia, Neorotalia*, and *Calcarina*: taxonomic revision. *J. Paleont, 65*, 18–33.
Hottinger, L. (1963). Quelques Foraminifères porcelanés oligocènes dans la série sédimentaire prébétique de Moratalla (Espagne méridionale). *Eclogae Geol. Helv. 56*, 963–972. https://doi.org/10.5169/seals-163053.
Hottinger, L. (1966). *Heterostegina*, *Grzybowskia* et *Spiroglypeus* néogènes du Maroc. *In* Committee on Mediterranean Neogene stratigraphy. Session 3, 61–69.
Hottinger, L. (1977). Foraminifères operculiniformes. Paris, *Muséum National d'Histoire Naturelle, 40*, 159 pp.
Hottinger, L. (1997). Shallow benthic foraminiferal assemblages as signals for depth of their deposition and their limitations. *Bulletin de la Société géologique de France*, 168(4), 491-505.
Hottinger, L. (2001). Archaiasinids and related porcelaneous larger foraminifera from the Late Miocene of the Dominican Republic. *Journal of Paleontology*, 75(3), 475–512.
Hottinger, L. (2006). The" face" of benthic Foraminifera. *Bolletino-Societá Paleontologica Italiana*, 45(1), 75.
Hottinger, L. (2014). *Neorotalia* Bermúdez, 1952. *In* D. Bassi (Ed.), Paleogene larger Rotaliid Foraminifera from the Western and Central Neotethys. Berlin, *Springer International Publishing Switzerland,* 153–157. 196 pp., 125 illus. Doi: 10.1007/978-3-319-02853-8.
Hottinger, L., Halicz, E. and Reiss, Z. (1993). Recent Foraminiferida from the Gulf of Aqaba, Red Sea (No. 563.12 HOT). Ljubljana. *Slovenska Akademija Znanosti in Umetnosti*, 179 pp., 230 pp. de láms.
Işik, U. (2010). Kahramanmaras-Adiyaman havzalari sig denizel sedimanlarin Oligo-Miyosen bentik foraminifer Tanimlamasi ve biyostratigrafisi [Benthic foraminiferal description and biostratigraphy of Oligo-Miocene shallow-water sediments of Kahramanmaras and Adiyaman basins]: Ph.D. Thesis, Ankara University, Faculty of Engineering, *Department Geological Engineering,* 234 pp. (In Turkish)
Jabaloy, A., Galindo-Zaldívar, J. and González-Lodeiro, F. (1992). The Mecina Extensional System: its relation with the post-Aquitanian piggy-back basins and the paleostresses evolution (Betic Cordilleras, Spain). *Geo-Marine Letters*, 12(2), 96–103.
Joly, N. and Leymerie, A. (1848). Mémoire sur les Nummulites considérées zoologiquement et géologiquement.

Mémoires de l'Académie des Sciences de Toulouse, v. 4, pp. 149–218.
Kleiber, G.W. (1991). *Nummuliten* der paläogenen Tethys in Axialschnitten. *Institut und Museum für Geologie und Paläontologie der Universität Tübingen, 9.*
Kuss, J. and Boukhary, M.A. (2008). A new upper Oligocene marine record from northern Sinai (Egypt) and its paleogeographic context. *GeoArabia, 13*(1), 59–84.
Kützing, F.T. (1843). Phycologia generalis: oder Anatomie, Physiologie und Systemkunde der Tange. *Leipzig: F.A. Brockhaus.*
Lange, H. (1968). Die evolution von *Nephrolepidina* und *Eulepidina* im Oligozän und Miozän der Insel Ithaka (Westgriechenland). Thesis, Universität München, München, 78 pp.
Langer, M. R. (2008). Assessing the contribution of foraminiferan protists to global ocean carbonate production 1. *Journal of Eukaryotic Microbiology*, *55*(3), 163–169.
Langer, M. R. and Hottinger, L. (2000). Biogeography of selected " larger" foraminifera. *Micropaleontology,* 46, 105–126.
Laursen, G.V., Monibi, S., Allan, T.L., Pickard, N.A.H., Hosseiney, A., Vincent, B., Hamon, Y., van Buchem, F.S.P., Moallemi, A. and Druillion, G. (2009). The Asmari Formation revisited: changed stratigraphic allocation and new biozonation. *In* Shiraz 2009-1st EAGE International Petroleum Conference and Exhibition (pp. cp-125). *European Association of Geoscientists & Engineers*.
Lemoine, P. and Douvillé, R. (1904). Sur le genre *Lepidocyclina* Gümbel. *Mémoires de la Société Géologique de France, sér. 12, 32*, 1–41.
Less, G. (1991). Upper Oligocene larger Foraminifers of the Bükk Mountains (NE Hungary). *Magyar Allami Földtani Intezet Evi Jelentése*, 1989, 411–465.
Less, G. (1999). The late Paleogene larger foraminiferal assemblages of the Bükk Mountains (NE Hungary). *Revista Española de Micropaleontología*, 31(3), 347–356.
Less, G. and Özcan, E. (2008). The late Eocene evolution of nummulitid foraminifer Spiroclypeus in the Western Tethys. *Acta Palaeontologica Polonica,* 53(2), 303–316.
Less, G., and Özcan, E. (2012). Bartonian-Priabonian larger benthic foraminiferal events in the Western Tethys. *Austrian Journal of Earth Sciences*, 105(1).
Less, G., Benedetti, A., Cahuzac, B., Parente, M., Pignatti, J. and Torres-Silva, A. (2015). Supposed trans-Atlantic migration of Heterostegina around the Eocene/Oligocene boundary. *Berichte des Institutes für Erdwissenschaften der Karl-Franzens-Universitat Graz*, Band 21, Graz 2015, Strati 2015, 222.
Less, G., Frijia, G., Özcan, E., Saraswati, P. K., Parente, M. and Kumar, P. (2018). Nummulitids, lepidocyclinids and Sr-isotope data from the Oligocene of Kutch (western India) with chronostratigraphic and paleobiogeographic evaluations. *Geodinamica Acta,* 30(1), 183–211.
Less, G., Kertész, B. and Özcan, E. (2006). Bartonian to end-Rupelian reticulate Nummulites of the Western Tethys. *Anuário do Instituto de Geociências*, 29(1), 334–335.
Less, G., Özcan, E. And Okay, A.I. (2011). Stratigraphy and larger foraminifera of the Middle Eocene to Lower Oligocene shallow-marine units in the northern and eastern parts of the Thrace Basin, NW Turkey. *Turkish Journal of Earth Sciences, 20*(6), 793–845.
Less, G., Özcan, E., Papazzoni, C.A. and Stockar, R. (2008). The middle to late Eocene evolution of nummulitid foraminifer Heterostegina in the Western Tethys. *Acta Palaeontologica Polonica*, 53(2), 317–350.
Loeblich, A.R. and Tappan, H. (1964). Foraminiferal classification and evolution. *Journal of Geological Society of India, 5*, 5–40.
Loeblich, A.R. and Tappan, H. (1986). Some new and redefined genera and families of Textulariina, Fusulinina, Involutinina and Miliolina (Foraminiferida). *J. Foramin. Res. 16* (4), 334–346. https://doi.org/10.2113/gsjfr.16.4.334.
Loeblich, A.R. Jr. and Tappan, H. (1987). Foraminiferal Genera and Their Classification*. Van Nostrand Reinhold Co.*, New York, 970 pp.
Lunt, P. and Allan, T. (2004). Larger foraminifera in Indonesian biostratigraphy, calibrated to isotopic dating. *Geol. Res. Dev. Cent. Mus.* 1–109. Workshop on Micropalaeontology, June 2004, Bandung.
Lupiani Moreno, E., Roldán García, F.J. and Villalobos Megía, M. (1994). Hoja 950, Huéscar. Mapa geológico de España, serie Magna 1:50000.
Maslov, V.P. (1956). Fossil calcareous algae of USSR. *Trudy Instituta geologicheskih nauk Akademii Nauk SSSR, 160*, 1–301 (in Russian).
Matsumaru, K. (1971). The genera *Nephrolepidina* and *Eulepidina* from New Zeland. *Transactions and proceedings of the Paleontological Society of Japan. New series, 84*, 179-189, pls. 22, 23.
Matsumaru, K. (1981). On Lepidocyclina (Trybliolepidina) ruueni van der Vlerk from Zone N17 at Mitsugane, Izu Peninsula, Shizuoka Prefecture, Japan. *Proceedings of the Japan Academy, Series B, 57*(4), 115-118.
Matteucci, R. and Schiavinotto, F. (1977). Studio biometrico di *Nephrolepidina, Eulepidina* e *Cycloclypeus* in

due campioni dell'Oligocene di Monte La Rocca, L'Aquila (Italia Centrale*). Geologica Romana, 16*, 141–171.
Michelotti, G. (1841). Saggio storico dei Rizopodi caratteristici dei terreni sopracretacei. *Memorie di matematica e di Fisica della Società Italiana delle Scienze*. Modena 22, 253–302.
Michelotti, G. (1861). Études sur le Miocène inférieur de l'Italie septentrionale. *Natuurkundige Verhandelingen van de Hollandsche Maatschappij der Wetenschappen te Haarlem, 15* (2), 1–183.
Moghadam, I.M., Borji, S., Amini, E., Azadbakht, S. and Abad, M.T.K. (2014). Microbiostratigraphy of the Qom Formation in Southwestern Tafresh, Central Iran. *Iranian Journal of Earth Sciences, 6*(1), 52–63.
Monfort, D. De (1808). Conchyliologie systématique et classification méthodique des coquilles. *F. Schoell*, Paris, 1, 409.
Muthukrishnan, S. and Saraswati, P.K. (2001). Shape analysis of the nucleoconch of *Lepidocyclina* from Kutch; a taxonomic interpretation. *Micropaleontology, 47*(1), 87–92.
Myftari, S., Bako, M. and Myftari, B. (2001). The study of lepidocyclina (*Eulepidina*)(Foraminifera) from middle Oligocene to lower Miocene of South Albania. *In* Proceedings of the 9th International Congress, Athens. *Bulletin of the Geological Society of Greece, 34*(2), 541–547.
Novak, V. (2014). Larger benthic foraminifera in Miocene carbonates of Indonesia. *Utrecht St. Earth Sci. 64*, 1–213.
Özcan, E. and Less, G. (2009). First record of the co-occurrence of western Tethyan and Indo-Pacific larger foraminifera in the Burdigalian of the Mediterranean province. *The Journal of Foraminiferal Research*, 39(1), 23–39.
Özcan, E., Less, G. and Baydogan, E. (2009b). Regional implications of biometric analysis of Lower Miocene larger foraminifera from Central Turkey. *Micropaleontology*, 559–588.
Özcan, E., Less, G., Báldi-Beke, M. and Kollányi, K. (2010). Oligocene hyaline larger foraminifera from Kelereşdere section (Muş, Eastern Turkey). *Micropaleontology*, 465–493.
Özcan, E., Less, G., Báldi-Beke, M., Kollányi, K. and Acar, F. (2009a). Oligo-Miocene foraminiferal record (Miogypsinidae, Lepidocyclinidae and Nummulitidae) from the Western Taurides (SW Turkey): biometry and implications for the regional geology. *Journal of Asian Earth Sciences*, 34(6), 740–760.
Özcan, E., Less, G., Báldi-Beke, M., Kollányi, K. and Kertész, B. (2006). Biometric analysis of middle and upper Eocene Discocyclinidae and Orbitoclypeidae (Foraminifera) from Turkey and updated orthophragmine zonation in the Western Tethys. *Micropaleontology,* 52(6), 485–520.
Özcan, E., Less, G., Jovane, L., Catanzariti, R., Frontalini, F., Coccioni, R., Giorgioni, Rodelli, D., Rego, E.S., Kayğılı, S. and Rostami, M.A. (2019). Integrated biostratigraphy of the middle to upper Eocene Kırkgeçit Formation (Baskil section, Elazığ, eastern Turkey): larger benthic foraminiferal perspective. *Mediterranean Geoscience Reviews*, 1(1), 55–90.
Özcan, E., Scheibner, C. and Boukhalfa, K. (2014). Orthophragminids (foraminifera) across the Paleocene–Eocene transition from North Africa: taxonomy, biostratigraphy, and paleobiogeographic implications. *The Journal of Foraminiferal Research*, 44(3), 203–229.
Papazzoni, C.A., Ćosović, V., Briguglio, A. and Drobne, K. (2017). Towards a calibrated larger foraminifera biostratigraphic zonation: celebrating 18 years of the application of shallow benthic zones. *Palaios*, 32(1), 1-4.
Parente, M. and Less, G. (2019). Nummulitids, Lepidocyclinids and strontium isotope stratigraphy of the Porto Badisco Calcarenite (Salento Peninsula, southern Italy). Implications for the biostratigraphy and paleobiogeography of Oligocene larger benthic foraminifera*. Italian Journal of Geosciences, 138*(2), 2391–261.
Parr, W.J. (1942). New genera of foraminifera from the Tertiary of Victoria. *Min. Geol. J. 2*, 361–363.
Pieroni, P.G. (1965). *Lepidocyclina* and *Miogypsina* from Opi, Sangro Valley (Central Apennines). *Geologica Romana, 4,* 161–180.
Pignatti, J. and Papazzoni, C.A. (2017). Oppelzones and their heritage in current larger foraminiferal biostratigraphy. *Lethaia,* 50(3), 369–380.
Racey, A. (1995). Lithostratigraphy and larger foraminiferal (nummulitid) biostratigraphy of the Tertiary of northern Oman. *Micropaleontology*, 1–123.
Rahaghi, A. (1973). Étude de quelques grands foraminifères de la Formation de Qum (Iran Central). *Revue de Micropaléontologie, 16*(1), 23–38.
Renema, W. (2007). Fauna development of larger benthic foraminifera in the Cenozoic of Southeast Asia. In Biogeography, Time, and Place: Distributions, Barriers, and Islands. Dordrecht, *Springer*, 179–215.
Riera, R., Haig, D.W., Bourget, J. (2019). Stratigraphic revision of the Miocene Trealla Limestone (Cape Range, western Australia): implications for Australasian foraminiferal biostratigraphy. *J. Foramin. Res. 49,* 318–338. https://doi.org/10.2113/gsjfr.49.3.318.

Robinson, E. (2003). Zoning the White Limestone Group of Jamaica using larger foraminiferal genera: a review and proposal. *Cainozoic research, 3*(1/2), 39–75.

Roozpeykar, A. and Moghaddam, M.I. (2016). Benthic foraminifera as biostratigraphical and paleoecological indicators: an example from Oligo–Miocene deposits in the SW of Zagros basin. Iran. *Geosci. Front. 7*, 125–140.

Sachs Jr, K.N. (1964). Multilocular embryonts in Lepidocyclina (Eulepidina) undosa Cushman from Puerto Rico. *Micropaleontology*, 323–329.

Sælen, G., Lunde, I.L., Porten, K.W., Braga, J.C., Dundas, S.H., Ninnemann, U.S., Ronen, Y. and Talbot, M.R. (2016). Oyster shells as recorders of short-term oscillations of salinity and temperature during deposition of coral bioherms and reefs in the Miocene Lorca Basin, SE Spain. *Journal of Sedimentary Research, 86*(6), 637–667.

Sanz de Galdeano, C. (1990). Geologic evolution of the Betic Cordilleras in the Western Mediterranean, Miocene to the present. *Tectonophysics,* 172(1-2), 107–119.

Sanz de Galdeano, C. (1997). La zona interna bético-rifeña: antecedentes, unidades tectónicas, correlaciones y bosquejo de reconstrucción paleogeográfica. Universidad de Granada. *Colección monográfica. Tierras del Sur* 18, 316 pp.

Sanz de Galdeano, C. and Vera, J.A. (1992). Stratigraphic record and palaeogeographical context of the Neogene basins in the Betic Cordillera, Spain. *Basin Research*, 4(1), 21–36.

Saraswati, P.K. (1995). Biometry of early Oligocene *Lepidocyclina* from Kutch, India. *Marine Micropalaeontology, 26*, 303–311.

Schaub, H. (1981). *Nummulites* et *Assilines* de la Tethys paleogene, taxinomie, phylogenie et biostratigraphie avec deux volumes d'atlas. *Schweitz. Palaeontol. Abh*., *104–106*, 236 p. ISSN 0080-7389.

Schefen, W. (1932). Zur morphologie und morphogenese der ‘‘Lepidocyclinen’’. *Paläontologische Zeitschrift, 14,* 233–256.

Schiavinotto, F. (1979). *Miogypsina* e *Lepidocyclina* del Miocene di Monte La Serra (L’Aquila-Appennino centrale). *Geologica Romana, 18*, 253–293.

Schiavinotto, F. (1995). Environmental influence on the neanic acceleration in Oligo-Miocene *Nephrolepidina*. *Geologica Romana, 31*, 273–283.

Schiavinotto, F. (2010). Neanic stage biometry in *Nephrolepidina* from the upper Oligocene of Lonedo (Lugo di Vicenza-Northern Italy*). Bollettino della Societá Paleontologica Italiana*, *49*, 173–194.

Schiavinotto, F. and Verrubbi, V. (1994). *Nephrolepidina* in the Oligo-Miocene section of the Gran Sasso (Central Apennines): environment-evolution relations. *Bollettino della Società Paleontologica Italiana, 33*, 375–406.

Schiavinotto, F. and Verrubbi, V. (1996). Middle-Upper Oligocene *Eulepidina* from Central Appennines: relations between evolution and environment. *In* Autoecology of selected fossil organisms: Achievements and problems. *Boll. Soc. Paleont. Ital., Spec., 3*, 213–221.

Schmarda, L.K. (1871). Zoologie. *Wilhelm von Braum€uller*, Vienna, 584 pp.

Seiglie, G.A. and Frost, S.H. (1979). Significance of middle Tertiary large foraminifera common to West Africa and Caribbean*. AAPG Bulletin, 63*(3), 525–525.

Serra-Kiel, J., Gallardo-Garcia, A., Razin, P.H., Robinet, J., Roger, J., Grelaud, C., Leroy, S. and Robin, C. (2016). Middle Eocene–Early Miocene larger foraminifera from Dhofar (Oman) and Socotra Island (Yemen). *Arab. J. Geosci. 9,* 344. https://doi.org/10.1007/s12517-015-2243-3.

Serra-Kiel, J., Hottinger, L., Caus, E., Drobne, K., Ferràndez, C., Jauhri, A.K., Less, G., Pavlovec, R., Pignatti, J., Samsó, J.M., Schaub, H., Sirel, E., Strougo, A., Tambareau, Y., Tosquella, J. and Zakrevskaya, E. (1998). Larger foraminiferal biostratigraphy of the Tethyan Paleocene and Eocene. *Bulletin de la Société Géologique de France*, 169, 281–299.

Setchell, W.A. and Mason, L.R. (1943). Goniolithon and Neogoniolithon: two genera of crustaceous coralline algae. *Proceedings of the National Academy of Sciences of the United States of America, 29*(3-4), 87.

Simmons, M.D. (2020). Larger benthic foraminifera. Subchapter 3H. *In* Gradstein, F.M., Ogg, J.G., Schmitz, M.D., Ogg, G.M. (Eds), Geologic Time Scale 2020. *Elsevier*, Amsterdam, 88–98.

Sirel, E. and Işik, U. (2011). *Marasella* n. gen.(Miogypsinidae, Foraminiferida) and re-description of *Risananeiza* Boukhary, Kuss & Abdelraouf, 2008 from the Late Chattian of the Maras Region (S of Turkey). *Revue de Paléobiologie, 30*(1), 31–43.

Sirel, E., Ayyildiz, T. and Deveciler, A. (2020). Foraminifera of shallow and very shallow facies from the upper Eocene–lower Oligocene Kazandere Member, Soğucak Formation, Thrace Basin, northwest Turkey. *Geologica acta: an international earth science journal, 18*(1), 13.

Sirel, E., Özgen-Erdem, O. and Kangal, Ö . (2013). Systematics and Oligocene (Rupelianearly Chattian) foraminifera from lagoonal-very shallow water limestone in the eastern Sivas Basin (central Turkey).

Geologia Croatica, 66, 83–109.
Tan Sin Hok (1936). Zur Kenntnis der Miogypsiniden. Ingenieur in Nederlandsch-Indië, *Mijnbouw en Geologie, 3,* 45–61.
Todd, R. And Low, D. (1960). Smaller Foraminifera from Eniwetok Drill Holes. *Geol. Surv. Prof. Pap*. *260-X*, 799–861.
Todd, R. and Post, R. (1954). Smaller Foraminifera from Bikini drill holes. Part 4, Paleontology of Bikini and nearby atolls. U.S. *Geol. Surv. Prof. Pap. 260N*, 547–568.
Todd, R. and Post, R. (1970). Smaller foraminifera from Midway drill holes. *Geol. Surv. Prof. Pap*. 680-E, E1–E49.
Tosquella, J., González-Regalado, M.L., Ruiz, F. and Baceta, J.I. (2001). El género *Heterostegina* (Nummulitidae, Foraminifera) en el Mioceno superior del SO de España. *Geobios, 34*(3), 278–290.
Uhlig, V. (1886). Über eine Mikrofauna aus dem Alttertiär der westgalizischen Karpathen. *Jahrbuch der Kaiserlich-Königlichen Geologischen Reichsanstalt, 36*, 141–214.
Vessem, E.J. Van (1978). Study of Lepidocyclinidae from South East Asia, particularly from Java and Borneo. *Utrecht Micropalaeontological Bulletins 19*, 162 pp.
Vlerk, I.M. Van der (1928). The genus *Lepidocyclina* in the Indo-Pacific. *Eclogae Geologicae Helvetiae, 21*, 182–211.
Vlerk, I.M. Van der (1929). Groote foraminiferen van N.O. Borneo. Dienst van den Mijnbouw in Nederlandsch-Indie, *Wetenschappelijke Mededee- lingen, 9*, 1–45.
Vlerk, I.M. Van der (1959). Problems and principles of Tertiary and Quaternary stratigraphy. *Quarterly Journal of Geological Society, London , 115,* 49–63.
Vlerk, I.M. Van der (1963). Biometric research on *Lepidocyclina*. *Micropalaeontology, 9*, 425–426.
Vlerk, I.M. Van der and Gloor, H. (1968). Evolution of an embryo. *Genetica , 39,* 45–63.
Wade, B.S., Pearson, P.N., Berggren, W.A. and Pälike, H. (2011). Review and revision of Cenozoic tropical planktonic foraminiferal biostratigraphy and calibration to the geomagnetic polarity and astronomical time scale. *Earth-Science Reviews*, *104*, 111-142.

Chapter 2. Biostratigraphic and Palaeobiogeographic patterns of the larger porcelaneous foraminifer *Austrotrillina* Parr, 1942

published in Marine Micropaleontology 169 (2021), 102058
doi: /10.1016/j.marmicro.2021.102058

Marine Micropaleontology 169 (2021) 102058

Contents lists available at ScienceDirect

Marine Micropaleontology

journal homepage: www.elsevier.com/locate/marmicro

Biostratigraphical and palaeobiogeographical patterns of the larger porcelaneous foraminifer *Austrotrillina* Parr, 1942

Davide Bassi [a,*], Md. Aftabuzzaman [b], Monica Bolivar-Feriche [a], Juan Carlos Braga [c], Julio Aguirre [c], Willem Renema [d,e], Hideko Takayanagi [b], Yasufumi Iryu [b]

[a] Dipartimento di Fisica e Scienze della Terra, Università degli Studi di Ferrara, via Saragat 1, 44122 Ferrara, Italy
[b] Institute of Geology and Paleontology, Graduate School of Science, Tohoku University, Aobayama, Sendai 980-8578, Japan
[c] Departamento de Estratigrafía y Paleontología, Universidad de Granada, Campus Fuentenueva s/n, 18002 Granada, Spain
[d] Naturalis Biodiversity Center, 9517, 2300 RA Leiden, the Netherlands
[e] Department of Ecosystem and Landscape Dynamics, Institute for Biodiversity and Ecosystem Dynamics, University of Amsterdam, P.O. Box 94240, 1090v Amsterdam, the Netherlands

ARTICLE INFO

Keywords:
Oligocene–Miocene
shallow-water carbonates
Miliolids
Systematics
Biostratigraphy
Tethys
Mediterranean
Indo-Pacific

ABSTRACT

Among the Tethyan larger porcelaneous foraminifera widespread from the middle–late Eocene to the middle Miocene, *Austrotrillina* Parr, 1942 is the only genus showing a non-homogeneous shell structure. This consists of a parakeriotheca, coated by a thin, dense tectum. Four *Austrotrillina* species (*A. brunni*, *A. eocaenica*, *A. howchini*, *A. striata*) have been often used as biostratigraphical markers in the Mediterranean and Indo-Pacific areas. New materials from southeastern Spain and Central Indo-Pacific (Indonesia, Kita-daito-jima, Kikai Seamount) were studied to assess their taxonomic status, species circumscription and palaeobiogeographical patterns. Based on re-assessed shell structures *A. asmariensis* Adams is considered a junior synonym of *A. brunni* Marie.

Austrotrillina eocaenica first appears in the middle–late Eocene of Iran. Two Rupelian descendants, *A. brunni* and *A. striata*, migrated from the Western Tethys into the Indo-Pacific. *Austrotrillina striata* reached Indonesia and Western Australia in the Chattian, then disappeared in the Langhian of Kita-daito-jima. *Austrotrillina brunni* first occurred in the Burdigalian of Indonesia and Western Australia and disappeared in the early Serravallian of Western and South Australia. *Austrotrillina brunni* and *A. striata* disappeared in the Serravallian westernmost Mediterranean (southeastern Spain). From the Burdigalian the exclusive occurrence of *A. howchini* in the Indo-Pacific areas is a possible result of the closing Tethyan Seaway, which differentiated the Mediterranean and Indo-Pacific bioprovinces. This species disappears in the latemost Langhian–early Serravallian of South Australia and in the Kikai Seamount. The palaeobiogeographical distribution of these species suggests an early Miocene active connection of Eastern Africa with the Central Indo–West Pacific.

1. Introduction

Austrotrillinids are fossil porcelaneous larger benthic foraminifera (LBF) widespread in the Western Tethys and in the Indo-Pacific from the middle–late Eocene to the middle Miocene (e.g., Adams et al., 1983; Cahuzac and Poignant, 1997; Renema, 2007). This group, with a miliolid, trilocular growth, differs from other porcelaneous LBF in having an alveolar exoskeleton formed by numerous secondary partitions (subepidermal mesh in Loeblich and Tappan, 1986, p. 345). The porcelaneous foraminiferal shell texture consists of calcite needle, rod, lath or plate-shaped crystals (Loeblich and Tappan, 1987; Parker, 2017). The crystal arrangement can change in the shell wall from the outer shell part, through exoskeletal to endoskeletal structures (Hottinger, 2006; Parker, 2017).

Exoskeletal structures have been described from microagglutinated larger lituolids (Hottinger, 1967), orbitolinids (e.g., Hofker Jr., 1963), soritins (Hottinger, 2001; see *Reticulotaberina jahrumiana* Nafarieh et al., 2019), and the austrotrillinids (Loeblich and Tappan, 1986). The austrotrillinid alveolar structure consists of branched or unbranched parapores with a blind ending, with exoskeletal elements, such as beams perpendicular to the septum (Hottinger, 2006). This alveolar structure

* Corresponding author.
E-mail addresses: bsd@unife.it (D. Bassi), ma.rony@yahoo.com (Md. Aftabuzzaman), blvmnc@unife.it (M. Bolivar-Feriche), jbraga@ugr.es (J.C. Braga), jaguirre@ugr.es (J. Aguirre), willem.renema@naturalis.nl (W. Renema), hideko.takayanagi.b4@tohoku.ac.jp (H. Takayanagi), yasufumi.iryu.d8@tohoku.ac.jp (Y. Iryu).

https://doi.org/10.1016/j.marmicro.2021.102058
Received 26 May 2021; Received in revised form 30 September 2021; Accepted 11 October 2021
Available online 18 October 2021
0377-8398/© 2021 Elsevier B.V. All rights reserved.

makes up the layered austrotrillinid shell along with a thin, outermost dense coating epiderm.

Among the porcelaneous LBF, *Austrotrillina* Parr, 1942 is the only genus showing a non-homogeneous shell texture and structure (i.e., exoskeleton). Seven *Austrotrillina* species have been described: *Austrotrillina asmariensis* Adams, 1968, *A. brunni* Marie *in* Brunn et al., 1955, *Austrotrillina eocaenica* Hottinger, 2007, *A. howchini* (Schlumberger, 1893), *A. laberynthica* Escandell and Colom, 1962, *A. paucialveolata* Grimsdale, 1952, and *A. striata* Todd and Post, 1954. As their peculiar shell structure is easily identifiable in random thin section analysis, *Austrotrillina* species have been used as biostratigraphical markers in the East Indian Letter Stages (Van Der Vlerk and Umbgrove, 1927; van Bemmelen, 1949; Marks, 1957; Cole, 1969; Todd and Post, 1970; Adams, 1984; BouDagher-Fadel and Banner, 1999; Renema, 2007). The shallow-water carbonate deposits with *Austrotrillina* species have been often related to settings above the fair-weather wave base (Buxton and Pedley, 1989; Hottinger, 1997; Beavington-Penney and Racey, 2004; Haig et al., 2020; Simmons, 2020).

Although frequently recorded in the Mediterranean region (e.g., Poignant and Lorenz, 1985), this genus has never been considered in the Western Tethyan shallow benthic zonation, which is based on Oppel zones defined by temporal ranges of nummulitids, lepidocyclinids and miogypsinids (Cahuzac and Poignant, 1997). The single exception was *Austrotrillina paucialveolata* that would mark the Mediterranean Chattian (Wielandt, 1996).

After Adams's (1968) revision of *Austrotrillina*, no re-assessment of morphological features, biostratigraphical ranges, and palaeobiogeographic patterns of species included in the genus has been performed. The purpose of this paper is to re-assess the *Austrotrillina* shell structure and, on the base of new data on species occurrences with improved age constraints, to understand the Tethyan evolutionary history and palaeobiogeography of its species. New records from southeastern Spain, Indonesia and northern Philippine Sea indicate that the genus appeared in the middle–late Eocene, diversified in the early Oligocene and the descendants disappeared in the Mediterranean and Indo-Pacific areas in the Langhian and Serravallian.

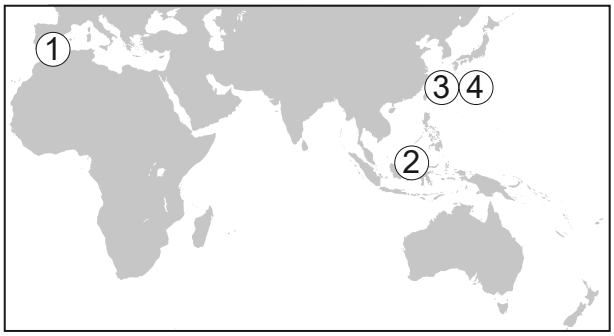

Fig. 1. Geographical locations of the newly studied *Austrotrillina* records. 1, southeastern Spain (Ibi and Sierra de Marmolance); 2, Mangkalihat and Wailawi, East Kalimantan, Indonesia; 3–4, northern Philippine Sea, Japan (3, Kita-daito-jima; 4, Kikai Seamount).

2. Materials and methods

Specimens in thin sections from hard-cemented limestone were examined, both from Hanzawa's (1940) collection from Kita-daito-jima housed at the Institute of Geology and Paleontology, Graduate School of Science, Tohoku University, Sendai (IGPS; Japan), and from newly collected samples from Spain, Indonesia and the Kikai Seamount (Northern Philippine Sea). The thin sections from Indonesia and southeastern Spain are housed at the Departamento de Estratigrafía y Paleontología, University of Granada (Spain), while the collection from the Kikai Seamount is stored at the Institute of Geology and Paleontology, Graduate School of Science, Tohoku University (IGPS). The isolated specimens from Wailawi, East Kalimantan (Indonesia), are housed at the Naturalis Biodiversity Center, Leiden (the Netherland).

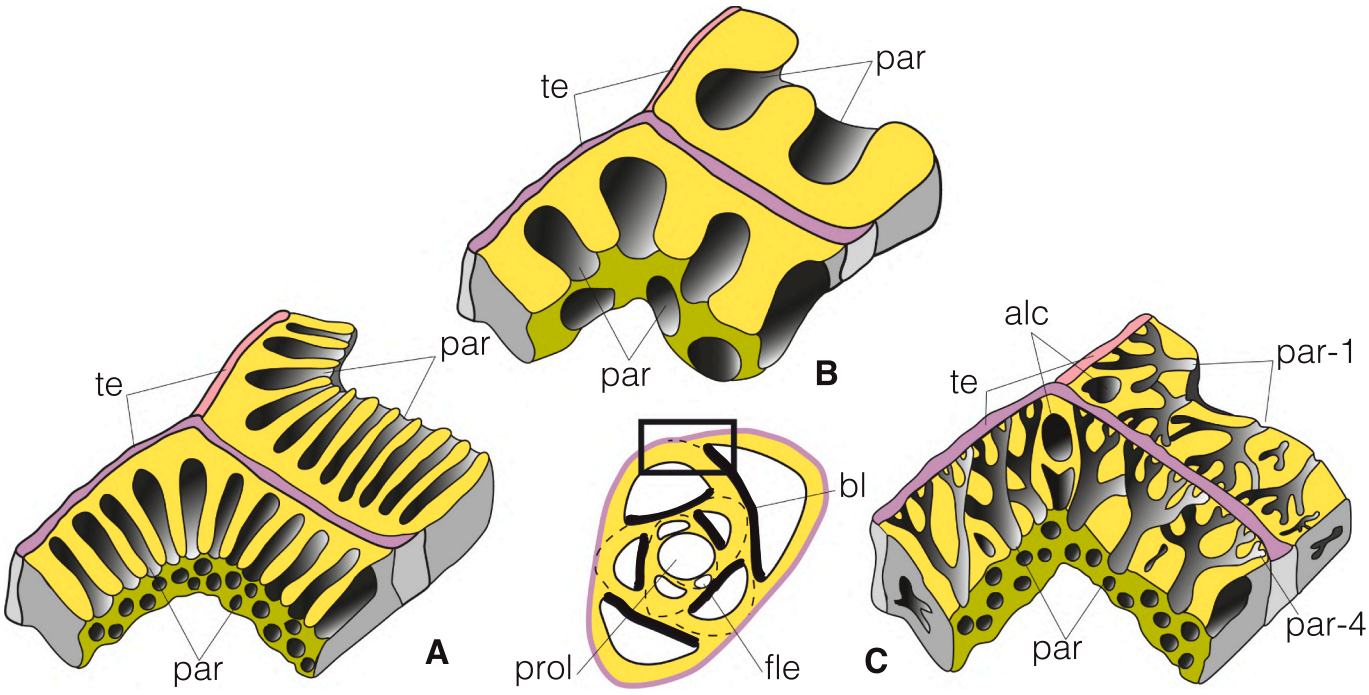

Fig. 2. Shell structures characterising the exoskeleton in *Austrotrillina* Parr, 1942. The schemes refer to the shell boundary between two successive chambers. A, *Austrotrillina brunni* Marie *in* Brunn et al., 1955. B, *Austrotrillina striata* Todd and Post, 1954. C, *Austrotrillina howchini* (Schlumberger, 1893). Shell structure of *A. eocaenica* differs from that of *A. striata* in having subsutural alcoves (see Table 1). Abbreviations: alc, alcove; bl, basal layer; fle, flexostyle; par, parapores; par-1, parapores of first order; par-4, parapores of four order; prol, proloculus; te, tectum. Schematic drawing, not to scale.

Table 1
Comparison of diagnostic shell characteristics of *Austrotrillina* species and related stratigraphical setting. Species are listed according to their first appearance reported in literature.

	age	prol (μm)	flexostyle	parakeriotheca	beams, subsut alcoves
A. eocaenica [1]	Lutetian–Priabonian	24–32	yes *	shallow, coarse parapores	yes
A. brunni [2]	Rupelian–Serravallian	(60) 100–250	yes *	fine parapores	no
A. striata [3]	Rupelian–Serravallian	50–130	yes **	coarse parapores	no
A. howchini [4]	Aquitanian–Langhian	70–150	no	branching parapores	yes

Based on data from: 1, Hottinger (2007), Serra-Kiel et al. (2016); 2, Marie (*in* Brunn et al., 1955), Adams (1968), Bassi et al. (2007), Sirel et al. (2013), Ferràndez-Cañadell and Bover-Arnal (2017), Riera et al. (2019), this study; 3, Todd and Post (1954), Adams (1968), this study; 4, Parr (1942), Carter (1964), Adams (1968), this study.
Abbreviations: subsut, subsutural; *, parakeriotheca not present in the wall of the nepionic apparatus; **, parakeriotheca not present in the first three chambers.

Table 2
Stratigraphical and palaeogeographical distribution of *Austrotrillina eocaenica* and *Austrotrillina brunni*. tran, transitional forms.

References	Referred to as	Age	Locality	Illustrations
Rahaghi (1980)	*A. paucialveolata*	(?) uppermost middle Eocene	Shiraz, Iran	pl. 7, figs 6–9
Hottinger (2007)	*A. eocaenica*	Bartonian–Priabonian	Shiraz, Iran	pl. 1, fig. 2; pl. 2, figs. 2–9; pl. 12, fig. 8
Wielandt-Schuster et al. (2004)	*A. asmariensis*	Rupelian	Greece	pl. 4, fig. 21
Sirel et al. (2013)	*A. brunni*	Rupelian	central Turkey	pl. 11, figs. 2–17
Serra-Kiel et al. (2016)	*A. brunni*	Rupelian	Dhofar, Socotra Island	figs. 14 (17–19), 16 (1–11)
Susanta (1990)	*A. howchini*	late Oligocene	western Kutch	pl. 57, fig. 23
Adams (1968)	*A. asmariensis*	Rupelian–Chattian	Kuh e Pataq	pl. 1, figs. 1–12
Sirel (2003)	*A. brunni*	Rupelian–Chattian	southern and eastern Turkey	pl. 10, figs. 10–16
Gedik (2014)	*A. brunni*	Rupelian–Chattian	eastern Turkey	pl. 3, figs. 12–16, 18–22
				pl. 3, fig. 25; pl. 4, figs. 1–13
	A. asmariensis			
Gedik (2015)	*A. brunni*	Chattian	eastern Turkey	pl. 1, figs. 19–23, 26, 27
Gedik (2020)	*A. asmariensis*	Rupelian–Chattian	Malatya, Turkey	fig. 14, L–P, A1, A6
				fig. 14, V–Z, A3, A4
	A. brunni			
BouDagher-Fadel (2018)	*A. asmariensis*	Oligocene	Iraq	pl. 6.3, figs. 7–9
Marie *in* Brunn et al. (1955)	*A. brunni*	Aquitanian	Greece	pl. 19, figs. 4–8
Lawa and Gafhur (2015)	*A. howchini*	Aquitanian	Kurdistan	pl. 4, figs. 2–3
Roozpeykar and Moghaddam (2016)	*A. asmariensis/A. howchini*	Aquitanian	Iran	fig. 9B, C, M
Eames et al. (1962)	*A. howchini*	Burdigalian	Kenya, Sabaki River	pl. 6, figs. A–B
Barberi et al. (1987)	*A.* sp.	Burdigalian	Sumbawa	pl. 5, fig. 10
Daneshian and Dana (2019)	*A. howchini*	Aquitanian–Burdigalian	Central Iran	fig. 5E
BouDagher-Fadel (2018)	*A. asmariensis*	Aquitanian	Iran	pl. 7.1, figs. 8–9
Dasgupta (1977)	*A. howchini*	Burdigalian	western India	pl. 1, figs. 2–3
Renz (1936)	*A. howchini*	Burdigalian	Apennines	pl. 15, figs 4–5
Ma et al. (2018)	*A. asmariensis*	Te5	South China Sea	fig. 7A–B
	A. brunni			fig. 7C–D
	A. howchini			fig. 7E–F
BouDagher-Fadel and Lokier (2005)	*A. asmariensis*	Langhian	Java	pl. 1, figs. 1–2
	A. howchini			pl. 1, fig. 3
Gedik (2015)	*A. asmariensis*	Burdigalian	eastern Turkey	pl. 1, figs. 12–16, 24, 29
Haig et al. (2020)	*A. asmariensis*	Burdigalian	Western Australia	fig. 8A–C
	A. sp.			fig. 8D–E
	A. howchini			fig. 8F–H
O'Connell et al. (2012)	*A. howchini*	early–middle Miocene	South Australia	fig. 5F
Riera et al. (2019)	*A. asmariensis*	Burdigalian–early Serravallian	Western Australia	fig. 8 (1–18), fig. 10 (1–6)
Riera et al. (2019)	tran *A. asmariensis/howchini*	Langhian–early Serravallian	Western Australia	fig. 14 (5–13)
This study	*A. brunni*	Langhian	Kita-daito-jima	Fig. 3A
This study	*A. brunni*	Serravallian	southeastern Spain	Figs. 3B–C

Structural and morphological terms are those used by Hottinger (2006). The suprageneric classification follows Loeblich and Tappan (1986, 1987). The descriptions of the analysed *Austrotrillina* species are ordered according to their stratigraphical appearance. References to published species and their records include only those in which structural diagnostic features were described and illustrated. Synonymy lists can be found in the Supplementary data.

Adams' (1968) species descriptions and illustrations (including types and topotypes) cover the main variability of parapores (i.e., alveoles), although he did not distinguish shell texture, shell structure and branching parapores.

In total 10 specimens from samples RGMS.603540 and RGMS.574854 (Wailawi, East Kalimantan) were micro-CT scanned using a Zeiss X-Radia versa 520 at Naturalis Biodiversity Center (by W. R.), Leiden, the Netherlands. Specimens were scanned at 80 kV and a voxel size of 0.9–1.4 μm. 3D-volumes were reconstructed and segmented using Avizo 2020.2 software (ThermoFisher Scientific, Watham MA, United States).

2.1. Southeastern Spain

The studied specimens were collected from two localities: Ibi and Sierra de Marmolance (Fig. 1).

Ibi is a town located in the Alicante province in southeastern Spain. The study samples were collected from Rupelian-lower Chattian limestones belonging to the Prebetic Domain of the External Zones of the

Table 3
Stratigraphical and palaeogeographical distribution of *Austrotrillina striata*.

References	Referred to as	Age	Locality	Illustrations
Grimsdale (1952)	*A. paucialveolata*	Oligocene	Kirkuk, Iraq	pl. 20, figs. 7–10
Boukhary et al. (2010)	*A. asmariensis*	Rupelian	UAE, Oman, western Egypt	pl. 7, fig. 8
Yazdi-Moghadam et al. (2018)	*A.* aff. *paucialveolata*	Rupelian	northwest Iran	fig. 8H–I
Serra-Kiel et al. (2016)	*A. paucialveolata*	Rupelian	Dhofar, Socotra Island	figs. 14(8–12)–15(9–20)
Seyrafian et al. (2011)	*A. howchini*	Rupelian	Iran	fig. 10p
Karevan et al. (2014)	*A. howchini*	Rupelian	Iran	fig. 6A
Susanta (1990)	*A. striata*	late Oligocene	western Kutch	pl. 57, fig. 21
Hottinger (1963)	*A. howchini*	Chattian	southern Spain	pl. 1, figs. 1–2
This study	*A. striata*	late Rupelian	southeastern Spain	Fig. 4
Gedik (2014)	*A. brunni*	Rupelian–Chattian	eastern Turkey	pl. 3, fig. 5
	A. howchini			pl. 3, figs. 17, 23–24
BouDagher-Fadel (2018)	*A. paucialveolata*	Oligocene	Iraq	pl. 6.9, figs. 15–17; pl. 6.10, figs. 1–2
Sajadi and Rashidi (2019)	*Austrotrillina*	Chattian	SE Persian Gulf	fig. 5N
Gedik (2017)	*A. brunni*	Chattian	eastern Turkey	fig. 6J–M
Gedik (2020)	*A. brunni*	Rupelian–Chattian	Malatya, Turkey	figs. 14, T–U
	A. howchini	Burdigalian		figs. 14, A2, A5
Adams (1965)	*A. howchini-striata*	Chattian	Indonesia	pl. 28, figs e–g
BouDagher-Fadel (2018)	*A. striata*	late Oligocene	Borneo	pl. 7.1, figs. 4–7
		early Miocene	Bikini	
Chaproniere (1984)	*A. striata*	Chattian–Aquitanian	Western Australia	no
Todd and Low (1960)	*A. striata*	lower Te	Eniwetok Atoll	pl. 261, fig. 22
Adams (1973)	*A. striata*	Te	Eniwetok Atoll	pl. 1, fig. 4
Gibson and Margerum (1991)	*A. striata*	lower Te	Eniwetok Atoll	no
Matsumaru (1996)	*A. howchini*	Te1–4	Ogasawara Islands (Japan)	pl. 84, figs. 3–6
Cole (1969)	*A. striata*	Te	Midway Atoll	pl. 4, fig. 27, pl. 5, figs. 4–5
Todd and Post (1970)	*A. striata*	Te	Midway Atoll	pl. 11, fig. 5 (outer surface)
Chaproniere (1983)	*A. striata*	upper Te	Western Australia	pl. 2, fig. 1
Todd and Post (1954)	*A. striata*	Te	Bikini	pl. 198, fig. 9
Cole (1954)	*A. striata*	Te	Saipan	pl. 210, figs. 6–9
Cole (1957)	*A. striata*	Te	Bikini	pl. 101, figs. 4–6
Todd and Post (1954)	*A. striata*	early Miocene	Bikini	pl. 198, fig. 9
Ma et al. (2018)	*A. brunni*	Te5	South China Sea	fig. 7C–D
Novak (2014)	*A. howchini*	Tf1	Indonesia	figs. 2B, 2C
BouDagher-Fadel (2018)	*A. brunni*	Burdigalian	Indonesia	pl. 7.1, fig. 11
Dasgupta (1977)	*A. striata*	Aquitanian	western India	pl. 1, figs. 4–6
Roozpeykar and Moghaddam (2016)	*A.* sp.	Aquitanian	Iran	fig. 9A
Daneshian and Dana (2019)	*A. howchini*	Aquitanian–Burdigalian	Central Iran	fig. 5F
Yazdi-Moghadam et al. (2021)	*A. asmariensis*	Burdigalian	NW Iran	Figs. 14 a–i
Renema (2007)	*A. striata*	Td	southeast Sulawasi	no
Betzler and Chaproniere (1993)	*A. striata*	early Miocene	Queensland Plateau	pl. 4, figs. 4–5
Haig et al. (2020)	*A. striata*	Burdigalian	Western Australia	fig. 8I
Adams and Belford (1974)	*A. striata*	Te (Aquitanian–Burdigalian)	Christmas Island	pl. 73, fig. 6
Hanzawa (1940)	*A. howchini*	Aquitanian	Kita-daito-jima	pl. 42, figs. 1–2
Lunt and Allan (2004)	*A. striata*	top Te	Indonesia	p. 45
Hanzawa (1957)	*A. howchini*	Aquitanian–Burdigalian	Micronesia	pl. 22, figs. 12–13, pl. 34, figs. 1–2
BouDagher-Fadel et al. (2000)	*A. striata*	Burdigalian	northeast Borneo	pl. 1, fig. 2
Chaproniere (1984)	*A. howchini*	middle Miocene	Western Australia	pl. 14, figs. 1–2
This study	*A. striata*	Aquitanian–Langhian	Kita-daito-jima	Fig. 5
This study	*A. striata*	Serravallian	southeastern Spain	Fig. 6

Table 4
Stratigraphical and palaeogeographical distribution of *Austrotrillina howchini*. *T*, *Trillina*.

References	Referred to as	Age	Locality	Illustrations
Adams (1968)	*A. howchini*	early Miocene	Tanzania (Pemba Island)	pl. 6, fig. 1
			Malabar	
		middle Miocene	South Australia	pl. 6, figs. 2, 4–5
				pl. 2, figs. 3–4, 6–7; pl. 6,
Adams (1973)	*A. howchini*	middle Miocene	South Australia	pl. 2, fig. 5
BouDagher-Fadel (2018)	*A. howchini*	early Miocene (lower Tf1)	Western Australia, Tanzania, Kenya	pl. 7.1, figs. 1–3, 12
				pl. 7.8, fig. 3
Schlumberger (1893)	*T. howchini*	Burdigalian	Australia, Philippines	text-fig. 1; pl. 3, fig. 6
Parr (1942)	*A. howchini*	Miocene	Parish, Pallarang, South Australia	fig. 1–3
Rögl and Briguglio (2018)	*A. howchini*	Burdigalian	southern India	pl. 4, figs. 19–22
Novak (2014)	*A. howchini*	late Te5–early Tf1	Indonesia	figs. 2A, D–F
This study	*A. howchini*	Tf1 (early Burdigalian)	East Kalimantan	Fig. 8
Binnekamp (1973)	*A. howchini*	Burdigalian–Langhian	New Britain, PNG	pl. 1, figs. 1–4
Barberi et al. (1987)	*A. howchini*	late Langhian–early Serravallian	Indonesia	pl. 7, fig. 6
This study	*A. howchini*	late Langhian–early Serravallian	East Kalimantan	Fig. 7
This study	*A. howchini*	latemost Langhian–early Serravallian	Kikai Seamount	Fig. 9

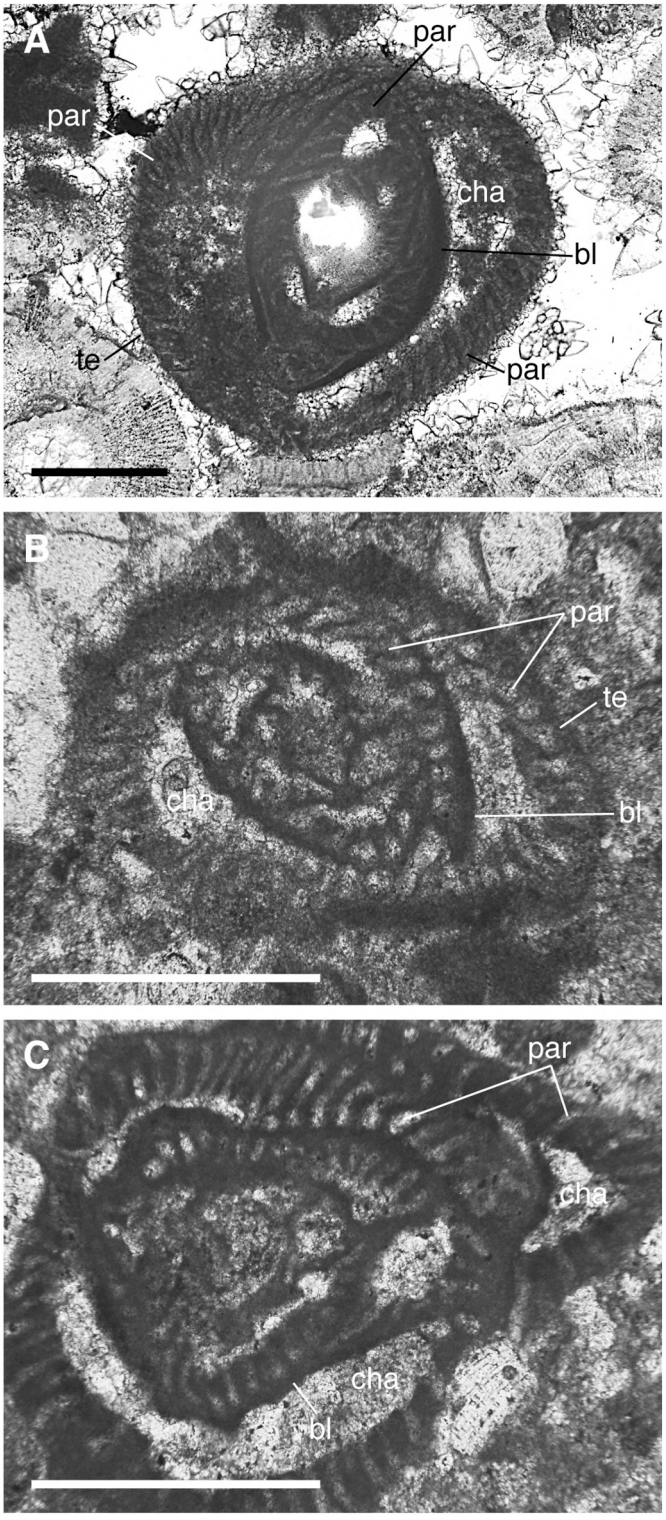

Fig. 3. *Austrotrillina brunni* Marie *in* Brunn et al., 1955. A, tangential subtransversal section showing the fine parakeriotheca and the basal layer; Burdigalian–Langhian boundary, Kita-daito-jima, Hanzawa's (1940) collection, sample 835 (202.66 m); Institute of Geology and Paleontology, Graduate School of Science, Tohoku University (IGPS), Sendai, Japan. B–C, tangential sections of deformed specimens showing the fine parakeriotheca coated by the tectum; Serravallian, Sierra de Marmolance. Abbreviations: bl, basal layer; cha, chamber; par, parapores; te, tectum. Scale bars represent 0.250 mm.

Betic Cordillera (Geel, 2000). During the Rupelian–early Chattian the Prebetic Domain was the proximal part of the Southern Iberian Margin (Geel, 1995; Höntzsch et al., 2013). The sampled Oligocene carbonates near Ibi formed in a back-reef setting (Geel, 1995). The study samples are from uppermost Rupelian deposits, characterised by 'a series of overlapping washover fans with intercalations of *Austrotrillina–Praerhapydionina* grainstone and coral rubble beds' (Geel, 2000). Upper Chattian deposits are missing in the area due to uplift and erosion.

The Serravallian specimens occur in middle Miocene limestones from the Sierra de Marmolance near Huéscar in the Granada province. This limestone succession belongs to the Subbetic Domain of the External Zones of the Betic Cordillera. The Subbetic was the distal domain of the Southern Iberian Margin, which in middle Miocene times was already deformed and partially emergent. Marls with Burdigalian–Serravallian planktonic foraminifera occur at the base and interfinger with limestones, constraining their age. The Serravallian *Austrotrillina* occurs in shallow-water bioclastic limestones rich in LBF and coralline red algae.

2.2. East Kalimantan, Indonesia

The studied specimens were collected from Mangkalihat and Wailawi (Fig. 1). The samples were collected along the banks of the Taballar River east of the Taballar village in the Mangkalihat peninsula in East Kalimantan (Borneo; Fig. 1). The Taballar limestone section cropping out in the sampled river stretch is late Aquitanian–early Burdigalian in age (Novak, 2014). The Taballar limestone is a shallow-water carbonate deposit formed in a low-energy inner platform (van der Vlerk, 1929; Wilson et al., 1999; Wilson, 2008; Novak, 2014).

Samples from the Wailawi 1 core are stored in the Naturalis Biodiversity Center collections. This core was drilled in the 1930s just south of Balikpapan Bay in East Kalimantan. The collections include well-preserved isolated LBF specimens at intervals between 320–350 m and 420–510 m depth. In both intervals *Austrotrillina* is observed in several samples. In the 510 m sample the planktonic foraminifera *Orbulina* (FO 15.1 Ma; Wade et al., 2011) and *Trilobus trilobota* have been found indicating a Langhian or younger age (Wade et al., 2011). In this interval *Planostegina* sp. is also abundant. In southeast Asia *Planostegina* occurs in the plankton zones M6–M9, roughly the middle to late Langhian, restricting the studied samples to the Langhian. Since *Planostegina* was not observed in the 320–350 m interval, an early Serravallian age for this interval is inferred from the combined occurrence of *Trybliolepidina martini* and *Nephrolepidina ferreroi*.

2.3. Northern Philippine Sea, southwestern Japan

The studied specimens were collected from Kita-daito-jima and the Kikai Seamount (Fig. 1).

Kita-daito-jima is a carbonate island located in the northwestern region of the Philippine Sea (25°55.6′–57.6′N, 131°16.9′–19.8′E). A deep borehole into atoll deposits was obtained from 431.7 m below the ground surface (mbgs) in 1934 and 1936 (Suzuki et al., 2006; Iryu et al., 2010). The material recovered from the Kita-daito-jima borehole consists exclusively of shallow-water carbonates distinguished in four lithologic units (C1, C2, C3, C4). The upper 100 m (Units C1 and C2) are pervasively dolomitised. The Oligocene to lower Miocene Unit C4 (209.3–431.7 mbgs), extending to the base of the borehole, consists of limestone probably originated from bioclastic packstone. The middle Miocene Unit C3, 105.9 m thick (103.4–209.3 mbgs), is composed of locally dolomitized rudstone along with grainstone and packstone. Studied samples were collected from Unit C4 (thin section labelled as 325.42–331.53 m; 21.7–22.1 Ma, Aquitanian) and Unit C3 (thin section 835, 15.8–16.4 Ma, Burdigalian–Langhian boundary; thin sections 753, 773–779, 14.8–15.2 Ma, Langhian). Numerical ages were determined by comparing the measured $^{87}Sr/^{86}Sr$ values (Ohde and Elderfield, 1992) with the global Sr calibration curve from McArthur et al. (2012), using the geologic time scale from Gradstein et al. (2012).

The Kikai Seamount (28°31′N, 131°05′E), near the axis of the Ryukyu Trench, the border between the Philippine Sea and Eurasia plates, constitutes an isolated flat-topped salient on the inner slope of the trench. The basement of the seamount continues to that of the Amami Plateau (Tokuyama et al., 1986), representing one of the Daito Ridge Group (Oki-Daito and Daito Ridges, and Amami Plateau) in the northern Philippine Sea (Hickey-Vargas, 2005). Carbonate rock cores drilled on the seamount comprise Miocene coral rudstone unconformably overlain by Early Pleistocene coral rudstone. The study specimens occur in thin sections from uppermost Langhian–lower Serravallian carbonates (Takayanagi et al., 2012).

3. Systematic palaeontology

Superfamily Miliolacea Ehrenberg, 1839.
Family Austrotrillinidae Loeblich and Tappan, 1986.
Genus *Austrotrillina* Parr, 1942.
Type species: *Trillina howchini* Schlumberger, 1893.

Remarks: The miliolid *Austrotrillina* shell is made up of randomly-oriented microcrystals of calcite giving rise to a porcelaneous texture (Loeblich and Tappan, 1987). The chamber wall consists of an exoskeleton made up of a tectum (i.e., organic lining in Hottinger, 2000) and an exoskeletal alveolar structure, the parakeriotheca (one-layered keriotheca). Tectum and parakeriotheca generally do not occur in the nepionic chambers, except in the first three in *A. striata* (Fig. 2). These two structural characters of the shell are diagnostic for distinguishing *Austrotrillina* (Adams, 1968, p. 82; Loeblich and Tappan, 1987, p. 355).

The tectum is a thin, dense outer layer about 8–15 μm in thickness. No tiny, pore-like gaps can be recognised. This tectum would correspond to the extrados described in the miliolids, which is an outer calcite lining bounded by an outer organic lining (Parker, 2017). However, since the *Austrotrillina* tectum does not subdivide chamber lumina (Hottinger, 2006), it cannot be considered a test structure as the extrados defined by Parker (2017). In modern miliolids the crystal elements that form the extrados exhibit different shapes, sizes and arrangements in different taxa (Parker, 2017). No comparison of tectum and extrados has been performed so far.

The tectum lines the parakeriotheca coating the lateral chamber wall. The alveole recesses are of varying depth and end blind beneath the tectum. Consequently, they are parapores sensu Hottinger (2006). The parakeriotheca is characterised by parapores. These parapores show different sizes and shapes, characterising three different alveolar arrangements.

Beams are exoskeletal partitions occurring in the proximal part of the chamber lumen near the previous chamber (Hottinger, 2006). The beams, perpendicular to the chamber septum and to the lateral chamber wall, produce subsutural alcoves with blind endings.

Among the seven *Austrotrillina* species known in literature

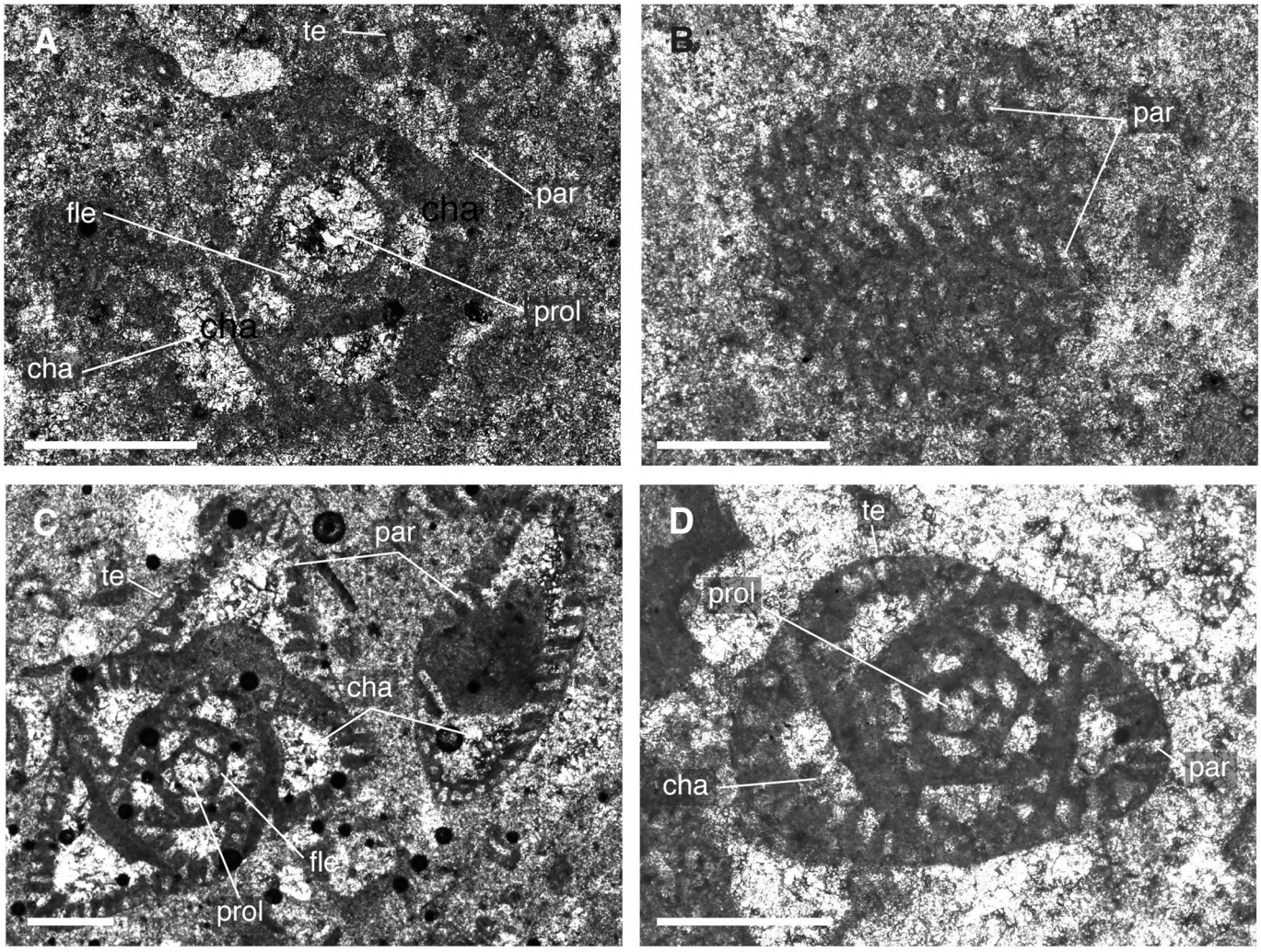

Fig. 4. *Austrotrillina striata* Todd and Post, 1954; latemost Rupelian, Ibi, Alicante; southeastern Spain. A, C–D, sub-transversal sections showing the nepionic apparatus and the coarse parakeriotheca coated by the tectum. B, tangential section showing the parapores. Abbreviations: cha, chamber; fle, flexostyle; par, parapores; prol, proloculus; te, tectum. Scale bars represent 0.250 mm.

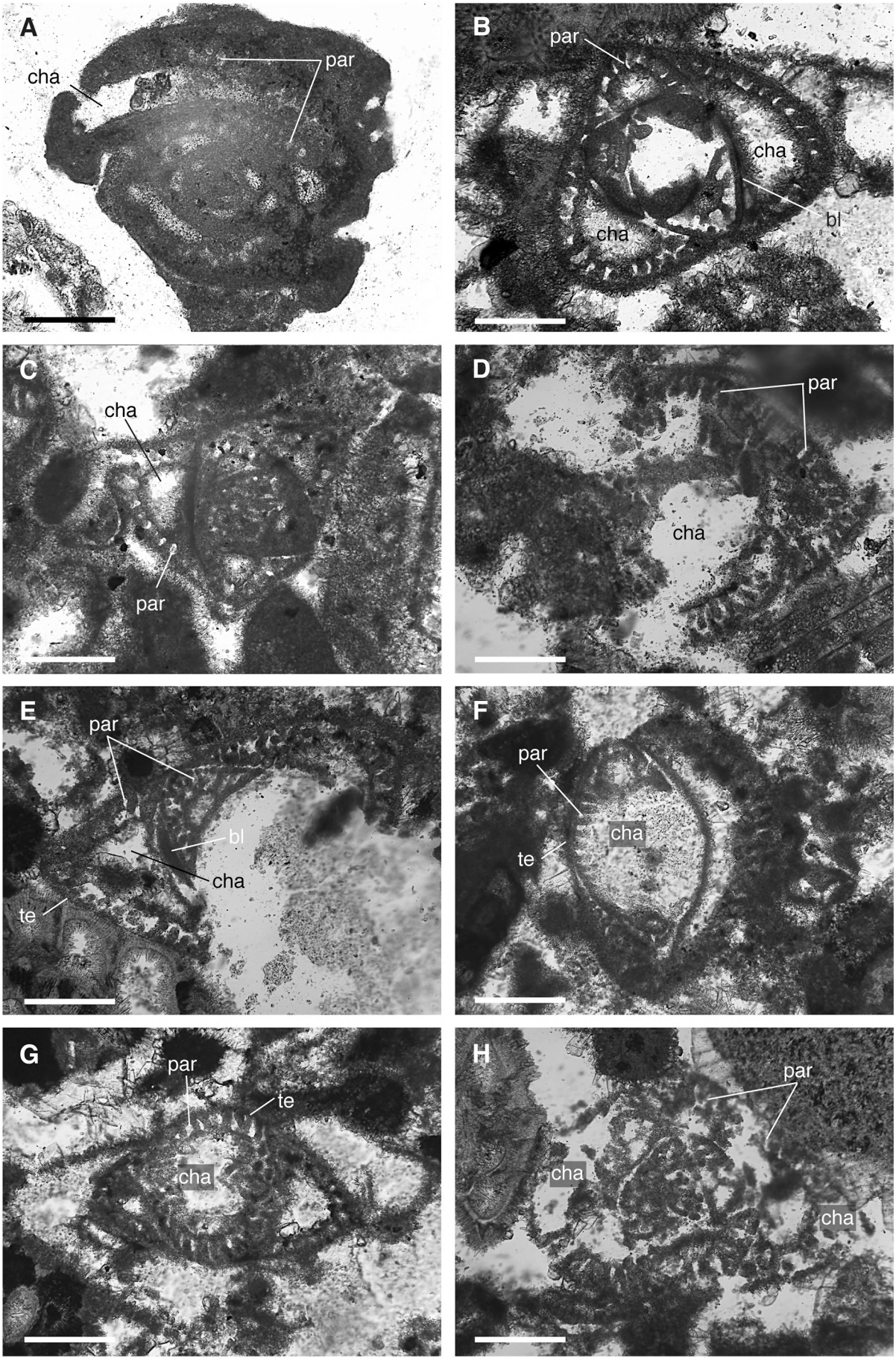

(caption on next page)

Fig. 5. *Austrotrillina striata* Todd and Post, 1954; Kita-daito-jima, northern Philippine Sea. A, Aquitanian; B–H, Langhian. A, core sample 325.42–331.53 m. B, core sample 753 (156.53 m). C, core sample 774 (166.39 m). D, core sample 775 (166.96 m). E, core sample 776 (167.52 m). F, core sample 777 (168.08 m). G, core sample 778 (168.61 m). H, core sample 779 (169.12 m). B, Hanzawa's (1940) collection; Institute of Geology and Paleontology, Graduate School of Science, Tohoku University (IGPS), Sendai, Japan; Langhian, Kita-daito-jima; tangential sub-transversal section, specimen illustrated in Hanzawa (1940), pl. 42, fig. 1, IGPS Coll. Cat. no. 21493). Abbreviations: bl, basal layer; cha, chamber; par, parapores; te, tectum. Scale bars represent 0.250 mm.

(*A. asmariensis*, *A. brunni*, *A. eocaenica*, *A. howchini*, *A. laberynthica*, *A. paucialveolata*, *A. striata*), the parakeriotheca, the diameter of the proloculus and the occurrence of beams and subsutural alcoves are reliable characters at species level distinguishing *A. eocaenica*, *A. brunni*, *A. striata* and *A. howchini* (Table 1). In Tables 2–4, the stratigraphical and palaeogeographical distributions of *Austrotrillina* species are listed.

Austrotrillina eocaenica Hottinger, 2007.

(see Supplementary data for the synonymy list)

Type reference and figures: *Austrotrillina eocaenica* Hottinger, 2007, p. 5, pl. 1, fig. 2 (bottom); pl. 2, figs. 2–9 (fig. 4, holotype); pl. 12,

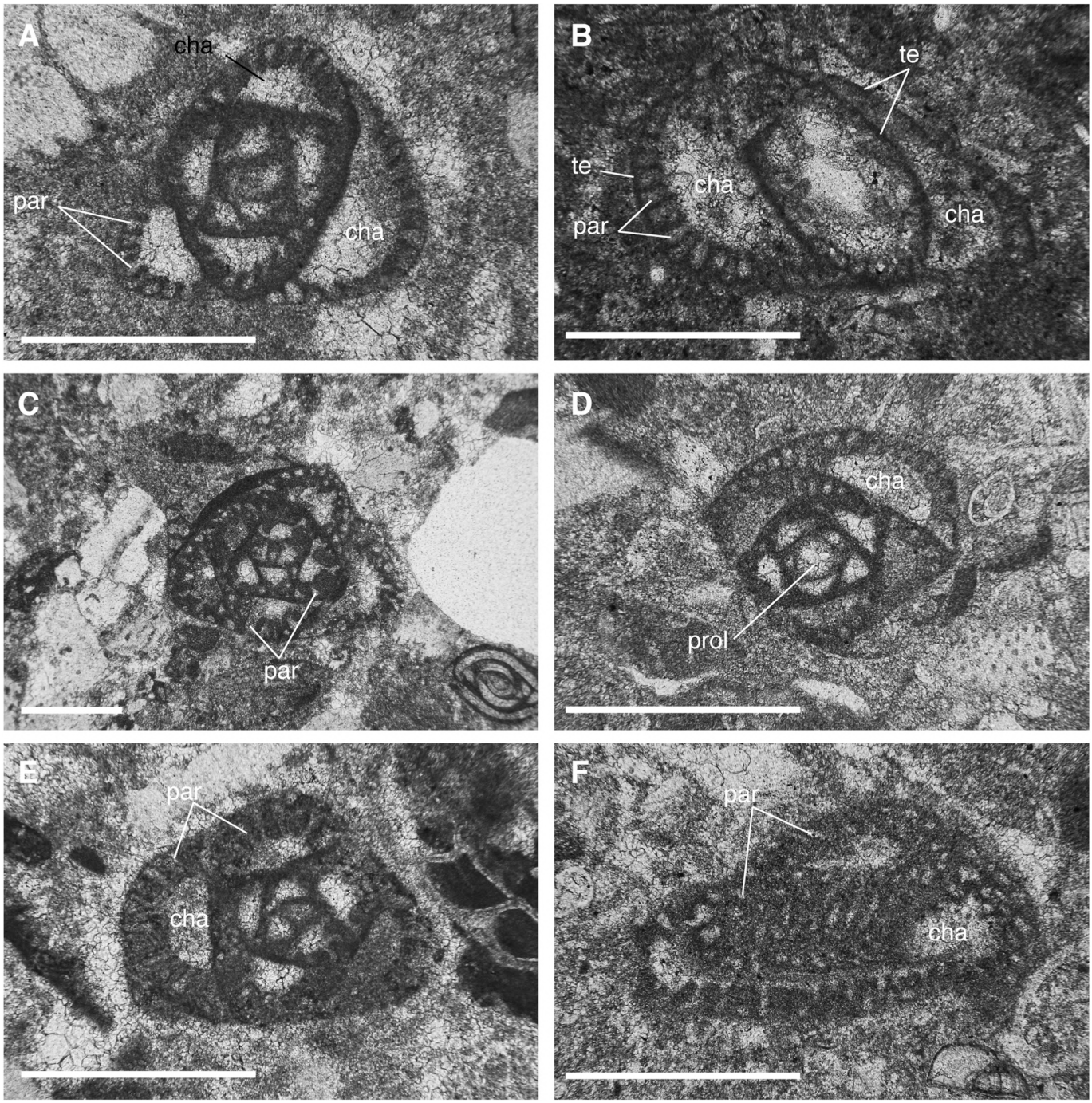

Fig. 6. *Austrotrillina striata* Todd and Post, 1954; Serravallian, Sierra de Marmolance; southeastern Spain. A, C–E, sub-transversal sections showing the miliolid trilocular growth and the coarse parakeriotheca underlying the tectum. B, F, tangential sections of deformed specimens. Abbreviations: cha, chamber; par, parapores; prol, proloculus; te, tectum. Scale bars represent 0.250 mm.

fig. 8 (left).

Diagnosis: Shallow and coarse parapores (i.e., alveoles in Hottinger, 2007, p. 5) arranged in parallel rows. Proloculus 24–32 μm in diameter with a narrow and low flexostyle (Hottinger, 2007, pl. 2, fig. 9). Nepionic apparatus (6–8 chambers) lacks parakeriotheca (Table 1). Beams between parapores and subsutural alcoves.

Stratigraphical distribution: *Austrotrillina eocaenica* has been found in the early?–middle Lutetian–Priabonian of western Dhofar (Oman) and Socotra Island (Serra-Kiel et al., 2016), Bartonian and Priabonian of Iran (Shiraz; Rahaghi, 1980, p. 31, fig. 14; Hottinger, 2007), and the Priabonian of Tunisia (Bonnefous and Bismuth, 1982) and southern Oman (Gallardo et al., 2001). The coarse parakeriotheca and the thick basal layer distinguish this species from *A. striata* (as *A. paucialveolata* in Rahaghi, 1980; Hottinger, 2007). Although assessing the shell structure is difficult in the low-quality photo of the single illustrated specimen from Tunisia (Bonnefous and Bismuth, 1982, pl. 4, fig. 1), the possible occurrence of shallow parapores ascribes the specimen to *A. eocaenica*. The only illustrated Priabonian specimen from southern Oman shows a coarse parakeriotheca comparable to that of *A. eocaenica* (Gallardo et al., 2001, pl. 1, fig. 12). The illustrated Eocene specimens from western Pakistan (Boukhari et al., 2016, figs. 5–7) are miliolids since they lack parakeriotheca.

Austrotrillina brunni Marie, 1955.

Fig. 3.

(see Supplementary data for the synonymy list)

Type reference and figures: *Austrotrillina brunni* Marie *in* Brunn et al., 1955, p. 203, pl. 9, figs 4–8 (fig. 5, holotype).

Diagnosis: Parallel fine parapores, almost with constant diameter. Proloculus ranging from 100 to 250 μm in diameter with narrow flexostyle. Parakeriotheca not present in the wall of the nepionic apparatus (Table 1). No beams, no subsutural alcoves.

Studied material: The analysed specimens are from the Burdigalian–Langhian boundary in Miocene limestones of Kita-daito-jima (Japan) and from Serravallian limestones of Sierra de Marmolance (southeastern Spain).

The parapores (*c.* 100 μm long and *c.* 20 μm in diameter), making up a fine alveolar parakeriotheca, are straight and sub-perpendicular to the overcoating tectum. The lateral chamber wall is tiny porous (i.e., thin parakeriotheca; Figs. 2A–3). The proloculus (*c.* 250 μm in diameter) has a narrow and low flexostyle. The very thin wall of the nepionic apparatus, with flexostyle, has no parakeriotheca.

Remark: Marie (*in* Brunn et al., 1955) introduced a new *Austrotrillina* species (*A. brunni* Marie, pl. 9, figs. 4–8) from the Chattian–Aquitanian of Greece. The illustrated specimens do not clearly show the characters of the parakeriotheca. However, Marie's (*in* Brunn et al., 1955) specimens of *A. brunni* were re-illustrated by Adams (1968), pl. 6, figs 6–8) showing a fine parakeriotheca with no branching parapores (Table 1). In re-assessing the stratigraphy and palaeoecology of Oligocene–lower Miocene sedimentary sequences of the Mesohellenic Basin, Wielandt-Schuster et al. (2004) illustrated a Rupelian *Austrotrillina* specimen from the Mesolouri stratigraphical section cropping out near Pentalofon (north-western Greece), the type locality of *A. brunni*. The specimen (as *A. asmariensis* in pl. 4, fig. 21 in Wielandt-Schuster et al., 2004) shows fine parapores. The occurrence of fine parapores which are not branching ascribe the specimen to *A. brunni*.

Adams (1968) introduced *A. asmariensis* because his specimens differed from *A. striata* in having an alveolar shell from the third chamber of the nepionic apparatus and thinner parapores. The nepionic apparatus of the Adams's specimens, showing a very thin wall with low and narrow flexostyle (see Adams, 1968, pl. 1, fig. 9 and pl. 5, fig. 8), has no parakeriotheca. The Adams's types differ from *A. howchini* in having non-branching parapores (Adams, 1968, p. 84). The occurrence of fine parapores from the third chamber and the absence of beams and subsutural alcoves are, therefore, distinctive characters of both *A. brunni* and *A. asmariensis* (Marie *in* Brunn et al., 1955, p. 203; Adams, 1968, pp. 82–83; Table 1).

The types of *A. asmariensis* (Adams, 1968, pl. 1, figs. 1–12) cannot be morphologically separated from the ones of *A. brunni* and, therefore, the former is considered a subjective junior synonym of the latter species (ICZN, 1999, Arts. 23.9.3 and 81.2.3). The affinities between *A. brunni* and *A. asmariensis* were highlighted by Adams (1968, p. 85) stating that *A. brunni* resembled the *A. striata/asmariensis* group. He considered *A. brunni* as a possible transitional form between *A. striata* and *A. howchini* (p. 89).

Stratigraphical distribution: In the Mediterranean area, *A. brunni* ranges from the Rupelian to the Serravallian, disappearing after the eastern closure of the Mediterranean Sea (Bassi et al., 2007, text-fig. 9; Fig. 10). Nonetheless, BouDagher-Fadel and Lokier (2005), fig. 3) considered *A. striata* and *A. brunni* restricted to the early Miocene. *Austrotrillina brunni* shows a wide geographical distribution from the Western Tethys (e.g., Gallardo et al., 2001; Bassi et al., 2007; Serra-Kiel et al., 2016; Ferràndez-Cañadell and Bover-Arnal, 2017) to Western Australia (Riera et al., 2019; Table 2).

In the Mediterranean area, the Serravallian records are represented by the studied specimens from the Sierra de Marmolance, while no Serravallian specimens have been found in the Middle East. Early Serravallian *A. brunni* is present in Western Australia, representing the youngest occurrence of *Austrotrillina* in the Pacific area (Riera et al., 2019). Upper Langhian–lower Serravallian specimens from the Trealla Limestones (Western Australia) have been considered to be '*Austrotrillina asmariensis* or transitional forms between *A. asmariensis* and *A. howchini*' (Riera et al., 2019, p. 331, figs. 14(5–13)). In the illustrated specimens the occurrence of the flexostyle (figs. 14 (5–6, 8a–9a)) and the absence of the parakeriotheca in the wall of the nepionic apparatus confirm the ascription to *A. brunni*. The coeval specimen from the lower–middle Miocene Nullabor Limestone (South Australia) is also

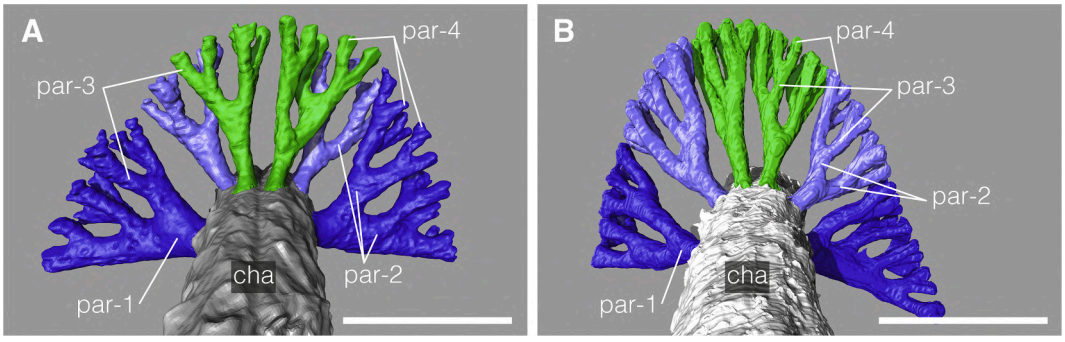

Fig. 7. *Austrotrillina howchini* (Schlumberger, 1893); middle–late Langhian (A) and Serravallian (B), Wailawi, East Kalimantan, Indonesia. A–B, micro-computed tomographic scanning 3-D rendered model with shell removed. Departing from the chamber (cha), the branching parapores of first order (par-1) bifurcate outwardly in subsequent order (from par-2 to par-4). The first-order parapores are longer (*c.* 75 μm long) than those in the subsequent orders (*c.* 35 μm long). Scale bars represent 0.250 mm.

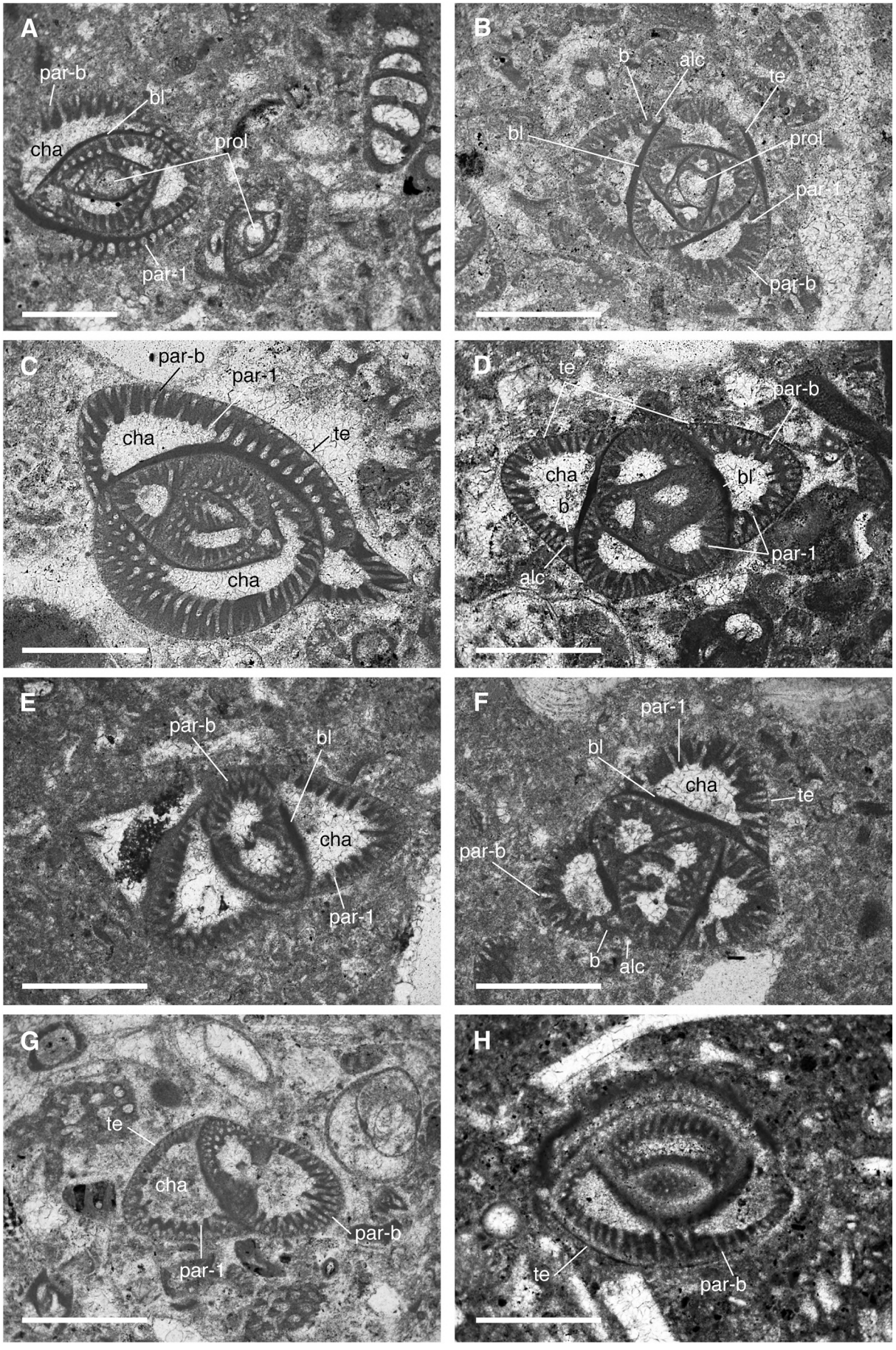

(caption on next page)

Fig. 8. *Austrotrillina howchini* (Schlumberger, 1893); (Tf1) early Burdigalian, Taballar limestone, Taballar river, East Kalimantan, Indonesia. A–F, tangential subtransversal sections showing the miliolid trilocular growth and the branching parapores of different orders (par-1, first order; par-b, second-to-fourth order) in the parakeriotheca underlying the tectum (te). G–H, tangential sections. Abbreviations: alc, alcove; b, beam; bl; basal layer; cha, chamber; prol, proloculus. Scale bars represent 0.250 mm.

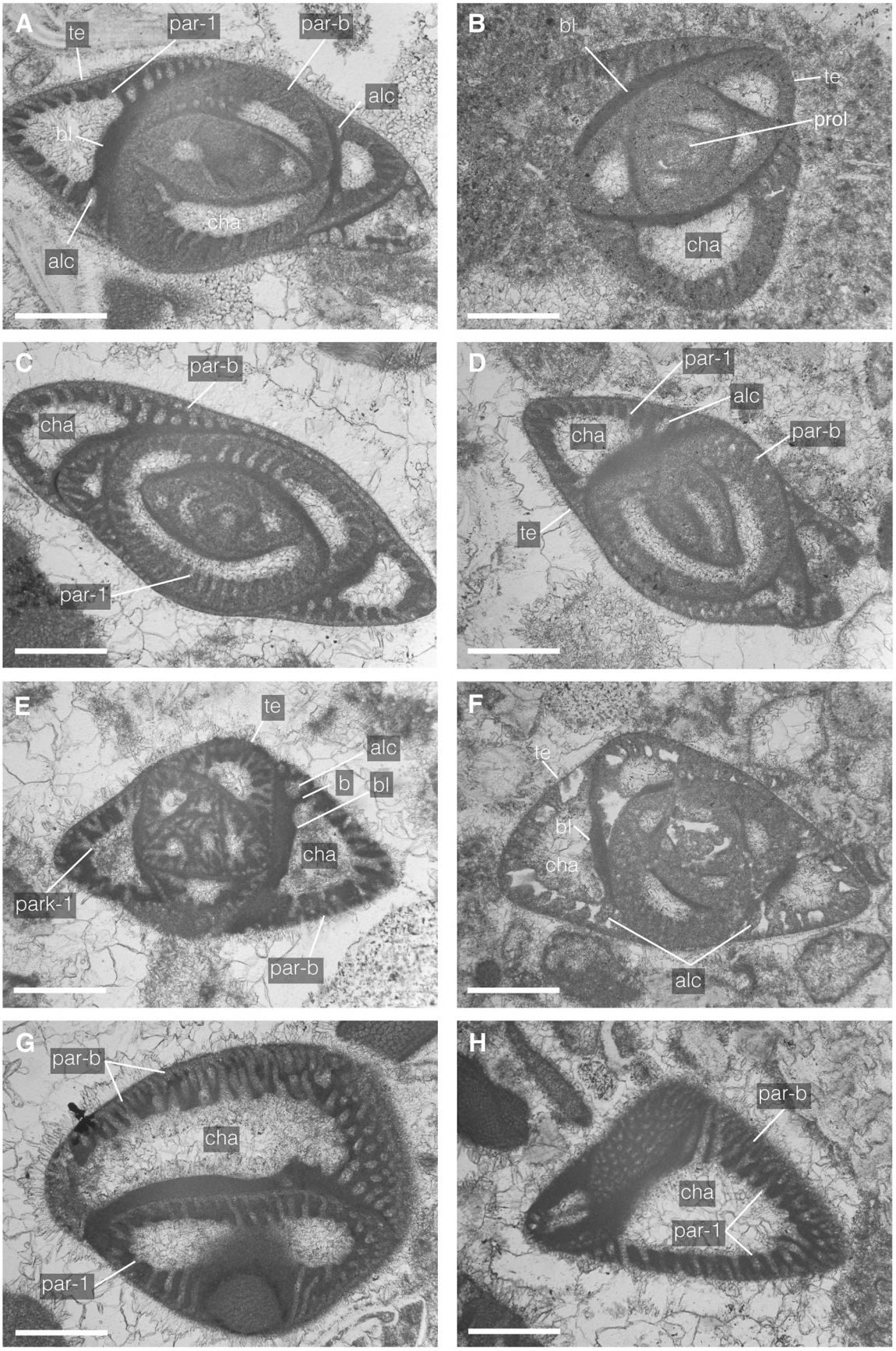

Fig. 9. *Austrotrillina howchini* (Schlumberger, 1893); latemost Langhian–early Serravallian, Kikai Seamount, northern Philippine Sea. A–F, tangential sub-transversal sections. G–H, tangential sections. Abbreviations: alc, alcove; b, beam; bl; basal layer; cha, chamber; par-1, parapores of first order; par-b, parapores of second-fourth order; te, tectum. Scale bars represent 0.250 mm.

ascribed to *A. brunni* because of the closed-spaced alveoli and absence of alcoves (O'Connell et al., 2012, fig. 5F; Table 2).

Austrotrillina striata Todd and Post, 1954.

Figs. 4–6.

(see Supplementary data for the synonymy list)

Type reference and figure: *Austrotrillina striata* Todd and Post, 1954, p. 555, pl. 198, fig. 9 (holotype).

Diagnosis: Coarse parapores. Proloculus 50–130 μm in diameter with narrow flexostyle. Parakeriotheca not present in the wall neither of the nepionic apparatus nor of the first three chambers (Table 1). No beams, no subsutural alcoves.

Studied material: The analysed specimens are from the latemost Rupelian of the Ibi area (southeastern Spain; Fig. 4), from the Aquitanian and Langhian limestones of Kita-daito-jima (Japan; Fig. 5), and from the Serravallian deposits of Sierra de Marmolance (southeastern Spain; Fig. 6).

The parapores (*c.* 90 μm long and *c.* 50 μm in diameter; Figs. 1B, 4B, 5F), rounded in transversal section, are large, straight, tubular in shape, perpendicular to the tectum. In the parakeriotheca, this alveolar arrangement makes the lateral chamber wall highly porous (i.e., coarse parakeriotheca; Figs. 1B, 4–6). The nepionic apparatus (proloculus *c.* 130 μm in diameter) has a flexostyle and the first three chambers do not show parakeriotheca.

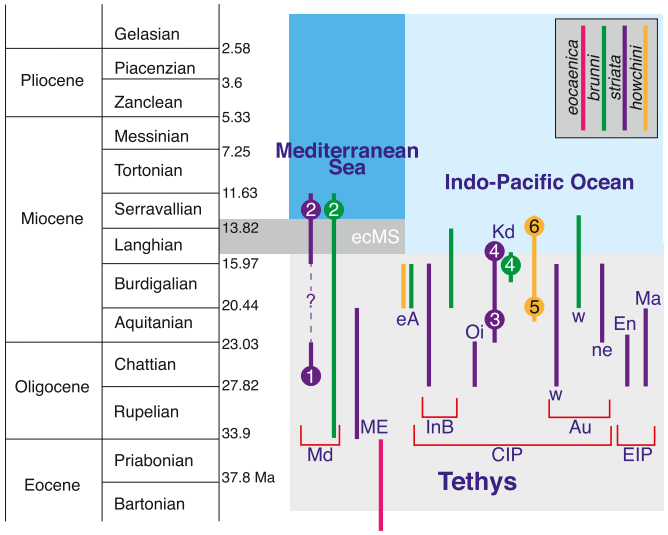

Fig. 10. Biostratigraphical patterns of the middle Eocene–Miocene *Austrotrillina* species. The middle Eocene *Austrotrillina eocaenica* is the ancestor of the Oligocene–Miocene species. *Austrotrillinabrunni* and *A. striata* appeared in the Rupelian of Western Tethys. Their westernmost occurrences are in southeastern Spain (1, Ibi; 2, Sierra de Marmolance; this study). These two species migrated eastward in the Indo-Pacific area via Indonesia reaching the Central Indo-Pacific in the latemost Rupelian and its northern part in the Aquitanian (3, Kita-daito-jima, this study). In this area both species disappeared in the early Langhian (4, this study). In Western Australia *A. brunni* lasted until the early Serravallian. The rarely recorded *A. howchini* occurs in the early Miocene of Kenya, Tanzania and Indonesia (5, this study), and disappeared in the latemost Langhian–early Serravallian in the central (Kalimantan, this study) and northern Central Indo-Pacific (6, Kikai Seamount, this study). Time scale after Cohen et al. (2021, updated).

Abbreviations: Au, Australia (w, western; ne, northeast); CIP, Central Indo-Pacific; eA, eastern Africa; ecMS, eastern closure of the Mediterranean Sea; EIP, eastern Indo-Pacific; En, Eniwetok Atoll; InB, Indonesia–Borneo; Kd, Kita-daito-jima; Ma, Midway Atoll; ME, Middle East; Md, Mediterranean area; Oi, Ogasawara Islands.

Remarks: No textural and structural differences were found between *A. striata* and *A. paucialveolata*. Their nepionic apparatus with flexostyle (Adams, 1968, pl. 3 and pl. 4, Figs. 10, 13) is followed by three first chambers with no parakeriotheca (Table 1). In addition, their overlapping stratigraphical and palaeogeographical distributions question the separation of these species (e.g., Adams, 1968; BouDagher-Fadel, 2018; Yazdi-Moghadam et al., 2018; Table 1).

Austrotrillina paucialveolata Grimsdale, 1952 has been described from Oligocene deposits of Kirkuk (Iraq). According to Grimsdale (1952, p. 229) the four illustrated types show throughout the shell large parapores 'coarser and less regular than in *Austrotrillina howchini*'. Adams (1968) stated that *A. asmariensis* and *A. paucialveolata* might be synonymous (p. 91) but the occurrence of large-sized parapores in *A. paucialveolata* disputes this interpretation. The single report of *Austrotrillina howchini* from the Chattian of southeastern Spain (Hottinger, 1963) corresponds in fact to *A. striata* (see also Adams, 1968, pl. 3, figs. 5–6 as *A. paucialveolata*).

Stratigraphical distribution: *Austrotrillina striata* appears from the Rupelian in the Western Tethys (Middle East; Serra-Kiel et al., 2016) and from the Chattian in the Indo-Pacific area (Indonesia; Table 3). In the Middle East, this species disappears in the early Burdigalian (e.g., Roozpeykar and Moghaddam, 2016; Daneshian and Dana, 2019). In the Western Tethys, the two records from the Rupelian and Chattian of southeastern Spain (Hottinger, 1963; see also Adams, 1968; Ibi, this study) are followed by a Serravallian occurrence in the southeastern Spain (this study).

In the Pacific area, *Austrotrillina striata* ranges from the Rupelian (Eniwetok, Todd and Low, 1960; Midway Atoll, Cole, 1969; Todd and Post, 1970) to the middle Miocene (Western Australia; Adams, 1984; Chaproniere, 1984; Lunt and Allan, 2004; Langhian in Kita-daito-jima, this study). This latter occurrence represents the northernmost record in the western Pacific marking the limit of shallow-water carbonate depositional systems. In Indonesia, it has been recorded from Tf1, roughly equivalent to the Burdigalian (Novak, 2014). The Serravallian record from southeastern Spain represents the last occurrence of this species in the Mediterranean area (Table 3, Fig. 10).

Austrotrillina howchini (Schlumberger) Parr, 1942.

Figs. 7–9.

(see Supplementary data for the synonymy list)

Type reference and figures: *Austrotrillina howchini* (Schlumberger) Parr, 1942, p. 361, fig. 1; holotype illustrated by Schlumberger (1893), pl. 3, fig. 6.

Diagnosis: Parakeriotheca with branching parapores in four bifurcating orders. Proloculus 70–150 μm. Beams occur approximately along the chamber suture, where they contact the basal layer at the chamber bottom forming a row of subsutural alcoves (Table 1).

Studied material: The analysed specimens are from lower Burdigalian deposits of East Kalimantan (Indonesia; early Tf1 in Novak, 2014), from the late Langhian–early Serravallian of Wailawi (East Kalimantan) and from the Langhian–early Serravallian of the Kikai Seamount. The parapores, decreasing in diameter outwardly, are branching in the parakeriotheca (Figs. 1C, 7, 8C). From the chamber lumen the first order of parapores bifurcates in the second order, which gives rise to the third and then to the fourth order. The parapores are rounded in transversal section (Fig. 7, 8C, H, 9A, C, G). The diameter of the parapores decreases from the first (*c.* 40–55 μm in diameter) to the fourth order (*c.* 25 μm; Fig. 7). The first-order parapores are longer (*c.* 75 μm long) than those in the subsequent orders (*c.* 35 μm long). Within specimens there is an ontogenetic increase in complexity of the parapores, with more orders of parapores in later chambers. The late

Aquitanian–lower Burdigalian specimens show thinner walls than the Serravallian ones and the parapores are usually of first to third orders. In the youngest thicker-shelled specimens the parapores are not perpendicular to the chamber, making the parakeriotheca pattern more complex. The walls of the nepionic apparatus (proloculus *c*. 150 μm in diameter) and of the first three chambers are lined by a parakeriotheca. No flexostyle has been recognised. Beams and subsutural alcoves present (Fig. 8B, F, 9A, E).

Remarks: Most of the *Austrotrillina howchini* reports are inadequately illustrated since they do not show the branching parapores in the parakeriotheca and subsutural alcoves (Table 1). The occurrence of branching parapores in the parakeriotheca is a distinctive character for this species which, together with *A. eocaenica*, bears subsutural alcoves (Table 1). The diameters of first-order parapores are larger than those of

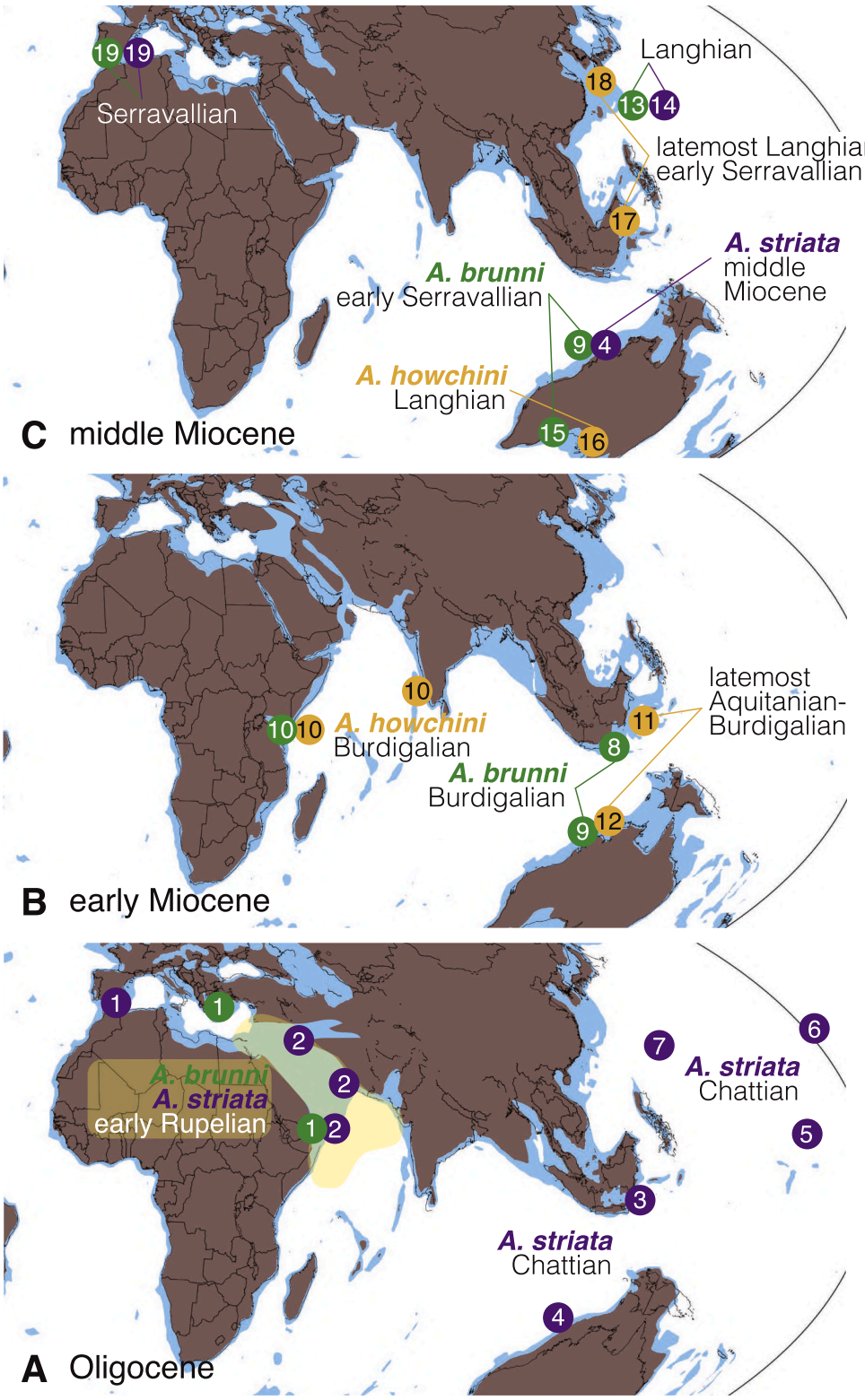

Fig. 11. Palaeogeographical locations of the first appearance data of *Austrotrillina brunni* (1, green) and *A. striata* (2, purple) in the eastern Western Tethys, and the first occurrence data of *Austrotrillina brunni* (8–9) and *A. striata* (3–7) in the Indo-Pacific (A). *A. brunni* and *A. striata* migrated from the eastern Western Tethys (Middle East areas) into the modern Arabian Sea during the early Rupelian (yellow shaded area). *A. striata* reached Indonesia and Western Australia in the Chattian (3–4), whilst *A. brunni* first occurs in these areas in the Burdigalian (8–10; B). *A. brunni* (9, 13, 17) and *A. striata* (4, 14) disappeared in the Pacific Langhian and in the Mediterranean Serravallian (18; C). The lower Miocene *A. howchini* appeared in eastern Africa, western Indian, Indonesia and Western Australia (10–12; B) and disappeared in the latemost Langhian–early Serravallian (16–18; C). Occurrences refer to citations in Tables 2–4 in which detailed information on each record can be found. Compare with Fig. 9. Palaeogeographical maps modified from Harzhauser and Piller (2007) and Kocsis and Scotese (2021).
Numbers refer to localities: 1, Wielandt-Schuster et al. (2004, Greece), Sirel et al. (2013, central Turkey), Serra-Kiel et al. (2016, Dhofar, Socotra Island), this study (Ibi); 2, Grimsdale (1952, Kirkuk, Iraq), Boukhary et al. (2010, UAE, Oman), Serra--Kiel et al. (2016, Dhofar, Socotra Island); 3, Adams (1965), BouDagher-Fadel (2018, Indonesia); 4, Chaproniere (1983, Western Australia); 5, Todd and Low (1960, Eniwetok atoll); 6, Cole (1969, Midway Atoll); 7, Matsumaru (1996, Ogasawara Island); 8, Barberi et al. (1987, Indonesia); 9, Riera et al. (2019, Western Australia), Haig et al. (2020, Western Australia); 10, Eames et al. (1962, Kenya, Sabaki River), Adams (1968, Pemba Island, Malabar); 11, Novak (2014), this study (Indonesia); 12, BouDagher-Fadel (2018, Western Australia); 13–14, this study (Kita-daito-jima); 15, O'Connell et al. (2012), South Australia); 16, Adams (1968, South Australia); 17, this study (Kalimantan); 18, this study (Kikai Seamount); 19, this study (southeastern Spain). (For interpretation of the references to colour in this figure legend, the reader is referred to the web version of this article.)

A. brunni (Marie *in* Brunn et al., 1955; Adams, 1968; Bassi et al., 2007; Ferràndez-Cañadell and Bover-Arnal, 2017) and comparable to those of *A. striata* (Todd and Post, 1954; Adams, 1968). This is the only *Austrotrillina* with no flexostyle (Table 1).

Stratigraphical distribution: Records of *Austrotrillina howchini* are from the early Miocene of Kenya and Tanzania (Williams, 1962, p. 18, Fundi Isa Limestones; Nyagah, 1995, Baratumu Formation; Banner and Highton, 1989; Table 4) and late Te5–early Tf1 from Indonesia (Novak, 2014; this study). Confirmed lower Miocene records are from Tanzania (Pemba Island; Adams, 1968, pl. 6, fig. 1; BouDagher-Fadel, 2018), western India (Adams, 1968; Banner and Highton, 1989), Philippines (Schlumberger, 1893) and Western Australia (BouDagher-Fadel, 2018; Table 4). The Burdigalian record in southern India is represented by isolated specimens whose shell shapes and decorticated shells do not show clearly the parakeriotheca of *A. howchini* (Rögl and Briguglio, 2018). The *Austrotrillina howchini* reported from the Australian Burdigalian (Chaproniere, 1976, 1977, 1984) corresponds to *A. brunni* (as *A. asmariensis* in Riera et al., 2019, p. 330; Table 2). Crespin's (1954, 1955) specimens from Southern Australia are inadequately illustrated since they do not show the alveoli. The Haig et al.'s (2020), figs. 8F–H) specimens from the Burdigalian Trealla Limestone, Western Australia, are characterised by the absence of alcoves and the occurrence of parakeriotheca in the first three chambers supporting placement in *A. brunni* (Tables 1–2). The studied late Aquitanian–lower Burdigalian *A. howchini* specimens along with the late Langhian–early Serravallian ones (Barberi et al., 1987) are the only illustrated records of this species in Indonesia (Fig. 9).

In the Langhian, *Austrotrillina howchini* is reported only from South Australia (Pata Formation in Lukasik and James, 1998; Adams, 1968, pl. 2, figs. 3–7; BouDagher-Fadel, 2018, pl. 7.1, figs. 1–3; Gallagher and Gourley, 2007, no illustration). The studied uppermost Langhian–lower Serravallian and Serravallian *A. howchini* from Kalimantan and from the Kikai Seamount respectively is the last occurrence of this taxon in the Indo-Pacific.

4. *Austrotrillina* shell structure

Symbiosis in LBF is performed by harbouring different microalgal (diatoms, dinoflagellates, chlorophytes, red algae) and bacterial communities in localised shell compartments (Hohenegger, 2009; Prazeres and Renema, 2019). The alveolar exoskeletal structures have been considered egg-holders hosting symbionts (e.g., Hottinger, 2000, 2006) and the different keriotheca types of fusulinids have been explained by relationships with symbiotic algae or cyanobacteria (Vachard et al., 2004). The wide parapores occurring in the coarse parakeriotheca of *Austrotrillina eocaenica* and *A. striata* likely hosted symbiotic microalgae which, in the narrow parapores in *A. brunni* and in the branching parapores in *A. howchini*, adjusted their optimal position according to irradiation intensity by displacement from exposed to the unexposed side of their host (e.g., Hottinger, 2006; Prazeres and Renema, 2019).

In all four species, the chamber floor is characterised by a basal layer, consisting of a thickening of the tectum of the previous whorl (Figs. 3–9; Adams, 1968, fig. 3A; Hottinger, 2007, p. 5; BouDagher-Fadel, 2018, p. 226). The basal layer, occurring in many imperforate LBF (fusulinids, alveolinoids; Loeblich and Tappan, 1987; Fleury and Fourcade, 1990; Hottinger, 2006), in miliolid *Austrotrillina* species becomes much thicker than the external chamber wall.

Among the miliolids, only *Pseudomassilina* Lacroix, 1938 shows a porcelaneous wall perforated by dense, anastomosing canaliculae (very thin parapores), which appear to only puncture the porcelain (Parker, 2017, p. 141). The canaliculae are similar in diameter and their density increases in later chambers. This rather complicated shell texture resembles those of *Austrotrillina brunni* and *A. howchini* but differs from them in having very tiny canaliculae opened to the exterior (parapores have a blind ending) and in the absence of the basal layer (which seems to be restricted to fossil taxa; Parker, 2017, p. 139). The Burdigalian *Pseudomassilina macilenta* and *P. quilonensis* occur in southern India (Kerala; Rögl and Briguglio, 2018). Present-day *Pseudomassilina australis*, *P. macilenta* and *P. robusta* (Chen and Lin, 2017; Parker, 2017) are the only larger porcelaneous foraminifera with a canaliculate shell wall in the Indo-Pacific area. A possible evolutionary link between *Austrotrillina* and *Pseudomassilina* requires further study.

5. Palaeobiogeography and evolutionary pattern

The four *Austrotrillina* species show different stratigraphical and biogeographic distributions in the Tethyan areas. The parakeriotheca characters, the diameter of the proloculus and the occurrence of beams and subsutural alcoves are diagnostic at species level (Table 1). The first appearance of shallow, coarse parapores in *A. eocaenica* followed by the appearance of fine and coarse parapores in *A. brunni* and *A. striata* respectively indicates that the two latter species derived from the Lutetian–Priabonian ancestor. This is supported by the increasing proloculus size over time (from the Lutetian–Priabonian to the Serravallian; Table 1), which is frequently observed in LBF lineages (de Mulder, 1975; Benedetti et al., 2010; Renema, 2015). After the biological crisis suffered by the larger foraminifera at the Eocene-Oligocene boundary, *Austrotrillina* species diversified in the Oligocene and migrated eastward. This diversification is nearly coeval with that of some nummulitids, the lepidocyclinids and the miogypsinids in the Western Tethys (de Mulder, 1975; Drooger, 1993; Cahuzac and Poignant, 1997). The successive changes in the complexity of the parakeriotheca represented by the branching parapores along with the absence of the flexostyle in *A. howchini* point to a subsequent evolutionary step from the ancestors *A. brunni–A. striata*. Increasing complexity in parakeriothecal structures has been recognised from early to advanced fusulinids (Hottinger, 2000) and in the alveolar exoskeleton and parapores of some larger agglutinated foraminifera (Hottinger, 1967, 2001; Banner et al., 1991; Kaminski, 2004).

Austrotrillina eocaenica occurs only in the Lutetian–Priabonian of the Middle East (Hottinger, 2007; Serra-Kiel et al., 2016). In the Mediterranean area, *Austrotrillina brunni* ranges from the Rupelian to the Serravallian, while *A. striata* ranges from the Chattian to the Serravallian (this study; Tables 2–3, Fig. 10).

From the eastern Western Tethys (Greece, Turkey, Iran; Adams, 1968) the Rupelian eastward migrants of *Austrotrillina brunni* and *A. striata* arrived in the modern Arabian Sea (Serra-Kiel et al., 2016; Tables 2–3, Fig. 11). The two species likely followed the shallow clockwise India to Indonesia current which flowed off the modern Andaman Sea coasts and finally mixed with western Pacific Ocean waters (Gourlan et al., 2008). This current potentially enhanced the eastward migration of *Austrotrillina* species by reducing transit times across the modern Central Indo-Pacific. After appearing in the Western Tethyan Rupelian, *Austrotrillina striata* reached Southeast Asia (Adams, 1965; Renema, 2007; BouDagher-Fadel, 2018) and Western Australia (Chaproniere, 1984) in the Chattian (Table 3, Figs. 10–11). Its last record in Indonesia is at the Aquitanian–Burdigalian boundary (top Te; Lunt and Allan, 2004), while in Borneo, Queensland Plateau and Western Australia it has been recorded from the Burdigalian (Chaproniere, 1983; Betzler and Chaproniere, 1993; BouDagher-Fadel et al., 2000; Haig et al., 2020). The species persisted until the Langhian of Kita-daito-jima in the northern Central Indo-Pacific (this study; Figs. 10–11).

In the Central Indo-Pacific, *Austrotrillina brunni* occurs first in the Burdigalian of Kenya (Eames et al., 1962) and Indonesia (Barberi et al., 1987; BouDagher-Fadel, 2018) and of Western Australia (Riera et al., 2019; Table 2, Fig. 11). The species reached Kita-daito-jima in northern Central Indo-Pacific (this study) at the Burdigalian–Langhian boundary. In the Central Indo-Pacific, its last occurrences are from the Langhian of Java (BouDagher-Fadel and Lokier, 2005) and from the Langhian–early Serravallian of Western and South Australia (O'Connell et al., 2012; Riera et al., 2019).

During the early Burdigalian, the closing Tethyan Seaway

represented a biogeographic barrier for the marine biota bringing about the differentiation into Mediterranean and Indo-Pacific bioprovinces (Reuter et al., 2009). As a possible result of such a biogeographic restriction, *Austrotrillina howchini*, which occurs in the early Miocene of Kenya and Tanzania (Williams, 1962; Adams, 1968; Kent et al., 1971; Adams et al., 1983; BouDagher-Fadel, 2018), has not been recorded in the Mediterranean and Middle East regions. *Austrotrillina howchini* appears in the Burdigalian in western India (Adams, 1968), Indonesia, Philippines (Schlumberger, 1893; Adams, 1965; Novak, 2014; BouDagher-Fadel, 2018; this study; Table 4, Fig. 10). The occurrences of *Austrotrillina howchini* in Eastern Africa and in the Central Indo-West Pacific area suggest an early Miocene active biogeographic connection between these two areas (Figs. 10–11). In the early Miocene, the Central Indo-Pacific area corresponds to the centre of marine biodiversity known as the Coral Triangle (e.g., Renema et al., 2008; Obura, 2016; Reuter et al., 2019). In this area, *Austrotrillina howchini* often occurs together with the alveolinoid *Flosculinella* species found in the early Miocene of Maldives, Indonesia and Ryukyu Islands (Lunt and Allan, 2004; Renema, 2007; Renema et al., 2015). The last occurrence of this species is in the early Serravallian of Indonesia (this study), the latemost Langhian–early Serravallian of the Kikai Seamount (this study; Table 4), and in the Langhian of South Australia (Adams, 1968).

As for the other characteristic LBF of the Western Tethyan and Indo-Pacific area (e.g., *Heterostegina* sensu *lato*, *Cycloclypeus*, reticulate nummulitids, alveolinoids), no record of *Austrotrillina* has been reported from the Oligocene–Miocene of the Caribbean realm (Robinson, 1995). This can be related to the fact that from the early Oligocene the Tethyan LBF migrants followed preferentially the eastward dispersal route (see Benedetti et al., 2018). Oligocene–Miocene westward migrations of nummulitids and alveolinoids from the Tethys to the Caribbean realm have never been recorded (e.g., BouDagher-Fadel, 2018; Bassi et al., 2021). The only possible westward migrants are the Burdigalian lepidocyclinids and *Cycloclypeus* from southeast Asia to eastern Mediterranean (Özcan and Less, 2009; Renema, 2015).

6. Concluding remarks

Four *Austrotrillina* species (*Austrotrillina brunni*, *Austrotrillina eocaenica*, *A. howchini* and *A. striata*) are widespread in the Western Tethys and in the Indo-Pacific from the middle Eocene to the middle Miocene. New records from southeastern Spain, Indonesia and western Pacific allowed defining the species descriptions according to the shell structure, which consists of a tectum and a parakeriotheca with subsutural alcoves. The parakeriotheca can be thin (*A. brunni*), coarse (*A. eocaenica*, *A. striata*) and with branching parapores (*A. howchini*).

The genus appeared in the Western Tethyan middle Eocene, diversified in the Early Oligocene and the descendants reached the Serravallian in the Mediterranean and Pacific areas. The Iranian Bartonian–Priabonian *Austrotrillina eocaenica* is the oldest austrotrillinid. The Western Tethyan Rupelian *Austrotrillina brunni* and *A. striata* migrated eastward in the Indo-Pacific region.

Austrotrillina striata reached Indonesia and Western Australia in the Chattian. The species persisted until the Langhian of Kita-daito-jima in the northern Central Indo-Pacific. *Austrotrillina brunni*, first occurring in the Burdigalian of Indonesia and Western Australia, reached Kita-daito-jima in northern Central Indo-Pacific at the Burdigalian–Langhian boundary. In the Central Indo-Pacific, its last occurrences are from the Langhian of Java and Kita-daito-jima, and from the early Serravallian of Western and South Australia. *Austrotrillina brunni* and *A. striata* disappeared in the westernmost Mediterranean (southeastern Spain) in the Serravallian.

Austrotrillina howchini, occurring in the early Miocene of eastern Africa, western Indian, Indonesia and Western Australia, has not been recorded in the Mediterranean region. Its lower Miocene occurrence in these areas is a possible result of the closing Tethyan Seaway which brought about the differentiation into Mediterranean and Indo-Pacific bioprovinces. This palaeobiogeographic distribution suggests an early Miocene active connection of Eastern Africa with the Central Indo–West Pacific. The last occurrence of this species is in the latemost Langhian–early Serravallian.

Author statement

D.B., J.C.B., Y.I. designed this study. Md.A., M.B.-F., J.A., W.R., H.T. contributed to sampling and analysis. Interpretation of data, discussion of the results, and writing of the manuscript were done by all authors.

Declaration of Competing Interest

None.

Acknowledgements

This study was supported by local research fund of the University of Ferrara (2016–2020) and FIR2018 (D.B.). This paper is a scientific contribution of the Project MIUR–Dipartimenti di Eccellenza 2018–2022 and of the PRIN 2017RX9XXXY (Biota resilience to global change: biomineralisation of planktic and benthic calcifiers in the past, present and future). Samples from the Tallabar limestone in East Kalimantan were collected in a field campaign (June 2011) in the frame of the Throughflow Initial Training Network, funded by the Marie Curie Actions Plan, Seventh Framework Programme of the European Union [grant 237922]. J.A. and J.C.B. were funded by the research project PGC2018-099391-B-100 of the Spanish Ministerio de Ciencia, Innovación y Competitividad, and the research group RMN190 of the Junta de Andalucía. DB sincerely acknowledges the International Joint Graduate Program in Earth and Environmental Sciences (GP-EES) for the invitation to the Tohoku University. We are grateful for the collection support from Mr. Jun Nemoto, curator of the Museum of Natural History, Tohoku University. We appreciated the Editor Richard Jordan and an anonymous reviewer for their constructive comments.

Appendix A. Supplementary data

Supplementary data to this article can be found online at https://doi.org/10.1016/j.marmicro.2021.102058.

References

Adams, C.G., 1965. The Foraminifera and stratigraphy of the Melinau Limestone, Sarawak, and its importance in Tertiary correlation. Q. J. Geol. Soc. Lond. 121, 283–338. https://doi.org/10.1144/gsjgs.121.1.0283.

Adams, C.G., 1968. A revision of the foraminiferal genus *Austrotrillina* Parr. Bull. Brit. Mus. (Nat. Hist.) 6 (2), 73–97.

Adams, C.G., 1973. Some Tertiary Foraminifera. In: Hallam, A. (Ed.), Atlas of Palaeobiogeography. Elsevier, Amsterdam, pp. 453–468.

Adams, C.G., 1984. Neogene larger foraminifera, evolutionary and geological events in the context of datum planes. In: Ikebe, N., Tsuchi, R. (Eds.), Pacific Neogene Datum Planes. University of Tokyo Press, Tokyo, pp. 47–68.

Adams, C.G., Belford, D.J., 1974. Foraminiferal biostratigraphy of the Oligocene–Miocene limestones of Christmas Island (Indian Ocean). Palaeontology 17, 475–506.

Adams, C.G., Gentry, A.W., Whybrow, P.J., 1983. Dating the terminal Tethyan event. In: Meulecamp, J.E. (Ed.), Reconstruction of Marine Paleoenvironments. Utrecht Micropaleontol. Bull, 30, pp. 273–298.

Banner, F.T., Highton, J., 1989. On *Pseudotaberina malabarica* (Carter) (Foraminiferida). J. Micropalaeontol. 8, 113–129. https://doi.org/10.1144/jm.8.1.113.

Banner, F.T., Simmons, M.D., Whittaker, J.E., 1991. The Mesozoic Chrysalinidae (Foraminifera, Textulariacea) of the Middle East: the Redmond (Aramco) taxa and their relatives. Bull. Br. Mus. (Nat. Hist.), Geol. Ser. 42 (2), 101–152.

Barberi, S., Bigioggero, B., Boriani, A., Cattaneo, M., Cavallin, A., Eva, C., Cioni, R., Gelmini, R., Giorgetti, F., Iaccarino, S., Innocenti, F., Marinelli, G., Slejko, D., Sudradjat, A., 1987. The Island of Sumbawa: a major structural discontinuity in the Indonesian Arc. Boll. Soc. Geol. Ital. 106, 547–620.

Bassi, D., Hottinger, L., Nebelsick, J.H., 2007. Larger foraminifera from the Late Oligocene of the Venetian area, north-eastern Italy. Palaeontology 50, 845–868. https://doi.org/10.1111/j.1475-4983.2007.00677.x.

Bassi, D., Braga, J.C., Di Domenico, G., Pignatti, J., Abramovich, S., Hallock, P., Könen, J., Kovács, Z., Langer, M.R., Pavia, G., Iryu, Y., 2021. Palaeobiogeography

and evolutionary patterns of the larger foraminifer *Borelis* de Montfort (Borelidae). Pap. Palaeontol. 7, 377–403. https://doi.org/10.1002/spp2.1273.
Beavington-Penney, S.J., Racey, A., 2004. Ecology of extant nummulitids and other larger benthic foraminifera: applications in palaeoenvironmental analysis. Earth-Sci. Rev. 67, 219–265. https://doi.org/10.1016/j.earscirev.2004.02.005.
Vachard, D., Munnecke, A., Servais, T., 2004. New SEM observations of keriothecal walls: implications for the evolution of Fusulinida. J. Foramin. Res. 34, 232–242. https://doi.org/10.2113/34.3.232.
van Bemmelen, R.W., 1949. The Geology of Indonesia. Government Printing Office, The Hague, Netherlands, 997 pp.
Benedetti, A., Di Carlo, M., Pignatti, J., 2010. Embryo size variation in larger foraminiferal lineages: stratigraphy *versus* paleoecology in *Nephrolepidina praemarginata* (R. Douvillé, 1908) from the Majella Mt. (Central Apennines). J. Med. Earth Sci. 2, 19–29. https://doi.org/10.3304/JMES.2010.003.
Benedetti, A., Less, Gy, Parente, M., Pignatti, J., Cahuzac, B., Torres-Siilvs, A.I., Buhl, D., 2018. *Heterostegina matteuccii* sp. nov. (Foraminiferida: Nummulitidae) from the lower Oligocene of Sicily and Aquitaine: a possible transatlantic immigrant. J. Syst. Palaeontol. 16, 87–110. https://doi.org/10.1080/14772019.2016.1272009.
Betzler, C., Chaproniere, G.C.H., 1993. Paleogene and Neogene larger foraminifers from the Queensland Plateau: biostratigraphy and environmental significance. In: McKenzie, J.A., Davies, P.J., Palmer-Julson, A., et al. (Eds.), Proceedings of the Ocean Drilling Program, Scientific Results, 133, pp. 51–66. https://doi.org/10.2973/odp.proc.sr.133.210.1993.
Binnekamp, J.G., 1973. Tertiary larger foraminifera from New Britain, PNG. Aust. Bur. Min. Res. Geol. Geophys. Bull. 140, 1–26.
Bonnefous, J., Bismuth, H., 1982. Les facies carbonates de plate-forme de l'Eocène moyen et supérieur dans l'offshore tunisien nord-oriental et en Mer Pélagienne: implications paléogéographiques et analyse micropaléontologique. Bull. Cent. Rec. Explor. Prod. Elf-Aquitaine 6, 337–403.
BouDagher-Fadel, M.K., 2018. Evolution and geological significance of larger benthic foraminifera, 2nd edition. University College London Press, London, UK. https://doi.org/10.14324/111.9781911576938. 693 pp.
BouDagher-Fadel, M.K., Banner, F.T., 1999. Revision of the stratigraphic significance of the Oligocene-Miocene "Letter-Stages". Rev. Micropaleontol. 42, 93–97. https://doi.org/10.1016/S0035-1598(99)90095-8.
BouDagher-Fadel, M.K., Lokier, S.W., 2005. Significant Miocene larger foraminifera from South Central Java. Rev. Paléobiol. 24, 291–309.
BouDagher-Fadel, M.K., Noad, J.J., Lord, A.R., 2000. Larger foraminifera from Late Oligocene-Earliest Miocene reefal limestones of north east Borneo. Rev. Esp. Micropaleontol. 32, 341–361.
Boukhari, S.W.H., Mohibullah, M., Kasi, A.K., Iqbal, H., 2016. Biostratigraphy of the Eocene Nisai Formation in Pishin belt, western Pakistan. J. Himal. Earth Sci. 49, 17–29.
Boukhary, M., Abdelghany, O., Hussein-Kamel, Y., Bahr, S., Razak Alsayigh, A., Abdelraouf, M., 2010. Oligocene larger foraminifera from United Arab Emirates, Oman and Western Desert of Egypt. Hist. Biol. 22, 348–366. https://doi.org/10.1080/08912960903570047.
Brunn, J.H., Chevalier, J.-P., Marie, P., 1955. Quelques formes nouvelles de Polypiers et de Foraminifères de l'Oligocene et du Miocene du NW de la Grèce. II. Foraminifères. Bull. Soc. géol. Fr. 5, 193–205. https://doi.org/10.2113/gssgfbull.S6-V.1-3.193.
Buxton, M.W.N., Pedley, H.M., 1989. A standardized model for Tethyan Tertiary carbonate ramps. J. Geol. Soc. 146, 746–748. https://doi.org/10.1144/gsjgs.146.5.0746.
Cahuzac, B., Poignant, A., 1997. Essai de biozonation de l'Oligo-Miocène dans les bassins européens à l'aide des grands foraminifères néritiques. Bull. Soc. Géol. Fr. 168 (2), 155–169.
Carter, A.N., 1964. Tertiary Foraminifera from Gippsland, Victoria, and their stratigraphical significance. Mem. Geol. Surv. Victoria 23, 1–154.
Chaproniere, G.C.H., 1976. The Bullara Limestone, a new rock stratigraphic unit from the Carnarvon Basin, Western Australia. Bur. Min. Res. Geol. Geophys. 1, 171–174.
Chaproniere, G.C.H., 1977. Studies on Foraminifera from Oligo-Miocene sediments, North West Western Australia. Unpubl. PhD thesis. The Univ. Western Australia, Crawley, 486 pp.
Chaproniere, G.C.H., 1983. Tertiary larger foraminiferids from the northwestern margin of the Queensland Plateau, Australia. Bur. Min. Res., Australia 217, 31–57.
Chaproniere, G.C.H., 1984. The Neogene larger foraminiferal sequence in the Australian and New Zealand regions, and its relevance to the East Indies Letter-stage Classification. Palaeogeogr. Palaeoclimatol. Palaeoecol. 46, 25–35. https://doi.org/10.1016/0031-0182(84)90023-3.
Chen, C., Lin, H.-L., 2017. Applying benthic foraminiferal assemblage to evaluate the coral reef condition in Dongsha Atoll lagoon. Zool. Stud. 56, e20 https://doi.org/10.6620/ZS.2017.56-20.
Cohen, K.M., Harper, D.A.T., Gibbard, P.L., 2021. The ICS International Chronostratigraphic Chart 2020/03. International Commission on Stratigraphy, IUGS. www.stratigraphy.org (visited: 2021/05/11).
Cole, W.S., 1954. Larger foraminifera and smaller diagnostic foraminifera from Bikini drill holes. U.S. Geol. Surv. Prof. Pap. 260-O, 569–608. doi: 10.3133/pp260O.
Cole, W.S., 1957. Variation in American Oligocene species of *Lepidocyclina*. Bull. Am. Paleontol. 38, 321–360.
Cole, W.S., 1969. Larger foraminifera from deep drill holes on Midway Atoll. U.S. Geol. Surv. Prof. Pap. 680-C, C1–C5. doi: 10.3133/pp680C.
Crespin, I., 1954. Stratigraphy and micropalaeontology of the marine Tertiary rocks between Adelaide and Aldinga, South Australia. Bur. Min. Res. Geol. Geophys. 12, 1–65.
Crespin, I., 1955. The Cape Range Structure, Western Australia. Part 2, Micropalaeontology. Bur. Min. Res. Geol. Geophys. 21, 49–82.
Daneshian, J., Dana, L.R., 2019. Benthic foraminiferal events of the Qom Formation in the north Central Iran Zone. Paleontol. Res. 23, 10–22. https://doi.org/10.2517/2018PR008.
Dasgupta, A., 1977. The species of *Austrotrillina* from Western Cutch. J. Geol. Soc. India 18, 65–71.
Drooger, C.W., 1993. Radial Foraminifera; morphometrics and evolution. Verh. Kon. Ned. Akad. Wetensch., Afd. Natuurk. 41, 1–242.
Eames, F., Banner, F., Blow, W., Clarke, W., 1962. Fundamentals of mid-Tertiary stratigraphical correlation. Cambridge Univ, Press, Cambridge, 163 pp.
Ehrenberg, C.G., 1839. Über die Bildung der Kreidefelsen und des Kreidemergels durch unsichtbare Organismen. Abh. Königl. Akad. Wiss. Berlin 59–147.
Escandell, B., Colom, G., 1962. Una revision del Nummulítico Mallorquín. Not. Com. Inst. Geol. Min. Esp. 66, 73–142.
Ferràndez-Cañadell, C., Bover-Arnal, T., 2017. Late Chattian larger foraminifera from the Prebetic Domain (SE Spain): new data on Shallow Benthic Zone 23. Palaios 32, 83–109. https://doi.org/10.2110/palo.2016.010.
Fleury, J.J., Fourcade, E., 1990. La Super-famille Alveolinacea (Foraminifères): systématique et essai d'interpretation phylogénétique. Rev. Micropaleontol. 33, 241–268.
Gallagher, S.J., Gourley, T.L., 2007. Revised Oligo-Miocene stratigraphy of the Murray Basin, southeast Australia. Austr. J. Earth Sci. 54, 837–849. https://doi.org/10.1080/08120090701392705.
Gallardo, A., Serra-Kiel, J., Ferrández-Cañadell, C., Razin, Ph., Roger, J., Boix, C., Caus, E., 2001. Macroforaminiferos porcelanados del Eoceno Superior–Oligoceno Inferior del Dhofar (Sultanato de Omán). In: Meléndez, G., Herrera, Z., Delvene, G., Azanza, B. (Eds.), Los fósiles y la paleogeografía. Actas de las 17° Jornadas de la Sociedad Española de Paleontología, Albarracín (Teruel), 5 (1). Pub. Sem. Paleontol. Zaragoza (SEPAZ), 83–89.
Gedik, F., 2014. Benthic foraminiferal fauna of Malatya Oligo-Miocene Basin, (eastern Taurids, eastern Turkey). Bull. Min. Res. Expl. 149, 93–136.
Gedik, F., 2015. Benthic foraminiferal biostratigraphy of Malatya Oligo-Miocene succession (eastern Taurids, eastern Turkey). Bull. Min. Res. Expl. 150, 19–50.
Gedik, F., 2017. First record of the new Neoplanorbulinid species (Foraminifera) from the Early Oligocene in Turkey, Malatya Basin, Eastern Taurids. Geodiversitas 39, 273–284. https://doi.org/10.5252/g2017n2a6.
Gedik, F., 2020. An example of evolutionary trends in the Miogypsinidae (Foraminiferida) from Turkey. Hist. Biol. 32, 386–408. https://doi.org/10.1080/08912963.2018.1497623.
Geel, T., 1995. Oligocene to early Miocene tectono-sedimentary history of the Alicante region (SE Spain): implications for Western Mediterranean evolution. Basin Res. 7, 313–336. https://doi.org/10.1111/j.1365-2117.1995.tb00120.x.
Geel, T., 2000. Recognition of stratigraphic sequences in carbonate platform and slope deposit: empirical models based on microfacies analysis of Palaeogene deposits in southeastern Spain. Palaeogeogr. Paleoclimatol. Palaeoecol. 155, 211–238. https://doi.org/10.1016/S0031-0182(99)00117-0.
Gibson, T.G., Margerum, R., 1991. Larger foraminifer biostratigraphy of PEACE boreholes, Enewetak Atoll, western Pacific Ocean. U.S. Geol. Surv. Prof. Pap. 1513-D, D1–D14. https://doi.org/10.3133/pp1513D.
Gourlan, A.T., Meynadier, L., Allègre, C.J., 2008. Tectonically driven changes in the Indian Ocean circulation over the last 25 Ma: Neodymium isotope evidence. Earth Planet. Sci. Lett. 267, 353–364. https://doi.org/10.1016/j.epsl.2007.11.054.
Gradstein, F.M., Ogg, J.G., Schmitz, M.D., Ogg, G.M., 2012. The geologic time scale (Volumes 1 and 2). Elsevier, Amsterdam, The Netherlands.
Grimsdale, T.F., 1952. Cretaceous and Tertiary foraminifera from the Middle East. Bull. Br. Mus. (Nat. Hist.). Geol. 1, 221–248.
Haig, D.W., Smith, M.G., Riera, R., Parker, J.H., 2020. Widespread seagrass meadows during the Early Miocene (Burdigalian) in southwestern Australia paralleled modern seagrass distributions. Palaeogeogr. Paleoclimatol. Palaeoecol. 555, 109846. https://doi.org/10.1016/j.palaeo.2020.109846.
Hanzawa, S., 1940. Micropaleontological studies of drill cores from a deep well in Kita-Daito-Zima (North Borodino Island). In: Committee on Jubilee Publication in the Commemoration of Prof. H. Yabe M. I. A. 60th birthday (ed.), Jubilee Publication in the commemoration of Prof. H. Yabe M. I. A. 60th birthday. Sasaki Shuppan Co. Ltd., Sendai, Miyagi, 755–802.
Hanzawa, S., 1957. Cenozoic Foraminifera of Micronesia. Geol. Soc. Am., Mem. 66 https://doi.org/10.1130/MEM66, 163 pp.
Harzhauser, M., Piller, W.E., 2007. Benchmark data of a changing sea – palaeogeography, palaeobiogeography and events in the Central Paratethys during the Miocene. Palaeogeogr. Palaeoclimatol. Palaeoecol. 253, 8–31. https://doi.org/10.1016/j.palaeo.2007.03.031.
Hickey-Vargas, R., 2005. Basalt and tonalite from the Amami Plateau, northern West Philippine Basin: new Early Cretaceous ages and geochemical results, and their petrologic and tectonic implications. Island Arc 14, 653–665. https://doi.org/10.1111/j.1440-1738.2005.00474.x.
Hofker Jr., J., 1963. Studies on the genus *Orbitolina* (Foraminiferida). Leidse. Geol. Meded. 29 (1963), 181–254.
Hohenegger, J., 2009. Functional shell geometry of symbiont-bearing benthic Foraminifera. Galaxea. J. Coral Reef St. 11, 81–89. https://doi.org/10.3755/galaxea.11.81.
Höntzsch, S., Scheibner, C., Brock, J.P., Kuss, J., 2013. Circum-Tethyan carbonate platform evolution during the Palaeogene: the Prebetic platform as a test for climatically controlled facies shifts. Turk. J. Earth Sci. 22, 891–918. https://doi.org/10.3906/yer-1207-8.
Hottinger, L., 1963. Quelques Foraminifères porcelanés oligocènes dans la série sédimentaire prébétique de Moratalla (Espagne méridionale). Eclogae Geol. Helv. 56, 963–972. https://doi.org/10.5169/seals-163053.

Hottinger, L., 1967. Foraminifères imperforés du Mézosoique marocain. Not. Serv. Géol. Maroc 209 (1967), 1–168.
Hottinger, L., 1997. Shallow benthic foraminiferal assemblages as signals for depth of their deposition and their limitations. Bull. Soc. Géol. Fr. 168, 491–505.
Hottinger, L., 2000. Functional morphology of benthic foraminiferal shells, envelopes of cells beyond measure. Micropaleontology 46, 57–86.
Hottinger, L., 2001. Archaiasinids and related porcelaneous larger foraminifera from the late Miocene of the Dominican Republic. J. Paleontol. 75, 475–512. https://doi.org/10.1017/S0022336000039627.
Hottinger, L., 2006. Illustrated glossary of terms used in foraminiferal research. Carnet Géol., Mém. https://doi.org/10.4267/2042/5832, 2006/02, 126 pp.
Hottinger, L., 2007. Revision of the foraminiferal genus *Globoreticulina* Rahaghi, 1978, and of its associated fauna of larger foraminifera from the late Middle Eocene of Iran., 2007/06 (CG2007-A06). Carnets Géol. 1–51. https://doi.org/10.4267/2042/9213. http://paleopolis.rediris.es/cg/07/A06/.
ICZN, 1999. International Code of Zoological Nomenclature, 4th edition. International Trust for Zoological Nomenclature. https://www.iczn.org/the-code/.
Iryu, Y., Inagaki, S., Suzuki, Y., Yamamoto, K., 2010. Late Oligocene to Miocene reef formation on Kita-daito-jima, northern Philippine Sea. In: Mutti, M., Piller, W.E., Betzler, C. (Eds.), Carbonate Systems During the Oligocene-Miocene Climatic Transition. Spec. Publ. Int. Ass. Sed., 42, pp. 243–254. https://doi.org/10.1002/9781118398364.ch14.
Kaminski, M.A., 2004. The year 2000 classification of the agglutinated foraminifera. In: Bubík, M., Kaminski, M.A. (Eds.), Proceedings of the Sixth International Workshop on Agglutinated Foraminifera. Grzybowski Found. Spec. Publ., 8, pp. 237–255.
Karevan, M., Vaziri-Moghaddam, H., Mahboudi, A., Moussavi-Harami, R., 2014. Biostratigraphy and paleo-ecological reconstruction on Scleractinian reef corals of Rupelian-Chattian succession (Qom Formation) in northeast of Delijan area. Geopersia 4, 11–24. https://doi.org/10.22059/jgeope.2014.51189.
Kent, P.E., Hunt, M.A., Johnstone, D.W., 1971. The geology and geophysics of coastal Tanzania. HMSO for the Inst. Geol. Sci. Geophys. Pap. 6, 1–101.
Kocsis, Á.T., Scotese, C.R., 2021. Mapping paleocoastlines and continental flooding during the Phanerozoic. Earth-Sci. Rev. 213, 103463. https://doi.org/10.1016/j.earscirev.2020.103463.
Lacroix, E., 1938. Révision du genre *Massilina*. Bull. Inst. Océanogr. 754, 1–11.
Lawa, F.A.A., Gafhur, A.A., 2015. Sequence stratigraphy and biostratigraphy of the prolific late Eocene, Oligocene and early Miocene carbonates from Zagros fold-thrust belt in Kurdistan region. Arab. J. Geosci. 8, 8143–8174. https://doi.org/10.1007/s12517-015-1817-4.
Loeblich, A.R., Tappan, H., 1986. Some new and redefined genera and families of Textulariina, Fusulinina, Involutinina and Miliolina (Foraminiferida). J. Foramin. Res. 16 (4), 334–346. https://doi.org/10.2113/gsjfr.16.4.334.
Loeblich, A.R., Tappan, H., 1987. Foraminiferal Genera and their Classification, 2 vols. Van Nostrand Reinhold Co, New York, p. 970+212.
Lukasik, J.J., James, N.P., 1998. Lithostratigraphic revision and correlation of the Oligo–Miocene Murray Supergroup, western Murray Basin, South Australia. Austr. J. Earth Sci. 45, 889–902. https://doi.org/10.1080/08120099808728443.
Lunt, P., Allan, T., 2004. Larger foraminifera in Indonesian biostratigraphy, calibrated to isotopic dating. Geol. Res. Dev. Cent. Mus. 1–109,. Workshop on Micropalaeontology, June 2004, Bandung.
Ma, Z.-L., Li, Q.-Y., Liu, X.-Y., Luo, W., Zhang, D.-J., Zhu, Y.-H., 2018. Palaeoenvironmental significance of Miocene larger benthic foraminifera from the Xisha Islands, South China Sea. Palaeoworld 27, 145–157. https://doi.org/10.1016/j.palwor.2017.05.007.
Marks, P., 1957. Stratigraphic lexicon of Indonesia. Djawatan Geol. Bandung, Publ. Keilmuan 31, 1–233.
Matsumaru, K., 1996. Tertiary larger foraminifera (Foraminiferida) from the Ogasawara Islands, Japan. Paleontol. Soc. Jpn. Spec. Pap. 36, 1–239.
McArthur, J.M., Howarth, R.J., Shields, G.A., 2012. Chapter 7, Strontium isotope stratigraphy. In: Gradstein, F.M., Ogg, G.O., Schmitz, M.D., Ogg, G.M. (Eds.), The Geologic Time Scale 2012, Volume 1. Elsevier, Amsterdam, pp. 127–144. https://doi.org/10.1016/B978-0-444-59425-9.00007-X.
Mulder, E.F.J., 1975. Microfauna and sedimentary-tectonic history of the Oligo-Miocene of the Jonian Islands and western Epirus (Greece). Utrecht Micropaleontol. Bull. 13, 1–140.
Nafarieh, E., Consorti, L., Ghassemi-Nejad, E., Caus, E., 2019. *Reticulotaberina* n. gen. *jahrumiana* n. sp., a new soritoidean (Praerhapydioninidae) from the Eocene of Iran. Rev. Micropaleontol. 65, 100382 https://doi.org/10.1016/j.revmic.2019.100382.
Novak, V., 2014. Larger benthic foraminifera in Miocene carbonates of Indonesia. Utrecht St. Earth Sci. 64, 1–213.
Nyagah, K., 1995. Stratigraphy, depositional history and environments of deposition of Cretaceous through Tertiary strata in the Lamu Basin, southeast Kenya and implications for reservoirs for hydrocarbon exploration. Sediment. Geol. 96, 43–71. https://doi.org/10.1016/0037-0738(94)00126-F.
O'Connell, L.G., James, N.P., Bone, Y., 2012. The Miocene Nullarbor Limestone, Southern Australia; deposition on a vast subtropical epeiric platform. Sediment. Geol. 253–254, 1–16. https://doi.org/10.1016/j.sedgeo.2011.12.002.
Obura, D.O., 2016. An Indian Ocean centre of origin revisited: Palaeogene and Neogene influences defining a biogeographic realm. J. Biogeogr. 43, 229–242. https://doi.org/10.1111/jbi.12656.
Ohde, S., Elderfield, H., 1992. Strontium isotope stratigraphy of Kita-daito-jima Atoll, North Philippine Sea: implications for Neogene sea-level change and tectonic history. Earth Planet. Sci. Lett. 113, 473–486. https://doi.org/10.1016/0012-821X(92)90125-F.
Özcan, E., Less, Gy, 2009. First record of the co-occurrence of Western Tethyan and Indo-Pacific larger foraminifera in the Burdigalian of the Mediterranean province. J. Foramin. Res. 39, 23–39. https://doi.org/10.2113/gsjfr.39.1.23.
Parker, J.H., 2017. Ultrastructure of the test wall in modern porcelaneous foraminifera: implications for the classification of the Miliolida. J. Foramin. Res. 47, 136–174. https://doi.org/10.2113/gsjfr.47.2.136.
Parr, W.J., 1942. New genera of foraminifera from the Tertiary of Victoria. Min. Geol. J. 2, 361–363.
Poignant, A., Lorenz, C., 1985. Répartition biogéographique de foraminifères benthiques à l'Oligocène et au Miocène inférieur dans la Téthys. Bull. Soc. Géol. Fr. 8, 771–779. https://doi.org/10.2113/gssgfbull.I.5.771.
Prazeres, M., Renema, W., 2019. Evolutionary significance of the microbial assemblages of larger benthic Foraminifera. Biol. Rev. 94, 828–848. https://doi.org/10.1111/brv.12482.
Rahaghi, A., 1980. Tertiary faunal assemblages of Qum-Kashan, Sabzerwar and Jahrum areas. Publ. Nat. Iran. Oil Comp. Geol. Lab. 8, 1–64.
Renema, W., 2007. Fauna development of larger benthic foraminifera in the Cenozoic of Southeast Asia. In: Renema, W. (Ed.), Biogeography, Time and Place: Distributions, Barriers and Islands. Springer-Verlag, Berlin, pp. 179–215. https://doi.org/10.1007/978-1-4020-6374-9_6.
Renema, W., 2015. Spatiotemporal variation in morphological evolution in the Oligocene–Recent larger benthic foraminifera genus *Cycloclypeus* reveals geographically undersampled speciation. GeoResJ 5, 12–22. https://doi.org/10.1016/j.grj.2014.11.001.
Renema, W., Bellwood, D.R., Braga, J.C., Bromfield, K., Hall, R., Johnson, K.G., Lunt, P., Meyer, C.P., McMonagle, L.B., Morley, R.J., O'Dea, A., Todd, J.A., Wesselingh, F.P., Wilson, M.E.J., Pandolfi, J.M., 2008. Hopping hotspots: global shifts in marine biodiversity. Science 321, 654–657. https://doi.org/10.1126/science.1155674.
Renema, W., Walter, V., Novak, V., Young, J.R., Marshall, N., Hasibuan, F., 2015. Ages of Miocene fossil localities in the northern Kutai Basin (east Kalimantan, Indonesia). Palaios 30, 26–39. https://doi.org/10.2110/palo.2013.127.
Renz, O., 1936. Stratigraphische und mikropaläontologische Untersuchung der Scaglia (Obere Kreide-Tertiär) im zentralen Appenin. Eclogae Geol. Helv. 29, 1–149.
Reuter, M., Piller, W.E., Harzhauser, M., Mandic, O., Berning, B., Rögl, F., Kroh, A., Aubry, M.-P., Wielandt-Schuster, U., Hamedani, A., 2009. The Oligo-Miocene Qom Formation (Iran): evidence for an early Burdigalian restriction of the Tethyan Seaway and closure of its Iranian gateways. Int. J. Earth Sci. 98, 627–650. https://doi.org/10.1007/s00531-007-0269-9.
Reuter, M., Bosellini, F.R., Budd, A.F., Coric, S., Piller, W.E., Harzhauser, M., 2019. High coral reef connectivity across the Indian Ocean is revealed 6–7 Ma ago by a turbid-water scleractinian assemblage from Tanzania (Eastern Africa). Coral Reefs 38, 1023–1037. https://doi.org/10.1007/s00338-019-01830-8.
Riera, R., Haig, D.W., Bourget, J., 2019. Stratigraphic revision of the Miocene Trealla Limestone (Cape Range, western Australia): implications for Australasian foraminiferal biostratigraphy. J. Foramin. Res. 49, 318–338. https://doi.org/10.2113/gsjfr.49.3.318.
Robinson, E., 1995. Larger foraminiferal assemblages from Oligocene platform carbonates, Jamaica: Tethyan or Caribbean? Mar. Micropaleontol. 26, 313–318. https://doi.org/10.1016/0377-8398(95)00020-8.
Rögl, F., Briguglio, A., 2018. The foraminiferal fauna of the Channa Kodi section at Padappakkara, Kerala, India. Palaeontogr. Abt. A, Paläozool.-Stratigr. 312, 47–101. https://doi.org/10.1127/pala/2018/0082.
Roozpeykar, A., Moghaddam, M.I., 2016. Benthic foraminifera as biostratigraphical and paleoecological indicators: an example from Oligo–Miocene deposits in the SW of Zagros basin. Iran. Geosci. Front. 7, 125–140. https://doi.org/10.1016/j.gsf.2015.03.005.
Sajadi, S.H., Rashidi, R.F., 2019. Paleoecology and sedimentary environments of the Oligo–Miocene deposits of the Asmari Formation (Qeshm Island, SE Persian Gulf). In: Aiello, G. (Ed.), New Insights into the Stratigraphic Setting of Paleozoic to Miocene Deposits. Case Studies from the Persian Gulf, Peninsular Malaysia and South-Eastern Pyrenees. IntechOpen Limited, London. https://doi.org/10.5772/intechopen.81402.
Schlumberger, C., 1893. Note sur les genres *Trillina* et *Linderina*. Bull. Soc. Géol. Fr. 21, 118–123.
Serra-Kiel, J., Gallardo-Garcia, A., Razin, P.H., Robinet, J., Roger, J., Grelaud, C., Leroy, S., Robin, C., 2016. Middle Eocene–Early Miocene larger foraminifera from Dhofar (Oman) and Socotra Island (Yemen). Arab. J. Geosci. 9, 344. https://doi.org/10.1007/s12517-015-2243-3.
Seyrafian, A., Vaziri-Moghaddam, H., Arzani, N., Taheri, A., 2011. Facies analysis of the Asmari Formation in central and north-central Zagros basin, southwest Iran: biostratigraphy, paleoecology and diagenesis. Rev. Mex. Cienc. Geológ. 28, 439–458.
Simmons, M.D., 2020. Larger benthic foraminifera. Subchapter 3H. In: Gradstein, F.M., Ogg, J.G., Schmitz, M.D., Ogg, G.M. (Eds.), Geologic Time Scale 2020. Elsevier, Amsterdam, pp. 88–98.
Sirel, E., 2003. Foraminiferal description and biostratigraphy of the Bartonian, Priabonian and Oligocene shallow-water sediments of the southern and eastern Turkey. Rev. Paléobiol. 22, 269–339.
Sirel, E., Özgen-Erdem, N., Özgen, K., 2013. Systematics an biostratigraphy of Oligocene (Rupelian–Early Chattian) foraminifera from lagoonal-very shallow water limestone in the eastern Sivas Basin (central Turkey). Geol. Croat. 66, 83–109. https://doi.org/10.4154/GC.2013.07.
Susanta, K., 1990. Stratigraphy of the Tertiary succession, exposed along the Waior-Cheropodi Nala section, south western Kutch, Gujarat, India, with special reference to foraminifera. Unpubl. PhD thesis. Univ. Calcutta, Calcutta, 313 pp.
Suzuki, Y., Iryu, Y., Inagaki, S., Yamada, T., Aizawa, S., Budd, D.A., 2006. Origin of atoll dolomites distinguished by geochemistry and crystal chemistry: Kita-daito-jima,

northern Philippine Sea. Sediment. Geol. 183, 181–202. https://doi.org/10.1016/j.sedgeo.2005.09.016.
Takayanagi, H., Iryu, Y., Oda, M., Sato, T., Chiyonobu, S., Nishimura, A., Nakazawa, T., Ishikawa, T., Nagaishi, K., 2012. Temporal changes in biotic and abiotic composition of shallow-water carbonates on submerged seamounts in the northwestern Pacific Ocean and their controlling factors. Geodiversitas 34 (1), 189–217. https://doi.org/10.5252/g2012n1a11.
Todd, R., Low, D., 1960. Smaller Foraminifera from Eniwetok Drill Holes. Geol. Surv. Prof. Pap. 260-X, 799–861.
Todd, R., Post, R., 1954. Smaller Foraminifera from Bikini drill holes. Part 4, Paleontology of Bikini and nearby atolls. U.S. Geol. Surv. Prof. Pap. 260N, 547–568.
Todd, R., Post, R., 1970. Smaller foraminifera from Midway drill holes. Geol. Surv. Prof. Pap. 680-E, E1–E49.
Tokuyama, H., Kagami, H., Nasu, N., 1986. Marine geology and subcrustal structure of the Shikoku Basin and the Daito Ridges region in the northern Philippine Sea. Bull. Ocean Res. Inst., Univ. Tokyo 22, 1–169.
Van Der Vlerk, I.M., 1929. Groote foraminiferen van N. O. Borneo. Dienst Mijnb. Wetensch. Meded. Nederlandsch-Oost-Indië, 9, pp. 1–45.
Van Der Vlerk, I.M., Umbgrove, J.H., 1927. Tertiarie gids foraminiferen uit Nederlandsch Oost-Indie. Wetensch. Meded., Dienst Mijnb. Bandoeng 6, 1–31.
Wade, B.S., Pearson, P.N., Berggren, W.A., Pälike, H., 2011. Review and revision of Cenozoic tropical planktonic foraminiferal biostratigraphy and calibration to the geomagnetic polarity and astronomical time scale. Earth-Sci. Rev. 104, 111–142. https://doi.org/10.1016/j.earscirev.2010.09.003.
Wielandt, U., 1996. Larger foraminifera around the Oligocene/Miocene boundary. Giorn. Geol. 58, 157–161.
Wielandt-Schuster, U., Schuster, F., Harzhauser, M., Mandic, O., Kroh, A., Rögl, F., Rreisinger, J., Liebetrau, V., Steininger, F.F., Piller, W.E., 2004. Stratigraphy and palaeoecology of Oligocene and Early Miocene sedimentary sequences of the Mesohellenic Basin (NW Greece). Cour. Forschungsinst. Senckenberg 248, 1–55.
Williams, L.A.J., 1962. Geology of the Hadu-Fundi Isa area, north of Malindi. Minist. Commer. Ind., Geol. Surv. Kenya 52, 1–62.
Wilson, M.E.J., 2008. Global and regional influences on equatorial shallow-marine carbonates during the Cenozoic. Palaeogeogr. Palaeoclimatol. Palaeoecol. 265, 262–274. https://doi.org/10.1016/j.palaeo.2008.05.012.
Wilson, M.E.J., Chambers, J.L.C., Evans, M.J., Moss, S.J., Nas, D.S., 1999. Cenozoic carbonates in Borneo: case studies from northeast Kalimantan. J. Asian Earth Sci. 17 https://doi.org/10.1016/S0743-9547(98)00045-2, 183–20.
Yazdi-Moghadam, M., Sadeghi, A., Hossein Adabi, M., Tahmasbi, A., 2018. Stratigraphy of the Lower Oligocene nummulitic limestones, North of Sonor (NW Iran). Riv. Ital. Paleontol. Stratigr. 124, 407–419. https://doi.org/10.13130/2039-4942/10271.
Yazdi-Moghadam, M., Sarfi, M., Ghasemi-Nejad, E., Sadeghi, A., Sharifi, M., 2021. Early Miocene larger benthic foraminifera from the northwestern Tethyan Seaway (NW Iran): new findings on Shallow Benthic Zone 25. Int. J. Earth Sci. 110, 719–740. https://doi.org/10.1007/s00531-021-01986-1.

Chapter 3. Coral-reef larger porcelaneous foraminifera with a common ancestor: the Miocene Indo-Pacific *Flosculinella* and *Alveolinella* (Alveolinoidea)

published in Marine Micropaleontology 173 (2022), 102124
doi: /10.1016/j.marmicro.2022.102124

Marine Micropaleontology 173 (2022) 102124

Contents lists available at ScienceDirect

Marine Micropaleontology

journal homepage: www.elsevier.com/locate/marmicro

Larger porcelaneous foraminifera with a common ancestor: the Neogene Indo-Pacific *Flosculinella* and *Alveolinella* (Alveolinoidea)

Davide Bassi [a,*], Monica Bolivar-Feriche [a], Willem Renema [b,c], Juan C. Braga [d], Johannes Pignatti [e], Giovanni Di Domenico [a], Kazuhiko Fujita [f], Jere H. Lipps [g], Jesús Reolid [d], Yasufumi Iryu [h]

[a] *Dipartimento di Fisica e Scienze della Terra, Università degli Studi di Ferrara, via Saragat 1, 44122 Ferrara, Italy*
[b] *Naturalis Biodiversity Center, 9517, 2300 RA Leiden, the Netherlands*
[c] *Department of Ecosystem and Landscape Dynamics, Institute for Biodiversity and Ecosystem Dynamics, University of Amsterdam, P.O. Box 94240, 1090 GE Amsterdam, the Netherlands*
[d] *Departamento de Estratigrafía y Paleontología, Universidad de Granada, Campus Fuentenueva s/n, 18002 Granada, Spain*
[e] *Dipartimento di Scienze della Terra, Università 'La Sapienza', P.le A. Moro 5, 00185 Rome, Italy*
[f] *Department of Physics and Earth Sciences, University of the Ryukyus, Senbaru 1, Nishihara, Okinawa 903-0213, Japan*
[g] *Department of Integrative Biology and Museum of Paleontology, University of California, Berkeley, California 94720, United States*
[h] *Institute of Geology and Paleontology, Graduate School of Science, Tohoku University, Aobayama, Sendai 980-8578, Japan*

ARTICLE INFO

Keywords:
Palaeobiogeography
Systematics
Shallow-water carbonates
Indo-Pacific Ocean
Miocene
Recent

ABSTRACT

Only two alveolinoid genera, *Borelis* de Montfort, 1808 and *Alveolinella* H. Douvillé, 1907 thrive in present-day Indo-Pacific coral-reef settings. The former is widespread from the Western (Red Sea) to the Central Indo-Pacific and Caribbean Sea coasts, whereas the latter occurs in the Central and Eastern Indo-Pacific area. A third Indo-Pacific alveolinoid genus, *Flosculinella* Schubert *in* Richarz, 1910, is exclusively fossil. New fossil and Recent material and a type collection were analysed to assess the taxonomic status of *Flosculinella* and *Alveolinella* species and understand alveolinoid phylogeny in the Indo-Pacific area.

The latest Oligocene–middle Miocene *Flosculinella globulosa*, the early–middle Miocene *F. reicheli*, *F. bontangensis*, *F. cucumoides*, *Alveolinella borneensis* and the middle Miocene–Recent *A. quoyi* are herein circumscribed in terms of shell length, diameter of the proloculus, whorl number of the first attic occurrence, and number of supplementary chamberlets in the attic floor per chamberlet in the main floor. The occurrence of the preseptal passage only and Y-shaped septula in *Borelis schlumbergeri*, *Flosculinella* and *Alveolinella* are characters of phylogenetic significance. Oligocene–early Miocene *Borelis philippinensis* is inferred as the common ancestor of these taxa.

The diversification of *Flosculinella* and *Alveolinella* occurred in the Coral Triangle of Southeast Asia during the early–middle Miocene. The northernmost occurrence of the Tortonian–Recent *A. quoyi*, widespread from Central to the Eastern Indo-Pacific areas, is in the Ryukyu Islands.

1. Introduction

Two alveolinoid genera *Borelis* Montfort, 1808 and *Alveolinella* H. Douvillé, 1907, which first appeared in the middle Eocene and in the middle Miocene, respectively (e.g., Hottinger, 1974; Loeblich and Tappan, 1987), live in present-day tropical shallow-water marine environments in the Indo-Pacific. A third alveolinoid genus, *Flosculinella* Schubert *in* Richarz, 1910, had a short evolutionary history limited to the latest Oligocene–middle Miocene (Hottinger, 1974; Lunt and Allan, 2004; Bassi et al., 2021a). The modern Indo-Pacific alveolinoid genera are represented by only two fusiform species, *Borelis schlumbergeri* (Reichel, 1937) and *Alveolinella quoyi* (d'Orbigny, 1826), and a single spherical species, *B. pulchra* (d'Orbigny, 1839). *Borelis schlumbergeri* is widespread from the Western (i.e., Red Sea) to the Central Indo-Pacific

* Corresponding author.
E-mail addresses: bsd@unife.it (D. Bassi), blvmnc@unife.it (M. Bolivar-Feriche), willem.renema@naturalis.nl (W. Renema), jbraga@ugr.es (J.C. Braga), johannes.pignatti@uniroma1.it (J. Pignatti), didomenico@fe.infn.it (G. Di Domenico), fujitaka@sci.u-ryukyu.ac.jp (K. Fujita), jlipps@berkeley.edu (J.H. Lipps), jreolid@ugr.es (J. Reolid), yasufumi.iryu.d8@tohoku.ac.jp (Y. Iryu).

https://doi.org/10.1016/j.marmicro.2022.102124
Received 13 December 2021; Received in revised form 8 March 2022; Accepted 1 April 2022
Available online 5 April 2022
0377-8398/© 2022 Elsevier B.V. All rights reserved.

(CIP), whereas *A. quoyi* occurs in the CIP and Eastern Indo-Pacific (from the Maldives to the Hawaii islands; Reiss and Hottinger, 1984; Hohenegger, 2000; Langer and Hottinger, 2000). *Borelis schlumbergeri* has been found in fringing reefs (back-reef to fore-reef), in rock pools and intertidal settings on rubble, coral sand and plants at water depths shallower than 40 m (Cole, 1957; Hottinger et al., 1993; Langer and Hottinger, 2000; Debenay, 2012; Fajemila et al., 2015; Weinmann and Langer, 2017). *Alveolinella quoyi*, the largest living porcelaneous foraminifer, lives on sandy slopes, coral rubble on the reef slope and in sandy inter-reef environments of the euphotic zone (e.g., Reiss and Hottinger, 1984; Hohenegger, 2000, 2006; Langer and Lipps, 2003; Debenay, 2012; Renema, 2018; Bassi et al., 2022).

In larger benthic foraminifera, the apertural face and shell morphology reflect functional adaptations related to their locomotion, feeding, and photosymbiosis (Hottinger, 2000, 2005; Hohenegger, 2018). Both *Alveolinella* and *Borelis* possess diatom symbionts (Hottinger, 1983). Photosymbiosis may be inferred from shell morphology and shell architecture to capture light (Leutenegger, 1984; Brasier, 1993; Hottinger, 2000; Hohenegger, 2011, 2018). The large fusiform tests of *Borelis schlumbergeri* and *Alveolinella quoyi* expand their surface through lengthening the skeleton in an axial direction which is occupied by the protoplasm with symbionts below the outer shell surface (Severin and Lipps, 1989; Hohenegger, 2009). Living individuals of *A. quoyi* can only fill an average of 39% of their chamber space with protoplasm (Severin and Lipps, 1989). The increase in their shell size during ontogeny is positively related to an increase in the number of apertures. These are likely to strengthen the fixation on substrate by multiplying the attachment through a bundle of pseudopods (Hottinger, 2006a; Hohenegger, 2018).

The purposes of this study are (1) to assess the taxonomic status of *Flosculinella* and *Alveolinella* species to understand their phylogeny in the Indo-Pacific area, (2) to describe newly discovered Y-shaped septula in *A. quoyi* already known in *B. schlumbergeri*, and (3) to assess the phylogenetic history of these taxa. The discovery of Y-shaped septula was possible due to analysis of modern and fossil material of *A. quoyi* from the Ryukyu Islands and Indonesia. Interestingly, the putative Indo-Pacific ancestor of *Flosculinella* appeared in the Oligocene while that of *Alveolinella* first occurs in the early Miocene. These taxa show shell traits in common with middle Eocene *Borelis* (aligned septula, only preseptal passage present and lack of postseptal passage).

2. Material and methods

This study was carried out on collected larger benthic foraminiferal specimens from fossil and modern coral-reef related settings. Fossil *Flosculinella globulosa*, *F. reicheli* and *F. bontangensis*, from Indonesia and the Maldives, and *Alveolinella quoyi* from Okinawa-jima (Ryukyu Islands), were examined in rock thin sections. The types of *F. cucumoides* are preserved as thin sections in the collections of the Museum Victoria, Melbourne, Australia, and were re-photographed for this study.

In the Taballar Limestone (Wilson et al., 2007; Novak, 2014; Renema et al., 2015). *globulosa* and *F. reicheli* were identified from the lower Burdigalian interval (Mankalihat, East Kalimantan, Indonesia). *F. bontangensis* is found in the Kutei Basin (East Kalimantan) from the upper Burdigalian to Serravallian interval (Bontang area, East Kalimantan, Indonesia; type area; Novak et al., 2013; Renema et al., 2015) and in Wailawi (south of Balikpapan Bay, East Kalimantan) from the Langhian or younger age (Bassi et al., 2021b). Additional material of *Flosculinella bontangensis* was studied also from the Serravallian platform carbonates in the Maldives (Reolid et al., 2020).

Specimens of *Alveolinella borneensis* were collected from close to the Langhian–Serravallian boundary of the Stadion stratigraphic section near Samarinda (East Kalimantan, Indonesia), from sediments inside a large strombid shell from the Serravallian of Pacitan (East Java, Indonesia; 12.2 Ma), and from several localities in the Tortonian of the Kutai basin (Sangatta, East Kalimantan, Indonesia) ranging from 11.6 Ma to 9.4 Ma in age (Renema et al., 2015). The Stadion specimens occur associated to *Nephrolepidina ferreroi* and *Cycloclypeus annulatus* suggesting an age older than the Langhian–Serravallian boundary (Marshall et al., 2015; Santodomingo et al., 2015).

Studied fossil *Alveolinella quoyi* occurs in the Calabrian–Chibanian (Pleistocene) Kourijima Formation of the Ryukyu Group cropping out in the Motobu Peninsula (samples M62_5 from Ohama, Motobu town; 167 Tobaru Core 12B-4–13.0 m and 16 Tobaru Core13B-7–5.98 m from Tobaru, Motobu town; N1_2_5 and N1_3_5 from Nakasone, Nakijin village; Yamamoto et al., 2006; Iryu et al., 2006) and in the Calabrian–Chibanian Sobe Formation in the Yomitan–Onna area (sample 362 from Maeda, Onna village; Muraoka et al., 2005), Okinawa-jima, Ryukyu Islands. Fossil *A. quoyi* was also studied from the Tortonian of Sangatta (Kalimantan; 8.9–9.3 Ma; Renema et al., 2015) and Messinian of Bengalon (Kalimantan; Renema et al., 2015), from the Pliocene of Malaysia (Togopi; Whittaker and Hodgkinson, 1979) and Waigeo (West Papua, Indonesia) and from the earliest Pleistocene of Cebu (Philippines).

The present-day *Alveolinella quoyi* was collected from Vanuatu and the Ryukyu Islands. The Vanuatu specimens were collected from the fore-reef of Espiritu Santo in 25–30 m water depth (15°33′11″S, 167°13′11″E). The Ryukyu specimens occurred in coral rubble on a fore-reef slope (15 m water depth) at Kushibaru, Aka-jima (26°12′46.7″N, 127°16′28.8″E), and in coral rubble on a fore-reef slope (35 m water depth) at northwest of Irabu-jima (24°51′53.5″N, 125°09′11.8″E).

The studied samples are stored in the Dipartimento di Fisica e Scienze della Terra of the University of Ferrara, in the Departamento de Estratigrafía y Paleontología of the Universidad de Granada, Naturalis Biodiversity Center (Leiden, the Netherlands), and in the Institute of Geology and Paleontology of the Tohoku University. The studied isolated specimens were micro-computed tomographic scanned in the Dipartimento di Fisica e Scienze della Terra of the University of Ferrara. The fossil specimens were, for the largest part, well without infillings of the chambers, allowing their volume segmentation, highlighting the complex shell structure. The internal cement was sparry calcite, not affecting the LBF microcrystalline texture (porcelaneous). The micro-computed tomographic scanning 3D-models were rendered with shell removed, in order to highlight the volumes occupied by protoplasm within the shell and the arrangement and communications among chambers and chamberlets. Detailed micro-computed tomographic methods performed on LBF have been described by Kellner et al. (2019) and Macher et al. (2021). The micro-computed tomographic system consists of a Hamamatsu L9421–02 tungsten X-ray microfocus tube with an anode voltage of 70 kVp. The used current was 100–110 uA. Rotation step ranges between 0.5° to 1°, with an exposure time of 1 s. The reconstructed voxel size was 5x5x5 um^3 with the reconstruction algorithm FDK on GPU. The X-ray detector collects hundreds of angular shadow images while the object rotates, thereafter, a computer program (Di Domenico, 2014), developed on CUDA framework and including alignment optimization, uses a modified Feldkamp algorithm allowing the reconstruction of data throughout the full 3D volume. Scanning Electron Microscopy analyses were performed at the University of Ferrara. Additional studied specimens were micro-computed tomographic scanned in the Zeiss XRadia Vera 520 at Naturalis Biodiversity Center.

Architectural and morphological terms are those used by Smout and Eames (1958), Hottinger (1960, 2006b) and Hottinger et al. (1993). The suprageneric classification follows Loeblich and Tappan (1987) and Fleury and Fourcade (1990). The analysed *Flosculinella* and *Alveolinella* species are listed in the systematic palaeontology chapter according to their stratigraphical appearance. Synonymy lists can be found in the Supplementary data.

3. Systematic palaeontology

Superfamily Alveolinoidea Ehrenberg, 1839.
Family Borelidae Schmarda, 1871.

Subfamily Borelinae Schmarda, 1871.

Remarks: In describing the foraminiferal shell structures Hottinger (2006b) redefined the terms floor and attic for endoskeletal elements. These terms still appear to be the only ones that can unambiguously be applied to these shell elements. Within the larger porcelaneous foraminifera of the superfamily Alveolinoidea in a chamber the floors ('planchers' in Reichel, 1937; Hottinger, 1960; Fleury and Fourcade, 1990) separate superposed regular layers of chamberlets. The foramina corresponding to the basal layer of chamberlets are named f1, those of the second layer f2, and those corresponding to the supplementary foramina in the attics f3. The attics ('mansardes' in Reichel, 1937) correspond to the outermost lateral or abaxial layer of tubiform chamberlets with smaller calibre/diameter than the less lateral or adaxial ones (f1, f2).

Genus *Flosculinella* Schubert *in* Richarz, 1910.

Type species: *Alveolinella bontangensis* L. Rutten, 1913, p. 221.

Diagnosis: Shell sub-spheroidal, ellipsoidal to fusiform in shape, up to 1.5 mm in diameter and up to 2.5 mm in length, no dimorphism, early whorls streptospiral, septula aligned, Y-shaped septula present, each chamber with one layer of main chamberlets and, in the adult stages, one layer of attics.

Remarks: *Flosculinella* species are exclusively known from fossil specimens (*F. globulosa*, *F. reicheli*, *F. bontangensis*; Figs. 1–2, 4, 7). Y-shaped septula occur in the whorls of adult stages (Figs. 1–2, 6; see also *F. globulosa* in Hottinger, 1974, pl. 103, fig. 4; *F. bontangensis* in Hottinger, 1974, pl. 104, figs. 1, 4). The length of the shell, the diameter of the proloculus, the number of whorls of the first attic occurrence, and the number of supplementary chamberlets in the attic layer per chamberlet in the main layer are reliable characters to distinguish the species (Table 1).

Flosculinella globulosa (Rutten, 1917).

Fig. 1A–E.

(see Supplementary data for the synonymy list)

Type reference and figures: *Alveolinella globulosa* Rutten, *in* Martin (1917), p. 277, pl. 5, figs. 140–141 (drawings), holotype not designated.

Lectotype of *F. globulosa*: In the original material illustrated as drawings Rutten (1917) did not designate a type. In accordance with Art. 74 of ICZN (1999), we designate hereby as lectotype the specimen originally illustrated by Rutten (1913, pl. 7, fig. 140), in order to clarify the application of this name.

Diagnosis: Sub-spheroidal to slightly sub-ellipsoidal shell 0.7–1.5 mm in diameter. Proloculus 35–50 μm in diameter with 2–3 streptospiral whorls. First attic occurs from the non-streptospiral second whorl. Less than 2 supplementary chamberlets in the attic (f3) per chamberlet in the basal layer (f1).

Studied material: The studied specimens are from the lower Burdigalian of the Taballar Limestone in the Mankalihat Peninsula (East Kalimantan, Indonesia; Fig. 1). Sub-spheroidal specimens 0.45–0.82 mm in length. Proloculus is *c.* 40 μm in diameter. Y-shaped septula occur in the whorls of adult stages (Fig. 1A). The first attic occurs in the second whorl with two supplementary chamberlets in the attic layer (f3) per chamberlet in the basal layer of chamberlets (f1).

Remarks: Two specimens were illustrated as drawings by Rutten (*in* Martin, 1917), representing tangential sub-axial and oblique sub-equatorial sections. The specimen illustrated in fig. 141 of Rutten *in* Martin (1917) shows the preseptal passage only and that in fig. 140 shows one layer of main chamberlets and one layer of attics, which are diagnostic characters for *Flosculinella*.

Flosculinella globulosa is separated from *F. reicheli* by having attics appearing from the second whorl and from *F. bontangensis* by its smaller size and by having less than two supplementary chamberlets in the attic per chamberlet in the basal layer of chamberlets (Table 1).

Stratigraphical distribution: Rutten's (*in* Martin, 1917) material was collected from the Burdigalian deposits of Kembang Sokkoh and Gunun Spolong, Yogyakarta, Java, Indonesia (Martin, 1911; Renema, 2008), which have been dated at 18.9 Ma (Reich et al., 2014). This species occurs from the late Chattian to the Langhian in Bikini Atoll, Midway Atoll, and the Philippines (Cole, 1954, 1969; Matsumaru, 2011, 2017), in the early Miocene (upper Te–lower Tf) of New Britain (Binnekamp, 1973), in the early Miocene of Indonesia (Hanzawa, 1957; Hottinger, 1974; Lunt and Allan, 2004; Renema, 2007, 2008; this study), in the late Aquitanian–Burdigalian of eastern and southwestern Australia (Haig et al., 2020) and in the late Langhian–early Serravallian of Western Australia (Chaproniere, 1984; Riera et al., 2019; Table 2, Fig. 7).

Flosculinella reicheli Mohler, 1949.

Fig. 2

(see Supplementary data for the synonymy list)

Type reference and figures: *Flosculinella reicheli* Mohler, 1949 (p. 151; only description); Mohler (1950), pp. 524–525, text-fig. 2 (1–6; fig. 5, holotype).

Diagnosis: Spheroidal shell 0.4–0.6 (maximum 0.8) mm in diameter. Proloculus 35–40 μm in diameter with 3–4 streptospiral whorls. Adult whorls with attics and one to two supplementary chamberlet (f3) per chamberlet in the basal layer of chamberlets (f1).

Studied material: The studied specimens are from the early Burdigalian of the Taballar Limestone in the Mankalihat Peninsula (East Kalimantan, Indonesia; Fig. 2). Sub-spheroidal and tightly coiled specimens with length up to 0.48 mm. Proloculus is 35–40 μm in diameter. The first attic occurs in the third whorl with one supplementary chamberlet (f3) in the attic layer per chamberlet in the basal layer of chamberlets (f1).

Remarks: The holotype of *F. reicheli* is an unsectioned, isolated specimen that does not show inner shell structures (Mohler, 1949). The occurrence of only the preseptal passage, aligned septula, one layer of main chamberlets and one layer of attics per chamber in the paratypes of *F. reicheli* (Mohler, 1949, fig. 2/1–3) indicate that it belongs to *Flosculinella*. *Flosculinella reicheli* differs from *F. globulosa* and *F. bontangensis* in having the attics appearing in the third or fourth whorls with only one supplementary chamberlet in the attic layer per chamberlet in the basal layer of chamberlets (Table 1, Fig. 2).

Stratigraphical distribution: The types of *F. reicheli* are from the Aquitanian of Hulu-Sungei, southern Borneo (Mohler, 1949). This species has only been found in the early Miocene of Indonesia (Adams, 1965, 1970; Hottinger, 1974; BouDagher-Fadel and Lokier, 2005; Renema, 2007; this study; Table 2, Fig. 7). Poorly preserved specimens identified as *F. reicheli* by Matsumaru (1996, pp. 212, 214, pl. 84, figs. 1–2) from the Oligocene of the Ogasawara Islands (Japan) do not appear to be conspecific or even congeneric.

Flosculinella bontangensis (Rutten, 1913).

Figs. 1F, 3–5.

(see Supplementary data for the synonymy list)

Repository data of *F. cucumoides*: Thin sections labelled '*Alveolina cucumoides* Chapman, New Hebrides pl. 38 f. 5, 6. 108' and '*Flosculinella cucumoides* (Chapman, 1908) Topotype Bartaleppe, Malekula, New Hebrides, Sample 108. P134790', '*Flosculinella cucumoides* (Chapman, 1908) Topotype Bartaleppe, Malekula, New Hebrides, Sample 108. P134791', '*Flosculinella cucumoides* (Chapman, 1908) Topotype Bartaleppe, Malekula, New Hebrides, Sample 108. P134792', and '*Flosculinella cucumoides* (Chapman, 1908) Topotype Bartaleppe, Malekula, New Hebrides, Sample 108. P134793'; housed at the Museum Victoria, Melbourne, Australia.

Type reference and figures of *F. cucumoides*: *Alveolina cucumoides* Chapman, 1908, pp. 754–755, pl. 38, figs. 5–6.

Type locality and horizon of *F. cucumoides*: Laleppe (Lalemba), along the track Laleppe Amil–Bartaleppe, northern Malakula Island, Vanuatu, Pacific Ocean. Miocene limestone and tuffs (Chapman, 1908, p. 746).

Diagnosis of *F. cucumoides* (modified from Chapman, 1908): Ellipsoidal to fusiform shell. Equatorial diameter of *c.* 1 mm and 1.8–2.5 mm in length. Proloculus *c.* 80 μm in diameter and 1–2 streptospiral whorls. Two supplementary chamberlets in the attic layer (f3) per

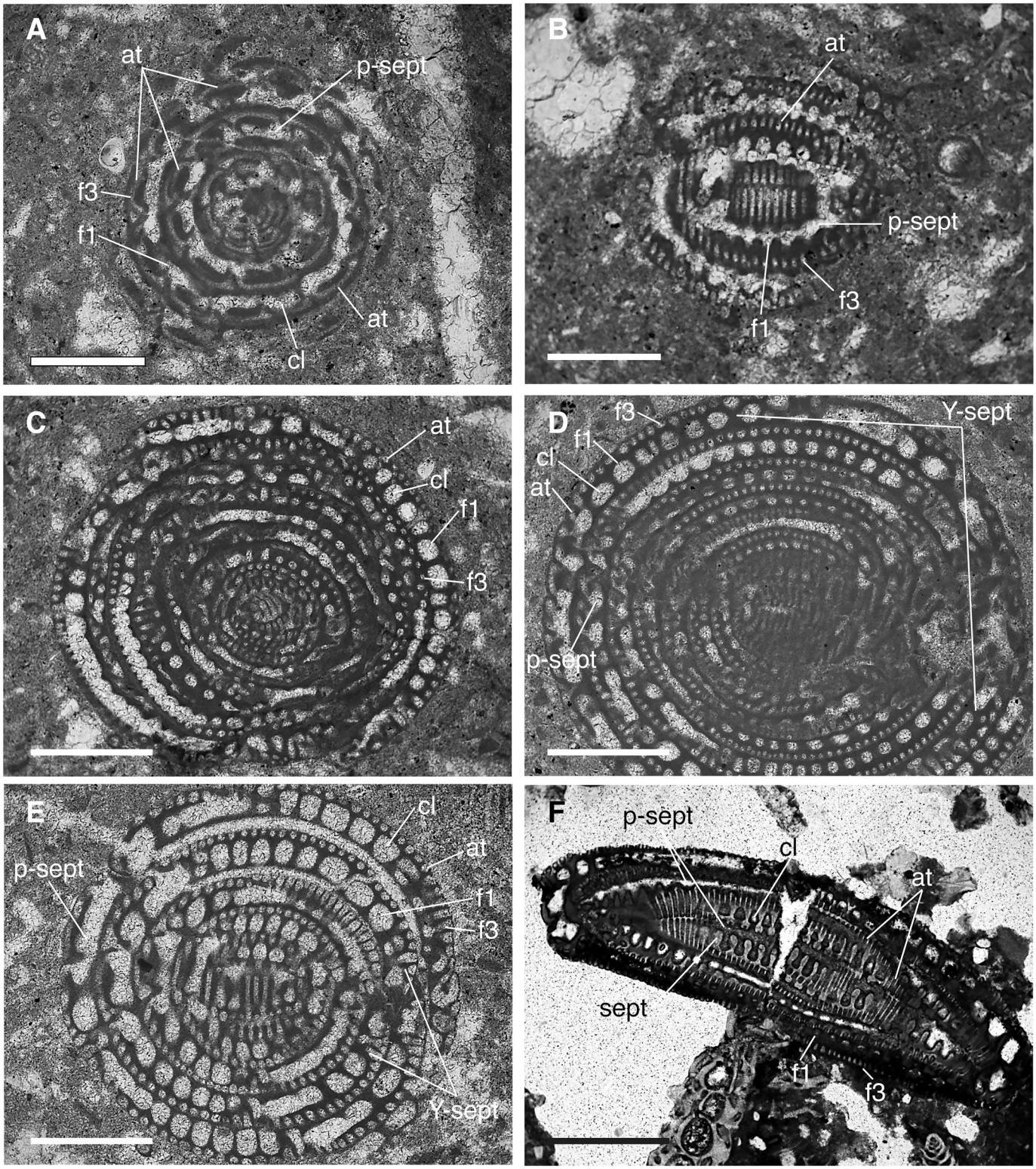

Fig. 1. *Flosculinella globulosa* (Rutten, 1917); A–E, early Burdigalian, Tallabar Limestone, Mankalihat Peninsula, East Kalimantan, Indonesia. A, sub-equatorial section showing preseptal passages, the basal layer of chamberlets overlain by attics (sample SA220c). B, tangential section showing alignment of septula and chamberlets with a single attic layer (sample SA220d). C–E, sub-axial sections showing the Y-shaped septula, basal layer of chamberlets and attics; note that there are more than 2 supplementary chamberlets in the attic layer per chamberlet in the basal layer (samples SA220f, SA220i, SA221g). *Flosculinella bontangensis* (Rutten, 1913); late Burdigalian, Kutai Basin, East Kalimantan, Indonesia. F, tangential sub-axial sections showing preseptal passage, aligned septula and chamberlets with attic (sample SA117). *Abbreviations*: at, attic; cl, chamberlet; f1, foramina in the basal layer of chamberlets; f2, foramina in the second layer of chamberlets; f3, supplementary foramina in the attic; prol, proloculus; p-sept, preseptal passage; sept, septula; Y-sept, Y-shaped septula. Scale bars represent 0.20 mm (A–E) and 0.50 mm (F).

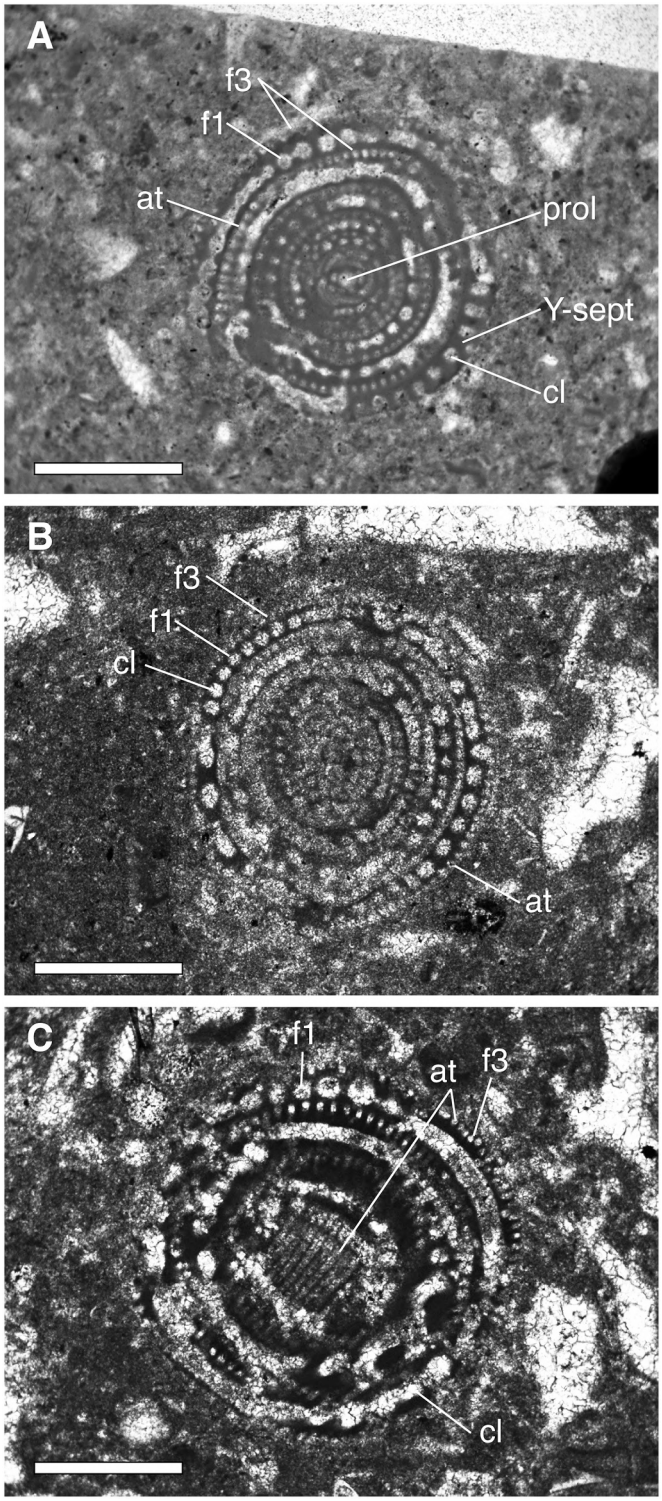

Fig. 2. *Flosculinella reicheli* Mohler, 1949; A–C, early Burdigalian, Tallabar Limestone, Mankalihat Peninsula, East Kalimantan, Indonesia. A–B, nearly axial sections showing the proloculus, single layer of chamberlets (cl) with attics (at) and Y-shaped septula (samples SA218, SA215). C, oblique tangential section showing attics (at); note more than 2 supplementary chamberlets in the attic (f3) per chamberlet in the basal layer of chamberlets (f1; sample SA216). *Abbreviations*: at, attic; cl, chamberlet; f1, foramina in the basal layer of chamberlets; f3, supplementary foramina in the attic; prol, proloculus; p-sept, preseptal passage; sept, septum. Scale bar represents 0.20 mm.

chamberlet in the basal layer of chamberlets (f1).

Lectotype of *A. cucumoides*: Chapman (1908) did not designate a holotype. The original material illustrated by Chapman (1908), pl. 38, figs. 5–6) occurs in the same thin section. In accordance with Art. 74 of ICZN (1999), we designate hereby as lectotype (Fig. 3A) the specimen in thin section '*Alveolina cucumoides* Chapman, New Hebrides pl. 38 f. 5, 6. 108', originally illustrated by Chapman (1908) in pl. 38, Fig. 5, with the purpose of clarifying the application of this name. The specimen illustrated by Chapman (1908) in pl. 38, fig. 6 becomes a paralectotype (Fig. 3B).

Type reference and figure: *Alveolinella Bontangensis* Rutten, 1913, pp. 221–224, text-figs. 1–2; pl. 14, figs. 1–3, holotype not designated.

Syntypes of *F. bontangensis*: Sample number RGM.17691 and labelled as '*Alveolinella bontangensis* Rutten; Bontang Borneo; Burdigalien; Rutten, Samml. Bd9, S221'. The type locality is *c.* 5 km to the north of the 3D-reef described in Novak et al. (2013) and dated as 15.6–16.0 Ma (Renema et al., 2015).

Studied material: The specimens are from the upper Burdigalian of the Bontang area in the Kutai Basin (East Kalimantan, Indonesia; Fig. 1F), from the early Langhian of Wailawi (East Kalimantan, Indonesia; Fig. 4), late Langhian–early Serravallian marls in Mankalihat (East Kalimantan; published before in van der Vlerk, 1929), and from Serravallian carbonates drilled in the western Kardiva Channel in Maldives (Site U1465, International Ocean Discovery Program (IODP) Expedition 359; Reolid et al., 2020; Fig. 5). Sub-ellipsoidal specimens *c.* 0.65–1.0 mm in diameter and c. 1.1–2.3 mm in length. Proloculus, only observed in the isolated specimens from East Kalimantan, ranges from *c.* 75 to 85 μm in diameter. The proloculus is elliptical, with a ratio of 0.95/1/1.05 (minimum diameter, max diameter, height). The orientation of the flexostyle, enveloping the proloculus for *c.* 270°, is variable with respect to the direction of the elongation axis of the shell. This increases the variability in observed proloculus size in oriented thin sections. The flexostyle is followed by 1/3–2 1/3 streptospiral whorls (1–8 streptospiral chambers) (Fig. 4A–B). The first attic occurs in the 14th– 17th chamber equal to the fourth to fifth whorl with one or two supplementary chamberlets (f3) per chamber (f1) in the basal layer, whereas in the later whorls with two supplementary chamberlets (f3) in the attic layer per chamberlet (f1) in the basal layer. From the second whorl the chambers (with two chamberlets or more each) increase in number at *c.* one chamber per whorl; the fourth whorl shows six chambers with six-seven chamberlets each (f1). This increase in number of chambers can be irregular. In the fourth whorl the chamber axis is at *c.* 60° angle to the previous chamber (Fig. 4E). In the fifth whorl this axis is at *c.* 30° (Fig. 4F), the chamberlets are *c.* eleven with up to eighteen supplementary chamberlets (f3). From the fifth whorl onwards the chamber axis becomes increasingly more parallel to the elongation axis of the test, and number of chamberlets increases to up to 20 f1 and 40 f3 per chamber. Up to 9 1/3 whorl in the Wailawi population, up to 11 whorls in the larger specimens in the Bontang and Mankalihat population. The number of chambers per whorl is highly variable from 8 to 11. Damage and repair is frequent in the Wailawi population (Fig. 4G).

Remarks: The occurrence of the preseptal passage only and aligned septula in the lectotype of *A. cucumoides* indicates that it belongs to *Flosculinella* (Fig. 3A, C–D).

The lectotype of *A. cucumoides* illustrated in pl. 38, fig. 5 (Chapman, 1908) represents a sub-equatorial section showing the proloculus, the preseptal passages and the attics (Fig. 3A). The first attic occurs in the second whorl. The paralectotype (pl. 38, fig. 6) is a sub-axial section, nearly tangential to the nepionic apparatus, showing preseptal passages, aligned septula, the basal layer of chamberlets and two supplementary chamberlets in the attic layer per chamberlet in the basal layer of chamberlets (Fig. 3C–D).

Rutten (1913) introduced the name *Alveolinella bontangensis* from the Burdigalian of Bontang (East Kalimantan, Borneo) with no mention of Chapman's species (see also Keijzer, 1940, p. 628). The name *cucumoides* has been rarely quoted in literature. Crespin (1955, p. 74, no

Table 1
Comparison of diagnostic shell characteristics of *Flosculinella* species and related stratigraphical distribution.

	Age	L (mm)	prol (μm), flexost	strsp	Attics
F. globulosa [1, 2]	late Chattian–Langhian	0.7–1.5	(16, 22) 35–50	2–3	(≥ 2) < 2
F. reicheli [1, 3]	Aquitanian–early Burdigalian	0.4–0.6 (0.8)	35–40	3–4	(3–4) 1–2
F. bontangensis [1, 2]	Burdigalian–early Serravallian	(1.1.–1.3) 2.1–3.4	75–90, flexost enveloping for c. 270°	1–2	(> 2) 2

Species are listed according to their first appearance reported in literature.
Based on data from: 1, Chapman (1908), Rutten (1913), Mohler (1949, 1950), Hanzawa (1957), Hottinger (1974), Hashimoto and Matsumaru (1975), Matsumaru (1996, 2017), this study; 2, Cole (1954), Chaproniere (1984), this study; 3, Adams (1965), this study.
Abbreviations: Attics, (number of whorl of their first occurrence) number of supplementary chamberlets in the attic floor per chamberlet in the main floor; flexost, flexostyle; L, length (max); prol, proloculus diameter (min); strsp, streptospiral whorls.

illustration) recorded *F. cucumoides* from the middle Miocene Trealla Limestone (Cape Range area, Western Australia). Adams (1970, p. 115) incorrectly stated that *A. cucumoides* is a junior synonym of *F. bontangensis* Rutten, 1913, as noted by Chaproniere (1984). The name *cucumoides* is, actually, a senior subjective synonym of *bontangensis*.

In contrast, *Flosculinella bontangensis* is a name that has been widely used in systematic and stratigraphical studies, having been used in at least twenty-five works by twenty authors in the immediately preceding fifty years. Thus, *Flosculinella cucumoides* precedes *F. bontangensis*, but priority is suppressed under Arts. 23.91.1 and 23.9.1.2 of the ICZN (1999). The younger valid name is *F. bontangensis* (*nomen protectum*) and the invalid, but older, name is *F. cucumoides* (*nomen oblitum*).

Table 2
Stratigraphical and geographical distribution of *Flosculinella* species.

References	Referred to as	Age	Locality	Illustrations
Cole (1954)	*F. globulosa*	Te	Bikini	pl. 209, fig. 9
Cole (1969)	*F. globulosa*	Te	Midway Atoll	pl. 4, figs. 24, 26
Matsumaru (2017)	*F. globulosa*	late Oligocene–early Miocene	Philippines	pl. 43, figs. 7–10
	F. bontangensis	early–middle Miocene		pl. 42, 10–14
	F. fusiformis	early Miocene		pl. 42, fig. 15; pl. 43, figs. 1–6
Matsumaru (2011)	*F. globulosa*	late Chattian–Burdigalian	Philippines	no
	F. bontangensis			no
	F. fusiformis			no
Leupold and van der Vlerk (1931)	*F. bontangensis*	early Burdigalian	Borneo	no
Eames et al. (1962)	*F. bontangensis*	Burdigalian	Kenya, Pemba Island	pl. 6, fig. C; pl. 7, fig. E
van der Vlerk (1922)	*F. globulosa*	Burdigalian–Langhian	Java	pl. 2, fig. 12
van der Vlerk (1929)	*A. boscii*	Burdigalian–Langhian	Mangkalihat, Indonesia	fig. 24
Binnekamp, (1973)	*F. globulosa*	late Te–early Tf	Nakanai Mountains, New	pl. 2, figs. 1–2
	F. borneensis	late Tf	Britain	pl. 2, figs. 3–6
Hottinger (1974)	*F. globulosa*	early Miocene	Java	pl. 103, figs. 3–4
Hottinger (1974)	*F. bontangensis*	early Miocene	east Borneo	pl. 103, figs. 1–2; pl. 104, figs. 1–4
BouDagher-Fadel and Price (2021)	*F. globulosa*	early Burdigalian	Indonesia	pl. 7, fig. 1
	F. bontangensis			pl. 7, fig. 2
Mohler (1949)	*F. reicheli*	Aquitanian	Borneo	text-figs. 1–2
Adams (1965)	*F. reicheli*	Aquitanian	Sarawak	pl. 27, fig. h
Adams (1965)	*F. reicheli*	lower Miocene	Melinau, Sarawak	pl. 2, fig. 4
Hottinger (1974)	*F. reicheli*	Te5, early Miocene	Borneo	pl. 103, figs. 5–7
Hashimoto and Matsumaru (1975)	*F. globulosa*	Aquitanian–Burdigalian	Palanan, Philippines	pl. 14, figs. 1–6
	F. fusiformis			pl. 14, fig. 8
Haig et al. (2020)	*F. globulosa*	Early Tf1	SW Australia	figs. M–N
	F. bontangensis			figs. L, O
	F. sp.			fig. J
Lunt and Allan (2004)	*F. globulosa/F. bontangensis*	late Aquitanian–Langhian	Indonesia	p. 43, 58
BouDagher-Fadel (2018)	*F. bontangensis*	Burdigalian–mid Serravallian	Borneo, east Java	pl. 7.2, figs. 9–11
Hanzawa (1957)	*F. globulosa*	Burdigalian	Saipan	pl. 23, fig. 1A–d
Renema et al. (2015)	*F. bontangensis*	Burdigalian–Langhian boundary	E Kalimantan	no
Renema (2007)	*F. globulosa*	late Chattian–early Burdigalian	SE Asia	no
	F. bontangensis	Serravallian		
	F. borneensis	Serravallian		
Barberi et al. (1987)	*F.* cf. *bontangensis*	early Burdigalian–early Serravallian	Indonesia	pl. 7, figs. 1, 7–9
	F. globulosa	late Aquitanian–early Burdigalian		pl. 7, figs. 10, 13–15
Novak (2014)	*F.* cf. *globulosa*	early Burdigalian	Indonesia	figs. E–F
This study	*F. globulosa, F. reicheli*	early Burdigalian	Indonesia	Figs. 1–2
This study	*F. bontangensis*	early Burdigalian Serravallian	Indonesia	Fig. 1F
			Maldives	Figs. 4–5
BouDagher-Fadel and Lokier (2005)	*F. bontangensis*	late Burdigalian–Serravallian	Java	pl. 1, fig. 4
Chaproniere (1984)	*F. bontagensis globulosa*	middle Miocene	N Australia	pl. 3, fig. 2a–b; pl. 14, fig. 22
	F. bontangensis bontangensis			pl. 14, figs. 18–19, 22
Lindsay (1969)	*F. bontangensis*	middle Miocene	S Australia	pl. 2, figs. 1, 3
Hallock et al. (2006)	*F. bontangensis*	Langhian	NE Australia	fig. F12B
Riera et al. (2019)	*F. globulosa*	late Langhian–early Serravallian	W Australia	table 4
	F. bontangensis			

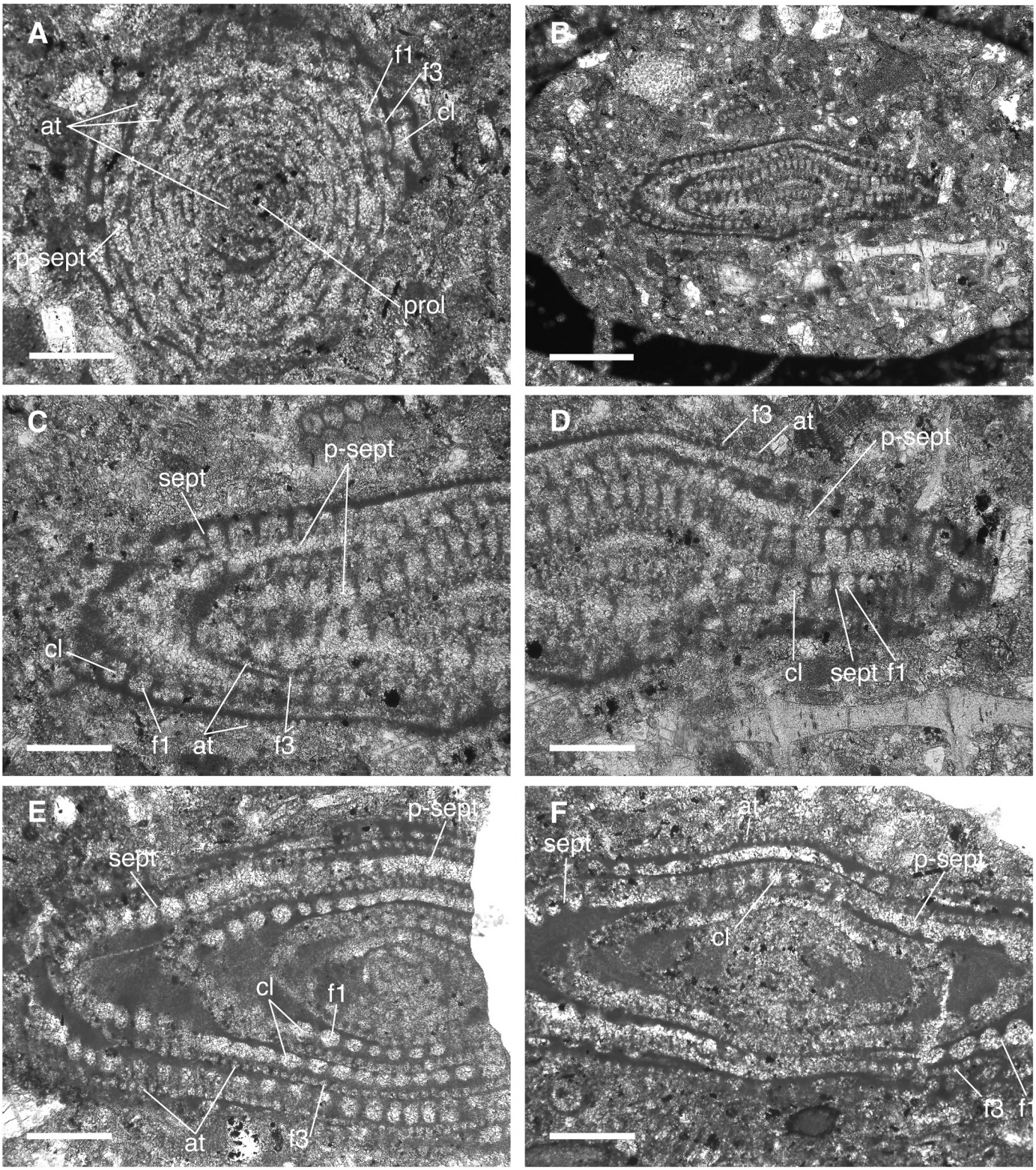

Fig. 3. *Flosculinella cucumoides* (Chapman, 1908), thin sections of types; Chapman collection; Museum Victoria, Melbourne, Australia. A, sub-equatorial section showing the proloculus and basal layer of chamberlets (f1) with attics (f3) (Chapman, 1908, pl. 38, fig. 5); lectotype of *Alveolina cucumoides* Chapman, 1908, designated herein; note that the first attic occurs in the second whorl. B, sub-axial section of the fusiform shell (Chapman, 1908, pl. 38, fig. 6); paralectotype. C-D, magnifications of the lectotype showing pre-septal passages, basal layer of chamberlets (f1) with two supplementary chamberlets in the attic (f3) per chamberlet in the basal layer. E–F, sub-axial sections showing the basal layer of chamberlets and attics (topotypes; E, '*Flosculinella cucumoides* (Chapman, 1908) Topotype Bartaleppe, Malekula, New Hebrides, Sample 108. P134791'; F, '*Flosculinella cucumoides* (Chapman, 1908) Topotype Bartaleppe, Malekula, New Hebrides, Sample 108. P134792'). *Abbreviations*: at, attic; cl, chamberlet; f1, foramina in the basal layer of chamberlets; f2, foramina in the second layer of chamberlets; f3, supplementary foramina in the attic; prol, proloculus; p-sept, preseptal passage; sept, septum. Scale bars represent 0.20 mm (A, C-F) and 0.50 mm (B).

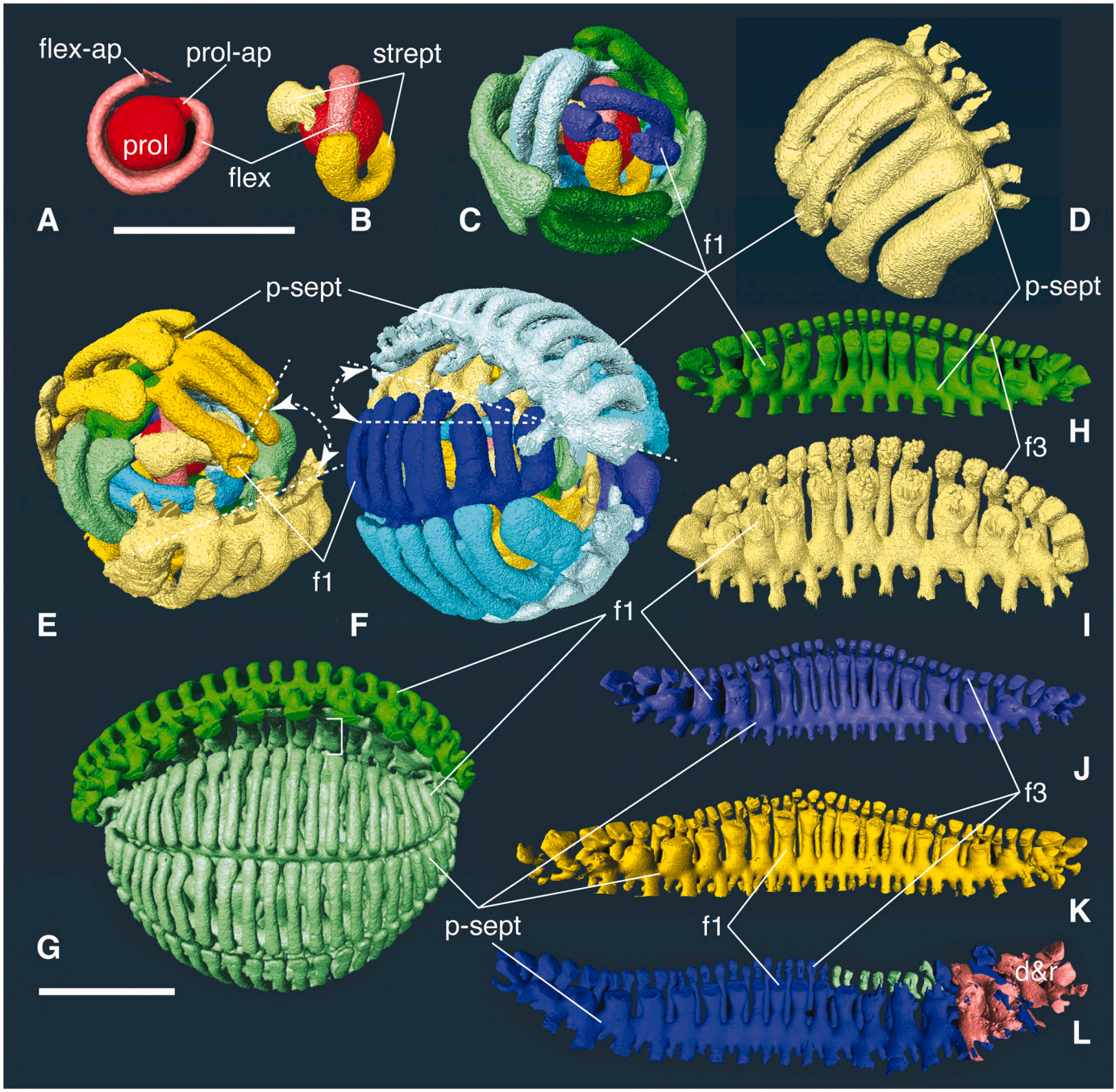

Fig. 4. *Flosculinella bontangensis* (Rutten, 1913); Langhian, Wailawi. Micro-computed tomographic scanning 3-D rendered models with shell removed (rendering by W.R.). A–B, the sub-spherical proloculus is enveloped by the flexostyle followed by two streptospiral whorls. Third whorl (C) with four chamberlets (f1) and fourth whorl (D–E) with six chamberlets (f1). The chamber axis is at *c*. 60° (dashed white line) to the previous chamber. Fifth whorl (F) with six chamberlets and up eleven supplementary chamberlets (f3). Chamber axis is at *c*. 30° (dashed white line) to the previous chamber. Six whorl (G) shows a thickening of the chamber shell whose coiling axis is unparallel to elongation axis. H, chamber 43 of the sixth whorl. I, last chamber of the sixth whorl. J, chamber 44 of the seventh whorl. K, chamber 52 of the eighth whorl. L, chamber 64 of the eight whorl. *Abbreviations*: d&r, damaged and repaired; f1, foramina in the basal layer of chamberlets; f3, supplementary foramina in the attics; flex, flexostyle; flex-ap, flexostyle aperture; p-sept, preseptal passage; prol, proloculus; prol-ap, proloculus aperture; strept, streptospire. Scale bars represent 0.10 mm in A–F and 0.20 mm in G–K.

Flosculinella bontangensis differs from *F. globulosa* and *F. reicheli* in being ellipsoidal to fusiform in shape and in having the attics appearing from the third whorl with two supplementary chamberlets in the attic layer per chamberlet in the basal layer (Table 1).

Hashimoto and Matsumaru (1975) described *Flosculinella fusiformis* from the Aquitanian–Burdigalian of the Philippines and separated it from *F. bontangensis* by its different growth rate. The single illustrated specimen is the holotype (Hashimoto and Matsumaru, 1975, pl. 14, fig. 8) showing a tangential section of a proloculus (34–36 μm in diameter in Hashimoto and Matsumaru, 1975) and about two supplementary chamberlets (f3) in the attic layer per chamberlet (f1) in the basal layer of chamberlets. The shell length (2.20 mm in length in Hashimoto and Matsumaru, 1975) and the number of supplementary chamberlets in the attic floor per chamberlet in the basal layer suggest that it cannot be separated from *F. bontangensis*.

Stratigraphical distribution: Chapman (1908) attributed his

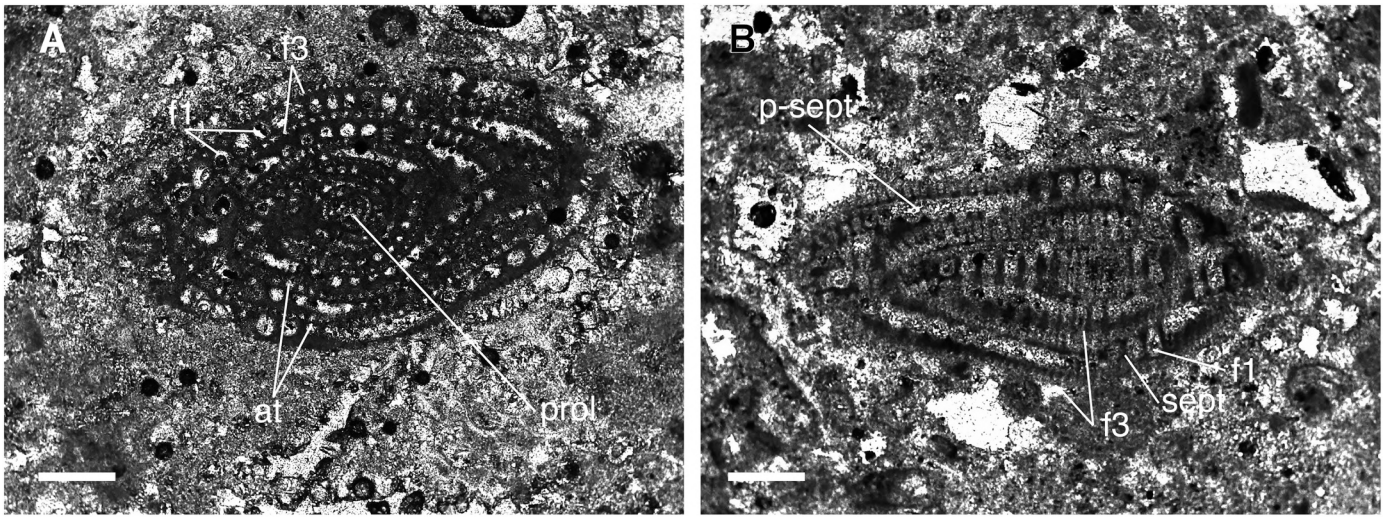

Fig. 5. *Flosculinella bontangensis* (Rutten, 1913); Serravallian, Maldives. A, sub-equatorial section (sample IODP 359, Site U1465, Hole B, Core 2, Section 1, at 17 cm). B, tangential sub-equatorial section (sample IODP 359, Site U1465, Hole A, Core 10, Section CC, at 1 cm). *Abbreviations*: at, attic; f1, foramina in the basal layer of chamberlets; f3, supplementary foramina in the attics; prol, proloculus; p-sept, preseptal passage; sept, septum. Scale bar represents 0.20 mm.

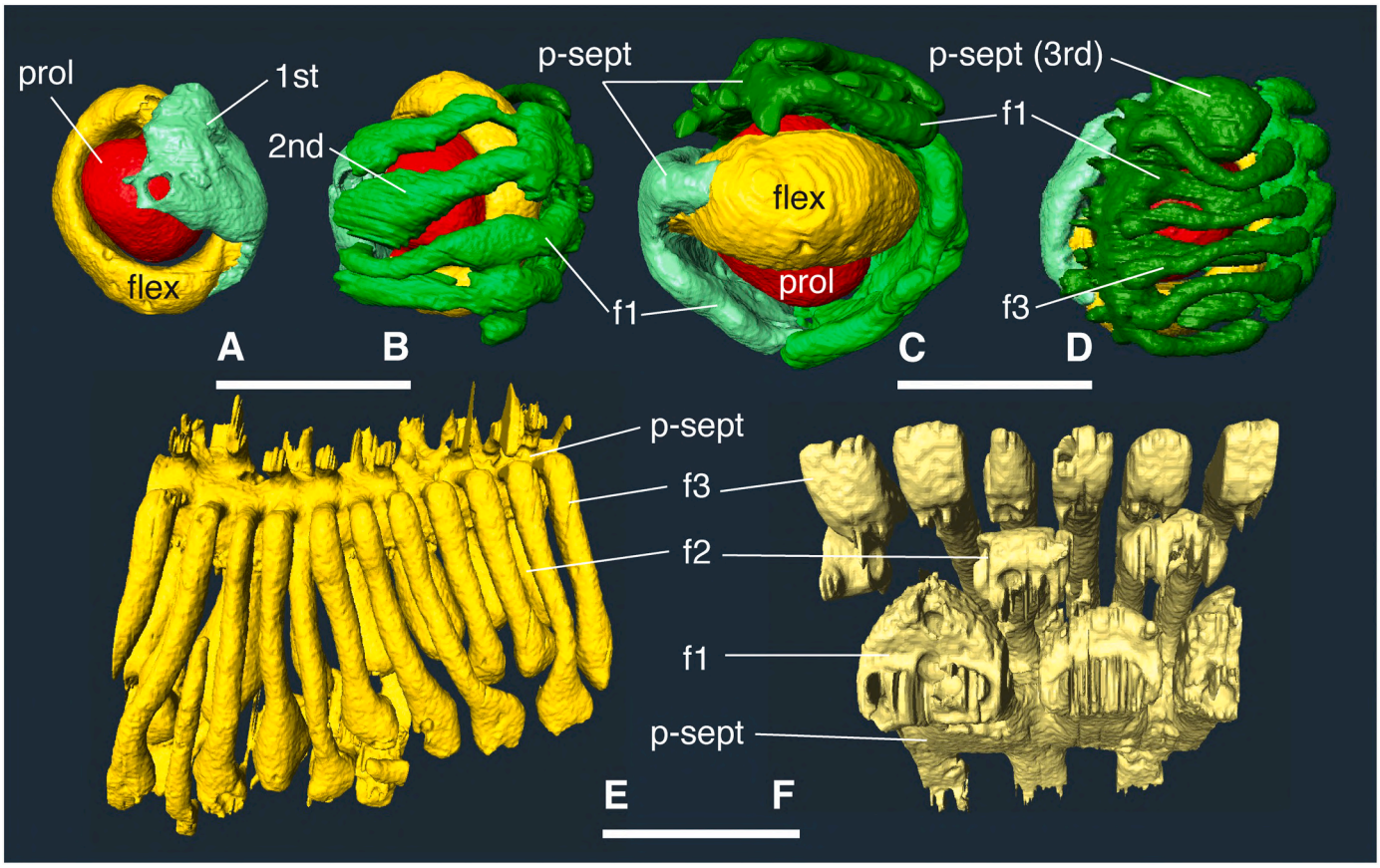

Fig. 6. *Alveolinella borneensis* Tan; Serravallian, Pacitan, East Java. Micro-computed tomographic scanning 3D-rendered models with shell removed (rendering by W. R.). A–D, the sub-ellipsoidal proloculus (prol) is followed by the flexostyle (flex). The first (1st) and second (2nd) chambers show the basal layer of chamberlets (f1). The supplementary chamberlets in the attics (f3) occur from the third (3rd) chamber (D). E–F, chambers in the penultimate (E) and last (F) whorls with two layers of chamberlets (f1, f2) and one layer of supplementary chamberlets (f3) in the attic. Scale bar represents 100 μm.

material from Malekula, New Hebrides, Vanuatu to the Miocene (1908, p. 758). *Flosculinella bontangensis* occurs in the early–middle Miocene of the Pemba Island (Kenya; Eames et al., 1962), Philippines (Matsumaru, 2011, 2017), Indonesia, Malaysia and Java (Hottinger, 1974; Barberi et al., 1987; Lunt and Allan, 2004; BouDagher-Fadel and Lokier, 2005; Renema, 2007; Renema et al., 2015; BouDagher-Fadel, 2018; Novak and Renema, 2018), southwestern Australia (Haig et al., 2020), and in the middle Miocene of the Maldives (Reolid et al., 2020; this study), Northern and Western Australia (Chaproniere, 1984; Riera et al., 2019), and Marion Plateau in northeastern Australia (Hallock et al., 2006;

Table 2, Fig. 7).

Genus *Alveolinella* H. Douvillé, 1907.

Type species: *Alveolina quoyi* d'Orbigny, 1826 (= *Alveolina quoii*, *nom. imperf.*).

Diagnosis: Prolate, fusiform shell with dimorphism. Early streptospiral whorl occurring in both generations. Septula aligned, Y-shaped septula in axial sections. Only preseptal passage present. Two or three layers with chamberlets (i.e., with foramina f1–f2) and one layer of attics (i.e., with foramina f3) per chamberlet in later whorls.

Remarks: The species dealt with here are known from exclusively fossil (*A. borneensis*) and from fossil and Recent (*A. quoyi*) specimens (Figs. 6–9). Y-shaped septula occur in the whorls of adult stages (Fig. 7C–D), marking even Y-shaped chamber sutures on the shell surface (Figs. 7–8). These septula are randomly distributed in the shell development. The index of elongation (I.E.), the number of floors and the whorl number of the attic first occurrence are reliable characters to separate species (Table 3).

Alveolinella borneensis and *A. quoyi* belong to the same evolutionary lineage and, therefore, represent successive chronospecies within the same lineage. The scattered stratigraphical data available prevent us from choosing a well-defined morphometric limit between these two chronospecies and instead we refer to a combination of characters. By definition (Drooger, 1993, p. 26), in every geological sample no more than a single chronospecies within a lineage is represented. Populations or specimens showing characters intermediate between the two chronospecies may be referred to either as *exemplum intercentrale* (*ex. interc.*) following the conventions set forth by Drooger (1993, p. 31) according to the biometrical approach, or as transitional specimens between *A. borneensis* and *A. quoyi* according to a typological approach.

Alveolinella borneensis Tan, 1936.

Fig. 6

(see Supplementary data for the synonymy list)

Neotype of *A. borneensis*: Tan (1936) introduced the new name *Alveolinella borneensis* for van der Vlerk's (1929, fig. 24) material, but no holotype nor lectotype have been designated. Although Hottinger (1974, p. 70) considered as the type the specimen illustrated by van der Vlerk (1929, fig. 24), he did not properly designate a neotype (ICZN, Art. 75.3.1). In accordance with Art. 75 of ICZN (1999), we designate herein the specimen illustrated in Fig. 6 as the neotype in order to clarify the taxonomic status of this species. The neotype is stored in the micropalaeontological collections of the Naturalis Biodiversity Center of Leiden (The Netherlands).

Diagnosis: Fusiform (prolate) shell (I.E. 3.4–4.2; Table 3) with early two whorls with one basal layer of chamberlets (f1) and one layer of supplementary chamberlets (f3) in the attic, later whorls with two layers of main chamberlets (f1, f2) and one layer of supplementary chamberlets (f3) in the attic per chamberlet. Slight polar torsion. The proloculus is globular (60–80 μm in diameter) with a flexostyle enveloping for 265°–280° and ending in a single aperture.

Studied material: The studied specimens are from the Serravallian–Langhian boundary of the Stadion stratigraphic section near Samarinda (East Kalimantan, Indonesia), from the Serravallian of Pacitan (Java) and the Tortonian of the Kutai basin (East Kalimantan, Indonesia). Fusiform (prolate) shell with globular proloculus (*c.* 70 μm in diameter) with the main axis not parallel to the coiling axis. Flexostyle, enveloping the proloculus by *c.* 270°, shows a single aperture. The first and second chambers with multiples apertures (f1) are followed by the third chamber characterised by one layer of supplementary chamberlets (f3) in the attics (Fig. 6A–D). Later whorls with two layers of chamberlets (f1, f2) and one layer of supplementary chamberlets (f3) in the attic per chamberlet (Fig. 6E–F). The supplementary chamberlets (f3) in the attics are larger than in *A. quoyi*.

Remarks: Verbeek and Fennema (1896) described and illustrated two alveolinoids from the Miocene of south Sindagsari (p. 1141, pl. 2, fig. 42) and Bautarguebang (p. 1142, pl. 2, fig. 43) in Java with no taxonomic ascription. Because their drawings do not show the earlier whorls with layers of chamberlets and related foramina, these specimens cannot be ascribed with any certainty to *Alveolinella*. In a footnote Checchia-Rispoli (1909, pp. 67–68) introduced two new names for Verbeek and Fennema's (1896) alveolinoid specimens: *Alveolina Verbeeki* and *Alveolina Fennemai*. These taxa, although insufficiently figured by Verbeek and Fennema (1896), were validly established, being species names by indication (ICZN, 1999, Art. 12.2).

Van der Vlerk (1922) recorded *Alveolinella boscii* Defrance (pp. 68–69) and *Alveolinella fennemai* (Checchia-Rispoli) (p. 69) from the Miocene of Sumbawa (Indonesia). The two figured specimens ascribed to *A. boscii* (pl. 2, fig. 10) are tangential sub-axial sections showing two layers of main chamberlets (f1, f2) and one layer of supplementary chamberlets (f3) in the attics. No features of the early whorls can be observed. However, van der Vlerk (1922, p. 70) states that the early whorls of *A. boscii* are comparable to those of *F. bontangensis*. Therefore, van der Vlerk's (1922) specimens can be ascribed to *Alveolinella* based upon the characteristics of the early whorls (Table 3). The specimen named as *A. fennemai* and illustrated in pl. 2, fig. 11 is a tangential sub-axial section which does not show clear diagnostic characters, hampering its generic ascription.

Tan (1936, p. 178, no illustration) introduced the new species *Alveolinella borneensis* for the Miocene specimen of van der Vlerk (1929, fig. 24 as *Alveolinella boscii*) recognising that 'it corresponds to the *bontangensis* type due to the chamber structure' (p. 178, transl. from German). Van der Vlerk's (1929, fig. 24) specimen, *c.* 1.6 mm long, shows one floor of chamberlets (f1) and supplementary chamberlets (f3) in the attic. Therefore, it cannot be ascribed to *Alveolinella* and, based upon the occurrence of first attic in the second whorl with two supplementary chamberlets (f3) in the attic layer per chamberlet in the basal layer of chamberlets (f1; Table 1), it belongs to *F. bontangensis*.

Hottinger (1974), pl. 105, figs. 1–2, pl. 106, fig. 5) named *A. borneensis* Miocene specimens from the Moluccas and Mangkalihat (Indonesia) with early whorls with one basal layer of chamberlets (f1) and one layer of supplementary chamberlets (f3) in the attic. The later whorls are characterised by two layers of main chamberlets (f1, f2) and one layer of supplementary chamberlets (f3) in the attic per chamberlet. The occurrence of chamberlets in more than two layers (f1, f2) in the neotype of *Alveolinella borneensis* (Fig. 5; compare with van der Vlerk, 1922, pl. 2, fig. 10) supports that it belongs to *Alveolinella*. Its status as a distinct species is confirmed by the occurrence of one layer of main chamberlets in the first two whorls along with the characters of the proloculus and the flexostyle (Table 3).

Based on material from the early to middle Miocene (Tf1–Tf2) of the Central Highlands, Papua New Guinea, Wonders and Adams (1991) introduced *Alveolinella praequoyi*. Wonders and Adams (1991), p. 173) did not rule out the possible synonymy of *A. praequoyi* and *A. fennemai*, the latter being a possible senior synonym. However, they mentioned neither *A. verbeeki* (Checchia-Rispoli) nor *A. borneensis* Tan. Wonders and Adams (1991) separated *A. praequoyi* from *A. quoyi* based on a distinct juvenile stage with only a single layer of chamberlets and attic, followed by an adult stage with two layers of chamberlets and one attic (p. 173, holotype figured in fig. 5a–b; see also BouDagher-Fadel, 2018, pl. 7.4, fig. 20). As described and illustrated by Hottinger (1974), these characters are in fact typical of *A. borneensis* which, therefore, is likely to be a senior synonym of *A. praequoyi*. However, detailed analysis of the early whorls are necessary to clarify its status as distinct species. These middle Miocene forms can be, therefore, referred as to *Alveolinella ex. interc. borneensis* Tan *et quoyi* (d'Orbigny) (Table 4).

Stratigraphical distribution: *Alveolinella borneensis* has been recorded from the late Burdigalian–early Tortonian of Indonesia, Papua New Guinea and northern Australia (Hottinger, 1974, 2006a; Wonders and Adams, 1991; Lunt and Allan, 2004; see Supplementary data, Table 4, Fig. 10).

The Langhian–Tortonian records of *A. quoyi* in Bikini (Todd and Post, 1954), Eniwetok (Cole, 1957) and *A. praequoyi* in Papua New Guinea (Wonders and Adams, 1991) show characters attributable to

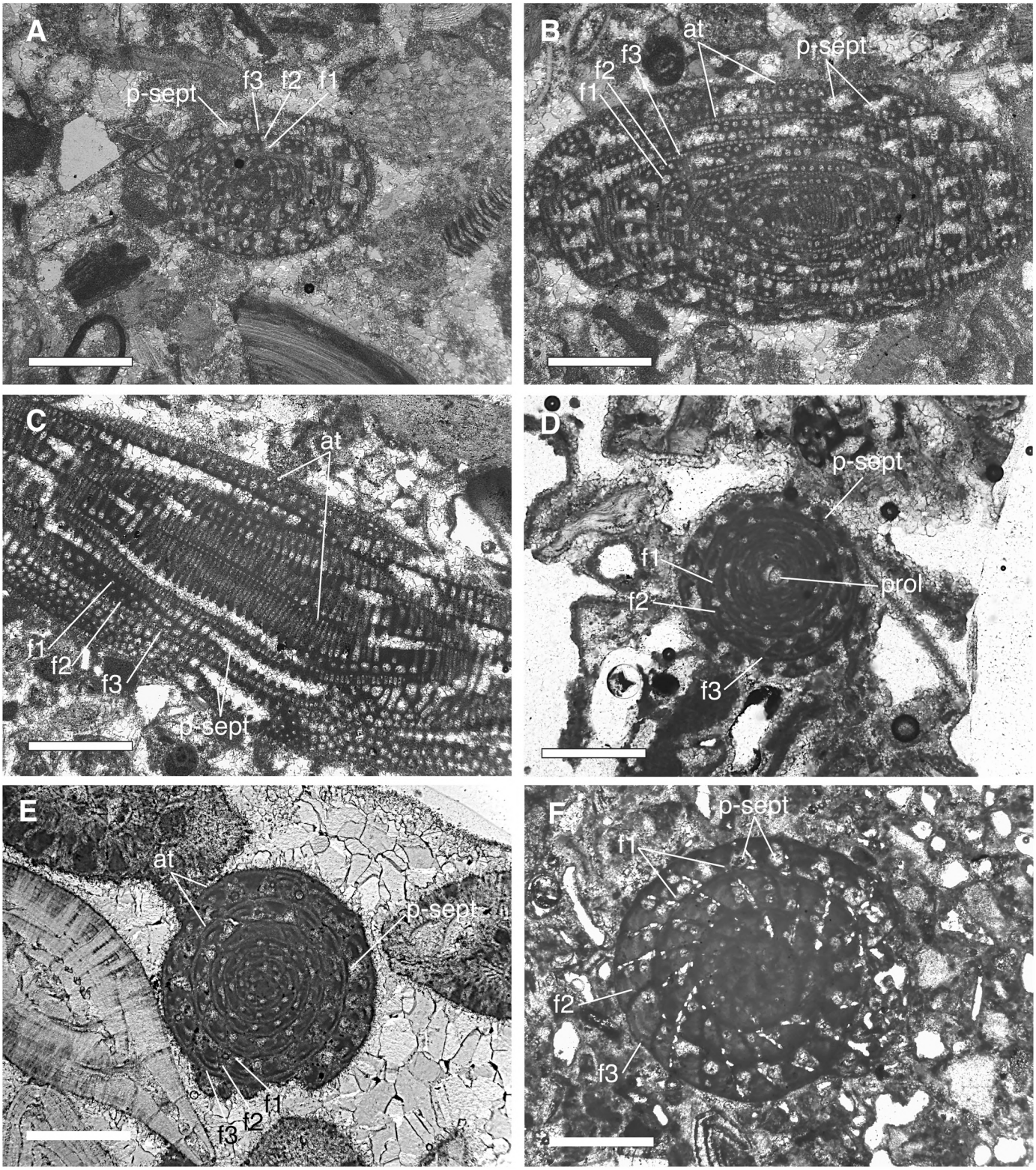

Fig. 7. *Alveolinella quoyi* (d'Orbigny, 1826); Calabrian–Chibanian Ryukyu Group, Okinawa-jima. A–B, Nakijin; C–E, Tobaru; Motobu peninsula; Kourijima Formation (Yamamoto et al., 2006). F, Maeda, Yomitan–Onna; Sobe Formation (Muraoka et al., 2005). A–B, tangential and oblique sub-equatorial sections (samples N1_3_5, N1_2_5). C, tangential sub-axial section (sample 167 Tobaru Core_12B-4–13.0 m). D-F, sub-equatorial section (samples 16 Tobaru Core 13B-7–5.98 m, M62_5, 362). *Abbreviations*: at, attic; cl, chamberlet; f1, foramina in the basal layer of chamberlets; f2, foramina in the second layer of chamberlets; f3, supplementary foramina in the attic; prol, proloculus; p-sept, preseptal passage; sept, septula; Y-sept, Y-shaped septula. Scale bar represents 0.50 mm.

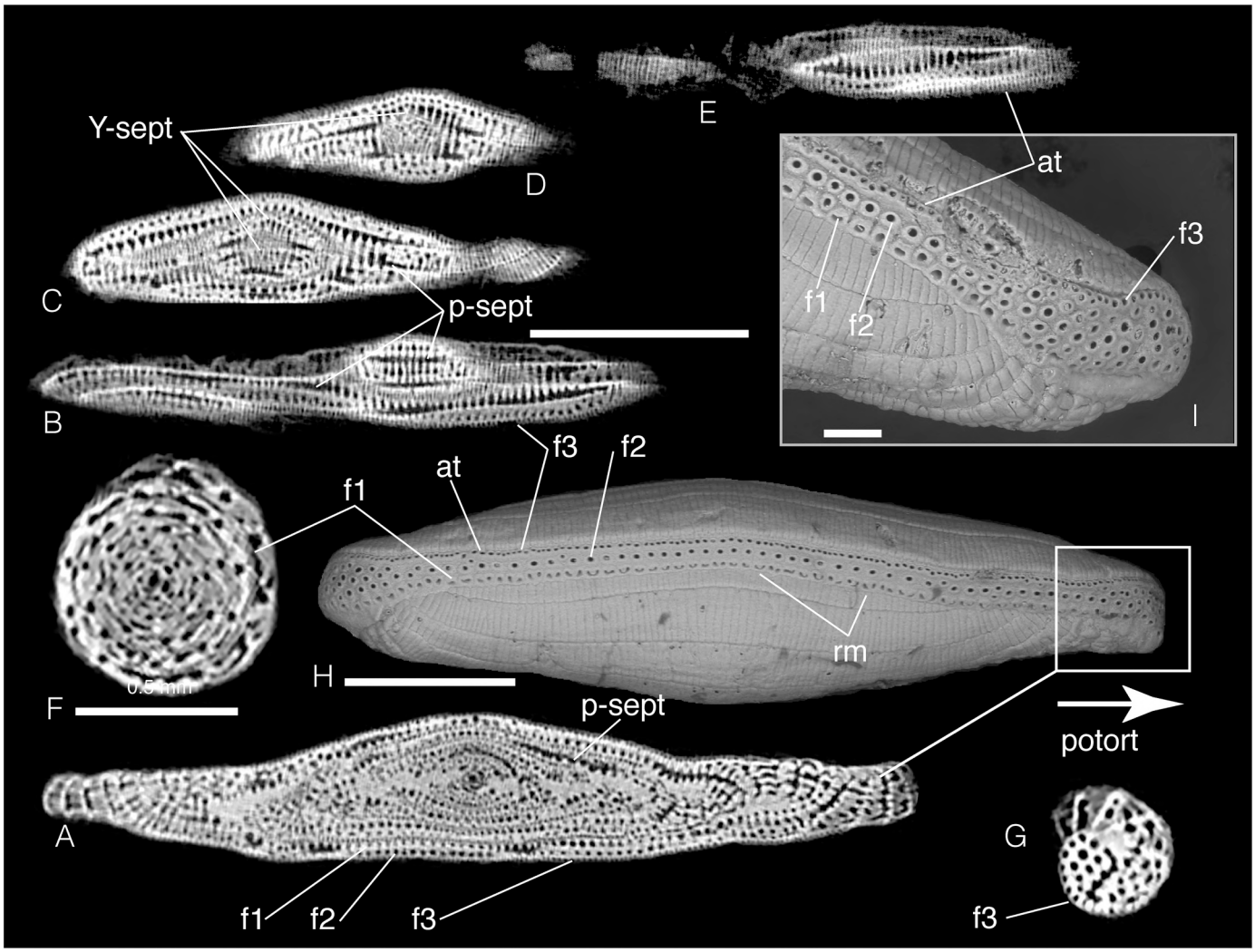

Fig. 8. *Alveolinella quoyi* (d'Orbigny, 1826); Recent material from coral rubble on a fore-reef slope (15 m water depth) at Kushibaru, Aka-jima, Okinawa-jima, Japan. Micro-computed tomographic analysis (A–G) and SEM details of the apertural face (H–I) of a specimen illustrating the foramina in the basal and second layers of chamberlets (f1, f2) and the attics (f3). *Abbreviations*: at, attic; cl, chamberlet; f1, foramina in the basal layer of chamberlets; f2, foramina in the second layer of chamberlets; f3, supplementary foramina in the attic; potort, polar torsion; prol, proloculus; p-sept, preseptal passage; rm., reverse masks; sept, septula; Y-sept, Y-shaped septula. Scale bars represent 1 mm (A–E), 0.5 mm (F-H) and 0.1 mm (I).

A. borneensis rather than to *A. quoyi sensu stricto* (see Tables 3–4).

Alveolinella quoyi (d'Orbigny, 1826).

Figs. 7–9.

(see Supplementary data for the synonymy list)

Type reference and figures: *Alveolinella quoyi* (d'Orbigny) Hofker, 1930, 166–170; d'Orbigny, 1826, pl. 17, figs. 11–13 (fig. 11, lectotype).

Diagnosis: Fusiform (prolate) shell (I.E. higher than 5; Table 3), the first whorl with one basal layer of main chamberlets (f1) and one layer of attic per chamberlet (f3). In the later whorls up to three layers of main chamberlets (f1, f2, f2) with one layer of attic (f3) per chamberlet. Polar torsion twisted/convoluted. Proloculus is sub-ellipsoidal (up to *c*. 80 μm in diameter and 160 μm in length) with the longest axis of the proloculus in the direction of the coiling axis and constrained at the position of the flexostyle (Fig. 9). The flexostyle envelopes the proloculus for 330° in the Recent specimens, 300°–320° in the upper Miocene specimens, and ends in multiple apertures.

Lectotype: In the original material illustrated as drawings d'Orbigny (1826) did not designate a type. In accordance with Art. 74 of ICZN (1999), we designate hereby as lectotype the specimen originally illustrated by d'Orbigny (1826, pl. 17, fig. 11).

Studied material: Late Tortonian of Sangatta (Kalimantan; Renema et al., 2015), Messinian of Bengalon (Kalimantan), Pliocene of Malaysia and Waigeo (West Papua New Guinea) and Pleistocene of Cebu (Philippines). These isolated specimens show proloculus shapes, flexostyle and initial chambers very similar in shape to those of Recent studied specimens. Most specimens are characterised by the occurrence of two or three layers with chamberlets (f1, f2, f2) and one layer of attics (f3) per chamberlet in later whorls.

Calabrian–Chibanian Kourijima (Pleistocene) Formation, Motobu Peninsula, Okinawa-jima, Ryukyu Islands (samples M62, 167 Tobaru Core 12B-4–13.0 m, 16 Tobaru Core13B-7–5.98 m, N1_2_5, N13_5) and Calabrian–Chibanian Sobe Formation, Yomitan to Onna area of Okinawa-jima (sample 362). The fossil specimens occur as random sections in thin sections from a hard-cemented limestone. Specimens, *c*. 1.0 mm in diameter and *c*. 4.0 mm in length, show two to three layers of chamberlets (f1, f2, f2) and one layer of attic with supplementary chamberlets (f3; Fig. 6). The studied Recent specimens are from coral rubble on a fore-reef slope (15 m water depth) at Kushibaru, Aka-jima, Okinawa-jima, Japan (Fig. 8), and from Vanuatu (Fig. 9). Prolate specimens with a diameter up to 1.0 mm and *c*. 3.8 mm long. Sub-ellipsoidal proloculus, up to *c*. 160 μm in diameter, with the flexostyle enveloping by *c*. 330° and multiple apertures (Fig. 9). Y-shaped septula present

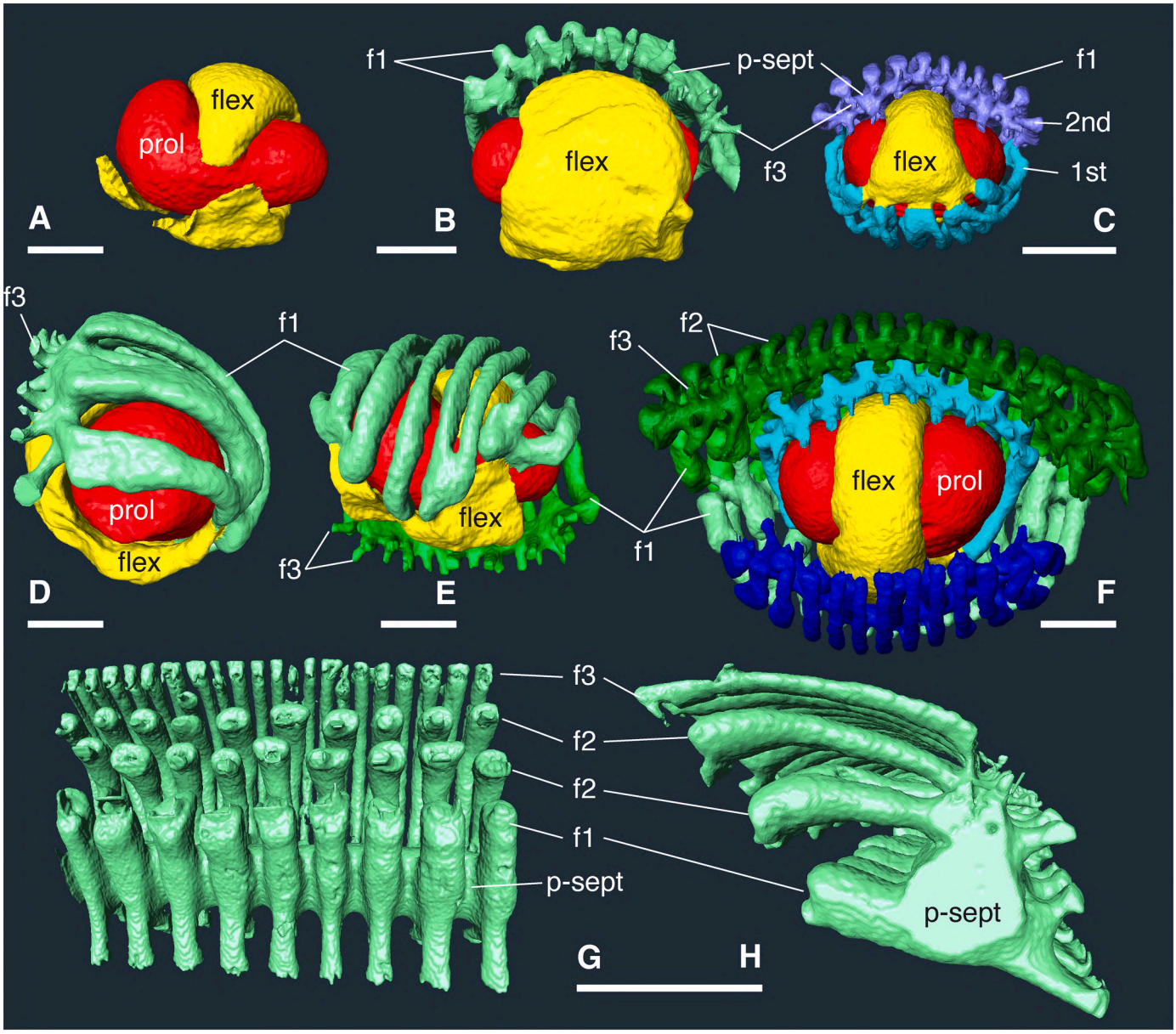

Fig. 9. *Alveolinella quoyi* (d'Orbigny, 1826); Recent material from Vanuatu. Micro-computed tomographic scanning 3D-rendered models with shell removed (rendering by W.R.). A–E, sub-ellipsoidal proloculus (prol) enveloped by the flexostyle (flex) and the first (1st) and second (2nd) chambers. The flexostyle shows multiple apertures. F, growth stage with four chambers showing the complicated superposition of layers of chamberlets and related attics. G–H, detail of the chamber in last whorl with three layers of chamberlets (f1, f2, f2) and one layer of attics (f3) per chamberlet. f1, foramina in the basal layer of chamberlets; f2, foramina in the second layer of chamberlets; f3, supplementary foramina in the attic; p-sept, preseptal passage. Scale bar represents 0.1 mm.

Table 3
Comparison of diagnostic shell characteristics of *Alveolinella* species and related stratigraphical distribution. Species are listed according to their first appearance reported in literature.

	Age	prol (μm)	prol sh, flexost	Diameter (mm)	Length (mm)	I.E.	f (wh)
A. borneensis [1]	late Burdigalian–early Tortonian	60–80	globular, flexost enveloping for <300°	1.03	2.4–3.40	3.4–4.2	f1 (1–2); f2, f3 (>3)
A. quoyi [2]	late Tortonian–Recent	50–78	sub-ellipsoidal (160), flexost enveloping for 330° in the Rs, 300°–320° in the uMs	0.74–1.36	3.41–4.50, pt	3.31–5.40	f1 (1); f1, f2, f2, f3 (>2)

Based on data from:
1, Tan (1936); Mohler (1949); Binnekamp (1973); Hottinger (1974); Wonders and Adams (1991, as *A. praequoyi*).
2, Hofker (1930); Cole (1957); Hottinger (1974); Zheng (1979); Matsumaru (2017); this study.
I.E., index of elongation; f (wh), number of layers of chamberlets (whorl number of the attic first occurrence); f1, foramina in the basal layer of chamberlets; f2, foramina in the second layer of chamberlets; f3, supplementary foramina in the attic; flexost, flexostyle; prol, proloculus diameter; prol sh, proloculus shape (length, μm); pt., polar torsion; Rs, Recent specimens; uMs, upper Miocene specimens.

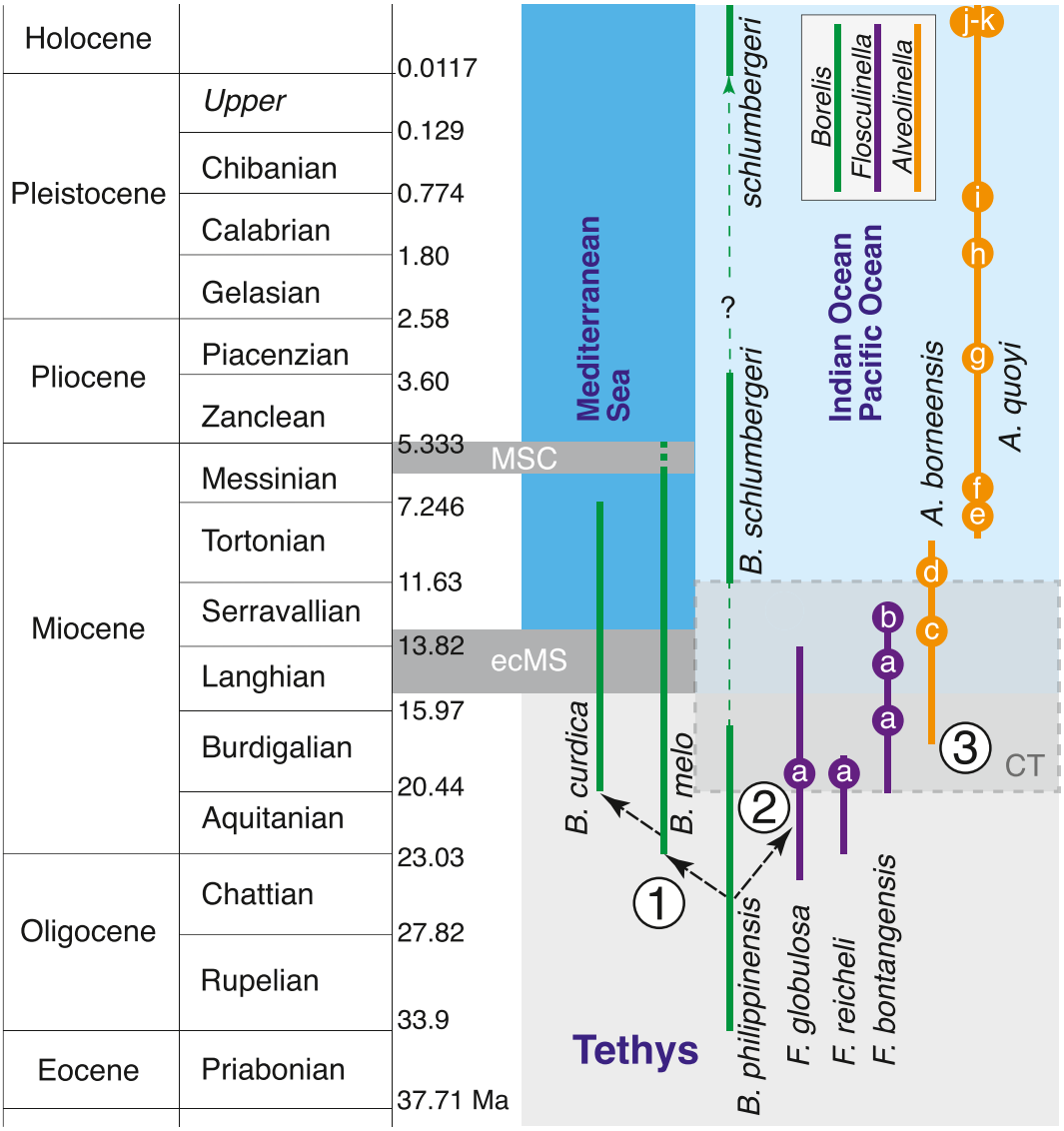

Fig. 10. Major events in the palaeobiogeographical history of the latest Oligocene–Miocene *Borelis* (*B.*), *Flosculinella* (*F.*) and *Alveolinella* (*A.*) species. The two present-day *B. schlumbergeri* and *A. quoyi*, both having only preseptal passages and bearing Y-shaped septula, are descendants of the Oligocene–early Miocene *B. philippinensis*. The Mediterranean *B. melo* and *B. curdica* also descended from *B. philippinensis* (1) and disappeared by the Messinian Salinity Crisis (MSC; Bassi et al., 2021a). *Flosculinella* appeared in the latest Oligocene giving rise to three early–middle Miocene species (*F. globulosa*, *F. reicheli*, *F. bontangensis*; 2). *Alveolinella* presumably appeared in the latest Burdigalian as *A. borneensis*, and *A. quoyi* in the late Tortonian (3). From the Central Indo-Pacific *F. bontangensis* and *A. borneensis* migrated southward reaching Western and Northern Australia and Bikini and Eniwetok in the Langhian. See text for details. This study: a, East Kalimantan, Indonesia; b, Maldives; c, Samarinda (East Kalimantan), Pacitan (Java); d–e, Sangatta (East Kalimantan); f, Bengalon (Kalimantan), g, Togopi (Malaysia), h, Cebu (Philippines); i, k, Okinawa-jima, Ryukyu Islands; j, Vanuatu. CT, Miocene Coral Triangle; ecMS, eastern closure of the Mediterranean Sea. Time scale after Cohen et al. (2021, updated). (For interpretation of the references to colour in this figure legend, the reader is referred to the web version of this article).

(Fig. 8). Later whorls with three layers of chamberlets (f1, f2, f2) and one layer of attics (f3) per chamberlet (Figs. 8A, 9G–H). Sinusoidal reverse masks in the apertural face (Fig. 8H).

Remarks: The analysed material is morphometrically and architecturally concordant with *Alveolinella quoyi* (Reichel, 1937; Hottinger, 1974; Table 5).

Alveolinella quoyi differs from *A. borneensis* in being longer (I.E. up to 5.4) and in having two layers of chamberlets (two layers with superposed foramina f1, f2) and one layer of attic (f3) per chamber from the first whorl (Table 3).

Stratigraphical distribution: This species has been identified exclusively in the CIP area, from the Tortonian to the Recent (Todd and Post, 1954; Hottinger, 1974, 1980; Hohenegger, 1994; Langer and Hottinger, 2000; Yordanova and Hohenegger, 2002; Renema et al., 2015; Table 5, Fig. 10). *A. quoyi* is reported from the late Langhian–Tortonian of Java with no illustrations (BouDagher-Fadel and Lokier, 2005, fig. 3).

4. Implications of Y-shaped septula for phylogeny

The early streptospiral whorls, the only preseptal passage and septula which are continuous in adjacent chambers (i.e., aligned) are diagnostic characters shared by *Borelis, Flosculinella* and *Alveolinella* (Reichel, 1937, 1964; Hottinger, 1974; Loeblich and Tappan, 1987). *Flosculinella* and *Alveolinella* differ from *Borelis* in having two or more layers of main chamberlets and one layer of attic per chamber in the adult growth stage (Hottinger, 1974; Loeblich and Tappan, 1987; Parker, 2009; Tables 1, 3).

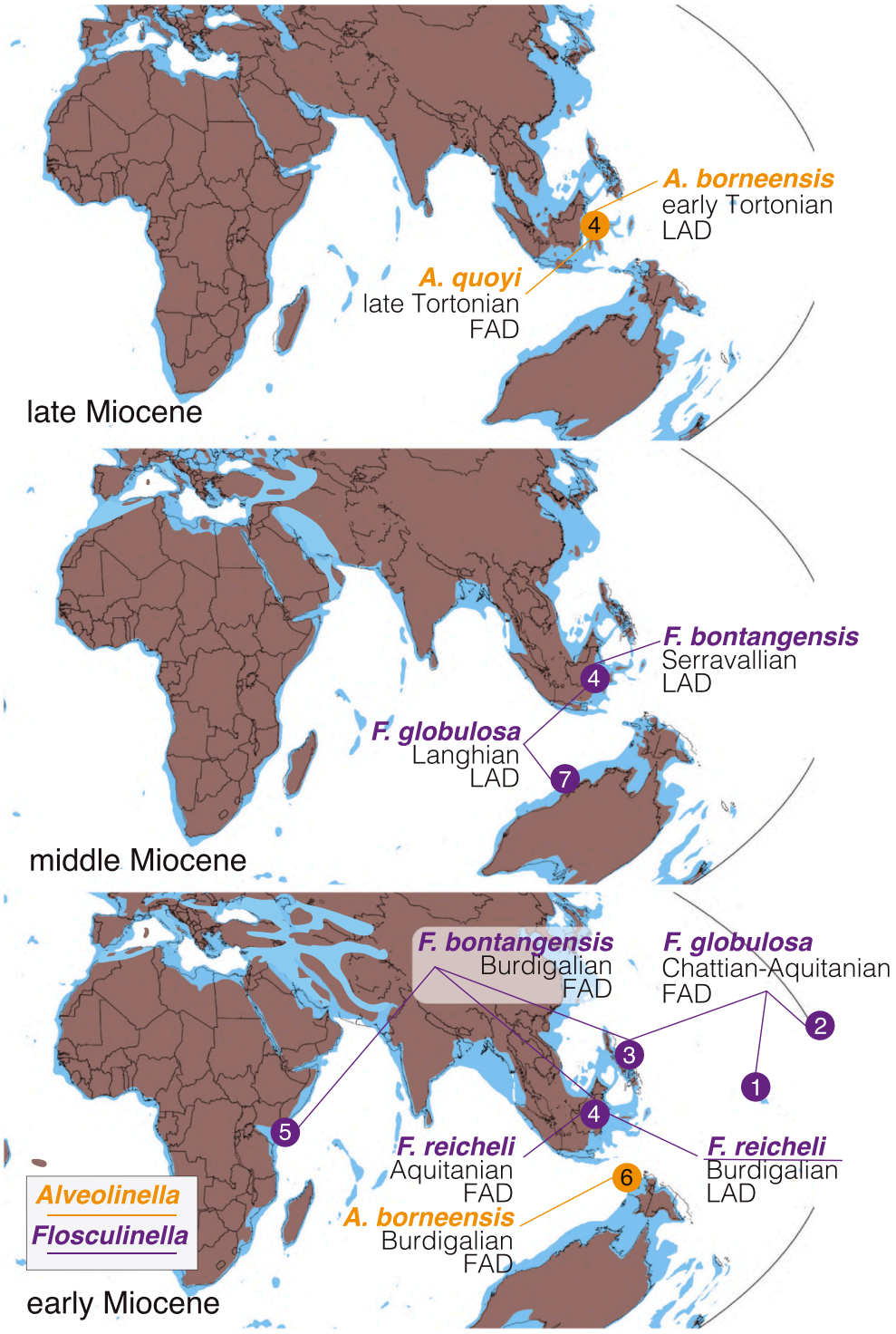

Fig. 11. Palaeogeographical locations of *Flosculinella* (*F.*) species and *Alveolinella* (*A.*) species in the Central Indo-Pacific. *Flosculinella* and *Alveolinella* speciation was in the Coral Triangle of Southeast Asia. *F. globulosa* appeared in the Chattian–Aquitanian of Bikini (1), Midway Atoll (2) and Philippines (3), whereas *F. reicheli* in the Aquitanian of Indonesia (4), and *F. bontangensis* in the Burdigalian of Philippines (3), Indonesia (4) and Pemba Island (5). The first and last appearances of *A. borneensis* are in the Burdigalian (6, Hottinger, 1974) and Serravallian (3, Mohler, 1949; 6, Hottinger, 2006a), whereas *A. ex. interc. borneensis et quoyi* first occurs in the Langhian of Bikini (1, Todd and Post, 1954). The short-lasting *F. reicheli* disappeared in the Burdigalian (4, this study), whilst *F. globulosa* (4, this study; 7, Riera et al., 2019) and *F. bontangensis* (4, this study) in the Langhian and Serravallian respectively. The present-day *A. quoyi* appeared in the Tortonian of Indonesia (Renema et al., 2015; see text). Occurrences refer to citations in Tables 2, 4-5 in which detailed information on each record can be found. Compare with Fig. 10. Palaeogeographical maps modified from Rögl (1998), Meulenkamp and Sissingh (2003) and Kocsis and Scotese (2021). Numbers refer to localities: 1, Cole (1954; Aq, Fg, Bikini), Todd and Post (1954; Ab, Bikini); 2, Cole (1969; Fg, Midway Atoll); 3, Matsumaru (2017; Fb, Fg, Philippines); 4, Mohler (1949; Ab, Fr, Borneo), Adams (1965; Fr, Sarawak), Hottinger (1974; Fr, Borneo), Renema et al. (2015; Aq, Indonesia); Leupold and van der Vlerk (1931; Fb, Borneo), Barberi et al. (1987; Fb, Indonesia), this study (Fb, Pacitan; Ab, Samarinda, East Kalimantan); 5, Eames et al. (1962; Fb, Pemba Island); 6, Hottinger (1974, 2006a, Ab, Moluccas); 7, Riera et al. (2019; Fg, W Australia). Ab, *A. borneensis*; Aq, *A. quoyi*; FAD, first appearance datum; Fb, *F. bontangensis*; Fg, *F. globulosa*; Fr, *F. reicheli*; LAD; last appearance datum. (For interpretation of the references to colour in this figure legend, the reader is referred to the web version of this article).

In *Borelis* the occurrence of Y-shaped septula is a diagnostic character (Bassi et al., 2021a) for the species lineage of *Borelis philippinensis* (*B. melo*, *B. curdica*, *B. schlumbergeri*). After the first occurrence of this shell feature in the Rupelian (early Oligocene) *Borelis* in the CIP area (e.g., Lunt and Allan, 2004; Matsumaru, 2011), westward migrants occur in the Mediterranean Miocene (*B. melo*, *B. curdica*; Bassi et al., 2021a; Fig. 10). In the Eastern Indo-Pacific area, the present-day *B. schlumbergeri* appeared in the late Miocene (Eniwetok and Bikini; Hanzawa, 1940; Cole, 1954, 1957; Adams, 1970; Matsumaru, 1974; Lunt and Allan, 2004), probably descendant from the Rupelian–Burdigalian *B. philippinensis* (Bassi et al., 2021a).

Borelis schlumbergeri, *Flosculinella* (*F. globulosa*, *F. reicheli*, *F. bontangensis*) and *Alveolinella* (*A. borneensis*, *A. quoyi*) are the only alveolinoids with Y-shaped septula in the Indo-Pacific area, and, therefore, they all are probably descendants from the common ancestor *B. philippinensis*.

The temporal ranges of *Flosculinella* species and *Alveolinella* species partially overlap and succeed each other in the Indo-Pacific. These temporal range setting supports the inference that Y-shaped septula are not a homoplastic character that independently appeared in separate

Table 4
Stratigraphical and geographical distribution of *Alveolinella borneensis* Tan.

References	Referred to as	Age	Locality	Illustrations
van der Vlerk (1922)	*A. boscii*	middle Miocene	Pulau, Indonesia	pl. 2, fig. 10
BouDagher-Fadel (2018)	*A. fennemai*[b]	Burdigalian	Borneo	pl. 7.2, fig. 8
BouDagher-Fadel and Price (2021)	*A. praequoyi*[b]	early middle Miocene	Borneo	pl. 7, fig. c
	A. fennemai[b]	Burdigalian		pl. 7, fig. d
Hottinger (1974)	*A. borneensis*	early Miocene	Moluccas, Mangkalihat	pl. 105, figs. 1–2, 4; pl. 106, fig. 5
Todd and Post (1954)	*A. quoii*[a]	Langhian–Serravallian	Bikini	pl. 202, figs. 5, 8
Wonders and Adams (1991)	*A. praequoyi*[a]	late Langhian–Serravallian	Papua New Guinea	figs. 4-7 (holotype)
	A. quoyi[a]			fig. 12
Lunt and Allan (2004)	*A. praequoyi*[a]	? middle Miocene–Recent	Papua New Guinea	p. 43
Hottinger (2006a)	*A. borneensis*	Miocene	Moluccas	fig. 14
BouDagher-Fadel (2018)	*A. praequoyi*[a]	Langhian–Serravallian	Papua New Guinea	pl. 7.1, fig. 20 (holotype); pl. 7.2, figs. 6–7
BouDagher-Fadel and Lokier (2005)	*A. praequoyi*[a]	Serravallian	Java	no
Mohler (1949)	*A. borneensis*	Serravallian–Messinian	Borneo	fig. 1
This study	*A. borneensis*	Serravallian	Pacitan	Fig. 6
		early Tortonian	Samarinda	
Cole (1957)	*A. quoyi*[a]	Tortonian	Eniwetok	pl. 240, figs. 23–25
Renema et al. (2015)	*A.* sp.[b]	Tortonian–Messinian	E Kalimantan	fig. 5A

[a] *Alveolinella ex. interc. borneensis* Tan *et quoyi* (d'Orbigny).
[b] See Remarks in the text for further details.

lineages but a synapomorphy of the *Borelis philippinensis* + *Flosculinella* + *Alveolinella* clade, which originated with the ancestral species (Fig. 10).

The appearance of two floors with chamberlets and one with attics is a synapomorphy of the *Flosculinella*+*Alveolinella* clade, whereas the occurrence of more than one chamberlet per chamber is an autapomorphy of *Alveolinella*.

Flosculinella appeared in the latest Oligocene of the CIP with *F. globulosa* (Lunt and Allan, 2004; Hallock et al., 2006; Renema et al., 2015; Table 3, Figs. 10–11). The single record of *F. bontangensis* in eastern Africa (Pemba Island) is Burdigalian in age (Eames et al., 1962). Often found together with *B. philippinensis* (Adams, 1965; Lunt and Allan, 2004; Renema, 2007; Matsumaru, 2011), *Flosculinella reicheli*, *F. bontangensis* and *Alveolinella borneensis* appeared in the CIP in the early Miocene (Tables 2, 4). This area corresponds to the Coral Triangle, the most important centre of marine biodiversity whose diversification started in the early Miocene (Renema et al., 2008; Veron et al., 2009; Förderer et al., 2018; Reuter et al., 2019; Fig. 11). As other larger porcelaneous forms such as *Borelis* and *Austrotrillina*, *Flosculinella* and *Alveolinella* thrived in shallow-water carbonate settings above the fair-weather wave base (Buxton and Pedley, 1989; Hottinger, 1997; Beavington-Penney and Racey, 2004; Haig et al., 2020; Simmons, 2020). From the late Oligocene the seagrass settings expanded (Brasier, 1975; Teske and Beheregaray, 2009) including vast areas of shallow-water habitats between Indonesia and Australia (Wilson and Rosen, 1998). Via these settings, *Flosculinella bontangensis* likely reached the Langhian seagrass habitats off northeastern Australia (Hallock et al., 2006), whilst *A. borneensis* and *Alveolinella ex. interc. borneensis et quoyi* the middle Miocene of Indonesia, Bikini and Eniwetok (Table 4). A similar eastward dispersion route has been found for the shallow-water larger porcelaneous foraminifer *Austrotrillina* (Bassi et al., 2021b) and the brown macroalga *Sargassum* (Yip and Quek, 2020).

Alveolinella quoyi has been identified from the Tortonian of Indonesia (Renema et al., 2015) to the Pliocene–Pleistocene of Palau (Hanzawa,

Table 5
Stratigraphical and geographical distribution of *Alveolinella quoyi* (d'Orbigny).

References	Referred to as	Age	Locality	Illustrations
Matsumaru (2011)	*A. quoyii*	Burdigalian–Pliocene–Holocene	Philippines	no
Wonders and Adams (1991)	*A. quoyi*	early Tf3	Papua New Guinea	fig. 12
Cole (1957)	*A. quoii*	post-Miocene	Eniwetok	pl. 240, figs. 16, 19
Renema (2007)	*A. quoyii*	Tortonian–Recent	SE Asia	no
Renema et al. (2015)	*A. quoyi*	Tortonian–Messinian	E Kalimantan	fig. 5B
Wonders and Adams (1991)	*A. quoyi*	middle Pliocene	Borneo	figs. 8–11
		Recent	New Caledonia, Maldives	
Whittaker and Hodgkinson (1979)	*A. quoyi*	Pliocene	Malaysia	pl. 8, fig. 11
Hanzawa (1957)	*A. quoii*	Pliocene–Pleistocene	Palau	pl. 23, fig. 2a–b
Matsumaru (1977)	*A. quoyii*	Pleistocene	Nansei Shoto Island	pl. 5, figs. 1–10, 15
Matsumaru (2017)	*A. quoyii*	Pliocene	Philippines	pl. 41, fig. 10; pl. 43, figs. 11–15
BouDagher-Fadel (2018)	*A. quoyi*	Recent	Papua New Guinea	fig. 7.2
		Holocene		pl. 7.2, figs. 2–4
Hofker (1930)	*A. Quoyi*	Recent	Kei Islands, Rotti Island, Indonesia	pl. 41, figs. 6–8; pl. 61, figs. 8–10, 12–13; pl. 64, figs. 1–4, 6
Cushman (1933)	*A. quoyi*	Recent	Pacific	pl. 19, fig. l0
Hofker (1952)	*A. Quoyi*	Recent	Pacific	figs. 61–62
Adams (1973)	*A. quoyi*	Recent	Pacific	pl. 2, fig. 6.
Hottinger (1974)	*A. quoyi*	Recent	Torres Strait, Australia	pl. 106, figs. 1–4
Zheng (1979)	*A. quoyi*	Recent	Xisha Islands	text-fig. 12, pl. 9, fig. 11, pl. 27, figs. 1–3, 5
Renema and Hoeksema (2001)	*A. quoyii*	Recent	Sulawasi	fig. 10e
Yordanova and Hohenegger (2002)	*A. quoyi*	Recent	Sesoko-jima	pl. 30, figs. 5–7
Förderer et al. (2018)	*A. quoyi*	Recent	geographic list	no
This study	*A. quoyi*	Pleistocene	Ryukyu Islands	Fig. 7
		Recent	Ryukyu Islands	Fig. 8
		Recent	Vanuatu	Fig. 9

1957). The northernmost occurrence of the species is in Okinawa-jima (Pleistocene–Recent; this study, Fig. 11). A Burdigalian record of *A. quoyi* needs further confirmation, since no illustrations were published (Matsumaru, 2011).

The present-day *Alveolinella* records from the Indian Ocean are inadequately illustrated since they often do not show the septula in alignment, two or more layers of main chamberlets and one layer of attics per chamber, considered to be diagnostic characters of this genus (e.g., Rana et al., 2007, fig. 2D; Mazumder et al., 2012, pl. 1, fig. 6; Panchang and Nigam, 2014, pl. 15, figs. 1–2; Sreenivasulu et al., 2017; Ranju et al., 2019, fig. 2f; Symphonia and Senthil, 2019, fig. 22(15)). In this area *Alveolinella quoyi* has been found only in the Maldives (Hottinger, 1980, p. 11; Parker and Gischler, 2011, pl. 3, figs. 16–17). The Maldives is considered the western limit of several Indo-Pacific larger foraminiferal taxa (Parker and Gischler, 2011). Because there are no fossil occurrences of this species in the Indian Ocean, the single occurrence in the Maldives may reflect a recent migration from the western CIP.

5. Concluding remarks

According to the species circumscriptions of latest Oligocene–middle Miocene *Flosculinella, F. globulosa* and *F. reicheli* are sub-spheroidal in shape, whereas *F. bontangensis* is ellipsoidal to fusiform and has the largest proloculus. *Flosculinella bontangensis* also differs from the other two species in having two supplementary chamberlets in the attic per chamberlet in the basal layer of chamberlets. *Flosculinella bontangensis* is considered a valid junior synonym of the *nomen oblitum F. cucumoides*.

The occurrence of the preseptal passage only (i.e., the lack of the postseptal passage) and Y-shaped septula in *Flosculinella* and *Alveolinella* are traits of phylogenetic significance. These shell characters can be considered as inherited from the common ancestor *Borelis philippinensis*, whose present-day descendant in the *Borelis* lineage is *B. schlumbergeri*.

Alveolinella borneensis appeared in the late Burdigalian of the Central Indo-Pacific area and disappeared in the Serravallian, whereas *A. quoyi* appeared in the Tortonian in the same area. Specimens with characters intermediate between *A. borneensis* and *A. quoyi,* referred to as *Alveolinella ex. interc. borneensis et quoyi*, range from the late Serravallian to the Tortonian.

The Coral Triangle in Southeast Asia was the centre of early Miocene *Flosculinella* and *Alveolinella* speciation. The south-eastward migrants of *F. bontangensis* and *A. borneensis* reached northeastern Australian and Bikini coral reef settings in the Langhian.

In modern coral reefs *Borelis schlumbergeri* occurs from the Western to the Central Indo-Pacific, and *Alveolinella quoyi* is widespread from Central to the Eastern Indo-Pacific areas. The northernmost occurrence of *A. quoyi* is in the Ryukyu Islands.

Author statement

All authors have contributed to data curation and interpretation, and critically reviewed the manuscript.

Declaration of Competing Interest

None.

Acknowledgements

This work was supported by local research funds at the University of Ferrara (FAR 2018–2021, FIR 2018). This paper is a scientific contribution of the MIUR-Dipartimenti di Eccellenza 2018–2022 Project and the PRIN 2017RX9XXXY (Biota resilience to global change: biomineralization of planktic and benthic calcifiers in the past, present and future). Samples from Miocene deposits of East Kalimantan were collected in two field campaigns in the frame of the Throughflow Initial Training Network, funded by the Marie Curie Actions Plan, Seventh Framework Programme of the European Union (Grant 237922). DB is grateful to the International Joint Graduate Program in Earth and Environmental Sciences (GP-EES) for inviting him to the Tohoku University. We are also grateful to Tim Ziegler, curator manager at the Museum Victoria, Melbourne (Australia), for photographs of the types of *F. cucumoides*. We thank David Haig (UWA) and an anonymous reviewer for their constructive comments.

Appendix A. Supplementary data

Supplementary data to this article can be found online at https://doi.org/10.1016/j.marmicro.2022.102124.

References

Adams, C.G., 1965. The foraminifera and stratigraphy of the Melinau Limestone, Sarawak, and its importance in Tertiary correlation. Q. J. Geol. Soc. Lond. 121, 283–338.
Adams, C.G., 1970. A reconsideration of the East Indian letter classification of the tertiary. Bull. Brit. Mus. (Nat. Hist.) Geol. 19, 1–137.
Adams, C.G., 1973. Some Tertiary foraminifera. In: Hallam, A. (Ed.), Atlas of Palaeobiogeography. Elsevier, Amsterdam, pp. 453–468.
Barberi, S., Bigioggero, B., Boriani, A., Cattaneo, M., Cavallin, A., Eva, C., Cioni, R., Gelmini, R., Giorgetti, F., Iaccarino, S., Innocenti, F., Marinelli, G., Slejko, D., Sudradjat, A., 1987. The island of Sumbawa; a major structural discontinuity in the Indonesian arc. Boll. Soc. Geol. Ital. 106, 547–620.
Bassi, D., Braga, J.C., Di Domenico, G., Pignatti, J., Abramovich, S., Hallock, P., Könen, J., Kovács, Z., Langer, M.R., Pavia, G., Iryu, Y., 2021a. Palaeobiogeography and evolutionary patterns of the larger foraminifer *Borelis* de Montfort (Borelidae). Pap. Palaeontol. 7, 377–403.
Bassi, D., Aftabuzzaman, Md., Bolivar-Feriche, M., Braga, J.C., Aguirre, J., Renema, W., Takayanagi, H., Iryu, Y., 2021b. Biostratigraphical and palaeobiogeographical patterns of the larger porcelaneous foraminifer *Austrotrillina* Parr, 1942. Mar. Micropaleontol. 169, 102058 https://doi.org/10.1016/j.marmicro.2021.102058.
Bassi, D., Pignatti, J., Abramovich, S., Fujita, K., Hohenegger, J., Lipps, J.H., Iryu, Y., 2022. Ephemeral masks in the ellipsoidal foraminifera *Alveolinella* and *Borelis* (Alveolinoidea): resilient solutions to stabilization in coral-reef settings. J. Foramin. Res. 50, 92–98.
Beavington-Penney, S.J., Racey, A., 2004. Ecology of extant nummulitids and other larger benthic foraminifera: applications in palaeoenvironmental analysis. Earth-Sci. Rev. 67, 219–265.
Binnekamp, J.G., 1973. Tertiary larger foraminifera from New Britain, PNG. Aust. Bur. Min. Res., Geol. Geophys. Bull. 140, 1–26.
BouDagher-Fadel, M.K., 2018. Evolution and Geological Significance of Larger Benthic Foraminifera, 2nd ed. University College London Press, London, UK. 693 pp.
BouDagher-Fadel, M.K., Lokier, S.W., 2005. Significant Miocene larger foraminifera from South Central Java. Rev. Paléobiol. 24, 291–309.
BouDagher-Fadel, M.K., Price, G.D., 2021. The geographic, environmental and phylogenetic evolution of the Alveolinoidea from the Cretaceous to the present day. UCL Open: environment 2, 1–34. https://doi.org/10.14324/111.444/ucloe.000015.
Brasier, M.D., 1975. An outline history of seagrass communities. Palaeontology 18, 681–702.
Brasier, M.D., 1993. Fossil indicators of nutrient levels. 2: Evolution and extinction in relation to oligotrophy. In: Bosence, D.W.J., Allison, P.A. (Eds.), Marine Palaeoenvironmental Analysis from Fossils, Geol. Soc. Spec. Publ, vol. 83, pp. 133–150.
Buxton, M.W.N., Pedley, H.M., 1989. A standardized model for Tethyan Tertiary carbonate ramps. J. Geol. Soc. 146, 746–748.
Chapman, F., 1908. On the Tertiary limestones and foraminiferal tuffs of Malekula, New Hebrides. Proc. Linnean Soc. NSW 32 (125–128), 745–760.
Chaproniere, G.C.H., 1984. Oligocene and Miocene larger foraminiferida from Australia and New Zealand. Bur. Mineral Resour. Geol. Geophys. Bull. 188, 1–98.
Checchia-Rispoli, G., 1909. Nuova contribuzione alla conoscenza delle Alveoline eoceniche della Sicilia. Palaeontogr. Ital. 15, 59–70.
Cohen, K.M., Harper, D.A.T., Gibbard, P.L., 2021. The ICS International Chronostratigraphic Chart 2021/07. International Commission on Stratigraphy, IUGS. www.stratigraphy.org (visited: 07/03/2022).
Cole, W.S., 1954. Larger foraminifera and smaller diagnostic foraminifera from Bikini drill holes. Prof. Pap. U.S. Geol. Surv. 260-O, 569–608.
Cole, W.S., 1957. Larger foraminifera from Eniwetok Atoll. Prof. Pap. U.S. Geol. Surv. 260–V, 743–784.
Cole, W.S., 1969. Larger foraminifera from deep drill holes on Midway Atoll. Prof. Pap. U.S. Geol. Surv. 680-C, 1–15.
Crespin, I., 1955. The Cape Range structure, Western Australia, 2nd edition, part 11, Micropalaeontology. Bull. Bur. Mineral Resour. Australia 21, 49–82.
Cushman, J.A., 1933. The foraminifera of the tropical Pacific collections of the "Albatross", 1899–1900, part 2. Lagenidae to Alveolinellidae. Bull. U.S. Nat. Mus. 161 (2), 1–79.
Debenay, J.-P., 2012. A Guide to 1,000 Foraminifera from Southwestern Pacific: New Caledonia. IRD Édit. Marseille, Muséum National d'Histoire Naturelle Paris (384 pp).

Di Domenico, G., 2014. Fast cone-beam CT reconstruction using GPU. In: Proc. Graph. Process. Units (GPU, meeting Pisa 2014, desy-proc-2015-05), pp. 193–198. https://doi.org/10.3204/desy-proc-2014-05/35.
Douvillé, H., 1907. Les calcaires à Fusulines de l'Indo-Chine. Bull. Soc. Géol. Fr. 4th Ser. 6 (588–587).
Drooger, C.W., 1993. Radial Foraminifera; morphometrics and evolution. Verh. Kon. Ned. Akad. Wetensch. Afd. Natuurk. 41, 1–242.
Eames, F., Banner, F., Blow, W., Clarke, W., 1962. Fundamentals of Mid-Tertiary Stratigraphical Correlation. Cambridge Univ. Press, Cambridge, p. 163.
Ehrenberg, C.G., 1839. Über die Bildung der Kreidefelsen und des Kreidemergels durch unsichtbare Organismen. Phys. Abh. Königl. Akad. Wiss. Berlin 59–147.
Fajemila, O.T., Langer, M.R., Lipps, J.H., 2015. Spatial patterns in the distribution, diversity and abundance of benthic foraminifera around Moorea (Society Archipelago, French Polynesia). PLoS One 10 (12), e0145752.
Fleury, J.-J., Fourcade, E., 1990. La super-famille Alveolinacea (foraminifères): systématique et essai d'interpretation phylogénétique. Rev. Micropaléontol. 33, 241–268.
Förderer, M., Rödder, D., Langer, M.R., 2018. Patterns of species richness and the center of diversity in modern Indo-Pacific larger foraminifera. Sci. Rep. 8, 8189. https://doi.org/10.1038/s41598-018-26598-9.
Haig, D.W., Smith, M.G., Riera, R., Parker, J.H., 2020. Widespread seagrass meadows during the early Miocene (Burdigalian) in Southwestern Australia paralleled modern seagrass distributions. Palaeogeogr. Palaeoclimatol. Palaeoecol. 555, 109846 https://doi.org/10.1016/j.palaeo.2020.109846.
Hallock, P., Sheps, K., Chaproniere, G.C.H., Howell, M., 2006. Larger benthic foraminifers of the Marion Plateau, Northeastern Australia (ODP leg 194): comparison of faunas from bryozoan (sites 1193 and 1194) and red algal (sites 1196–1198) dominated carbonate platforms. In: Anselmetti, F.S., Isern, A.R., Blum, P., Betzler, C. (Eds.), Proceedings of the Ocean Drilling Program, Scientific Results 194. College Station, Texas, pp. 1–31. https://doi.org/10.2973/odp.proc.sr.194.009.2006.
Hanzawa, S., 1940. Micropaleontological studies of drill cores from a deep well in Kita-Daito-Zima (North Borodino Island). In: Commemoration of Prof. H. Yabe M. I. A. 60th birthday (Ed.), Jubilee Publication in the Commemoration of Prof. H. Yabe M. I. A. 60th Birthday. Sasaki Shuppan Co. Ltd, Sendai, Miyagi, pp. 755–802.
Hanzawa, S., 1957. Cenozoic foraminifera of Micronesia. Geol. Soc. Am. Mem. 66, 1–163. https://doi.org/10.1130/MEM66.
Hashimoto, W., Matsumaru, K., 1975. Larger foraminifera from the Philippines part 3. Limestones from eastern coastal ranges of north and Central Luzon. Geol. Palaeont. Southeast Asia 16, 117–125.
Hofker, J., 1930. The foraminifera of the Siboga expedition. Part 2. Siboga-Exped. Monogr. 4a (2), 79–170.
Hofker, J., 1952. Recent Peneroplidae. Part 4. J. R. Microscop. Soc. 72, 102–122.
Hohenegger, J., 1994. Distribution of living larger foraminifera NW of Sesoko-Jima, Okinawa, Japan. Mar. Ecol. 25, 291–334.
Hohenegger, J., 2000. Coenoclines of larger foraminifera. Micropaleontology 46, 127–151.
Hohenegger, J., 2006. The importance of symbiont-bearing benthic foraminifera for West Pacific carbonate beach environments. Mar. Micropaleontol. 61, 4–39.
Hohenegger, J., 2009. Functional shell geometry of symbiont-bearing benthic foraminifera. Galaxea J. Coral Reef Stud. 11, 81–89.
Hohenegger, J., 2011. Large Foraminifera. Greenhouse Constructions and Gardeners in the Oceanic Microcosm. The Kagoshima University Museum, Kagoshima (81 pp).
Hohenegger, J., 2018. Foraminiferal growth and test development. Earth-Sci. Rev. 185, 140–162.
Hottinger, L., 1960. Recherches sur les alvéolines du Paléocène et de l'Eocène. Mém. Suisses Paléontol. 75–76, 1–243.
Hottinger, L., 1974. Alveolinids, Cretaceous-Tertiary larger Foraminifera. Rapport EPR-E-1sp74, 2 vols. Esso Production-Research-European Laboratories, pp. 1–84.
Hottinger, L., 1980. Repartition comparée des grands foraminifères de la Mer Rouge et de l'Océan Indien. Ann. Univ. Ferrara (N. S.) Geol. Paleontol. 7 (suppl), 1–13.
Hottinger, L., 1983. Processes determining the distribution of larger foraminifera in space and time. Utrecht Micropaleontol. Bull. 30, 239–253.
Hottinger, L., 1997. Shallow benthic foraminiferal assemblages as signals for depth of their deposition and their limitations. Bull. Soc. Géol. Fr. 168, 491–505.
Hottinger, L., 2000. Functional morphology of benthic foraminiferal shells, envelopes of cells beyond measure. Micropaleontology 46 (Suppl. 1), 57–86.
Hottinger, L., 2005. Geometrical constraints in foraminiferal architecture: consequences of change from planispiral to annular growth. Stud. Geol. Pol. 124, 99–115.
Hottinger, L., 2006a. Illustrated glossary of terms used in foraminiferal research. Carnets Géol. Mém. 2006/02, 1–126.
Hottinger, L., 2006b. The "face" of benthic foraminifera. Boll. Soc. Paleontol. Ital. 45, 75–89.
Hottinger, L., Halicz, E., Reiss, Z., 1993. Recent Foraminifera from the Gulf of Aqaba, Red Sea, 33(3). Academia Scientiarum et Artium Slovenica, Classis 4, Historia Naturalis, Paleontološki inštitut Ivana Rakovca, Ljubljana, pp. 1–179 (179 pp).
ICZN, 1999. International Code of Zoological Nomenclature, 4th edition. International Trust for Zoological Nomenclature. https://www.iczn.org/the-code/.
Iryu, Y., Matsuda, H., Machiyama, H., Piller, W.E., Quinn, T.M., Mutti, M., 2006. An introductory perspective on the COREF Project. Island Arc 15, 393–406.
Keijzer, F., 1940. A contribution to the geology of Bawean. Proc. Kon. Ned. Akad. Wetensch. 43, 620–629.
Kellner, S.K., Knappertsbusch, M.W., Costeur, L., Müller, B., Schulz, G., 2019. Imaging the internal structure of *Borelis schlumbergeri* Reichel (1937): advances by high-resolution hard X-ray microtomography. Palaeontol. Electron. 22, 1–19.
Kocsis, Á.T., Scotese, C.R., 2021. Mapping paleocoastlines and continental flooding during the Phanerozoic. Earth-Sci. Rev. 213, 103463 https://doi.org/10.1016/j.earscirev.2020.103463.
Langer, M.R., Hottinger, L., 2000. Biogeography of selected larger foraminifera. Micropaleontology 46 (Suppl. 1), 105–126.
Langer, M.R., Lipps, J.H., 2003. Assembly and persistence of foraminifera in introduced mangroves on Moorea, French Polynesia. Micropaleontology 52, 343–355.
Leupold, W., van der Vlerk, I.M., 1931. The tertiary. Leidse. Geol. Meded. 5 (1), 54–78.
Leutenegger, S., 1984. Symbiosis in benthic foraminifera: specificity and host adaptation. J. Foramin. Res. 14, 16–35.
Lindsay, J.M., 1969. Cainozoic foraminifera and stratigraphy of the Adelaide Plains sub-basin, South Australia. Geol. Surv. S. Austr. Bull. 42, 7–54.
Loeblich, A.R., Tappan, H., 1987. Foraminiferal genera and their classification, 2 vols. Van Nostrand Reinhold Co., New York, p. 970+212.
Lunt, P., Allan, T., 2004. Larger Foraminifera in Indonesian Biostratigraphy, Calibrated to Isotopic Dating. Geological Research Development Centre Museum, Workshop on Micropalaeontology, June 2004, Bandung (109 pp).
Macher, J.-N., Prazeres, M., Taudien, S., Jompa, J., Sedekov, A., Renema, W., 2021. Integrating morphology and metagenomics to understand taxonomic variability of *Amphisorus* (Foraminifera, Miliolida) from Western Australia and Indonesia. PLoS One 16, e0244616.
Marshall, N., Novak, V., Cibaj, I., Krijgsman, W., Renema, W., Young, J., Fraser, N., Limbong, A., Morley, R., 2015. Dating Borneo's deltaic deluge: middle Miocene progradation of the Mahakam Delta. Palaios 30, 7–25.
Martin, K., 1911. Vorläufiger Bericht über geologische Forschungen auf Java. Erster Theil. Samm. Geol. Reichs-Mus. Leiden, Ser. 1, Beitr. Geol. Ost-Asiens Austral, 9, pp. 1–76.
Martin, K., 1917. Die altmiocäne Fauna des West-Progogebirges auf Java. Samm. Geol. Reichs-Mus. Leiden *N. F.* 2 (7), 276–277.
Matsumaru, K., 1974. The transition of the larger foraminiferal assemblages in the Western Pacific Ocean, especially from the Tertiary period. J. Geogr. (Chigaku Zasshi) 83, 281–301 (in Japanese, English abstract).
Matsumaru, K., 1977. Larger foraminifera from the Ryukyu Group, Nansei Shoto Islands, Japan. In: Marit. Sedim. Spec. publ. 1, pp. 401–424.
Matsumaru, K., 1996. Tertiary larger foraminifera (Foraminiferida) from the Ogasawara Islands, Japan. Palaeontol. Soc. Jpn. Spec. Pap. 36, 1–239.
Matsumaru, K., 2011. A new definition of the letter stages in the Philippine archipelago. Stratigraphy 8, 237–252.
Matsumaru, K., 2017. Larger foraminifera from the Philippine Archipelago. Micropaleontology 63 (2–4), 77–253.
Mazumder, A., Nigam, R., Henriques, P.J., 2012. Deterioration of early Holocene coral reef due to sea level rise along west coast of India: benthic foraminiferal testimony. Geosci. Front. 3 (5), 697–705.
Meulenkamp, J.E., Sissingh, W., 2003. Tertiary palaeogeography and tectonostratigraphic evolution of the Northern and Southern Peri-Tethys platforms and the intermediate domains of the African-Eurasian convergent plate boundary zone. Palaeogeogr. Palaeoclimatol. Palaeoecol. 196, 209–228.
Mohler, W.A., 1949. *Flosculinella reicheli* n. sp. aus dem Tertiär e5 von Borneo. Verh. Schweiz. Naturforsch. Ges, 129, p. 151.
Mohler, W.A., 1950. *Flosculinella reicheli* n. sp. aus dem Tertiär e5 von Borneo. Eclogae Geol. Helv. 42 (1949), 521–527.
Montfort de, D., 1808. Conchyliologie Systématique et Classification Méthodique des Coquilles., 1. F. Schoell, Paris, pp. 1–409.
Muraoka, A., Iryu, Y., Odawara, K., Yamada, T., Sato, T., 2005. Stratigraphy of the Ryukyu Group in Maeda-Misaki area, Okinawa-jima, Ryukyu Islands, Japan. Galaxea J. Coral Reef Stud. 7, 23–36 (in Japanese with English abstract).
Novak, V., 2014. Larger benthic foraminifera in Miocene carbonates of Indonesia. Utrecht Stud. Earth Sci. 64, 1–213.
Novak, V., Renema, W., 2018. Ecological tolerances of Miocene larger benthic foraminifera from Indonesia. J. Asian Earth Sci. 151, 301–323.
Novak, V., Santodomingo, N., Rösler, A., Di Martino, E., Braga, J.C., Taylor, P.D., Johnson, K., Renema, W., 2013. Environmental reconstruction of a late Burdigalian (Miocene) patch reef in deltaic deposits (East Kalimantan, Indonesia). Palaeogeogr. Palaeoclimatol. Palaeoecol. 374, 110–122.
Orbigny, A.d', 1826. Tableau méthodique de la classe des céphalopodes. Ann. Sci. Nat. 7, 245–314.
Orbigny, A.d', 1839. Foraminiféres. In: de la Sagra, R. (Ed.), Historia fisica, politica y natural de la Isla de Cuba. A. Bertrand ed., Paris.
Panchang, R., Nigam, R., 2014. Benthic ecological mapping of the Ayeyarwady delta shelf off Myanmar, using foraminiferal assemblages. J. Palaeontol. Soc. India 59 (2), 121–168.
Parker, J.H., 2009. Foraminifera from Ningaloo Reef, Western Australia. Mem. Ass. Australas. Palaeontol. 36, 1–810.
Parker, J.H., Gischler, E., 2011. Modern foraminiferal distribution and diversity in two atolls from the Maldives, Indian Ocean. Mar. Micropaleontol. 78, 30–49.
Rana, S.S., Nigam, R., Panchang, R., 2007. Relict benthic foraminifera in surface sediments off central east coast of India as indicator of sea level changes. Indian J. Mar. Sci. 36, 355–360.
Ranju, R., Nandini Menon, N., Menon, N.R., 2019. Observations on some symbiont bearing Foraminifera from the shelf and slope sediments of Eastern Arabian Sea. J. Mar. Biol. Assoc. India 60 (2), 53–58.
Reich, S., Wessenlingh, F., Renema, W., 2014. A highly diverse molluscan seagrass fauna from the early Burdigalian (early Miocene) of Banyunganti (south-Central Java, Indonesia). Ann. Naturhist. Mus. Wien Ser. A 116, 5–129.
Reichel, M., 1937. Étude sur les Alvéolines. Mém. Soc. Paléontol. Suisse 57, 93–147.

Reichel, M., 1964. The Alveolinidae. In: Moore, R.C. (Ed.), Treatise on Invertebrate Paleontology. C (Protista 2). University of Kansas Press, Boulder/Lawrence, pp. C503–510a.
Reiss, Z., Hottinger, L., 1984. The Gulf of Aqaba: Ecological Micropaleontology. In: Ecological Studies, 50. Springer-Verlag, Berlin (354 pp).
Renema, W., 2007. Fauna development of larger benthic foraminifera in the Cenozoic of Southeast Asia. In: Renema, W. (Ed.), Biogeography, Time and Place: Distributions, Barriers and Islands. Springer-Verlag, Berlin, pp. 179–215.
Renema, W., 2008. Internal architecture of Miocene *Pseudotaberina* and its relation to Caribbean archaiasins. Palaeontology 51, 71–79.
Renema, W., 2018. Terrestrial influence as a key driver of spatial variability in large benthic foraminiferal assemblage composition in the central Indo-Pacific. Earth-Sci. Rev. 177, 514–544.
Renema, W., Hoeksema, B.W., van Hinte, J.E., 2001. Larger benthic foraminifera and their distribution patterns on the Spermonde shelf, South Sulawesi. Zool. Verh. 334, 115–149.
Renema, W., Bellwood, D.R., Braga, J.C., Bromfield, Kk, Hall, R., Johnson, K.G., Lunt, P., Meyer, C.P., McMonagle, L.B., Morley, R.J., O'Dea, A., Todd, J.A., Wesselingh, F.P., Wilson, W.E.J., Pandolfi, J.M., 2008. Hopping hotspots: global shifts in marine biodiversity. Science 321, 654–657.
Renema, W., Walter, V., Novak, V., Young, J.R., Marshall, N., Hasibuan, F., 2015. Ages of Miocene fossil localities in the northern Kutai Basin (East Kalimantan, Indonesia). Palaios 30, 26–39.
Reolid, J., Betzler, C., Braga, J.C., Lüdmann, T., Ling, A., Eberli, G.P., 2020. Facies and geometry of drowning steps in a Miocene carbonate platform (Maldives). Palaeogeogr. Palaeoclimatol. Palaeoecol. 538, 109455 https://doi.org/10.1016/j.palaeo.2019.109455.
Reuter, M., Bosellini, F.R., Budd, A.F., Coric, S., Piller, W.E., Harzhauser, M., 2019. High coral reef connectivity across the Indian Ocean is revealed 6–7 Ma ago by a turbid-water scleractinian assemblage from Tanzania (Eastern Africa). Coral Reefs 38, 1023–1037.
Richarz, P.S., 1910. Der geologische Bau von Kaiser Wilhelms-Land nach dem heutigen Stand unseres Wissens. Neues Jahrb. Min. Geol. Paläontol. Beilagebände 29, 406–536.
Riera, R., Haig, D.W., Bourget, J., 2019. Stratigraphic revision of the Miocene Trealla Limestone (Cape Range, Western Australia): implications for Australasian foraminiferal biostratigraphy. J. Foramin. Res. 49, 318–338.
Rögl, F., 1998. Palaeogeographic considerations for Mediterranean and Paratethys seaways (Oligocene to Miocene). Ann. Naturhist. Mus. Wien 99A, 279–310.
Rutten, L., 1913. Studien über Foraminiferen aus Ost-Asien. 3. Eine neue Alveolinella von Ost-Borneo. Samml. Geol. Reichs-Mus. Leiden, Ser. 1 9 (1), 219–224.
Rutten, L., 1917. Rhizopoda. In: Martin, K. (Ed.) Die altmiocäne Fauna des West-Progogebirges auf Java. Samml. Geol. Reichs-Mus. Leiden, N. F. 2 (7), 276–277.
Santodomingo, N., Novak, V., Pretković, V., Marshall, N., Di Martino, E., Capelli, E.L.G., Rösler, A., Reich, S., Braga, J.C., Renema, W., Johnson, K.G., 2015. A diverse patch reef from turbid habitats in the middle Miocene (East Kalimantan, Indonesia). Palaios 30 (1), 128–149.
Schmarda, L.K., 1871. Zoologie. I. Band. Wilhelm von Braumüller, Wien (372 pp).
Severin, K.P., Lipps, J.H., 1989. The weight-volume relationship of the test of *Alveolinella quoyi*: implications for the taphonomy of large fusiform foraminifera. Lethaia 22, 1–12.
Simmons, M.D., 2020. Larger benthic foraminifera. Subchapter 3H. In: Gradstein, F.M., Ogg, J.G., Schmitz, M.D., Ogg, G.M. (Eds.), Geologic Time Scale 2020. Elsevier, Amsterdam, pp. 88–98.
Smout, A.H., Eames, F.E., 1958. The genus *Archaias* (Foraminifera) and its stratigraphical distribution. Palaeontology 1, 207–225.
Sreenivasulu, G., Jayaraju, N., Sundara Raja Reddy, B.C., Lakshmi Prasad, T., Nagalakshmi, K., Lakshmanna, B., 2017. Foraminiferal research in coastal ecosystems of India during the past decade: a review. GeoResJ 13, 38–48. https://doi.org/10.1016/j.grj.2017.02.003.
Symphonia, T.K., Senthil, N.D., 2019. Taxonomic notes on recent foraminifera from the continental shelf-slope region of Southwestern Bay of Bengal, East Coast of India. Palaeontol. Electron. 22.3.55A, 1–89. https://doi.org/10.26879/811.
Tan, S.H., 1936. Over verschillende paleontologische criteria voor de geleding van het Tertiair. Ingenieur in Nederlandsch-Indië. Neth. J. Geosci. 3 (9), 173–179.
Teske, P.R., Beheregaray, L.B., 2009. Evolution of seahorses' upright posture was linked to Oligocene expansion of seagrass habitats. Biol. Lett. 5 (4), 521–523.
Todd, R., Post, R., 1954. Smaller foraminifera from Bikini drill holes. US Geol. Surv. Prof. Pap. 260-n, 547–568.
van der Vlerk, I.M., 1922. Studien over Nummulinidae en Alveolinidae. Thesis Utrecht (Mouton and Co., 's-Gravenhage) (140 pp., 3 pls).
van der Vlerk, I.M., 1929. Groote Foraminiferen van N. O. Borneo. Wetensch. Meded. Dienst Mijnbouw in Nederlandsch-Oost-Indië, 9, pp. 1–45.
Verbeek, R.D.M., Fennema, R., 1896. Description Géologique de Java et Madoura, 2 vols. Stemler J.G., Amsterdam, pp. 1–1183.
Veron, J.E.N., Devantier, L.M., Turak, E., Green, A.L., Sininmonth, S., Stafford-Smith, M., Peterson, N., 2009. Delineating the Coral Triangle. Galaxea J. Coral Reef Stud. 11, 91–100.
Weinmann, A.E., Langer, M.R., 2017. Diverse thermotolerant assemblages of benthic foraminiferal biotas from tropical tide and rock pools of eastern Africa. Rev. Micropaléontol. 60, 511–523.
Whittaker, J.E., Hodgkinson, R.L., 1979. Foraminifera of the Togopi Formation, Eastern Sabah, Malaysia. Bull. Brit. Mus. Nat. Hist. (Geol.) 31, 1–120.
Wilson, M.E., Rosen, B.R., 1998. Implications of paucity of corals in the Paleogene of SE Asia: Plate tectonics or Centre of origin? In: Hall, R., Holloway, D. (Eds.), Biogeography and Geological Evolution of SE Asia. Backhuys Publishers, Leiden, pp. 165–195.
Wilson, M.I.J., Evans, M.J., Oxtoby, N.H., Nas, D.S., Donnelly, T., Thirwall, M., 2007. Reservoir quality, textural evolution, and origin of fault-associated dolomites. Am. Assoc. Pet. Geol. Bull. 91, 1247–1272.
Wonders, A.A.H., Adams, C.G., 1991. The biostratigraphical and evolutionary significance of *Alveolinella praequoyi* sp. nov. from Papua New Guinea. Bull. Brit. Mus. Nat. Hist. (Geol.) 47, 169–175.
Yamamoto, K., Iryu, Y., Sato, T., Chiyonobu, S., Sagae, K., Abe, E., 2006. Responses of coral reefs to increased amplitude of sea-level changes at the mid-Pleistocene climate transition. Palaeogeogr. Palaeoclimatol. Palaeoecol. 241, 160–175.
Yip, Z.T., Quek, R.Z.B., 2020. Historical biogeography of the widespread macroalga *Sargassum* (Fucales, Phaeophyceae). J. Phycol. 56, 300–309.
Yordanova, E.K., Hohenegger, J., 2002. Taphonomy of larger foraminifera: relationships between living individuals and empty tests on flat reef slopes (Sesoko Island, Japan). Facies 46, 169–204.
Zheng, S.-Y., 1979. The Recent foraminifera of the Xisha Islands, Guangdong Province, China. II. [in Chinese, English descriptions of new taxa]. Stud. Mar. Sin. 15, 101–232.

CONCLUSIONS

The new records of LBF and planktonic foraminifera from southeastern Spain (Sierra de Marmolance) allowed a re-assessement of the age range of Miocene SBZs for the western Mediterranean area.

According to the planktonic foraminifera identified in the studied area, the base of the studied succession characterized by marls is middle Miocene (Langhian–Serravallian) in age. The overlying LBF limestones should be at least early Serravallian in age.

The LBF record in the Sierra de Marmolance extends from the Rupelian to the early Serravallian the time ranges of ten LBF species: *Eulepidina formosoides*, *Eulepidina* ex.interc *dilatata et formosoides*, *Heterostegina assilinoides*, *Neorotalia viennoti, Nephrolepidina* ex.interc. *morgani et praemarginata*, *Nephrolepidina tournoueri, Nummulites fichteli*, *Nummulites kecskemetii, Nummulites vascus* and *Risananeiza crassaparies*. These species have been so far considered Neogene biochronostratigraphic markers, so this study highlights the need of a substantial revision of the Oligocene–Miocene SBZs.

These LBF deposited in the Sierra de Marmolance carbonate ramp, from the inner to the middle ramp settings.

The new records of *Austrotrillina* from southern Spain (Ibi and Sierra de Marmolance), Indonesia (Mankalihat and Wailawi) and western Pacific (Kitadaito-jima and Kikai Seamount) allowed defining the species descriptions according to the shell structure (tectum and a parakeriotheca with subsutural alcoves).

The biostratigraphic record of *A.striata* and *A.brunni* extends up to the Langhian (Last Appearance Datum), representing the westernmost record in the Medirerranean area.

The exclusive occurrence of *A. howchini* in the Indo-Pacific areas is a possible result of the closing Tethyan Seaway, which differentiated the Mediterranean and Indo-Pacific bioprovinces.

The palaeobiogeographic distribution of these species suggests an early Miocene active connection of Eastern Africa with the Central Indo–West Pacific.

The new records of *Flosculinella* and *Alveolinella* from the Maldives, Indonesia and Ryukyu Islands (Okinawa) allowed the circumscription of species according to the shell structure (shell length, diameter of the proloculus, whorl number of the first attic occurrence, and number of supplementary chamberlets in the attic floor per chamberlet in the main floor)

Oligocene–early Miocene *B.philippinensis* is inferred as the common ancestor of *Alveolinella* and *Flosculinella* (shell traits in common: occurrence of the preseptal passage only and Y-shaped septula).

The diversification of *Flosculinella* and *Alveolinella* speciation occurred in the Coral Triangle of SE Asia during the early–middle Miocene.

Università degli Studi di Ferrara

Sezioni

Dottorati di ricerca

Dichiarazione di conformità

AL MAGNIFICO RETTORE

UNIVERSITÀ DEGLI STUDI DI FERRARA
UFFICIO IUSS
Corso Porta Mare, n. 2 – 44121 Ferrara
e-mail dottorato@unife.it

ATTENZIONE: Il presente modulo è da stampare, firmare e rilegare alla tesi in formato cartaceo, in quanto parte integrante; va inoltre caricato nella procedura informatica Esse3 come file formato PDF/A.

Il tuo indirizzo e-mail Inserisci qui l'e-mail che ti ha fornito l'Università
blvmnc@unife.it
Oggetto: Indicare qui: "Dichiarazione di conformità della tesi di Dottorato"
Dichiarazione di conformità della tesi di c
Io sottoscritto Dott. (Cognome e Nome)
Bolívar Feriche, Mónica
Nato a: Indicare il Comune di nascita
Granada
Provincia: Scrivere per esteso la provincia di nascita oppure lo Stato (se nato all'estero)
Spagna
Il giorno: Trascrivere la data di nascita
16/06/1993
Avendo frequentato il Dottorato di Ricerca in: Specificare il nome del corso
Scienze della Terra e del Mare (EMAS)
Ciclo di Dottorato Scrivere in cifre (es. 26)
34
Titolo della tesi: Attenzione: deve essere lo stesso riportato sulla tesi cartacea
MIOCENE LARGER FORAMINIFERAL BIOSTRATIGRAPHY IN THE MEDITERRANEAN AND THE INDO-PACIFIC AREAS

Titolo della tesi (traduzione): Se la stesura della tesi è autorizzata dal Collegio dei docenti in una lingua diversa dall'italiano, è obbligatorio compilare il campo secondo queste modalità: - Tesi in inglese: traduzione in lingua italiana - - Tesi in francese, spagnolo, tedesco etc.: traduzione del titolo sia in italiano che in inglese
Biostratigrafia dei Macroforaminiferi nel Miocene del Mediterraneo e dell'Indo-Pacifico

Tutore: Prof. (Cognome e Nome)
Bassi, Davide; Braga, Juan Carlos; Coltorti, Massimo

Settore Scientifico Disciplinare (S.S.D.) Indicare il settore della tesi. Ad esempio, BIO/01
GEO/01
Parole chiave della tesi (max 10): In Italiano, Inglese ed eventuale terza lingua
Miocene, biostratigraphy, larger benthic foraminifera, Mediterranean, Indo-Pacific

Consapevole, dichiara Selezionare con un click
◉ CONSAPEVOLE: (1) del fatto che in caso di dichiarazioni mendaci, oltre alle sanzioni previste dal codice penale e dalle Leggi speciali per l'ipotesi di falsità in atti ed uso di atti falsi, decade fin dall'inizio e senza necessità di alcuna formalità dai benefici conseguenti al provvedimento emanato sulla base di tali dichiarazioni; (2) dell'obbligo per l'Università di provvedere al deposito di legge delle tesi di dottorato al fine di assicurarne la conservazione e la consultabilità da parte di terzi; (3) della procedura adottata dall'Università di Ferrara ove si richiede che la tesi sia consegnata dal dottorando in 1 originale cartaceo e 1 in formato PDF/A caricata sulla procedura informatica Esse3 secondo le istruzioni pubblicate sul sito: http://www.unife.it/studenti/dottorato alla voce ESAME FINALE – disposizioni e modulistica; (4) del fatto che l'Università, sulla base dei dati forniti, archivierà e renderà consultabile in rete il testo completo della tesi di dottorato di cui alla presente dichiarazione attraverso la pubblicazione ad accesso aperto nell'Archivio Istituzionale dei Prodotti della Ricerca IRIS-UNIFE (www.iris.unife.it) oltre che attraverso i Cataloghi delle Biblioteche Nazionali Centrali di Roma e Firenze; DICHIARO SOTTO LA MIA RESPONSABILITA': (1) che la copia della tesi depositata presso l'Università di Ferrara in formato cartaceo è del tutto identica a quella caricata in formato PDF/A sulla procedura informatica Esse3, a quelle da inviare ai Commissari di esame finale e alla copia che produrrò in seduta d'esame finale. Di conseguenza va esclusa qualsiasi responsabilità dell'Ateneo stesso per quanto riguarda eventuali errori, imprecisioni o omissioni nei contenuti della tesi; (2) di prendere atto che la tesi in formato cartaceo è l'unica alla quale farà riferimento l'Università per rilasciare, a mia richiesta, la dichiarazione di conformità di eventuali copie; (3) che il contenuto e l'organizzazione della tesi è opera originale da me realizzata e non compromette in alcun modo i diritti di terzi, ivi compresi quelli relativi alla sicurezza dei dati personali; che pertanto l'Università è in ogni caso esente da responsabilità di qualsivoglia natura civile, amministrativa o penale e sarà da me tenuta indenne da qualsiasi richiesta o rivendicazione da parte di terzi; (4) che la tesi di dottorato non è il risultato di attività rientranti nella normativa sulla proprietà industriale, non è stata prodotta nell'ambito di progetti finanziati da soggetti pubblici o privati con vincoli alla

divulgazione dei risultati, non è oggetto di eventuali registrazioni di tipo brevettale o di tutela. PER ACCETTAZIONE DI QUANTO SOPRA RIPORTATO

Firma del dottorando

Ferrara, il 07/06/2022 (data)

Firma del Dottorando

Firma del Tutore

Visto: Il Tutore
Si approva

Firma del Tutore

Selezionando il tasto "**INVIA**" in fondo alla pagina, la dichiarazione di conformità viene spedita automaticamente alla posta elettronica dell'**Ufficio IUSS**. Per ottenerne una copia in **FORMATO PDF**, fare click sull'icona della stampante del proprio browser (Internet Explorer, Firefox, Google Chrome etc.), quindi selezionare l'opzione Pdf Creator o simili (a seconda del programma in uso).